MOLECULAR BASIS OF INVASIVE GROWTH DURING MOULD INFECTION OF THE LUNG

A THESIS SUBMITTED TO THE UNIVERSITY OF MANCHESTER FOR THE DEGREE OF

DOCTOR OF PHILOSOPHY IN MEDICINE

IN THE FACULTY OF BIOLOGY, MEDICINE AND HEALTH

2017

UJU J ICHEOKU, BPharm., MRes

SCHOOL OF MEDICAL SCIENCES/DIVISION OF INFECTION, IMMUNITY AND RESPIRATORY MEDICINE

TABLE OF CONTENTS

Final word count: 57,522

LIST OF FIGURES

LIST OF TABLES

ABSTRACT

Uju Joy Icheoku; BPharm, MRes

PhD Medicine: Molecular basis of invasive growth during mould infection of the lung

This study reports a previously unappreciated degree of mechanistic complexity occurring in three sequential phases and involving: contact-mediated perturbation; physical invasion of the epithelial stratum by *A. fumigatus* germlings, and hyphae and lytic activity of soluble effectors.

This study provides evidence that airway epithelial cells respond in a distinctive and dynamic manner to *A. fumigatus* infection during the early (conidia), intermediate (germlings/immature hyphae) and late (mature hyphae/secreted effector) phases of infection via an immediate and sustained activation of the canonical NF-κB signaling circuit, an intermediate JNK and NF-κB activation in response to swollen conidia and early germlings and a late phase of MAPK JNK, p38 activation in response to hyphae and hyphae-derived secreted soluble effectors .

In tandem with activation of host signalling pathways, changes in DNA binding activities of transcription factors occurred in three distinct pattern. Early and intermediate infection increased the transcriptional activity of p65 and p50 with an increase in RelB DNA binding activity during late infection.

The events identified from this study as leading to epithelial cell decay appear to be mechanistically due to a combination of factors under the *A. fumigatus* master regulator PacC .

Finally, by using siRNA targeted at NIK, it was found that the non-canonical NF-κB signalling via RelB was a protective epithelial cell response to *A. fumigatus* induced damage, likely mediated via inflammatory modulation and or upregulation of pro-survival genes.

DECLARATION

I hereby declare that no portion of the work referred to in the thesis has been submitted in support of an application for another degree or qualification of this or any other university or other institute of learning. Wherever contributions of others are involved, and other sources of information have been used, they have been properly acknowledged.

Signed

Date:

COPYRIGHT STATEMENT

i. The author of this thesis (including any appendices and/or schedules to this thesis) owns certain copyright or related rights in it (the "Copyright") and s/he has given The University of Manchester certain rights to use such Copyright, including for administrative purposes.

ii. Copies of this thesis, either in full or in extracts and whether in hard or electronic copy, may be made only in accordance with the Copyright, Designs and Patents Act 1988 (as amended) and regulations issued under it or, where appropriate, in accordance with licensing agreements which the University has from time to time. This page must form part of any such copies made.

iii. The ownership of certain Copyright, patents, designs, trademarks and other intellectual property (the "Intellectual Property") and any reproductions of copyright works in the thesis, for example graphs and tables ("Reproductions"), which may be described in this thesis, may not be owned by the author and may be owned by third parties. Such Intellectual Property and Reproductions cannot and must not be made available for use without the prior written permission of the owner(s) of the relevant Intellectual Property and/or Reproductions.

iv. Further information on the conditions under which disclosure, publication and commercialisation of this thesis, the Copyright and any Intellectual Property and/or Reproductions described in it may take place is available in the University IP Policy (see http://documents.manchester.ac.uk/DocuInfo.aspx?DocID=2442 0), in any relevant Thesis restriction declarations deposited in the University Library, The University Library's regulations (see http://www.library.manchester.ac.uk/about/regulations/) and in The University's policy on Presentation of Theses.

ACKNOWLEDGEMENTS

First of all, I would like to express my sincere gratitude to my supervisor Dr. Elaine Bignell for being such an inspiration, for her continuous support, guidance, mentorship and all the uphill tasks that has helped me grow as a scientist. A special thank you goes to my clinical supervisor, Prof David Denning for the indispensable career mentorship and trainings.

I would like to thank our external collaborator, Dr Julian Naglik for his support and advice during the most challenging days of starting my PhD and through the first year. I would also like to thank Dr David Moyes for teaching me research and encouraging me to grow to an amazing scientist I am today-thank you Dave!

I want to thank Dr Margherita Bertuzzi for her assistance and support in setting up and continuing my research in Manchester. Huge thanks goes to Dr Lea Gregson for her help and support with cell culture. Thank you Darren Thomson for the training and help with the microscopy works. Thanks to all members of Bignell group for their friendship and co-operation. Thanks to all the MFIG members for their friendship and support one way or the other. A special thanks goes to Narjes Alfuraji, a friend turned sister for being there always and being so genuinely caring in trouble times.

I want to thank my family starting with my Daddy, Aunty obioma, Oyibo, mama Chidi, Chika, Amara, Ebere, Nmasi, KC and Chibuike for their prayers, undiluted love, patience and all the sacrifices made toward the success of this 4 years journey away from them. This journey would have been much more challenging without you guys! I love you all always.

This PhD wouldn't have happened without the mentorship, guidance, support from my role models, Dr Ken Ngwoke and Prof Charles Esimone. I am ever grateful to you both for believing so much in me! I want to thank Dr Stanley Dimkpa for all the tips and encouragement that helped me complete this PhD in time. Thanks to my Uncle Mr Godwin Okafor (and his wife) for fathering me so well and given me a home in away from home in London and for all the nice memories ☺ too.

Thanks to my inlaws especially my Dad inlaw, Justice Okaa for his love, understanding and prayers. Dad you know how we roll na ☺.

Now to the most amazing creature and gift from God, my Cherry Okaa Chibuzor Valentine-thank you for being such an awesome husband and friend, so loving, so patient, so tolerant, so supportive as ever. Thanks for giving me your lifting shoulders to lean on, for walking through the tears, frustrations and difficult times with me. How would I have done this without you Hun? My body, my money and my love na your own oo baby!

Lastly, I am forever grateful to the Almighty God who made all things possible!!!

DEDICATION

In loving memory of my dearest Mum, ***Mrs Esther Ugochi Icheoku,*** *of the blessed memory! Rest on and be rest assured of your lasting legacies.*

We miss You!!!

LIST OF ABBREVIATIONS

%	Percentage
°C	Degrees Celsius
H_2SO_4	Sulfuric acid
ABPA	Allergic broncho pulmonary aspergillosis
AECs	Airway epithelial cells
AIDS	Acquired immune deficiency syndrome
AM	Active motif
ANOVA	Analysis of variance
AP-1	Activator protein-1
ALI	Air liquid interface
BAL	Bronchioalveolar lavage
BCA	Bicinchoninic
BSA	Bovine serum albumin
CNA	Chronic necrotising aspergillosis
CARD	Cytoplasmic caspase recruiting domain
CCPA	Chronic cavitary pulmonary aspergillosis
cDNA	Complementary deoxyribonucleic acid
CF	Culture filtrate
CT	Computed tomography
CFTR	Cystic fibrosis transmembrane conductance regulator
CTLR	C-type lectin receptor
cm	Centimetre
CO_2	Carbon dioxide
COPD	Chronic obstructive pulmonary disease
CPA	Chronic pulmonary aspergillosis
Cu	Copper
DAMPs	Danger associated molecular patterns
DMSO	Dimethylsulfoxide
DNA	Deoxyribonucleic acid
dNTPs	Dinucleotide triphosphates
dsRNA	Double-stranded ribonucleic acid

DUSP	Dual specific phosphatase
ECs	Epithelial cells
ECM	Extracellular matrix
eDNA	Extracellular DNA
ELISA	Enzyme linked immunosorbent assay
ERK	Extracellular signal-regulated kinases
FBS	Foetal bovine serum
g	Grams
GAG	Galactosaminogalactan
G-CSF	Granulocyte colony-stimulating factor
GM	Galactomannan
GM-CSF	Granulocyte-macrophage colony-stimulating factor
h	Hour
HIV	Human immunodeficiency virus
HRP	Horseradish peroxidase
IFN-γ	Interferon gamma
HSC	haematopoietic stem cell
IA	Invasive aspergillosis
Ig	Immunoglobulin
IL	Interleukin
IPA	Invasive pulmonary aspergillosis
IRAK	Interleukin-1 receptor associated kinase
JNK	c-Jun N-terminal kinases
L	Litre
LDH	Lactate dehydrogenase
LPS	Lipopolysaccharide
M	Molar
MAL	MyD88 adaptor like
MAPK	Mitogen-activated protein kinase
MCP	Monocyte chemoattractant protein
min	Minutes
MIP	Macrophage inflammatory protein

MKP	MAP kinase phosphatase
m	Micro
mg	Milligram
ml	Millilitres
MOI	Multiplicity of infection
mTOR	Mammalian target of rapamycin
mRNA	Messenger RNA
mU	milli unit
NF-κB	Nuclear factor kappa-light-chain-enhancer of activated B cells
NOD	Nucleotide binding oligomerization domain
NLR	Nod like receptor
NLRP3	NLR family pyrin domain containing 3
nm	Nanometres
PAMPs	Pathogen associated molecular patterns
PAR	Protease activated receptor
PBS	Phosphate buffered saline
pg	Picogram
PI3K	Phosphoinositide 3-kinase
PRR	Pattern recognition receptor
PTX	Pentraxin
qRT-PCR	Quantitative real time polymerase chain reaction
RAGE	Receptor for advanced glycosylation end product
RIPA	Radio-Immunoprecipitation assay
RLR	RIG-like receptor
RNA	Ribonucleic acid
ROS	Reactive oxygen species
rpm	Rotations per minute
RPMI	Roswell Park Memorial Institute
SDS	Sodium dodecyl sulfate
SEM	Standard error of the mean
sp	Species
SPA	Simple pulmonary aspergillosis

TB	Tuberculosis
TLR	Toll-like receptor
TRAF	Tumor necrosis factor receptor associated factor
TRIF	TIR-domain-containing adapter-inducing interferon-β
UV	Ultra violet

CHAPTER 1: INTRODUCTION

1.0 Preface

The global burden of fungal diseases on human health and associated mortality is widely under-recognized compared to other infectious diseases (Brown et al., 2012). Consequently, there has been a steadily increasing number of new cases of fungal infection due to increasing prevalence of risk factors such as immunosuppression, transplantation, chemotherapy, and aging (Takazono and Sheppard, 2017). Of particular concern in fungal infection research is the ubiquitous and airborne opportunistic pathogen, *Aspergillus fumigatus.*

A. fumigatus is the major cause of a diverse spectrum of human lung diseases which are directly dependent upon underlying host immune status. (Fig 1.1). *A. fumigatus* causes >200000 cases of fatal invasive disease also known as invasive aspergillosis per annum. Of major concern, is the high mortality rate of 30-95% associated with invasive aspergillosis which results from poor understanding of disease pathobiology, poor diagnosis as well as paucity of therapeutics and preventive agents (Brown et al., 2012). The last two decades have seen an expanding interest and advancement towards understanding of the pathobiology of fungal disease development. Prior to the twentieth century, the study of microbial pathogenicity was focused predominantly on the ability of pathogen to cause disease, while assuming the host to be a passive factor in disease outcome (Casadevall et al., 2011). The early twentieth century was however graced with an understanding that pathogenicity is a variable and unstable property of most microbes, which in most cases depends on the host immune status, thus; host damage can equally result from both pathogen activity and host activity (Casadevall and Pirofski, 2014).

Rather than focusing on the fungus or host in isolation as key drivers of human diseases, current research has adopted a host-pathogen interaction model to simultaneously study *A. fumigatus* factors and the host variables that contribute to invasive disease phenotype during *A. fumigatus* infection. Elucidation of pathogenicity mechanisms of *A. fumigatus* in susceptible humans and more thorough

understanding of host biology including the distinct roles of epithelial barriers and immune function during *A. fumigatus* infection is a critical step to improving the therapeutic and preventive arsenals against the life threatening invasive aspergilloses.

1.1 Aspergillosis

Aspergillosis is a term that describes the wide spectrum of diseases caused by the genus *Aspergillus*. The pathobiology of the disease can vary depending on factors including host immune status, and the presence of underlying illness such as tuberculosis as well as the interaction between the host and the fungus (Kosmidis and Denning, 2015). The spectrum (Fig 1.1) of *Aspergillus* related syndromes includes the non/semi-invasive chronic pulmonary aspergillosis (CPA), simple pulmonary aspergilloma (SPA), invasive pulmonary aspergillosis (IPA) and allergic aspergillosis commonly seen in the form of allergic bronchopulmonary aspergillosis, (ABPA) (Fig1.1) (Tochigi et al., 2013, Kousha et al., 2011, Chabi et al., 2015). The different syndromes can manifest singly or in combination in a given host (Takazono and Sheppard, 2017).

1.1.1 Allergic aspergillosis

Allergic aspergilloses may arise in individuals exerting hypersensitive responses upon repeated exposure to components of *Aspergillus* species such as conidia or hyphae. Allergic aspergillosis in atopic individuals usually manifests as allergic bronchopulmonary aspergillosis (ABPA), allergic sinusitis, *Aspergillus*-induced asthma and less commonly as hypersensitive pneumonitis. ABPA occurs as a direct consequence of immune-mediated damage and dysfunction of the airways triggered in hypersensitive individuals by *Aspergillus* antigens (Shah and Panjabi, 2014, Shah and Panjabi, 2016). The resulting immune responses to *Aspergillus* antigens are characterized by polarized activation of T-helper (Th) 2 responses leading to an increase in IgE levels, as opposed to the Th1 response seen in non-allergic humans. The skewed Th2 response seen in ABPA has been linked to vitamin D deficiency and dysfunctional T- regulatory (Treg) cells (Chambers and Hawrylowicz, 2011, Hewison,

2012). The reaction of IgE with the antigen leads to combined mast cell degranulation, increased capillary permeability and eosinophilic infiltration (Shah, 2008). Type III (IgG mediated) and type IV (cell mediated) hypersensitivity responses have also been observed in ABPA patients. The current global prevalence of ABPA is thought to be greater than 4.5 million cases per annum (Denning et al., 2013), the majority of which affects asthmatics or cystic fibrosis sufferers who have significant defects in mucociliary-mediated clearance of the airways, thus increasing the likelihood of spore germination and exposure to more allergens.

1.1.2 Chronic aspergilloses

1.1.2.1 Chronic pulmonary aspergillosis

Chronic pulmonary aspergillosis (CPA) is the most common form of aspergillosis and occurs in individuals with mild or no apparent systemic immunosuppression. Presence of underlying lung disease such as chronic obstructive pulmonary disease, (COPD) is a prerequisite for development of CPA because of the induced local pulmonary immunosuppression (Godet et al., 2014). The pathophysiology of the disease shows minimal hyphal invasion following infection by *Aspergillus* species (Tochigi et al., 2013). CPA can be further divided into two classes on the basis of histopathologic features: chronic cavitary pulmonary aspergillosis (CCPA) and chronic necrotising aspergillosis (CNA), both of which are associated with high morbidity (Patterson and Strek, 2014, Denning et al., 2003, Chabi et al., 2015). CNA could be considered as a semi invasive or subacute form of invasive pulmonary aspergillosis (IPA) (Barac et al., 2017). However, CNA has a slow progression course of weeks to months (unlike IPA), with only minimal invasion, which is often limited to the lung tissues (Kousha et al., 2011). CNA was previously described as a complex form of aspergilloma because of the frequency with which it can invade the lung cavity, causing local destruction, a hallmark of the now termed CAN (Gefter et al., 1981).

1.1.2.2 Simple pulmonary aspergillosis or aspergilloma

Aspergilloma/Simple Pulmonary Aspergillosis (SPA) is a macroscopic ball composed of fungal mycelia, inflammatory immune cells, mucus, fibrin and tissue debris usually

seen in pre-existing lung cavities and sinuses such as those seen in tuberculosis (TB) or sarcoidosis, cystic fibrotic and bronchiectasis patients (Denning et al., 2003). It occurs following repeated exposure to, and inhalation of, conidia. Interestingly, an aspergilloma may increase in size, or move within the cavity but doesn't invade the lung or vascular tissues. Patients with aspergilloma are mostly asymptomatic. Rarely, mild haemoptysis may be present particularly in tuberculosis patients. The dense fungal mass of an aspergilloma is more resistant to conventional antifungal agents than invasive hyphae. Surgical interventions are the most common methods of treatment although not without risks (Kim et al., 2005).

1.1.3 Invasive aspergillosis

Invasive aspergillosis (IA) is characteristically seen in patients with severely compromised immune function, such as lung, or solid organ or haematopoietic stem cell (HSC) transplantees, HIV/AIDS patients, neutropenic patients and patients receiving chemotherapy or corticosteroids (Kosmidis and Denning, 2014, Patterson and Strek, 2014, Panjabi and Shah, 2011). IA is the most severe form of all *Aspergillus* infections, with evidence of both acute invasion of pulmonary tissues and parenchyma as well as angioinvasive growth of the fungal hyphae (Desoubeaux et al., 2014). The severity of hyphal invasion observed is generally dependent on the degree of host immune deficiency. Thus angioinvasive IA is seen in severely immunocompromised individuals whereas the subtler broncho-invasive IA is observed in patients with mild immunosuppression and with predisposing lung diseases. Damage in broncho-invasive IA is limited to the bronchial walls (Bergeron et al., 2012). On the other hand, hyphal invasion into blood vessels (angioinvasion) leads to systemic dissemination of fungus to other organs such as brain, eyes, skin, gut and kidney (Hope et al., 2005, Eggimann et al., 2006, Panjabi and Shah, 2011). Invasion of the central nervous system results in very severe consequences, almost always resulting in death in the light of limited treatment options (Desoubeaux et al., 2014). Generally, the onset of symptoms in IA is relatively quick, occurring from between a few days to weeks after conidial inhalation (Hohl and Feldmesser, 2007, Shah, 2008, Shah and Panjabi, 2014). The mortality rate of IA has been rising as the risk factors are expanding, currently ranging from 50% in neutropenia to 90% in haematopoietic

transplant patients (Denning et al., 2011, Zmeili and Soubani, 2007, Lin et al., 2001, Pappas et al., 2010, Fukuda et al., 2003, Shah and Panjabi, 2014) (http://www.gaffi.org/why/fungal-disease-frequency/ 05/10/2017). IA is one of the four most fatal fungal infections contributing to over 30% of approximately 1 million deaths due to fungal infections per year (Rajasingham et al., 2017, Brown et al., 2012). Current therapeutic options for the management of IA are limited to only three classes of antifungal agents (Tissot et al., 2017, Campoy and Adrio, 2016). However, increase in rate of resistance and poor safety profile associated with these drugs necessitates an urgent and undeniable need for better understanding of the disease mechanisms that will lead to the development of new and effective antifungal agents.

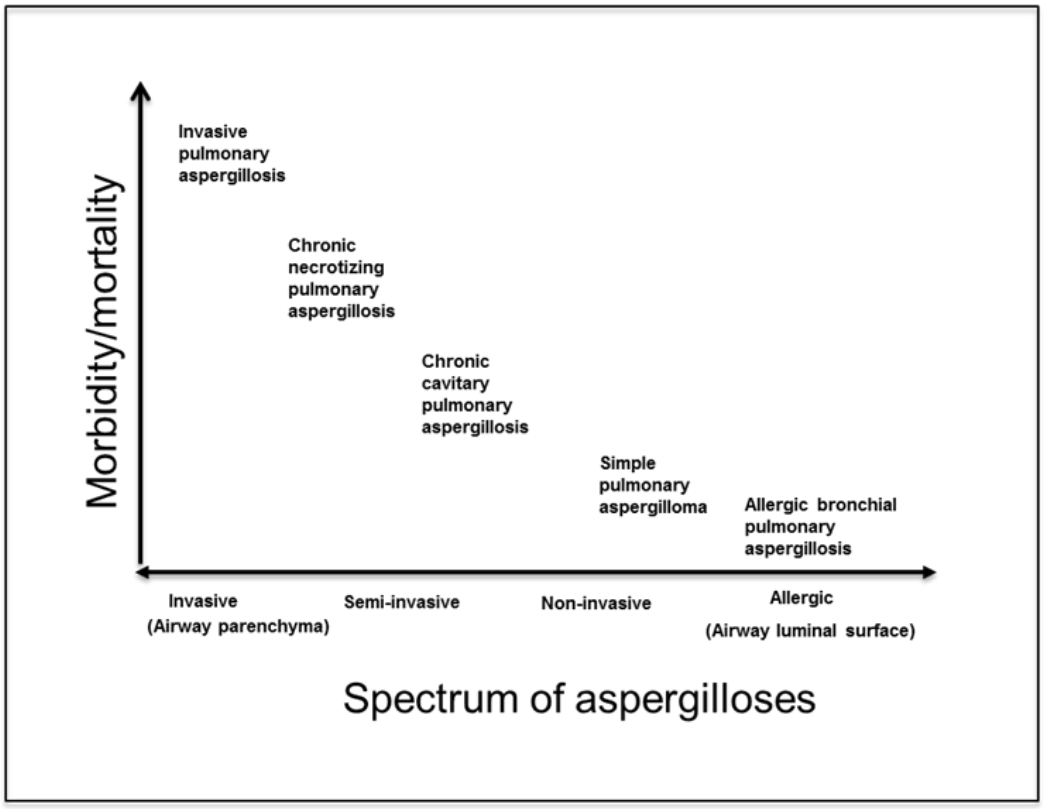

Figure 1.1: Spectrum of *Aspergillus* related diseases.

Aspergillus fumigatus causes a range of human disease which varies from invasive to allergic aspergillosis depending on the immune status (x-axis). Mortality and morbidity rate (y-axis) increases with the degree of immune-suppression. Figure was adapted from (Takazono and Sheppard, 2017, Kurza, 2014).

Table 1.1: Clinical manifestations of aspergillosis

Disease features	Invasive aspergillosis	Semi-invasive aspergillosis	Non-invasive aspergillosis	Allergic aspergillosis	References
Major manifestation	Invasive pulmonary aspergillosis, angioinvasive disease, invasive tracheobronchial disease.	Chronic cavitary pulmonary aspergillosis (CCPA), chronic necrotizing CNA.	Simple pulmonary aspergilloma, colonisation.	ABPA, SAFS, AAS, AIA hypersensitive pneumonitis, extrinsic allergic alveolitis.	(Zmeili and Soubani, 2007, Shah and Panjabi, 2016, Sherif and Segal, 2010, Gefter et al., 1981)
Risk factors/susceptibility	Neutropenia, AIDS, critically ill, lung/ allogenic stem cell transplant chronic pulmonary or liver disease, COPD, alcoholic hepatitis, diabetes mellitus.	Classic TB, thoracic surgery, rheumatoid arthritis, sarcoidosis, pneumonia, COPD, ABPA, emphysema, lung cancer survivor.	History of mycobacterial disease, ABPA, fibrotic sarcoidosis, COPD, bronchiectasis, treated lung cancer, pneumothorax.	Bronchial asthma, cystic fibrosis, genetic factors, bronchiectasis, hypersensitivity.	(Smith and Denning, 2011, Sethi et al., 2012, Chabi et al., 2015)
Clinical presentations	Overt respiratory failure, dyspnea, fever, necrosis, unilateral wheeze, ulcerative and pseudomembranous atelectasis.	Fever, malaise, productive cough, haemoptysis, pleural thickening.	Pleural thickening, chest pain, weight loss, cough, haemoptysis, pulmonary fibrosis.	Poorly controlled asthma, haemoptysis, cough, breathlessness, wheezing, fever, malaise.	(Kosmidis and Denning, 2015, Patterson and Strek, 2014, Campoy and Adrio, 2017)
Diagnosis	Positive culture, galactomannan (GM), multiplex PCR, Matrix Assisted Laser Desorption/Ionization-Time of Flight Mass Spectrometry, microscopy, bronchioalveolar lavage (BAL)/serum/sputum GM positivity, chest CT scan.	CT scan imaging, positive mycological culture, BAL sensitivity, serum precipitin test for *Aspergilllus* specific IgG.	Radiological scan, positive culture from BAL/sinus lavage.	Elevated *Aspergillus* specific and total serum IgE test, positive Aspergillus skin prick test, total eosinophil count >500 cells/µl, radiological scanning.	(McCarthy and Walsh, 2017, Arvanitis and Mylonakis, 2015, Richardson and Page, 2017, Prasad et al., 2016)

Treatments	Isavuconazole, Voriconazole , liposomal amphotericin B , caspofungin IV, micafungin IV.	Surgical resection, micafungin, Voriconazole IV/PO, Itraconazole PO, Amphotericin B IV.	Surgical resection, Bronchial artery embolization, Voriconazole IV/PO, Itraconazole PO, Amphotericin B IV.	Corticosteroids (prednisone), immunotherapy (omalizumab), surgery, nebulized amphotericin B, Itraconazole PO, Voriconazole PO.	(Tissot et al., 2017, Campoy and Adrio, 2017, Godet et al., 2014, Natesan and Chandrasekar, 2016, Li et al., 2017)

Footnote: ABPA: Allergic bronchopulmonary aspergillosis, AAS: Allergic *Aspergillus* sinusitis, COPD: chronic obstructive pulmonary diseases, PCR: polymerase chain reaction, IV: intravenous, PO: per oral, SAFS: severe asthma with fungal sensitization, AIA: *Aspergillus* induced asthma.

1.2 *Aspergillus* Species

Aspergillus species are ancient lineages of globally ubiquitous and saprophytic fungi (Cornell et al., 2007, Gugnani, 2003). They are mainly found growing in ecological niches such as soil or decaying organic matters, where they play significant roles in carbon and nitrogen recycling (Tekaia and Latge, 2005). In addition to their primary ecological niche, *Aspergillus* species can also survive in a range of other environmental conditions, in the asexual form known as conidia. The genus *Aspergillus* includes over 350 known species (Samson et al., 2014) but only a few are clinically relevant in impacting on human and animal health (Thompson and Patterson, 2011, Sherif and Segal, 2010, Shah and Panjabi, 2014, Lamoth, 2016, Cray et al., 2013, Paulussen et al., 2017). Some of the pathogenic species of *Aspergillus* are *Aspergillus flavus, Aspergillus terreus, Aspergillus niger, A. fumigatus, Aspergillus nidulans, Aspergillus clavatus, Aspergillus glaucus, Aspergillus oryzae, Aspergillus versicolor* amongst several other rarely isolated species (Denning, 1998, Perfect et al., 2001, Frisvad and Larsen, 2015, Baddley et al., 2013). *Aspergillus* species are also of tremendous economic relevance due to their grave impact on public health, their beneficial application in food industries such as citric fermentation and their negative effects as agents of food spoilage (de Vries et al., 2017).

1.2.1 *Aspergillus fumigatus*

A. fumigatus is the major cause of human aspergilloses accounting for >90% of all cases of invasive aspergillosis (Balajee et al., 2009). Recent advances in fungal genome studies have shown that *A. fumigatus* can reproduce both sexually and asexually giving rise to ascospores as well as the reproductive conidia, spores (O'Gorman et al., 2009, Dyer and O'Gorman, 2012). The capability of sexual cycle in *A. fumigatus* is of considerable medical importance. Research has suggested a possible link between the mating type 1 locus (MAT1-1) and increased virulence and antifungal resistance (Alvarez-Perez et al., 2010, Di-Giovanni, 1995). Asexual reproduction is through mitotic division of haploid cells leading to formation of asexual conidiospores which are readily released into the environment in the form of

airborne asexual conidia (Fig 1.2 and 1.3). It has been shown that the airborne burden of spores can vary significantly from 0 to 5000 spores/m^3 of inhaled air (Tovey and Green, 2005, Gots et al., 2003), depending on factors such as relative humidity, wind velocity and direction, and seasonal changes (McGinnis, 2007). By this means, all humans are frequently exposed to *Aspergillus* spores, but to varying degrees, through inhalation as the primary route of exposure; although spores can also enter the body through the eyes, ears, broken skin and gastrointestinal tract (Denning, 1998, Shah and Panjabi, 2014, Margalit and Kavanagh, 2015, Hospenthal et al., 1998, Anaissie and Costa, 2001). *A. fumigatus* is a known opportunistic pathogen, and as such, the propensity of an individual to develop aspergillosis depends upon their immune status and not solely on exposure level because inhaled fungal spores are quickly cleared by the pulmonary immune system in immunocompetent individuals, in contrast to immunocompromised hosts. However, the incidence of community acquired and nosocomial cases of invasive aspergillosis has been directly correlated with the daily load of airborne spores and fungal fragments in at-risk groups with immune deficiency (Brenier-Pinchart et al., 2011). This is logical because the higher the concentration of *A. fumigatus* spores in the air, the greater the probability that a predisposed individual will inhale a sufficient number to establish an infection. It is therefore important to keep the level of atmospheric spores to a minimum in high-risk patient areas. This has been achieved by the use of mobile air decontamination units in high-risk hospital wards (Bergeron et al., 2007, Poirot et al., 2007), in addition to other nosocomial preventive measures such as dust containment, cleaning, chemoprophylaxis and education (Brenier-Pinchart et al., 2011). A study by Green et al (2006) characterised the composition of mycoaerosols and showed that airborne hyphae and other subcellular fragments also contribute to allergic sensitization and aspergillosis. Further studies by the same group highlighted the existence of a wider community of fungi in the environment, the majority of which were not *A. fumigatus*. *A. fumigatus* is not the most abundant airborne fungus (Green et al., 2006), but remains the most frequently isolated mould clinically. It could therefore be argued that *A. fumigatus* possesses unique virulence and adaptation factors that permit a unique interaction between inhaled conidia and the host (Green et al., 2006, Nielsen et al., 2014, Dagenais and Keller, 2009, Bultman et al., 2017). The conidia of

A. fumigatus are naturally adapted for dispersal in air, and are highly tolerant to a range of adverse conditions such as very high temperature and nutrient starvation. Their small size (2-3 µm) sustains them in the air for extended periods of time (Smith, 1977). Scanning electron microscopy (SEM) has shown that *A. fumigatus* conidia have a somewhat shiny and rough (echinulate) surface, which confers resistance to air pressure while encouraging airborne dispersion (Afanou et al., 2014). The outer layer of the conidium (rodlet layer) is highly enriched with melanin pigmentation. The melanin protects the conidial genome from ultraviolet (UV) radiation while in the air, and also confers thermotolerance for their survival (O'Gorman et al., 2009, Afanou et al., 2015). Di-Giovann et al (1995) tested the settling velocity of conidia from 49 different airborne pathogens and showed that *A. fumigatus* conidia have the lowest settling velocity of approximately 0.03 cm/s (Di-Giovanni, 1995). This finding suggests that the concentration of *A. fumigatus* in the air relative to other airborne pathogens is largely dependent on the time after dispersal. *A. fumigatus* conidia can adhere to surfaces they come in contact with upon settlement; on which they can grow and become airborne again.

1.2.2 Structural organization and life cycle of *A. fumigatus*

The lifecycle of *A. fumigatus* includes the formation of both conidia and mycelium (hyphae) in each single cycle. Macroscopically, *A. fumigatus* cultured on Sabouraud dextrose agar presents as a bluish-green woolly colony of up to 1 cm in diameter at 7 days old, often having a thin white fringe edge (Figure 1.2).

Figure 1.2: Macroscopic structure of *Aspergillus fumigatus*

A. fumigatus cultured on Sabouraud dextrose agar. The white woolly edge is composed of new mycelial tips. The bluish-green centre composed of the older and sporulating mycelia originating from the colony at the slightly depressed centre

Microscopically, the vegetative fungal cells (hyphae) are filamentous showing parallel septation. Aerial hyphae terminate in cone-shaped conidiophores. The conidiophore can be up to 300 µm long and is capped with dome-shaped vesicles, 20-30 µm in diameter. Phialides cover the upper two thirds of the vesicles from where chains of spherical, smooth to finely roughened conidia radiate, (Figure 1.3). Although conidia and mycelia are successive structural morphotypes arising from the same growth cycle, the molecular organization of their cell wall differs. The cell wall of *A. fumigatus* conidia is composed of two layers; the dense pigmented outer layer and the translucent inner layer (Fig 1.4). The outermost layer as revealed by electron microscopy and biochemical analysis exhibit the presence of a clustered layer of proteinaceous microfibrils called rodlets (Dague et al., 2008). Rodlets are highly enriched with the hydrophobin RodA and are important in maintaining conidia in the resting (non-germinating) state. Research has shown that the RodA layer is crucial for adhesion to host tissues, and protection against immune mediated recognition and

phagocytosis. However, deletion of the *rodA* gene does not affect pathogenesis and virulence (Dague et al., 2008, Paris et al., 2003).

1.2.3 Germination of conidia

Following inhalation, conidia settle and gradually adhere to suitable human tissues before initiating the process of germination. Before germination, the conidial surface progressively sheds the outer rodlet/hydrophobic layer, exposing an electron-translucent hydrophilic surface as shown by real-time atomic force microscopy (Dague et al., 2008, Paris et al., 2003). Following this is the exposure of antigenic molecules in the cell wall largely composed of polysaccharide. Cell wall polysaccharides of *A. fumigatus* include α-(1,3) glucan, β-D(1,3) glucan, chitin, galactomannan and cell wall associated proteins (Abad et al., 2010, Hohl and Feldmesser, 2007, Bernard and Latge, 2001, Paris et al., 2003, Latge et al., 1993) all of which confer immunogenicity to the now swollen conidia. Nutrient and water absorption by the germinating conidium induces an isotropic swelling to up to double the diameter of the metabolically inactive conidium and *de novo* synthesis of a new electron lucent layer (Paris et al., 2003, Latge et al., 2005). Morphologically, the resting conidium (Fig. 1.5A) appears different from the swollen conidium (Fig. 1.5B) as it loses the smooth appearance of the inert spore and assumes a more complex surface topology characteristic of a brain structure (Figure 1.5A and B). The next observable step in the germination process is a gradual constriction of the swollen conidium at one pole, giving rise to a germ tube, which grows into hyphae following the initial septation event. Similarly, the morphology and surface features of the newly formed germ tube and hypha (Fig. 1.5C) are distinct from that of the swollen conidium (Figure 1.5B). The surface appendages expressed by the resting conidia, swollen conidia, germ tube and hyphae are different. For example, the growing germ tube is characteristically covered with filamentous appendages between 2–7 μm in length from the base of the outgrowth, which are absent on a fully germinated hypha(Rohde et al., 2002, Paris et al., 2003). As a consequence, different growth stages of *A. fumigatus* drive specific immune responses during infection and interaction with the host.

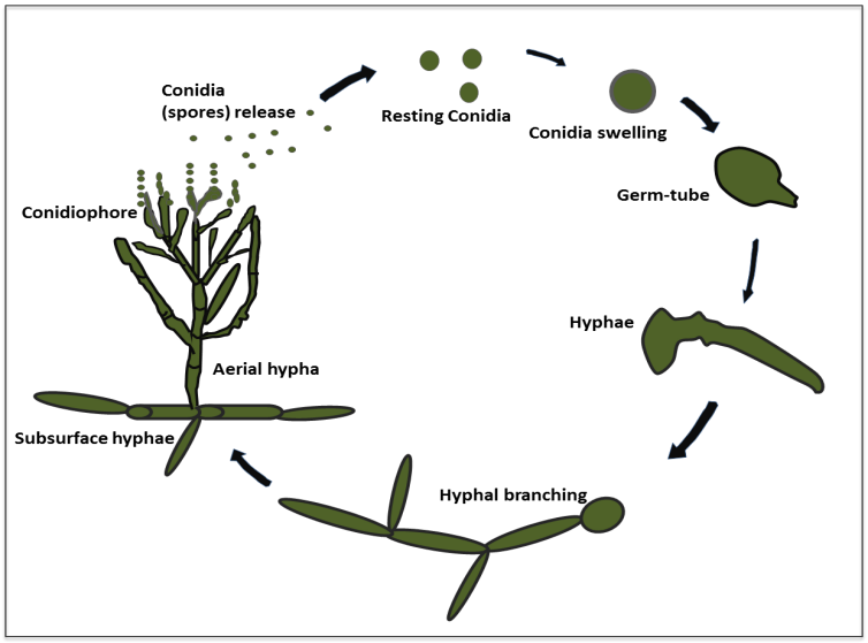

Figure 1.3: Growth and life cycle of *A. fumigatus* at 37°C

Absorption of moisture from suitable substrate causes resting *A. fumigatus* conidia to germinate and grow into hyphae. The hyphal cells are divided by parallel septa to form a multicellular branching filament. The aerial hyphae terminate in cone-shaped conidiophores covered with chains of newly formed conidia ready for dispersion

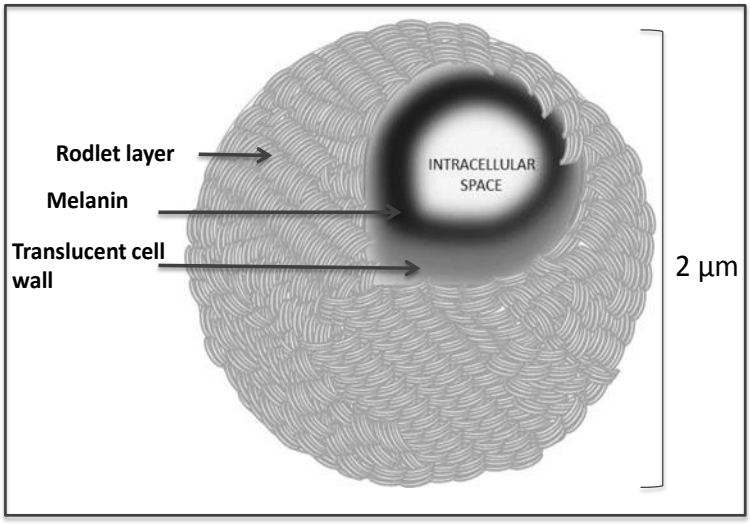

Figure 1.4: Structure of *Aspergillus* conidia

A. fumigatus conidia are structurally divided into multiple physiologically important layers: The outer hydrophobic layer covered by rodlet protein RodA which is important for conidia dispersability, the inner cell wall (translucent) layer which

houses the cell wall antigens important for immune sensing and recognition and the innermost melanin layer which is important in environmental and immune tolerance. An average *A. fumigatus* conidium measures approximately 2 µm in diameter.

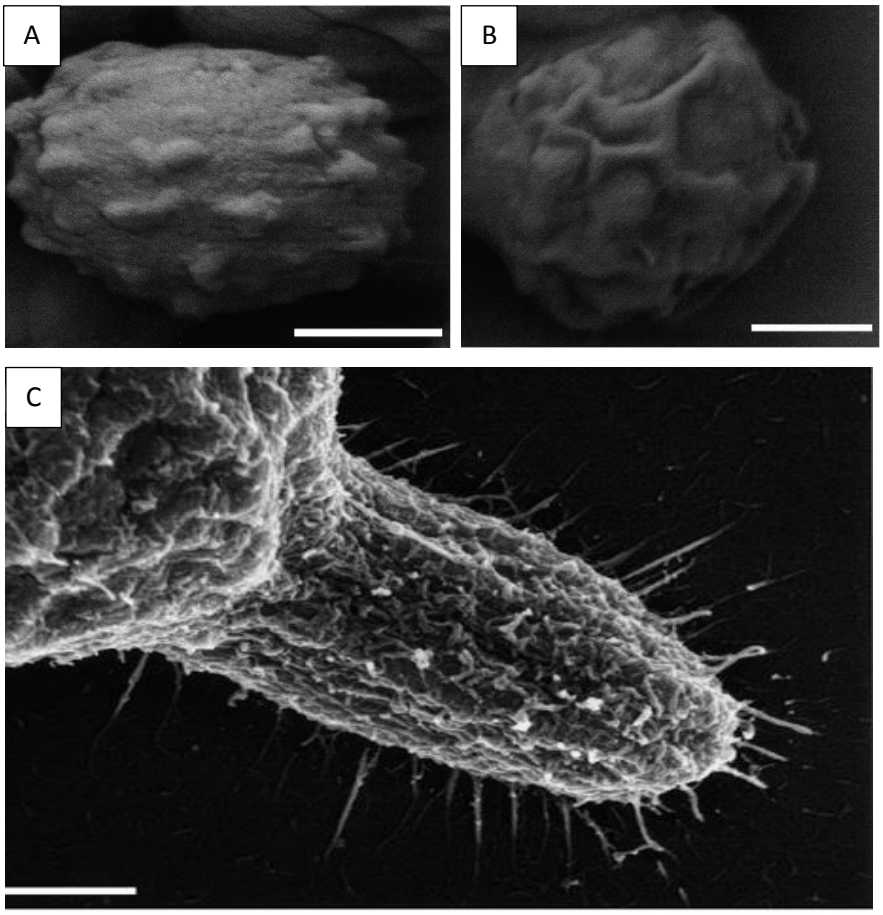

Figure 1.5 : Physical appearance of germinating *A. fumigatus* conidia.

Resting conidia (A), swollen conidia (B) and growing germ-tube (C) of *A. fumigatus* analysed by scanning electron microscope (SEM) after 0 h, 4-6 h and 7 h incubation at 37^{o}C respectively. Scale bars = 1 µm. Adapted from (Rohde et al., 2002).

1.3 Pathogenesis and virulence factors of *A. fumigatus*

The clinical outcome of *Aspergillus* infection is not only decided by the immune status of individuals but also by the virulence of the infecting strain. There are several key virulence factors associated with *A. fumigatus* pathogenicity also reflected by the predominance of *A. fumigatus* related aspergilloses. This ability to thrive in the host results in aspergilloses (McCormick et al., 2010). Pathogenicity-related traits can potentially be grouped based on the biological process they are involved in and include: transcription factors, secondary metabolites/mycotoxins, secreted proteases and structural and adaptation components. These factors individually or most likely in combination contribute to the success of *A. fumigatus* as an opportunistic pathogen.

Table 1.2: *A. fumigatus* transcription factors having significant impacts on virulence *in vivo*, updated from (Bultman et al., 2017)

Gene name	Function	Disease model of study	Impact of deletion on virulence	Reference(s)
ace2	Conidiation and conidia pigmentation	Non-neutropenic corticosteroid treated murine model of invasive pulmonary aspergillosis (IPA)	Increased	(Ejzykowicz et al., 2009)
acuK	Gluconeogenesis, iron acquisition	Non-neutropenic corticosteroid-treated murine model of IPA	Reduced	(Pongpom et al., 2015)
acuM	Gluconeogenesis, iron acquisition	*Galleria mellonella* larva model of invasive aspergillosis, neutropenic model of hematogenously disseminated disease and non-neutropenic cortisone treated murine model IPA	Reduced	(Liu et al., 2010, Pongpom et al., 2015)
areA	Nitrogen utilization	Low dose neutropenic murine model of IPA	Reduced	(Hensel et al., 1998, Krappmann and Braus, 2005)
cipC	Unknown	Neutropenic murine model of IPA	Reduced	(Canela et al., 2017)
cpcA	Cross-pathway control system	Neutropenic murine model of IPA	Reduced	(Krappmann et al., 2004)
crzA	Calcium homeostasis	Neutropenic murine model of IPA	Abrogated	(de Castro et al., 2014, Soriani et al., 2008) (Cramer et al., 2008)
dvrA	Host cell damage and modulation of inflammation	Non-neutropenic murine model of IPA	Increased	(Ejzykowicz et al., 2010)
gliZ	Gliotoxin production	Neutropenic murine model of IPA	No impact	(Bok et al., 2006)
gliP	Gliotoxin synthase	Neutropenic murine model of IPA	No impact	(Kupfahl et al., 2006)
hacA	Unfolded protein response	Neutropenic and non-neutropenic murine model IPA	Reduced	(Richie et al., 2009)
hapX	Iron homeostasis	Leukopenic murine model and non-leukopenic murine model IPA	Reduced	(Brandon et al., 2015, Schrettl et al., 2010)

hasA	hexadehydro-astechrome production	Neutropenic murine model of IPA	Increased	(Yin et al., 2013)
laeA	Conidial pigmentation and morphology	Neutropenic murine model IPA	Abrogated	(Sugui et al., 2007, Bok et al., 2005)
medA	Biofilm formation, adherence	*G. mellonella* larva and non-neutropenic murine model of IPA	Reduced	(Gravelat et al., 2010, Al Abdallah et al., 2012)
metR	Acquisition of inorganic sulfur	*G. mellonella* larva and leukopenic murine model of IPA	Reduced	(Amich et al., 2013)
mtfA	Conidiation, protease and gliotoxin production	*G. mellonella* model	Reduced	(Smith and Calvo, 2014)
pacC	Alkaline pH response	Neutropenic murine model of IPA	Avirulent	(Bertuzzi et al., 2014, Amich et al., 2010) (Tilburn et al., 1995)
rlmA	Cell wall integrity and DHN melanin sythesis	Neutropenic murine model of IPA	Reduced	(Rocha et al., 2016, Valiante et al., 2016)
sebA	Heat shock, nutrient and oxidative stress	Neutropenic murine model of IPA	Avirulent	(Dinamarco et al., 2012)
somA	Conidiation, adhesion	Egg infection and neutropenic murine model of IPA	Reduced	(Lin et al., 2015)
srbA	Hypoxia response, ergosterol biosynthesis, siderophore biosynthesis	Non-neutropenic murine model of IPA	Reduced	(Blatzer et al., 2011, Chung et al., 2014) (Willger et al., 2008)
srbB	Hypoxia response, carbohydrate metabolism, heme biosynthesis	Neutropenic murine model of IPA	Reduced	(Chung et al., 2014)
sreA	Iron homeostasis (replete conditions)	Neutropenic murine model of IPA	No impact	(Brandon et al., 2015) (Schrettl et al., 2008)
stuA	Asexual reproduction, secondary metabolite pathways	Neutropenic murine model of IPA	No impact	(Sheppard et al., 2005, Twumasi-Boateng et al.,

				2009)
yap1	Oxidative stress response	Neutropenic murine model of IPA	No impact	(Lessing et al., 2007, Qiao et al., 2008)
zafA	Zinc homeostasis	Neutropenic murine model of IPA	Avirulent	(Amich et al., 2010, Amich et al., 2014) (Moreno et al., 2007)

1.3.1 Transcription factors (TFs)

Currently, many of the studies directed towards the identification of the virulence factors of *A. fumigatus* primarily focus on transcriptional regulators for insight on individual gene products. Studying virulence at transcriptional level helps to accommodate the complex genetic interaction/genetic redundancy involved in different stress responses but under a single TF control. A major caveat to this approach is that, mutation of a single TF may lead to loss of virulence but the study of a single downstream target gene maybe either impossible (for essential genes) or without a phenotype. Regardless of the advantages and disadvantages of using TFs to probe virulence, a significant number of TFs have been reported which may impact on *A. fumigatus* virulence (Table 1.2).

1.3.2 Secondary metabolites

A. fumigatus produces enzymes and secreted proteins to aid the digestion and utilization of substrates and nutrient sources (including host tissues) and secondary metabolites as chemical weapons against predators in the environment. Although the secreted proteases and secondary metabolites are ultimately regulated by transcription factors, significant effort is being made to identify and characterise at single gene level, molecules important for pathogenicity in *A. fumigatus*.

Production of toxic secondary metabolites and siderophore biosynthesis are the most widely studied virulence features of *A. fumigatus* at single gene level. These toxic secondary metabolites (also known as mycotoxins) are the major known cause of damage in the host during *Aspergillus* infection and have been extensively reviewed (Abad et al., 2010, Schwienbacher et al., 2005, Bignell et al., 2016). Mycotoxin production can be associated with all growth stages of *A. fumigatus* including spores and hyphae. Tryptoquivaline F, Fumiquinazoline C, questin, monomethylsulochrin and trypacidin are all spore borne secondary metabolites (Gauthier et al., 2012). Fumigaclavine C and aurasperone C toxins associated with DNA synthesis inhibition and nerve dysfunction respectively are also produced by *A. fumigatus* conidia (Coyle et al., 2007, Gauthier et al., 2012). Similarly the most well-characterised *A. fumigatus* mycotoxin, gliotoxin has demonstrated strong bioactivities on macrophages,

especially cytotoxicity, and inhibition of the respiratory burst in human neutrophils (Comera et al., 2007, Mitchell et al., 1997). In addition, gliotoxin also negatively impacts epithelial barrier integrity by causing complete ciliostasis and epithelial cell rupture (Amitani et al., 1995, Eichner et al., 1986, Gauthier et al., 2012). Gliotoxin synthesis is transcriptionally regulated by GliZ, Glip and PacC and is already reported to be important for virulence in *A. fumigatus* (Table 1.2) (Priyadarsiny et al., 2003, Gauthier et al., 2012). Another mycotoxin family known as ribotoxins appear to be important in the formation of conidiophores (Kao and Davies, 1995, Gauthier et al., 2012), where the major allergenic ribotoxins in *A. fumigatus* are mitogillin and restrictocin. Both could be exploited positively in clinical mycology diagnostics because they are easily detected in urine of infected patients during active fungal growth (Gauthier et al., 2012, Abad et al., 2010). *A. fumigatus* hyphae are associated with production of mycotoxins such verruculogen (Steffan et al., 2009, Gauthier et al., 2012), fumigallin (Bunger et al., 2004, Gauthier et al., 2012), gliotoxin and helvonic acids (Mitchell et al., 1997, Gauthier et al., 2012). Fumigallin directly inhibits ciliary functions of human respiratory epithelium

1.3.3 Secreted products

As a saprophytic mould, *A. fumigatus* produces large amounts of degradative and proteolytic enzymes such as proteases and elastases. At least three major classes of proteases produced by *A. fumigatus* have been studied in murine models of inhalation: serine proteases, metalloproteases and aspartic proteases (Namvar et al., 2015, Vickers et al., 2007), functional groupings which include a large proportion of the major *A. fumigatus* allergens (designated Asp-f) family. Extracellular/secreted metalloproteinase, aspartic protease, alkaline serine protease, subtilisin, vacuolar serine protease, enolase and hemolysin are some examples of the known secreted proteases of *A. fumigatus* that contribute to tissue damage and cell lysis in *in vitro* infection studies (Gautam et al., 2007, Kurup et al., 1998, Kurup, 2005, Markaryan et al., 1994, Alp and Arikan, 2008). These groups form a large proportion of major *A. fumigatus* allergens (Asp f) family. Host allergic inflammatory reactions are heightened by proteases that damage the epithelial barrier thereby allowing the movement of antigens across the epithelium. *A. fumigatus* uses degradative enzymes

with elastinolytic and collagenolytic properties of to break the structural barrier of pulmonary epithelium during infection (Rementeria et al., 2005, Kurup et al., 1998, Namvar et al., 2015).

Table 1.3: Secondary metabolites and secreted products having significant impacts on *A. fumigatus* virulence

Genes/Molecules	Function/category	Model used in study	Impact of deletion on virulence	References
Aspergillopepsin	Secreted secondary metabolite	Guinea pig model of IPA	No impact	(Schwienbacher et al., 2005, Reichard et al., 1997)
Fumiquinazoline C, aurasperone C and trypacidin	Secondary metabolite	*In vitro* cell culture	Increased cytotoxity	(Gauthier et al., 2012)
Haemolysin	Degradative enzyme	Non-neutropenic murine infection model IPA	No impact	(Wartenberg et al., 2011)
PLD	Phospholipases	Non-neutropenic but not neutropenic murine model of IPA	Reduced	(Li et al., 2012)
Proteases	Aspartic, vacuolar serine, alkaline proteases	Leukopenic murine model of pulmonary aspergillosis	No impact	(Kurup, 2005, Alp and Arikan, 2008, Bergmann et al., 2009)
rdbB	Regulates protein level of SREBP	Non-neutropenic murine model of IPA	Reduced	(Dhingra et al., 2016)
Ribotoxin	Secreted proteins/ secondary metabolite	Neutropenic murine model of IPA	No impact	(Smith et al., 1994)
Protein phosphatase A2 (sitA)	Cell wall integrity pathway	Leukopenic murine model of IPA	Avirulent	(Bom et al., 2015)

Table 1.4: Cell wall components with potential significance on *A. fumigatus* virulence

Genes	Functional category	Study model	Impact of deletion on virulence	Reference
GAG	Mediates adherence to host constituents	Neutropenic and non-neutropenic murine model of IPA	Reduced	(Lee et al., 2015, Gravelat et al., 2013)
beta-(1-3)-glucan glycosyltransferase	Cell wall beta-(1-3)-glucan synthesis	*Galleria mellonella* model	Increased	(Samar et al., 2015)
Chitin synthase *chsE*	Cell wall chitin synthesis	Neutropenic murine model of PA	No impact	(Aufauvre-Brown et al., 1997)
rodA	Adhesion and spore dispersion	Non-neutropenic murine model of IPA	No impact	(Thau et al., 1994, Aimanianda et al., 2009)
alb1	Conidial melanin production	Neutropenic murine model of IPA	Reduced	(Jahn et al., 1997)

1.3.4 Structural components

Many cell wall components, such as beta-(1-3)-glucan, galactosaminoglycan (GAG), galactomannan, chitin (Chs; *chsE* and *chsG*), rodlets layer (RodA), the conidial DHN melanin (*pksP*/*alb1* gene) as well as others have been implicated in pathogenicity as mutants lacking these genes were attenuated in virulence (Gresnigt et al., 2014, Lee et al., 2015, Briard et al., 2016, Thau et al., 1994, Sugui et al., 2007).

1.3.5 *Aspergillus* Biofilm

A biofilm is a complex community of microorganisms attached to a substrate or surface or one another and enclosed in an extracellular polymeric substance (EPS) (Ramage et al., 2011). There has been an increasing body of clinical and experimental evidence to support the relevance of biofilms by *A. fumigatus* during pathogenicity (Williams et al., 2016, Borghi et al., 2016, Sanguinetti and Posteraro, 2016, Reichhardt et al., 2016). *A. fumigatus* can form both planktonic and mixed biofilm with other fungal or bacterial species *in vitro* (Gutierrez-Correa et al., 2012) as well as *in vivo* (Boase et al., 2011). Most clinical diseases caused by *A. fumigatus* have characteristics of a biofilm. A typical example is the spherical mass of hyphae seen in aspergilloma. A mast-like structure containing mucus and mycelia as in bronchitis, a complex multicellular mycetoma structure in CPA and filamentous intertwined hyphae visible in invasive fungal disease tissues are other features of *Aspergillus* biofilm (Ramage et al., 2011). *A. fumigatus* can form biofilms on any accessible substrate including upper and lower airways, wounds and medical devices. For example, the characteristic filamentous growth morphology of *A. fumigatus* is a fundamental feature of A*spergillus* biofilms (Beauvais et al., 2007). Biofilms are characterised by the presence of extracellular matrix (ECM) also known as extracellular polymeric susbstance (EPS) as the primary defining feature. *A. fumigatus* has been shown to produce ECM *in vivo* during inversive aspergillosis and aspergilloma (Seidler et al., 2008) similar to that observed in *in vitro* settings. *A. fumigatus* also produces galactomannan and galactosaminogalactan (GAG) which are the major components of ECM (Briard et al., 2016). The formation, maintenance and stability of the ECM of *A.fumigatus* biofilm is mediated through eDNA because of its critical role in promoting conidial and hyphal

surface adhesion during biolfilm formation (Shopova et al., 2013). Similar to an infection process by *A. fumigatus*, development of biofilm on plastic surfaces *in vitro* occurs in three major stages: a) Early phase of conidia adhesion and germling formation before or at 8 h b) intermediate phase characterised by mass of intertwined hyphae occurring between 8 h and 12 h c) Matured filamentous biomass enclosed within an EPS reached after about 24 h (Mowat et al., 2007, Joubert et al., 2017). The eDNA content of the biofilm increases with each stage during biofilm formation. The most clinically significant aspect of fungal biofilm growth is the high level of resistance to both host immune cells and antifungal agents (Borghi et al., 2016), thus, the stage of biofilm development plays a key role in the outcome of antifungal treatment (Rajendran et al., 2011). Heightened resistance to antifungal agents can be directly linked to the eDNA content as reported by Krappmann and Ramage (Krappmann and Ramage, 2013) who showed that treatment of an *A. fumigatus* biofilm with DNAse significantly improved fungal susceptibility to amphotericin B and Caspofungin. Mucolytic agents and natural products such as chitosan have shown some anti biofilm properties and are currently being investigated for clinical use (Kvasnickova et al., 2016, Cobrado et al., 2013). Depending on the site of biofilm formation, surgical debridement can be effective if possible (Warkentien et al., 2012). *In vitro* studies of mixed culture biofilm showed that *Pseudomonas aeruginosa* inhibited *A. fumigatus* biofilms via two mechanisms, namely: via acontact-dependent mechanism and vis production of a secreted heat-stable soluble factor described as a quorum sensing molecule (Mowat et al., 2010). This suggests that in light of poly-antifungal resistance by biofilms, secreted products and secondary metabolites present potential sources of future effective therapeutics. However, the most logical approach to curb biofilm related cases is to prevent their development. This could be achieved easily by increasing clinical awareness, removal and replacement of medical devices and debridement.

1.4 Recognition of *A. fumigatus* by the innate immune system

The innate immune system is the first line of defence used by the host to respond to pathogens in a rapid and conserved manner. In addition to the constitutive defence

mechanisms present at the site of contact with pathogens, which include the barrier functions, the innate immune system also relies heavily on pathogen recognition by evolutionarily conserved germline encoded receptors referred to as pattern recognition receptors (PRR) present on the on host cells (Mortaz et al., 2017, Romani, 2011). PRRs typically recognise highly conserved microbial molecules associated with pathogens and known as pathogen associated molecular patterns (PAMPs). Microbial PAMPs are often components of the cell wall and common examples include lipopolysaccharides, peptidoglycans, lipotechoic acids and others well reviewed in (Akira et al., 2006). In fungal pathogens, especially multi-morphic species like *Aspergillus*, recognizable motifs (PAMPs) vary according to the growth stage, morphotype and the extracellular environment. The three major fungal PAMPs are the β-glucans (1,3, 1,2 and 1,6 branches), chitin and mannans (Medzhitov, 2007). During an infection, multiple PRRs are likely to be stimulated by the PAMPs in several different combinations leading to the activation of several immune responses. PRRs are broadly classified into three major groups based on their cellular localization: cell membrane bound PRRs, cytosolic/cytoplasmic PRRs and soluble or secreted molecule PRRs in serum and tissue fluid (Broz and Monack, 2013, Kumar et al., 2009).

1.4.1 Toll Like Receptor signalling

There are several, distinct classes of cell membrane bound PRRs with diverse functions (Figure 3). PRRs present on the cell membrane are important in presentation of PAMPs to other PRRs, promotion of microbial uptake by phagocytes and in initiating downstream signalling pathways (Lee and Kim, 2007). The most widely studied membrane bound PRRs are the toll like receptors (TLRs). There are currently ten well studied TLRs encoded by the human genome, designated TLR 1 through TLR 10 (Bryant et al., 2015). Whereas TLR1, 2, 4, 5, 6 and 10 are located extracellularly, TLR3, 7, 8 and 9 are found in the cytoplasm. Individually, each TLR recognizes a specific subset of pathogenic ligands but more than one TLR can recognize the same ligand.

TLRs are coupled to several cytosolic adaptor molecules such as MyD88, TRIF, TRAM and MAL permitting the activation of one or more independent intracellular

pathways. TLR stimulation always leads to activation of 2 major pathways depending on the primary adaptor recruited: the classical and non-classical pathways. The classical pathway involves the IL-1R- associated kinases (IRAK) adaptor complex leading to activation of both nuclear factor κB (NF-κB) and mitogen-activated protein kinases (MAPKs). The non-classical pathway on the other hand is dependent on the TRIF adaptor and sometimes MyD88 (Mortaz et al., 2017). The classical pathway through NF-κB and AP-1 transcriptional processes leads to release of pro- and inflammatory cytokines and chemokines such as IL-1β, −6, −8, −12 and TNF-α. More details on the role of NF-κB signalling in *A. fumigatus* infection are provided in section 1.6.5.

1.4.2 C-Type Lectin like receptors

The C-type lectin like receptors (CLRs) belong to another class of cell membrane bound PRRs. The most well studied CTLRs involved in recognition and phagocytosis of *A. fumigatus* are Dectin-1, Dectin-2, and dendritic cell-specific ICAM-3-grabbing non-integrin (DC-SIGN) (Hardison and Brown, 2012). Dectin-1 is pivotal in antifungal immunity being the main receptor for the β-glucan component of fungal cell walls including hyphae and conidia of *A. fumigatus* (Brown, 2006, Palma et al., 2006, Taylor et al., 2007). Signalling through Dectin-1 is achieved through two distinct Ca^{2+} independent pathways: the spleen tyrosine kinase (Syk) dependent-caspase recruitment domain containing protein 9 (CARD9) pathway and the Syk independent RAF pathway. In Syk dependent responses, Syk is recruited to the cytoplasmic tail of the phosphorylated ITAM motif of Dectin-1. The generated signal is relayed by CARD9 interacting protein to B-cell lymphoma (BcL) 10 and mucosal associated lymphoid tissue (Malt)-1 (Bcl10-Malt1) complex (Fig 1.6) (Gross et al., 2006), which mediates activation of NF-κB pathway, a key mediator of inducible inflammatory gene expression. The overall outcome of Dectin-1 activation depends on the cell type activated, the activating ligand and cross talk between other PRRs.

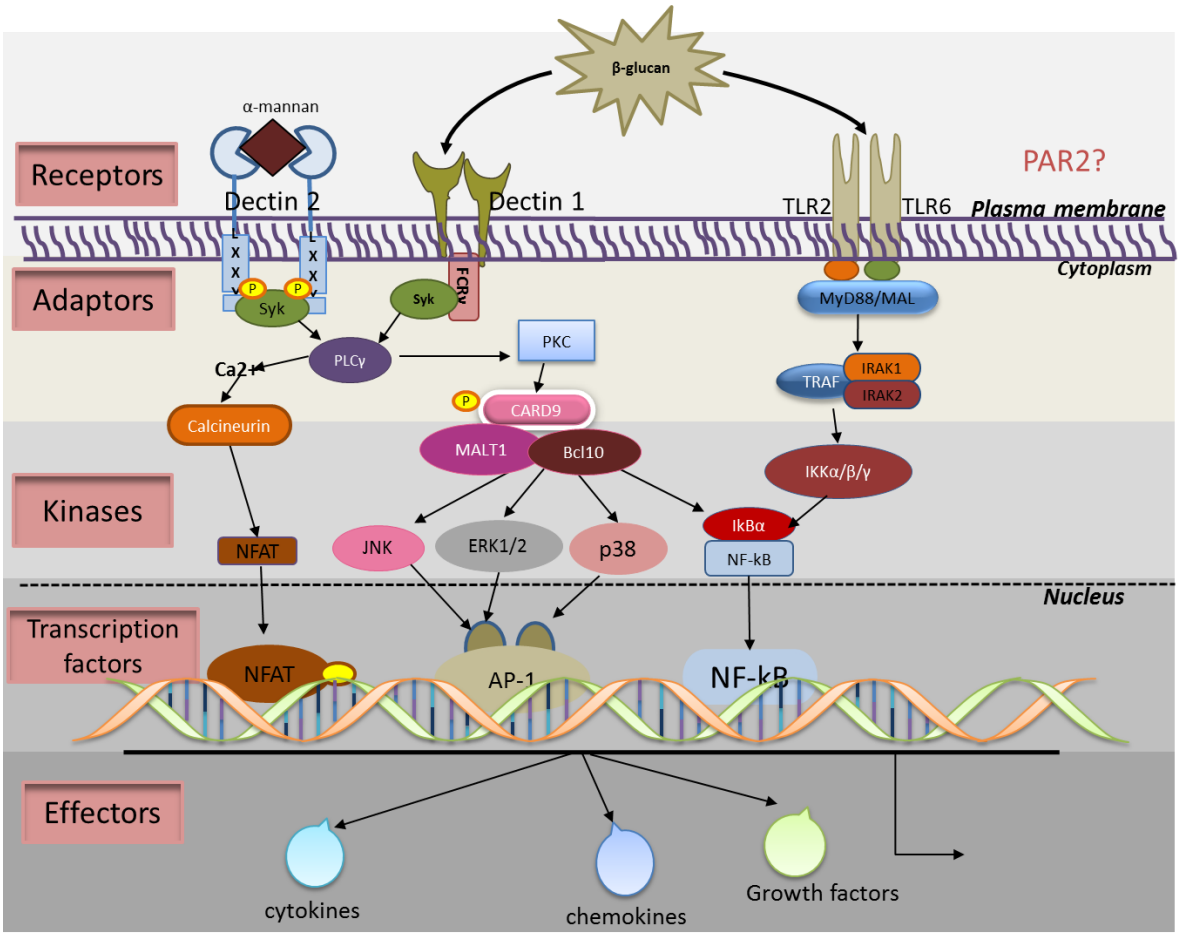

Figure 1.6: Main receptors and signalling pathways involved in innate immune responses against *A. fumigatus*. Innate immune response to *A. fumigatus*: First, recognition of appropriate fungal antigen (PAMP) by a range of host cell receptors (PRRs); Secondly, recruitment of appropriate receptor associated intracellular adaptors; Thirdly, activation and phosphorylation of kinases and ultimately the phosphorylation and activation of transcription factors leading to expression of effector molecules such as cytokines, chemokines, growth factors and others.

1.4.3 Cytoplasmic/cytosolic bound receptors

In addition to the membrane bound PRRs, there are cytosolic and secreted PRRs that recognize intracellular/cytosolic pathogen derived PAMPs mostly in the form of viral ssRNA, dsRNA, and DNA as well as components of internalized extracellular bacteria and fungi. Two well-studied cytosolic receptors are the retinoid acid-inducible gene 1 (RIG-1) like receptors (RLRs) and the nucleotide-binding oligomerization domain (NOD)-like receptors (NLRs) (Broz and Monack, 2013). The RLRs are crucial in sensing cytoplasmic uncapped RNAs, ultimately resulting in antiviral immunity mediated by type I IFN production. The NLR family plays a broader role in infection and immunity. They are key sensors for intracellular bacteria and danger associated molecular patterns (DAMPs). Two major characterized receptors in this family are NOD1 and NOD2. They recognize bacterial products derived from synthesis and degradation of peptidoglycan in the phagolysosome. Although fungal ligands for cytosolic PRRs are yet to be described, there are several reports implicating the NLRs in fungal recognition (Romani, 2011).

1.4.4 Secreted/Soluble PRRs

Secreted PRRs include a range of proteins present in the blood or body fluid, which identify molecular patterns from both non-self and altered-self components. They include the collectins, pentraxin 3, ficollins, and complement (Bidula et al., 2015). Collectins are the soluble forms of the C-type lectin superfamily. Surfactant protein A (SP-A), D (SP-D) and mannose/mannan binding lectin (MBL) are the main collectins that are potentially involved in *A. fumigatus* recognition.

1.4.5 Danger associated molecular patterns, DAMPs

Mammalian antigen presenting cells (APCs) do not only recognise PAMPs but also DAMPs which are highly immunogenic. Some of the known DAMPs include ROS, alarmins, nucleic acids, and heat shock protein (Bianchi, 2007). The cross talk between TLR and RAGE, a known DAMP receptor is thought to protect the host against *A. fumigatus* induced inflammation in the airways (Sorci et al., 2011).

1.5 Structure and role of bronchial and alveolar epithelia in immunity against *Aspergillus* species

1.5.1 The bronchial epithelium

The main route of *A. fumigatus* infection is via inhalation of airborne conidia into the bronchioles and alveoli. The respiratory airway epithelium and its secretions represent the first structures in the host to come in contact with *A. fumigatus* and constitute the first line defence of the innate immune system against this pathogen. The airway is structurally divided into two zones: the conducting zone (trachea, bronchi and secondary bronchioles) and the respiratory zone for gas exchange. The respiratory zone consists of the bronchioles, alveolar ducts and the primary alveoli. The entire length of the human airway epithelium is comprised of about 10^{10} pseudo-stratified cells covering an area of approximately 2500 cm^2 (Mercer et al., 1994). The upper respiratory tract (conducting zone) is lined with ciliated columnar cells (250 cilia on apical surface of each cell), mucus secreting goblet cells, undifferentiated basal cells and micro-villiated brush cells (Lale et al., 1998, Rokicki et al., 2016). Within the respiratory zone, the respiratory bronchioles are lined in the most part by ciliated cells and clara cells now known as club cells. The epithelium of the pulmonary alveoli comprises of three unique cell types: also known as pneumocytes: Type I, Type II and Type III (rare) and also alveolar macrophages. Epithelial cells lining the airways provide a physical barrier to inhaled particles. Within the scope of this study, emphasis will be placed upon the epithelium of the respiratory zone of the airway. Structurally, the epithelium of the respiratory airway is comprised of three layers: the outer layer of ciliated pseudostratified columnar and mucus-secreting goblet cells, a middle layer of connective tissue (basal lamina) and the innermost layer of smooth muscle and extra-cellular matrix (ECM). As well as fulfilling a mechanical barrier function, human mucus also contains immunological and antimicrobial molecules such as lactoferrin, beta-defensins (HBD), immunoglobulin A (IgA), IgG, IgM, and IgE, lysozymes, chitinases, and collectins (Brandtzaeg, 1995, Tilley et al., 2015, Rackley and Stripp, 2012). Mucociliary escalator function implicates effective hydration by mucins produced by the secretory cells and mucociliary dysfunction results in marked decrease in epithelial defence and lung disease (Tilley et al., 2015)

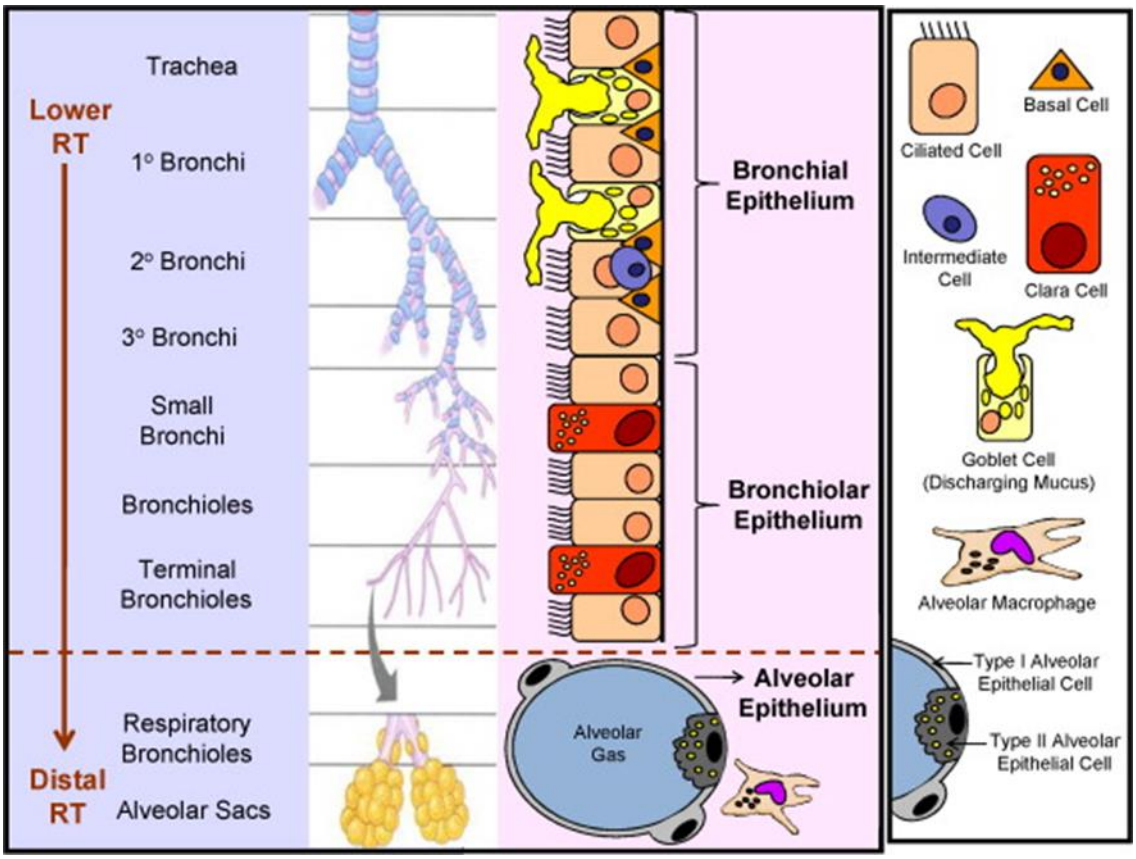

Figure 1.7: The anatomy and cellular composition of human respiratory airway epithelium.

The airway epithelium is composed of diverse cell types with specific functions. The cell types at the different regions of the airway are adapted to accommodate the functions and defence mechanisms required of the region (Berube et al., 2010).

1.5.2 The alveolar epithelium

The alveolar epithelium covering a surface of approximately 100 m^2 is composed of approximately 700 million individual alveoli. Alveolar Type I pneumocytes (ATI) cells are thin, terminally differentiated, non-dividing cells covering over 95% of the total alveolar surface, but only account for approximately 8% of the total cells in an adult human lung (Rackley and Stripp, 2012, Matthay et al., 2005, Brandtzaeg, 1995). The flatness (depth <0.5 microns) of these cells (Figure 1.7), facilitates rapid gas exchange and possibly fluid and ion transport. It is suggested that this flatness is associated with a large surface area which increases the risk of interaction with inhaled toxins

and a limited number of mitochondria which increases the sensitivity to damage from inhaled toxins (Brandtzaeg, 1995, Herzog et al., 2008).

Type II pneumocytes (ATII) are cuboidal and sometimes granular. ATII cells account for about 15% of total lung cells but only cover approximately 5% of the alveolar surface area. Their function is mostly house-keeping to maintain normal alveolar function. ATII cells are responsible for producing, secreting, and recycling lipid and protein components of the pulmonary surfactants: dipalmitoylphosphatidylcholine A, B, C and D (Evans et al., 1975, Agassandian and Mallampalli, 2013). Surfactant proteins A and D act primarily to lower the surface tension exerted by the blood–air interface on the luminal surface (Guillot et al., 2013).

Surfactant proteins A and D act as opsonins on *A. fumigatus* conidia, enhancing phagocytosis and killing by neutrophils and alveolar macrophages (Chroneos et al., 2010, Chroneos et al., 2009). ATII pneumocytes also play immunomodulatory roles through secretion of cytokines, chemokines and antimicrobial peptides such as tumour necrosis factor-alpha (TNF-α), granulocyte macrophage-colony stimulating factor (GM-CSF), macrophage inflammatory protein (MIP)-1α, interleukin (IL)-6 and IL-1β (Yamamoto et al., 2012). During alveolar repair, ATII cells differentiate into ATI cells (Evans et al., 1975), although it is still unclear how they themselves are repopulated in human lungs. Lineage studies have shown that ATII cells can develop from bronchoalveolar stem cells (BASCs) or from embryologic precursors expressing surfactant protein (SP) C (Evans et al., 1975). Studies with ATI cells have been hampered by their extremely thin morphology and difficulties in culturing ATI cells of primary human origin, although a stable transformed ATI cell line has been generated (Thorley et al., 2011). When a foreign body successfully evades the mucociliary clearance and comes into contact with the epithelium, the epithelial cells (ECs) secrete several molecules involved in host protection and also activate the more specific adaptive immune response (Iosifidis et al., 2016). Pathologic deficiencies and dysregulation of the anti-microbial properties of EC secretions are the cause of airway allergic disorders and inflammation such as seen in ABPA (Roth et al., 2012).

1.5.3 The alveolar epithelial tight junction

The barrier function of airway epithelium is highly dependent on heteromeric protein complexes known as tight junctions (TJs). TJs maintain epithelial barriers by connecting neighbouring epithelial cells with each other by forming a sealed interface. Exchange of materials between the air-filled apical compartment of the airway and the aqueous interstitial compartment on the basolateral surface occurs via two well-established routes: the paracellular route and the transcellular route. Transcellular transport route depends on polarisation of epithelial cells and the polarisation of transport channels and receptors on the apical and basolateral membranes to facilitate entry and exit of substances respectively. Paracellular movement of molecules involves passage through the interepithelial cells extracellular compartments and is dependent on tight junctional complexes. Although tight junctions are important in sealing the epithelium, they also allow a certain level of permeability to ensure optimal exchange of molecules across the epithelium. The TJ is composed of four broad classes of proteins: The integral membrane proteins, the tight junction-associated Marvel domain-containing proteins (TAMPs), the junctional adhesion molecules-A (JAMs) and the scaffolding proteins (Van Itallie and Anderson, 2014). The unique 27 member claudin family are the main component of TJ integral membrane proteins with relative molecular weights of between 21 and 34 kDa (Cording et al., 2013). Claudin proteins contain four membrane spanning domains which enable them to self-organize into different scaffolding architecture. Depending on their ability to restrict paracellular permeability, claudins are further classified in two: the tight junction forming (sealing) claudins and the non-tight junction (pore) forming claudins (Gunzel and Yu, 2013). Of the 27 claudins, claudins-1,- 3,-4,-5, 7, -8 and 18 have been confirmed to be highly expressed in human lung because of their ability to form sealing TJs. The three members of the TAMPs group of TJ proteins are occludin, tricellulin and MarvelD3. The role of occludin in regulating paracellular permeability is unclear as occludin -/- mice had normal paracellular permeability with some un explained phenotypes that may result from permeability dysregulation (Saitou et al., 2000). Similarly, the role of tricellulin and MarvelD3 in airway permeability is still controversial (Van Itallie and Anderson, 2014). JAM is known to

concentrate at epithelial and endothelial tight junctions where it localizes to the tight junctional fibrils formed by claudins (Itoh et al., 2001). The scaffolding of the TJs is formed by the zonula occludins (ZO)- 1, 2,3 proteins. The ZO-1 is the most studied ZO. ZO are positioned just below the tight junction membrane contact.

1.6 Interaction between *A. fumigatus* and respiratory epithelia

Airway epithelial cells (AECs) are amongst the first cells to encounter inhaled fungal pathogens with alveolar macrophages and dendritic cells (Espinosa and Rivera, 2016). The following sections will focus on specific interactions between airway ECs and *A. fumigatus* during the various stages of morphogenetic transitions of *A. fumigatus*, from primary pathogen encounter to pathogen clearance, and the processes leading to epithelial damage and diseases (Osherov, 2012, Croft et al., 2016). The interaction between AECs and *A. fumigatus* is thought to occur in physiologically distinct phases. First inhaled spores, if not cleared by mucociliary processes and the innate immune system, reach and adhere to the epithelial cells. Secondly, adherent spores may either be internalized by epithelial cells (ECs) and killed or germinate on the host cell. Thirdly, the epithelium, in response, releases effector molecules through inflammatory pathways directed against the fungus. Most of the studies on AEC-*A. fumigatus* interaction have used *in vitro* models of bronchial and alveolar epithelial cell lines (Foster et al., 2000, Hirakata et al., 2010, Balloy et al., 2008, Oguma et al., 2011, Fekkar et al., 2012). So far, inducing *A. fumigatus* infection in these systems has been achieved in two main ways depending on the aim. Airway epithelial cell (AEC) lines can be infected with live pathogen in the form of conidia or hyphae to study *A. fumigatus* and AEC interactions. Alternatively, culture filtrate (CF) from which *A. fumigatus* cells have been removed can be added to cell lines to study the effect of fungal secreted factors as a mimic for late infections which is difficult to achieve with live fungal infections because mature hyphae destroy host cells.

1.6.1 Mechanisms of *A. fumigatus* adherence to epithelial cells and other host constituents

The adhesion process is of primary importance in the establishment of *A. fumigatus* infections and a prerequisite for host tissue invasion. In immunocompromised individuals, inhaled conidia have been shown to adhere rapidly to the pulmonary epithelium, which provides plenty of suitable substrates (de Groot et al., 2013, Sheppard, 2011). Studies have shown that *A. fumigatus* adheres to the apical surface of the epithelium as well as to extracellular matrix proteins in the basal membrane depending on the stage of fungal development (Sheppard, 2011, DeHart et al., 1997, Wasylnka and Moore, 2000). In general, both host and fungal components are required for successful adhesion.

1.6.1.1 Host factors involved in adhesion

The main host component involved in fungal adhesion is the basal lamina in patients with diseased lung. However, basal lamina is inaccessible in healthy lung suggesting the importance of underlying lung disease/damage in fungal adhesion, persistence and invasion. It has been previously demonstrated experimentally that adhesion of conidia and hyphae of *A. fumigatus* to alveolar type II like epithelial (A549) cells is rapid, and increases with time up to a maximum as early as 40 minutes post-infection (DeHart et al., 1997). Bertuzzi et al (2014) recently observed that initial contact of *A. fumigatus* with A549 cells causes disaggregation of A549 monolayers in two mechanistically distinct processes. It is also suspected that this process exposes the basal membrane for adhesion. Addition of CF to EC monolayers increases the adhesion of conidia to A549 cells (Yang et al., 2000), further highlighting the importance of fungal secreted factors in mediating damage and exposure of the basal lamina. Also, Sharon et al, (2011) and Kogan et al (2004) showed that live *A. fumigatus* conidia initiated cell rounding, loss of focal adhesion and F-actin cytoskeletal depolymerisation in A549 cells within 2 h of infection suggesting that binding to conidia increases the exposure of basal lamina to spores (Kogan et al., 2004, Sharon et al., 2011). Type II alveolar epithelia produce H-ficolin, a soluble lectin-like opsonin. H-ficolin has been shown to enhance conidia binding to A549 cell lines *in*

vitro. These studies suggest that there are potential receptors/ligands on *A. fumigatus* that are capable of binding to host basal lamina or ECM.

1.6.1.2 Fungal factors mediating adherence to host tissues

A number of fungal molecules and or proteins involved in *A. fumigatus* adhesion to host tissues have been characterised (Croft et al., 2016). Proteinaceous sialic acids detectable on the *A. fumigatus* surface have been shown to mediate adherence to ECM components (Bouchara et al., 1997, Wasylnka et al., 2001). The exopolysaccharide, glycosaminoglycan (GAG) and galactomannan of *A. fumigatus* cell wall can also mediate adherence to the GAG binding domain of fibronectin (Gravelat et al., 2013, Wasylnka and Moore, 2000). In general, selective binding/cooperation between fungal components and a compatible host substrate is necessary for strong adhesion. For example, clustered *A. fumigatus* hydrophobin RodA protrusions on the outer surface of the conidia cell wall appear to be important for adhesion to host components such as albumin and collagen but not to laminin and fibrinogen, nor the epithelial cell surface (Aimanianda et al., 2009, Akira et al., 2006). The extracellular/secreted Fucose-specific Lectin A or FLeA, is another conidial surface protein which binds to fucose moieties such as those present on the host cell surface (Houser et al., 2013). The role of conidial adherence *in vivo* and the host receptors involved in mediating adherence are currently unclear. Just recently, a group described integrin alpha5beta1 to be the first host cell receptor for *A. fumigatus* CalA which mediates fungal adhesion and endocytosis (Liu et al., 2016).

1.6.2 Conidial internalization by airway epithelial cells

As well as uptake by professional phagocytes, studies have shown that *A. fumigatus* conidia can be internalized by epithelial cells following adherence (Paris et al., 1997, Botterel et al., 2008, Wasylnka and Moore, 2002, Zhang et al., 2005). The role of internalization in disease progression and outcome is still a subject for debate. Some reports hypothesize that intracellular occupation by internalized spores serves as a reservoir for them to evade immune responses and thus might provide a source of spores for later dissemination (Amin et al., 2014, Wasylnka and Moore, 2003). Contrary to this, Chaudhary et al (2012) reported that endocytosis by ECs was

important in killing and clearance of spores, as cystic fibrosis transmembrane conductance regulator (CFTR) deficient ECs demonstrated impaired conidia uptake and killing (Chaudhary et al., 2012). Primary human nasal epithelial cells, A549 cells and transformed human bronchial epithelial cells (16HBE140o) internalize 30-50% of spores they encounter and all but 3% of the internalized spores are killed in the acidic phagosome whilst about 34% percent of the viable 3% population germinate at least 24 h following internalization (Wasylnka and Moore, 2003). Internalization is temperature dependent and involves rearrangement of the host cell actin cytoskeleton, since cytochalasin D, an inhibitor of actin polymerization inhibited 75% of uptake of conidia (Wasylnka and Moore, 2003). Internalization did not depend on recognition of viable or heat labile antigen, as both live and heat-killed conidia were equally internalized by A549 cells (Wasylnka and Moore, 2002). Spore internalization by A549 cells was demonstrated to depend on the Dectin-1 receptor (Heyl et al., 2014, Sun et al., 2012). However, treating epithelial monolayers with an anti Dectin-1 neutralising antibody prior to conidial challenge reduces the number of internalized spores by only 20-30% (Wasylnka and Moore, 2002, Bertuzzi et al., 2014), suggesting the involvement of an additional spore-sensing mechanism and/or endocytic receptor on AECs. Dectin-1 dependent internalization was mediated by phospholipase D (PLD) activity as demonstrated by Han et al (Han et al., 2011). Also, decreasing E-cadherin reduced the rate of conidia internalization by A549 cells (Yan et al., 2015). The process of conidia internalization neither stimulates nor damages epithelial cells, as surface E-cadherin and electrophysiological properties remain intact and lactose dehydrogenase (LDH) levels measured as a marker of damage were not elevated compared to controls (Botterel et al., 2008). On the contrary, Bertuzzi et al (2014) demonstrated that detachment of A549 cells from *in vitro*-cultured monolayers is dependent on actin-mediated spore internalization. A non-invasive *A. fumigatus* mutant was internalized less than wild type progenitors and showed less perturbation to epithelial integrity both *in vivo* and *in vitro*. Blocking internalization with anti-Dectin-1 antibody significantly reduced epithelial damage caused by wild type *A. fumigatus* (Bertuzzi et al., 2014).

There is clear, consistent and growing evidence of conidia internalization by different epithelial cell types. However, whether or not this process is relevant *in vivo* and or clinically is yet to be ascertained. Using a novel single cell approach, Bertuzzi et al, 2017 have successfully demonstrated the presence of conidia in alveolar epithelial cells from mice following infection (in preparation).

1.6.3 Growth of *A. fumigatus* on airway epithelial cells

Inhaled conidia reaching the epithelium can begin germination on the host epithelium within 2 h. Hyphal extension and initial tissue penetration likely causes tissue damage in a number of ways: digestion of intraepithelial cell tight junctions and direct penetration of pneumocytes (Naglik et al., 2011, Amitani and Kawanami, 2009, Akira et al., 2006). Internalized *A. fumigatus* might also survive and germinate inside acidic phagosomes and subsequently exit into the extracellular environment without lysing the cells. Interestingly, extracellular germlings are usually longer than their intracellular counterparts (Wasylnka and Moore, 2003, Akira et al., 2006, Wasylnka et al., 2005), suggesting an inhibitory role of the intracellular compartment of the epithelium on fungal growth. An interesting aspect of conidia germination and hyphal growth is the production of degradative enzymes by the pathogen, which are the hallmark of tissue damage during *A. fumigatus* infection. Secreted proteases and other enzymes produced by hyphae can directly cause epithelial monolayer disintegration, as observed in co-culture of airway epithelial cells (AECs) with *A. fumigatus* 48 h CF (Tomee et al., 1997).

1.6.4 Airway epithelial cell immune responses to *A. fumigatus*

The view of the function of epithelial cells has changed from being a passive physical barrier to that of a non-classical innate immune cell having non-professional phagocytic properties. There has been a growing interest in the involvement of airway and alveolar epithelial cells in immunity against *A. fumigatus* (Kato and Schleimer, 2007, Vareille et al., 2011). Airway ECs (AECs) express a range of PRRs with which they recognise *A. fumigatus* and are thus able to generate appropriate effector responses such as cytokine production. By this means, epithelial cells can actually initiate and bridge the innate and adaptive responses through production of

cytokines, chemokines and cell differentiating molecules. The likely roles of AECs in mediating anti- *A. fumigatus* immunity have been demonstrated through both proteomics and transcriptomic studies.

The following sub-sections will review the specific epithelial PRRs, pathways and gene products involved in *A. fumigatus* induced immune responses.

1.6.4.1 Pattern recognition and activation of signalling pathways in airway epithelia cells by *A. fumigatus*

In order to mount an immune response against inhaled spores, AECs must first recognize the pathogen. Similar to innate immune cells, pathogen recognition by AECs is likely to rely heavily on the use of PRRs present on the EC surface, however, the identity of these PRRs is still largely unknown. Irrespective of that, there are numerous reports describing AEC signalling in response to live *A. fumigatus*, the majority of which have focused on signalling pathways and the effector cytokines produced. Borger et al (1999) first discovered that IL-8 and IL-6 signalling occurs via the NF-κB signalling pathway in the ATII like A549 epithelial cell line (Borger et al., 1999). Studies with spores and CF of *A. fumigatus* identified two independent signalling pathways both leading to NF-κB activation in the bronchial BEAS-2B epithelial cell line: the TLR independent MyD88 dependent pathway and the MyD88 independent p38/PI3K/ERK1/2 pathways leading to IL-8 synthesis. The MyD88 NF-κB pathway is regulated by three kinases, PI3K, MAPK, and ERK1/2 (Balloy et al., 2008). Sharon et al (2011) substantiated the involvement of MAPK/ERK1/2 by showing that *A. fumigatus* CF induced phosphorylation of p38, ERK1/2 and JNK in alveolar A549 cells (Sharon et al., 2011). Notably, no phosphorylation was induced by CF of an *A. fumigatus* strain lacking the PrtT transcription factor that regulates fungal protease gene expression (Sharon et al., 2011). CF of *A. fumigatus* induced the release of lysosomal enzymes from human bronchial BEAS-2B cells through P13K and p38 MAPK pathways. This response was independent of spore internalization into the phagosome (Fekkar et al., 2012).

In addition to its role in fungal internalization, the Dectin-1 receptor has a demonstrated role in fungal recognition in AECs. Exposure of bronchial epithelial cells to *A. fumigatus* conidia lead to increased Dectin-1 expression and concomitant up-

regulation of mRNA of pro-inflammatory cytokines TNFα, GM-CSF, IL8, HBD2, and HBD9 (Sun et al., 2012). Loss of Dectin-1 on ATII alveolar cells correlated with increased lung damage and epithelial cell damage *in vivo* due to *A. fumigatus* infection, strongly indicating the protective role of PRRs (Bertuzzi et al., 2014). Some TLR family members have been shown to be important in anti-*A. fumigatus* responses in AECs. The inducible expression of Dectin-1 described above was directly related to TLR-2 expression as silencing TLR-2 resulted in decreased Dectin-1 expression (Sun et al., 2012). TLR-2 role in the anti-*A. fumigatus* response has been demonstrated in corneal epithelial cells as well (Wu et al., 2015). CF-activated IFN-β and IL-10 signalling through the RIP-1/ TBK1 pathway in human bronchial epithelial cells (HBECs) was dependent on TLR3 (Beisswenger et al., 2012).

Current data on the molecular basis of the outcome of the EC- *A. fumigatus* interaction is scarce and has focused on the role of secreted factors, mainly fungal proteases, in activating host inflammatory responses. Further work is clearly required to clarify and substantiate the signalling pathways activated by different morphotypes of *A. fumigatus* during its contact with AECs. Notably, Moyes et al (2010) described a biphasic MAPK signalling response used by oral epithelial cells to distinguish between the yeast and hyphal forms of *Candida albicans*. *C. albicans* is another opportunistic fungal pathogen of humans that forms hyphae and which is known to activate epithelial responses, at different mucosal sites (Moyes et al., 2010, Moyes et al., 2016). *C. albicans* induces an initial NF-κB and MAPK response leading to activation of transcription factors c-Jun (MAPK) and p65 (NF-κB). Initial activation events require low fungal burdens, are independent of morphology and do not induce an inflammatory response. However, *C. albicans* also induces a "danger response" which is dependent on hyphal formation and increased fungal burden. The danger response comprises MKP1 phosphorylation via ERK1/2 and c-Fos activation via p38, which together with p65 (NF-κB) activation results in strong proinflammatory responses. Thus, it will be interesting to investigate how AECs respond to *A. fumigatus* conidia and hyphae in terms of signal and transcription factor activation. This will help us to better characterise the innate immune response of AECs against *A. fumigatus.*

1.6.5 NF-KB signalling

The process of recognition and clearance of fungal pathogens by the immune system largely depends on the activation of various inducible transcription factors, a role which NF-κB transcription factors have been evolutionarily conserved to play. NF-κB transcription factors are ubiquitously expressed in virtually all cell types (May and Ghosh, 1998), where they play a variety of roles in immune and stress responses, apoptosis, proliferation and differentiation, as well as in cellular development. Similarly, the signalling pathways leading to the activation of these transcription factors are receptive to diverse sources of external stimuli (O'Dea and Hoffmann, 2010). The pleotropic nature of NF-κB function derives from the fact that the majority of the genes important in the above physiological process contain kB sites in their regulatory region, thereby creating potential targets for NF-κB -mediated activation or repression (Fig 1.8).

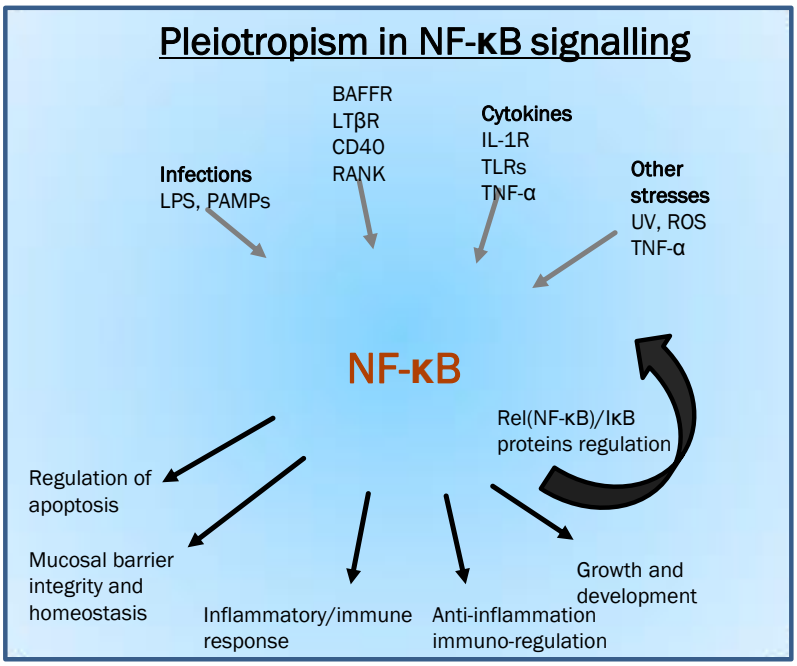

Figure 1.8: The diverse role of NF-κB signalling in mammalian immune system.

NF-κB signalling can be activated by various different stimuli and receptors (grey arrows). and has a range of biological functions (black straight arrows) in host cells. NF-κB transcription factors are autoregulated (Black rotatory arrow).

Composed of five related transcription factors, the NF-κB family of the mammalian proteins can be divided into two groups: the Rel proteins (RelA (p65), RelB and c-Rel) and the NF-κB proteins (NFκB1 (p105/p50) and NFκB2 (p100/p52). In contrast to the Rel proteins, NF-κB proteins 1 and 2 are synthesized *de novo* as precursor proteins p105 and p100 respectively, which upon detection of adequate stimuli are proteasomally processed to p50 and p52 (Betts and Nabel, 1996, Fan and Maniatis, 1991). Whereas all five NF-κB transcription factors share a 300 amino acid Rel homology domain (RHD) located towards the N-terminus of the protein, and which is essential for DNA binding, dimerization and inhibition of κB (IκB) interaction, only the Rel proteins contain the C-terminal transcription activation domains (TADs) that enable co-activator recruitment, nuclear translocation and target gene expression (Hayden and Ghosh, 2011). The NF-κB proteins can form up to 15 different combinatorial dimers having distinct physiological roles (O'Dea and Hoffmann, 2010, Shih et al., 2011). The various dimer combinations of the NF-κB subunits have distinct DNA binding specificities and may serve to activate specific sets of genes (Shih et al., 2011). Upon stimulation, the NF-κB proteins are freed from the cytoplasmic inhibitors to translocate into the nuclear compartment where they bind to consensus sequences in the target gene. The DNA binding targets of the NF-κB proteins are made up of different loose consensus sequences of approximately 9-11 base pairs. These sequences are embedded in the promoter or enhancer regions of the target genes known as the κB site or the κB response element (Kunsch et al., 1992).

Due to the absence of TAD in p50 and p52 protein sequences, homodimers of these proteins lack the ability to activate transcription and as a result act as transcriptional repressors when bound to actives sites of gene regulators. However, p50 and p52 transcription factors can act as transcriptional activators by dimerizing with any of the TAD-containing Rel family proteins (RelA (p65), c-Rel, or RelB) or by recruiting other TAD containing proteins. As much as is known currently, the p50/p65 heterodimer remains the most abundant transcriptionally active form present in most cell types (reviewed by (Hayden and Ghosh, 2004, Hayden and Ghosh, 2012). In a resting cell, the NF-κB transcription factors are bound in inactive forms in the cytoplasm by

inhibitory IκB proteins (IκBα, IκBβ, IκBε, IκBζ, p100, p105, Bcl3) until activation by appropriate stimuli.

Depending on the type of activating stimuli and signalling pathways, NF-κB transcription factors are regulated by two pathways; the canonical and non-canonical pathways (Fig. 1.9). The canonical NF-κB signalling pathway leads to activation of dimers composed of a p50 and RelA/p65 subunit occurring in response to stimulation of most stress responsive receptors (such as the TLRs or TNFR) by typical stimuli such as PAMPs (LPS), or inflammatory cytokines (TNF-α and IL-1). Stimulation leads to activation of the NEMO containing IKK complex, which in turn phosphorylates IκBα primarily by IKKβ leading to the release of the p65/p50 dimer for translocation into the nucleus.

The activation of non-canonical NF-κB transcription factors occurs independently of NEMO and primarily via IKKα. Activation begins with the induction of a specific subset of TNFR family members including BAFF-R, receptor activator of NF-κB (RANK), Lymphotoxin β-receptor (LTβR) and CD40 leading to activation of the NF-κB inducing kinase (NIK), which phosphorylates IKKα. Phosphorylation of p100 by IKKα triggers partial degradation to p52 which is capable of forming transcriptionally active RelB/p52 dimers of the non-canonical pathway (Mitchell et al., 2016).

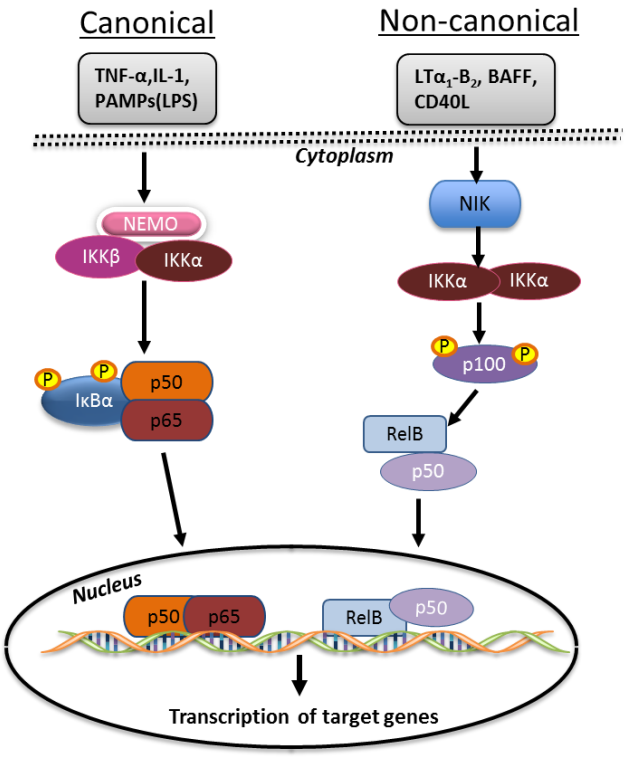

Figure 1.9: Canonical and non-canonical NF-κB signalling pathways

Depending on the nature of the activating stimuli, signalling pathways leading to the activation of NF-κB can be divided into canonical and non-canonical subtypes. Canonical signalling is activated by multiple stress-responsive receptors such as the TLRs or TNFR leading to activation of dimers composed of a p50 and a RelA/p65 subunit of NF-κB via the NEMO containing IKK complex. Non-canonical signalling is activated by more specific TNFR family members such as BAFF-R, receptor activator of NF-κB (RANK), Lymphotoxin β-receptor (LTβR) and CD40 via NIK phosphorylation leading to activation of RelB/p52 dimers

More recently, a third activation mechanism of NF-κB signalling, termed alternative NF-κB signalling has been described although the detailed mechanism is yet to be deciphered. Alternative NF-κB signalling occurs in response to ribotoxic stress induced by UV, genotoxic or shear stress deriving from mechanical forces which prompt activation of NF-κB signalling by overriding the requirement to phosphorylate cytoplasmic inhibitors (Mitchell et al., 2016). UV or mechanical stress can activate NF-κB by inhibiting translation of IκBα (O'Dea et al., 2008) or by up-regulation of

intracellular calcium level (Chen et al., 2003) respectively. As stated earlier, the components and regulation of this pathway is yet to be completely elucidated.

1.6.6 Mitogen Activated Protein Kinase (MAPK) signalling pathways

Mitogen-activated protein kinases (MAPKs) are serine threonine kinases that mediate a range of intracellular signals in response to diverse extracellular and intracellular stimuli (Kim and Choi, 2015). The mammalian MAPK family comprises the c-Jun NH_2-terminal kinase (JNK), the extracellular signal-regulated kinase (ERK), and p38. Each of the MAPKs exists as several isoforms. ERK exists as ERK 1 through 8, JNK has three isoforms, JNK1 to JNK 3, while p38 exist as p38-α, -β, -γ, and –δ (Kim and Choi, 2015). The JNK and p38 MAPK pathways are also known as stress activated protein kinases (SAPKs) derived from their primary role in mediating cellular stress responses usually to pro-inflammatory cytokines such as tumor necrosis factor (TNF)-α or interleukin (IL)-1β as well as cellular stresses including genotoxic, osmotic, hypoxic, or oxidative stress (Kyriakis and Avruch, 2001). However, the ERK pathway especially ERK1/2 are mainly responsive to growth factors (Ramos, 2008).

MAPK-mediated signalling comprises an axis of three step wise phosphorylation events (Fig1.10) initiating with MAPK kinase kinases (MAP3Ks)-mediated phosphorylation of MAPK kinases (MAP2Ks) which subsequently phosphorylate MAPKs. Activation of MAPKs involves a double phosphorylation on threonine and tyrosine residues (Whitmarsh and Davis, 1996). Activated MAPKs target and phosphorylate various downstream substrates the majority of which are transcription factors.

Some of the mammalian transcription factors which are under the regulation of MAPKs are listed in Table 1.5 below and include: ATF-2, c-Myc, STAT-1α, and MEF-2 as well as the AP-1 transcription factor complex comprising of the Jun (c-Jun, Jun B, and Jun D) and Fos (c-Fos, Fos B and Fra-1) families (Yang et al., 2003). Activation of transcription factors by MAPKs leads to increased (or repressed) gene transcription and production (or attenuation) of inflammatory cytokines which underlies both the protective and pathologic roles of MAPK-mediated signalling.

Table 1.5: Summary of the intracellular substrates of MAPK-mediated signalling

MAPK	Activating stimuli	Nuclear Substrate
ERK1/2	Growth Factors, Serum, Hormones, Cytokines, Small molecules	ATF-2, Elk-1, c-Fos, c-Myc, SAPs, c-Jun, NeuroD1, PDX-1, STAT3, RSKs, Mnks, MSK
ERK5	Growth factors, Serum, Hormones, Osmotic stress	MEF2, RSKs
p38	Hormones, Cytokines, Osmotic stress, Heat shock	ATF-2, Elk-1, MEF2, SAPs, STAT1, STAT3, MAPKAPs, Mnks, MSK
JNK	Hormones, Cytokines, DNA/protein synthesis inhibitors, Osmotic stress	ATF-2, c-Jun, Elk-1, STAT1, STAT3

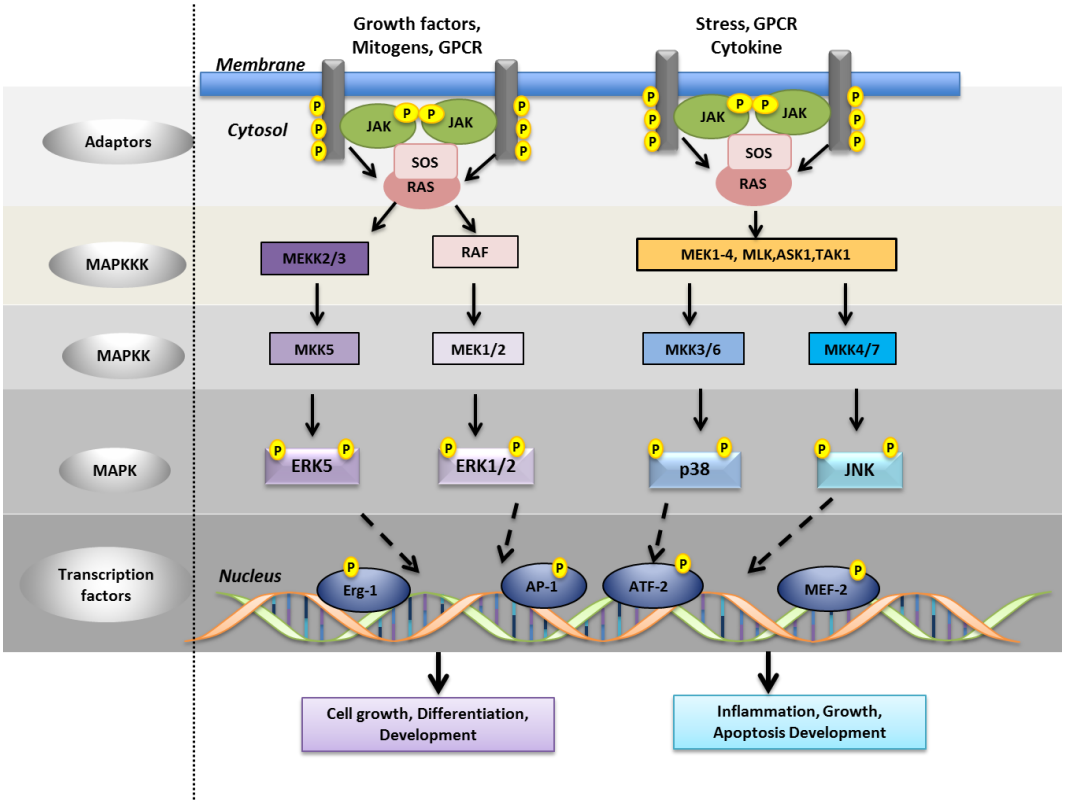

Figure 1.10: Overview of mammalian MAPK signalling cascades

MAPK signalling pathways are activated following the recognition of ligands by specific membrane receptors. Ligand receptor binding leads to the recruitment of intracellular adaptor molecules to the cytoplasmic domain of the receptors. Adaptor recruitment leads to the activation of three-tier step-wise phosphorylation cascade starting with the MAPKKs, MAPKKs and then MAPKs. Phosphorylation of MAPKs results in their activation. Activated MAPKs target and phosphorylate the downstream transcription factors leading to expression of genes involved in various biological processes.

1.6.7 Inflammatory and effector molecules produced by AEC, in response to *A. fumigatus*

Following recognition of *A. fumigatus*, AECs are capable of mounting protective immune responses. Most immune effector responses against *A. fumigatus* result from up regulation of pro-inflammatory cytokines and chemokines (Chen et al., 2015, Gomez et al., 2010, Borger et al., 1999, Zhang et al., 2008). A549 cells secrete IL-8, TNF-α and GM-CSF in response to *A. fumigatus* germ tubes (Bellanger et al., 2009)

and respond to live swollen conidia by secreting beta-defensin 2 (HBD-2) and HBD-9 (Alekseeva et al., 2009). BEAS-2B cell lines showed a time-dependent expression of IL-8 in response to swollen conidia and hyphae only, and not to resting conidia (Balloy et al., 2008). IL-8 production is highest between 8 and 15 h coinciding with *A. fumigatus* germination. This suggests that spore germination and fungal growth is necessary for generation of effector molecules. Similarly, internalization of live but not heat inactivated *A. fumigatus* conidia induced expression of IL-8, TNF-α and GM-CSF, HBD2, and HBD9 mRNA in human bronchial epithelial (HBE) cells (Sun et al., 2012). An increase in the mRNA level of these cytokines reached the maximum at 6-8 h, again correlating with *A. fumigatus* germination (Sun et al., 2012). *A. fumigatus* hyphae stimulated production of MIP2, CXCL-1 and MCP-1 in bronchial epithelial cells having cystic fibrosis transmembrane conductance regulator (CFTR) mutations (Chaudhary et al., 2012). Differentiated human bronchial epithelial cells (HBECs) expressed IFN-β upon internalization of heat or UV-inactivated resting conidia in a dose dependent manner (Beisswenger et al., 2012). Heat or paraformaldehyde (PFA) treated hyphae and conidia or culture supernatants could not induce inflammatory responses as shown by Fekkar et al (Fekkar et al., 2012). Together, these data generated by using whole fungus indicate that interaction of AEC PRRs and fungal PAMPs as well as fungal viability is necessary for induction of inflammatory responses.

Zhang et al, (2005) demonstrated that CF of *A. fumigatus* induced significant IL-6 and IL-8 production from A549 cells after 6 h. Cytokine production was not or only partly dependent on TLR-2 and TLR-4 even though they are expressed by A549 cells (Zhang et al., 2005). This response was absent when the cells were stimulated with either swollen conidia or hyphae. Also, IL-6, IL-8, MCP-1 and mucin production induced by CF in NCI-H292 bronchial and primary nasal epithelial cells was blocked by addition of serine protease inhibitors suggesting a role for proteases in mediating these responses (Tomee et al., 1997). It is clear so far that *A. fumigatus* induces inflammatory responses in AECs but the exact contribution of secreted molecules and surface antigens is yet to be resolved. Most inflammatory cytokine gene expressions results from the activation of intracellular pathways with associated transcriptional events and only IL-8 synthesis has been characterised. IL-8 is a pro-inflammatory

cytokine and a potent chemo-attractant for neutrophils (Baggiolini and Clark-Lewis, 1992). IL-8 synthesis in response to *A. fumigatus* is regulated by MAPK pathways especially p38 MAPK-, and ERK1/2- (Balloy et al., 2008, Sharon et al., 2011, Bidula et al., 2015) and NF-κB -mediated transcriptional induction (Balloy et al., 2008).
Therefore, characterising the specific pathways leading to activation of the different pro-inflammatory molecules by different *A. fumigatus* morphotypes and secreted products will help to better understand the epithelial-fungal interaction. In addition, elucidating the specific role of these cytokines in the context of pulmonary defence against aspergillosis is necessary.

1.7 Mechanistic basis of host damage during AEC- *A. fumigatus* interaction

One key pathological feature observed in invasive and non-invasive aspergillosis is a gross destruction of lung parenchyma following damage to the epithelium. The exact mechanism(s) by which the fungus damages epithelial cells to penetrate the lining of the lung are unknown. Current hypotheses suggest that fungal proteases are critical for damage induction.

Two major features of *C. albicans* induced epithelial damage are necrosis and apoptosis (Naglik et al., 2011, Moyes et al., 2016) but studies into the interactions between AEC and *A. fumigatus* are still in their infancy and little is presently known about the cause or mechanism of damage.

Activities of ECs during interaction with respiratory pathogens might be protective and/or prompt further damage. Internalization of spores by AECs might aid immune evasion by providing a hiding place, thereby serving as source of germination and further dissemination (Osherov, 2012). Alternatively, internalization of conidia might enhance killing of *A. fumigatus* and improve disease outcomes (Chaudhary et al., 2012). Exposure of cultured bronchial or alveolar cells to *A. fumigatus* CF causes massive destruction of the mammalian F-actin cytoskeleton and loss of tight junction integrity, presumably predisposing lung tissues to additional disruption and damage (Sharon et al., 2011, Bertuzzi et al., 2014). CF of *A. fumigatus* exacerbates mucociliary impairment and cilia beat velocity after 6 h in human neck epithelial cells (HNEC). This

effect was attributed to the fungal mycotoxins, gliotoxin and verruculogen (Khoufache et al., 2007). A549 cell monolayer disaggregation has been observed in the presence of *A. fumigatus*. However, whether monolayer disaggregation is a cause or consequence of EC death is a subject for study. *A. fumigatus* CF and purified AspF allergen caused detachment of A549 epithelial cells from basement membrane and detachment of A549 cells was prevented by heating the CF and adding serine protease inhibitor suggesting a role for fungal proteases in epithelial damage (Kogan et al., 2004). In addition to monolayer damage, fungal gliotoxin induced apoptosis of BEAS-2B cells following their detachment from the basement membrane. This was evidenced by clear membrane blebbing, cell shrinkage, actin-depolymerization, disruption of focal adhesions and was further confirmed by Annexin V staining (Geissler et al., 2013).

Activation of host signalling pathways in ECs is one host response that has been identified as a contributing factor to epithelial damage in response to *A. fumigatus*. Protease-induced ERK/JNK MAPK signalling in A549 cells caused *in vitro* lung cell peeling and death by necrosis, and heat inactivation of the CF neutralized its ability to peel the cells (Sharon et al., 2011). Recently, Bertuzzi et al (2014), discovered an *A. fumigatus* mutant lacking the transcription factor PacC, which could form hyphae but was unable to damage airway epithelium or invade lung tissues during murine infection. Studying the interaction of this mutant with AECs, the mutant was found to lack two distinct and morphotype-dependent modes of interaction with ECs: an early, actin-and Dectin-1-dependent internalization of spores and subsequent epithelial decay induced by secreted fungal components (Bertuzzi et al., 2014). This suggests a hypothesis that epithelial damage occurs as a result of both pathogen and host activities. Specifically, intracellular host signalling pathways activated in response to pathogens do have some additional effects on the activated host cells. A notable example is PI3K signalling in myeloid cells which can positively and negatively regulate PRR responses, particularly, TLR-mediated proinflammatory responses (Hazeki et al., 2007). Excessive production of pro-inflammatory cytokines in airways resulting from activation of intracellular signalling pathways can lead to tissue damage as seen in ABPA patients (Fukahori et al., 2014). However, little is known about the role of PI3K

signalling in epithelial PRR-mediated intracellular signalling pathways. Moyes et al (2014) described a damage protection PI3K pathway in oral epithelial cells, whereby protection against epithelial damage induced by *C. albicans* was mediated by PI3K-Akt–mToR signalling (Moyes et al., 2014). This study will consider the possibility of a similar mechanism in protecting against *A. fumigatus* induced AEC damage. Table 1.6 below summarises the current understanding regarding *A. fumigatus* and AECs and the unanswered questions. This study intends to elucidate the kinetics of host signalling pathways and effector molecules activated upon contact with *A. fumigatus* and the outcome of this activation on epithelial integrity.

Table 1.6 What is known currently about the outcome of AECs-*A. fumigatus* interaction and the existing knowledge gap

Fungal morphotypes	Epithelial cell type	Signal protein phosphorylated	Transcription factor activated	Cytokine expression (experimental approach)	Effect of interaction on host	References
Conidia	A549	?	?	?	Epithelial deaggregation	(Bertuzzi et al., 2014)
	A549	?	?	hBD2 and hBD9 (RT-qPCR)	?	(Alekseeva et al., 2009)
	HBECs	?	NF-ķB	IFN-β, IP-10, TNFα, GM-CSF, IL8, hBD2 and hBD9 (RT-qPCR)	?	(Beisswenger et al., 2012)
Hyphae	A549	?	?	IL-6 and IL-8 (ELISA)	?	(Zhang et al., 2005)
	A549	?	?	TNF-alpha, IL-8, IL-6 and GM-CSF (RT-PCR)	?	(Bellanger et al., 2009) (Borger et al., 1999)
	HBECs	?	?	TNF-α, IL-6, IP-10, MCP- 1, MIP- 2 (Luminex multiplex technology)	?	(Chaudhary et al., 2012)
	BEAS-2B	Phosphatidylinositol 3-kinase, p38 MAPK, and ERK1/2	NF-ķB	IL-8 (RT-qPCR)	?	(Balloy et al., 2008)
	A549	JNK and ERK1/2	?	?	Cell peeling, actin- skeleton damage, necrosis	(Sharon et al., 2011)

Culture filtrate	A549	?	?	?	Disruption of the actin fiber cytoskeleton and loss of focal adhesion sites (Kogan et al., 2004)

Footnote: HBECs: Human bronchial epithelial cells, IFN: interferon gamma, TNF: Tumour necrosis factor, IL: interleukin, IP: IFN-gamma-inducible protein, HBD: human beta defensin, MCP: monocyte chemotactic protein, MIP: Macrophage inflammatory protein, GM-CSF: Granulocyte-macrophage colony stimulating factor, BEAS-2B: Transformed human bronchial epithelial cell, A549: carcinomic human alveolar basal epithelial cell.

1.8 Objectives of study

In vitro and *in vivo* studies have revealed that during interaction with lung epithelial cells, *A. fumigatus* spores germinate and form hyphae, which may penetrate and damage the surrounding tissue (Osherov, 2012). Apart from physical invasion, pathogenicity of *A. fumigatus* has also been attributed to several key secreted small molecules produced by the fungus, such as proteases and immunotoxins (Watanabe et al., 2003). In this study, the differential contribution and timing of fungal contact and secreted products to epithelial damage was elucidated (Chapter 3) as this will aid in the identification of a druggable single gene product essential for epithelial disruption.

Upon breaking dormancy *A. fumigatus* undergoes an obligatory morphological switch which, due to altered presentation of pathogen associated molecular patterns (PAMPs), constitutes a pivotal aspect of the host-pathogen interaction. Morphotype-specific activation of immune responses at the oral mucosa has been demonstrated for *Candida albicans* (Moyes et al., 2010, Achterman et al., 2015) but the relevance of morphotype switching upon respiratory epithelial responses to *A. fumigatus* has yet to be clarified. This study establishes a model of interaction between respiratory epithelial cells and different growth morphotypes of *A. fumigatus*, which enabled the study of global and dynamic immune responses of the airway epithelia to these morphotypes (Chapter 4).

Many studies have implicated activation of intracellular signalling pathway in resident tissue such as epithelial cells in cell death and loss in viability during interaction with fungal pathogens (Moyes et al., 2014, Sharon et al., 2011). In other to understand the contribution of immune activation in weakening of the epithelium, we characterised the role of the signalling pathways and endocytosis identified in Chapter 4 in epithelial cell decay events described in Chapter 3 using chemical or genetic inhibitors of the pathways (Chapter 5 and Chapter 7).

Finally, for the ultimate purpose of finding a specific gene products or groups of molecule responsible for directly damaging the host or inducing damaging responses

in epithelial cells, we studied the interaction between *A. fumigatus* mutant strains lacking the transcription factors PacC, PrtT, GliP as well as mutants lacking secreted products under the control of these transcription factors and epithelial cells to find which fungal effector proteins are responsible for epithelial damage and via which mechanisms (Chapter 6).

1.9 Bibliography

ABAD, A., FERNANDEZ-MOLINA, J. V., BIKANDI, J., RAMIREZ, A., MARGARETO, J., SENDINO, J., HERNANDO, F. L., PONTON, J., GARAIZAR, J. & REMENTERIA, A. 2010. What makes *Aspergillus fumigatus* a successful pathogen? Genes and molecules involved in invasive aspergillosis. *Rev Iberoam Micol,* 27**,** 155-82.

ACHTERMAN, R. R., MOYES, D. L., THAVARAJ, S., SMITH, A. R., BLAIR, K. M., WHITE, T. C. & NAGLIK, J. R. 2015. Dermatophytes activate skin keratinocytes via mitogen-activated protein kinase signaling and induce immune responses. *Infect Immun,* 83**,** 1705-14.

AFANOU, K. A., STRAUMFORS, A., SKOGSTAD, A., NILSEN, T., SYNNES, O., SKAAR, I., HJELJORD, L., TRONSMO, A., GREEN, B. J. & EDUARD, W. 2014. Submicronic fungal bioaerosols: high-resolution microscopic characterization and quantification. *Appl Environ Microbiol,* 80**,** 7122-30.

AFANOU, K. A., STRAUMFORS, A., SKOGSTAD, A., SKAAR, I., HJELJORD, L., SKARE, O., GREEN, B. J., TRONSMO, A. & EDUARD, W. 2015. Profile and Morphology of Fungal Aerosols Characterized by Field Emission Scanning Electron Microscopy (FESEM). *Aerosol Sci Technol,* 49**,** 423-435.

AGASSANDIAN, M. & MALLAMPALLI, R. K. 2013. Surfactant phospholipid metabolism. *Biochim Biophys Acta,* 1831**,** 612-25.

AIMANIANDA, V., BAYRY, J., BOZZA, S., KNIEMEYER, O., PERRUCCIO, K., ELLURU, S. R., CLAVAUD, C., PARIS, S., BRAKHAGE, A. A., KAVERI, S. V., ROMANI, L. & LATGE, J. P. 2009. Surface hydrophobin prevents immune recognition of airborne fungal spores. *Nature,* 460**,** 1117-21.

AKIRA, S., UEMATSU, S. & TAKEUCHI, O. 2006. Pathogen recognition and innate immunity. *Cell,* 124**,** 783-801.

AL ABDALLAH, Q., CHOE, S. I., CAMPOLI, P., BAPTISTA, S., GRAVELAT, F. N., LEE, M. J. & SHEPPARD, D. C. 2012. A conserved C-terminal domain of the *Aspergillus fumigatus* developmental regulator MedA is required for nuclear localization, adhesion and virulence. *PLoS One,* 7**,** e49959.

ALEKSEEVA, L., HUET, D., FEMENIA, F., MOUYNA, I., ABDELOUAHAB, M., CAGNA, A., GUERRIER, D., TICHANNE-SELTZER, V., BAEZA-SQUIBAN, A., CHERMETTE, R., LATGE, J. P. & BERKOVA, N. 2009. Inducible expression of beta defensins by human respiratory epithelial cells exposed to *Aspergillus fumigatus* organisms. *BMC Microbiol,* 9**,** 33.

ALP, S. & ARIKAN, S. 2008. Investigation of extracellular elastase, acid proteinase and phospholipase activities as putative virulence factors in clinical isolates of *Aspergillus* species. *J Basic Microbiol,* 48**,** 331-7.

ALVAREZ-PEREZ, S., BLANCO, J. L., ALBA, P. & GARCIA, M. E. 2010. Mating type and invasiveness are significantly associated in *Aspergillus fumigatus*. *Med Mycol,* 48**,** 273-7.

AMICH, J., SCHAFFERER, L., HAAS, H. & KRAPPMANN, S. 2013. Regulation of sulphur assimilation is essential for virulence and affects iron homeostasis of the human-pathogenic mould *Aspergillus fumigatus*. *PLoS Pathog,* 9**,** e1003573.

AMICH, J., VICENTEFRANQUEIRA, R., LEAL, F. & CALERA, J. A. 2010. *Aspergillus fumigatus* survival in alkaline and extreme zinc-limiting environments relies on

the induction of a zinc homeostasis system encoded by the zrfC and aspf2 genes. *Eukaryot Cell,* 9**,** 424-37.

AMICH, J., VICENTEFRANQUEIRA, R., MELLADO, E., RUIZ-CARMUEGA, A., LEAL, F. & CALERA, J. A. 2014. The ZrfC alkaline zinc transporter is required for *Aspergillus fumigatus* virulence and its growth in the presence of the Zn/Mn-chelating protein calprotectin. *Cell Microbiol,* 16**,** 548-64.

AMIN, S., THYWISSEN, A., HEINEKAMP, T., SALUZ, H. P. & BRAKHAGE, A. A. 2014. Melanin dependent survival of *Apergillus fumigatus* conidia in lung epithelial cells. *Int J Med Microbiol,* 304**,** 626-36.

AMITANI, R. & KAWANAMI, R. 2009. Interaction of *Aspergillus* with human respiratory mucosa: a study with organ culture model. *Med Mycol,* 47 Suppl 1**,** S127-31.

AMITANI, R., TAYLOR, G., ELEZIS, E. N., LLEWELLYN-JONES, C., MITCHELL, J., KUZE, F., COLE, P. J. & WILSON, R. 1995. Purification and characterization of factors produced by *Aspergillus fumigatus* which affect human ciliated respiratory epithelium. *Infect Immun,* 63**,** 3266-71.

ANAISSIE, E. J. & COSTA, S. F. 2001. Nosocomial aspergillosis is waterborne. *Clin Infect Dis,* 33**,** 1546-8.

ARVANITIS, M. & MYLONAKIS, E. 2015. Diagnosis of invasive aspergillosis: recent developments and ongoing challenges. *Eur J Clin Invest,* 45**,** 646-52.

BADDLEY, J. W., STEPHENS, J. M., JI, X., GAO, X., SCHLAMM, H. T. & TARALLO, M. 2013. *Aspergillosis* in Intensive Care Unit (ICU) patients: epidemiology and economic outcomes. *BMC Infect Dis,* 13**,** 29.

BAGGIOLINI, M. & CLARK-LEWIS, I. 1992. Interleukin-8, a chemotactic and inflammatory cytokine. *FEBS Lett,* 307**,** 97-101.

BALAJEE, S. A., KANO, R., BADDLEY, J. W., MOSER, S. A., MARR, K. A., ALEXANDER, B. D., ANDES, D., KONTOYIANNIS, D. P., PERRONE, G., PETERSON, S., BRANDT, M. E., PAPPAS, P. G. & CHILLER, T. 2009. Molecular identification of *Aspergillus* species collected for the Transplant-Associated Infection Surveillance Network. *J Clin Microbiol,* 47**,** 3138-41.

BALLOY, V., SALLENAVE, J. M., WU, Y., TOUQUI, L., LATGE, J. P., SI-TAHAR, M. & CHIGNARD, M. 2008. *Aspergillus fumigatus*-induced interleukin-8 synthesis by respiratory epithelial cells is controlled by the phosphatidylinositol 3-kinase, p38 MAPK, and ERK1/2 pathways and not by the toll-like receptor-MyD88 pathway. *J Biol Chem,* 283**,** 30513-21.

BARAC, A., VUKICEVIC, T. A., ILIC, A. D., RUBINO, S., ZUGIC, V. & STEVANOVIC, G. 2017. Complications of chronic necrotizing pulmonary aspergillosis: review of published case reports. *Rev Inst Med Trop Sao Paulo,* 59**,** e19.

BEAUVAIS, A., SCHMIDT, C., GUADAGNINI, S., ROUX, P., PERRET, E., HENRY, C., PARIS, S., MALLET, A., PREVOST, M. C. & LATGE, J. P. 2007. An extracellular matrix glues together the aerial-grown hyphae of *Aspergillus fumigatus*. *Cell Microbiol,* 9**,** 1588-600.

BEISSWENGER, C., HESS, C. & BALS, R. 2012. *Aspergillus fumigatus* conidia induce interferon-beta signalling in respiratory epithelial cells. *Eur Respir J,* 39**,** 411-8.

BELLANGER, A. P., MILLON, L., KHOUFACHE, K., RIVOLLET, D., BIECHE, I., LAURENDEAU, I., VIDAUD, M., BOTTEREL, F. & BRETAGNE, S. 2009. *Aspergillus fumigatus* germ tube growth and not conidia ingestion induces expression of

inflammatory mediator genes in the human lung epithelial cell line A549. *J Med Microbiol,* 58**,** 174-9.

BERGERON, A., PORCHER, R., SULAHIAN, A., DE BAZELAIRE, C., CHAGNON, K., RAFFOUX, E., VEKHOFF, A., CORNET, M., ISNARD, F., BRETHON, B., LACROIX, C., POIROT, J. L., BOUGES, C., DEROUIN, F., TAZI, A. & RIBAUD, P. 2012. The strategy for the diagnosis of invasive pulmonary aspergillosis should depend on both the underlying condition and the leukocyte count of patients with hematologic malignancies. *Blood,* 119**,** 1831-7; quiz 1956.

BERGERON, V., REBOUX, G., POIROT, J. L. & LAUDINET, N. 2007. Decreasing airborne contamination levels in high-risk hospital areas using a novel mobile air-treatment unit. *Infect Control Hosp Epidemiol,* 28**,** 1181-6.

BERGMANN, A., HARTMANN, T., CAIRNS, T., BIGNELL, E. M. & KRAPPMANN, S. 2009. A regulator of *Aspergillus fumigatus* extracellular proteolytic activity is dispensable for virulence. *Infect Immun,* 77**,** 4041-50.

BERNARD, M. & LATGE, J. P. 2001. *Aspergillus fumigatus* cell wall: composition and biosynthesis. *Med Mycol,* 39 Suppl 1**,** 9-17.

BERTUZZI, M., SCHRETTL, M., ALCAZAR-FUOLI, L., CAIRNS, T. C., MUNOZ, A., WALKER, L. A., HERBST, S., SAFARI, M., CHEVERTON, A. M., CHEN, D., LIU, H., SAIJO, S., FEDOROVA, N. D., ARMSTRONG-JAMES, D., MUNRO, C. A., READ, N. D., FILLER, S. G., ESPESO, E. A., NIERMAN, W. C., HAAS, H. & BIGNELL, E. M. 2014. The pH-Responsive PacC Transcription Factor of *Aspergillus fumigatus* Governs Epithelial Entry and Tissue Invasion during Pulmonary Aspergillosis. *PLoS Pathog,* 10**,** e1004413.

BERUBE, K., PRYTHERCH, Z., JOB, C. & HUGHES, T. 2010. Human primary bronchial lung cell constructs: the new respiratory models. *Toxicology,* 278**,** 311-8.

BETTS, J. C. & NABEL, G. J. 1996. Differential regulation of NF-kappaB2(p100) processing and control by amino-terminal sequences. *Mol Cell Biol,* 16**,** 6363-71.

BIANCHI, M. E. 2007. DAMPs, PAMPs and alarmins: all we need to know about danger. *J Leukoc Biol,* 81**,** 1-5.

BIDULA, S., SEXTON, D. W., YATES, M., ABDOLRASOULI, A., SHAH, A., WALLIS, R., REED, A., ARMSTRONG-JAMES, D. & SCHELENZ, S. 2015. H-ficolin binds *Aspergillus fumigatus* leading to activation of the lectin complement pathway and modulation of lung epithelial immune responses. *Immunology*.

BIGNELL, E., CAIRNS, T. C., THROCKMORTON, K., NIERMAN, W. C. & KELLER, N. P. 2016. Secondary metabolite arsenal of an opportunistic pathogenic fungus. *Philos Trans R Soc Lond B Biol Sci,* 371.

BLATZER, M., BARKER, B. M., WILLGER, S. D., BECKMANN, N., BLOSSER, S. J., CORNISH, E. J., MAZURIE, A., GRAHL, N., HAAS, H. & CRAMER, R. A. 2011. SREBP coordinates iron and ergosterol homeostasis to mediate triazole drug and hypoxia responses in the human fungal pathogen *Aspergillus fumigatus*. *PLoS Genet,* 7**,** e1002374.

BOASE, S., VALENTINE, R., SINGHAL, D., TAN, L. W. & WORMALD, P. J. 2011. A sheep model to investigate the role of fungal biofilms in sinusitis: fungal and bacterial synergy. *Int Forum Allergy Rhinol,* 1**,** 340-7.

BOK, J. W., BALAJEE, S. A., MARR, K. A., ANDES, D., NIELSEN, K. F., FRISVAD, J. C. & KELLER, N. P. 2005. LaeA, a regulator of morphogenetic fungal virulence factors. *Eukaryot Cell,* 4**,** 1574-82.

BOK, J. W., CHUNG, D., BALAJEE, S. A., MARR, K. A., ANDES, D., NIELSEN, K. F., FRISVAD, J. C., KIRBY, K. A. & KELLER, N. P. 2006. GliZ, a transcriptional regulator of gliotoxin biosynthesis, contributes to *Aspergillus fumigatus* virulence. *Infect Immun,* 74**,** 6761-8.

BOM, V. L., DE CASTRO, P. A., WINKELSTROTER, L. K., MARINE, M., HORI, J. I., RAMALHO, L. N., DOS REIS, T. F., GOLDMAN, M. H., BROWN, N. A., RAJENDRAN, R., RAMAGE, G., WALKER, L. A., MUNRO, C. A., ROCHA, M. C., MALAVAZI, I., HAGIWARA, D. & GOLDMAN, G. H. 2015. The *Aspergillus fumigatus* sitA Phosphatase Homologue Is Important for Adhesion, Cell Wall Integrity, Biofilm Formation, and Virulence. *Eukaryot Cell,* 14**,** 728-44.

BORGER, P., KOETER, G. H., TIMMERMAN, J. A., VELLENGA, E., TOMEE, J. F. & KAUFFMAN, H. F. 1999. Proteases from *Aspergillus fumigatus* induce interleukin (IL)-6 and IL-8 production in airway epithelial cell lines by transcriptional mechanisms. *J Infect Dis,* 180**,** 1267-74.

BORGHI, E., BORGO, F. & MORACE, G. 2016. Fungal Biofilms: Update on Resistance. *Adv Exp Med Biol,* 931**,** 37-47.

BOTTEREL, F., GROSS, K., IBRAHIM-GRANET, O., KHOUFACHE, K., ESCABASSE, V., COSTE, A., CORDONNIER, C., ESCUDIER, E. & BRETAGNE, S. 2008. Phagocytosis of *Aspergillus fumigatus* conidia by primary nasal epithelial cells *in vitro*. *BMC Microbiol,* 8**,** 97.

BOUCHARA, J. P., SANCHEZ, M., CHEVAILLER, A., MAROT-LEBLOND, A., LISSITZKY, J. C., TRONCHIN, G. & CHABASSE, D. 1997. Sialic acid-dependent recognition of laminin and fibrinogen by *Aspergillus fumigatus* conidia. *Infect Immun,* 65**,** 2717-24.

BRANDON, M., HOWARD, B., LAWRENCE, C. & LAUBENBACHER, R. 2015. Iron acquisition and oxidative stress response in *Aspergillus fumigatus*. *BMC Syst Biol,* 9**,** 19.

BRANDTZAEG, P. 1995. Immunocompetent cells of the upper airway: functions in normal and diseased mucosa. *Eur Arch Otorhinolaryngol,* 252 Suppl 1**,** S8-21.

BRENIER-PINCHART, M. P., LEBEAU, B., BOREL, J. L., QUESADA, J. L., MALLARET, M. R., GARBAN, F., BRION, J. P., MOLINA, L., BOSSON, J. L., THIEBAUT-BERTRAND, A., GRILLOT, R. & PELLOUX, H. 2011. Community-acquired invasive aspergillosis and outdoor filamentous fungal spore load: a relationship? *Clin Microbiol Infect,* 17**,** 1387-90.

BRIARD, B., MUSZKIETA, L., LATGE, J. P. & FONTAINE, T. 2016. Galactosaminogalactan of *Aspergillus fumigatus*, a bioactive fungal polymer. *Mycologia,* 108**,** 572-80.

BROWN, G. D. 2006. Dectin-1: a signalling non-TLR pattern-recognition receptor. *Nat Rev Immunol,* 6**,** 33-43.

BROWN, G. D., DENNING, D. W., GOW, N. A., LEVITZ, S. M., NETEA, M. G. & WHITE, T. C. 2012. Hidden killers: human fungal infections. *Sci Transl Med,* 4**,** 165rv13.

BROZ, P. & MONACK, D. M. 2013. Newly described pattern recognition receptors team up against intracellular pathogens. *Nat Rev Immunol,* 13**,** 551-65.

BRYANT, C. E., GAY, N. J., HEYMANS, S., SACRE, S., SCHAEFER, L. & MIDWOOD, K. S. 2015. Advances in Toll-like receptor biology: Modes of activation by diverse stimuli. *Crit Rev Biochem Mol Biol,* 50**,** 359-79.

BULTMAN, K. M., KOWALSKI, C. H. & CRAMER, R. A. 2017. *Aspergillus fumigatus* virulence through the lens of transcription factors. *Med Mycol,* 55**,** 24-38.

BUNGER, J., WESTPHAL, G., MONNICH, A., HINNENDAHL, B., HALLIER, E. & MULLER, M. 2004. Cytotoxicity of occupationally and environmentally relevant mycotoxins. *Toxicology,* 202**,** 199-211.

CAMPOY, S. & ADRIO, J. L. 2016. Antifungals. *Biochem Pharmacol*.

CAMPOY, S. & ADRIO, J. L. 2017. Antifungals. *Biochem Pharmacol,* 133**,** 86-96.

CANELA, H. M., TAKAMI, L. A. & DA SILVA FERREIRA, M. E. 2017. cipC is important for *Aspergillus fumigatus* virulence. *APMIS,* 125**,** 141-147.

CASADEVALL, A., FANG, F. C. & PIROFSKI, L. A. 2011. Microbial virulence as an emergent property: consequences and opportunities. *PLoS Pathog,* 7**,** e1002136.

CASADEVALL, A. & PIROFSKI, L. A. 2014. Microbiology: Ditch the term pathogen. *Nature,* 516**,** 165-6.

CHABI, M. L., GORACCI, A., ROCHE, N., PAUGAM, A., LUPO, A. & REVEL, M. P. 2015. Pulmonary aspergillosis. *Diagn Interv Imaging,* 96**,** 435-42.

CHAMBERS, E. S. & HAWRYLOWICZ, C. M. 2011. The impact of vitamin D on regulatory T cells. *Curr Allergy Asthma Rep,* 11**,** 29-36.

CHAUDHARY, N., DATTA, K., ASKIN, F. B., STAAB, J. F. & MARR, K. A. 2012. Cystic fibrosis transmembrane conductance regulator regulates epithelial cell response to *Aspergillus* and resultant pulmonary inflammation. *Am J Respir Crit Care Med,* 185**,** 301-10.

CHEN, F., ZHANG, C., JIA, X., WANG, S., WANG, J., CHEN, Y., ZHAO, J., TIAN, S., HAN, X. & HAN, L. 2015. Transcriptome Profiles of Human Lung Epithelial Cells A549 Interacting with *Aspergillus fumigatus* by RNA-Seq. *PLoS One,* 10**,** e0135720.

CHEN, N. X., GEIST, D. J., GENETOS, D. C., PAVALKO, F. M. & DUNCAN, R. L. 2003. Fluid shear-induced NFkappaB translocation in osteoblasts is mediated by intracellular calcium release. *Bone,* 33**,** 399-410.

CHRONEOS, Z. C., MIDDE, K., SEVER-CHRONEOS, Z. & JAGANNATH, C. 2009. Pulmonary surfactant and tuberculosis. *Tuberculosis (Edinb),* 89 Suppl 1**,** S10-4.

CHRONEOS, Z. C., SEVER-CHRONEOS, Z. & SHEPHERD, V. L. 2010. Pulmonary surfactant: an immunological perspective. *Cell Physiol Biochem,* 25**,** 13-26.

CHUNG, D., BARKER, B. M., CAREY, C. C., MERRIMAN, B., WERNER, E. R., LECHNER, B. E., DHINGRA, S., CHENG, C., XU, W., BLOSSER, S. J., MOROHASHI, K., MAZURIE, A., MITCHELL, T. K., HAAS, H., MITCHELL, A. P. & CRAMER, R. A. 2014. ChIP-seq and in vivo transcriptome analyses of the *Aspergillus fumigatus* SREBP SrbA reveals a new regulator of the fungal hypoxia response and virulence. *PLoS Pathog,* 10**,** e1004487.

COBRADO, L., SILVA-DIAS, A., AZEVEDO, M. M., PINA-VAZ, C. & RODRIGUES, A. G. 2013. *In vivo* antibiofilm effect of cerium, chitosan and hamamelitannin against usual agents of catheter-related bloodstream infections. *J Antimicrob Chemother,* 68**,** 126-30.

COMERA, C., ANDRE, K., LAFFITTE, J., COLLET, X., GALTIER, P. & MARIDONNEAU-PARINI, I. 2007. Gliotoxin from *Aspergillus fumigatus* affects phagocytosis and the organization of the actin cytoskeleton by distinct signalling pathways in human neutrophils. *Microbes Infect,* 9**,** 47-54.

CORDING, J., BERG, J., KADING, N., BELLMANN, C., TSCHEIK, C., WESTPHAL, J. K., MILATZ, S., GUNZEL, D., WOLBURG, H., PIONTEK, J., HUBER, O. & BLASIG, I. E. 2013. In tight junctions, claudins regulate the interactions between occludin, tricellulin and marvelD3, which, inversely, modulate claudin oligomerization. *J Cell Sci,* 126**,** 554-64.

CORNELL, M. J., ALAM, I., SOANES, D. M., WONG, H. M., HEDELER, C., PATON, N. W., RATTRAY, M., HUBBARD, S. J., TALBOT, N. J. & OLIVER, S. G. 2007. Comparative genome analysis across a kingdom of eukaryotic organisms: specialization and diversification in the fungi. *Genome Res,* 17**,** 1809-22.

COYLE, C. M., KENALEY, S. C., RITTENOUR, W. R. & PANACCIONE, D. G. 2007. Association of ergot alkaloids with conidiation in *Aspergillus fumigatus*. *Mycologia,* 99**,** 804-11.

CRAMER, R. A., JR., PERFECT, B. Z., PINCHAI, N., PARK, S., PERLIN, D. S., ASFAW, Y. G., HEITMAN, J., PERFECT, J. R. & STEINBACH, W. J. 2008. Calcineurin target CrzA regulates conidial germination, hyphal growth, and pathogenesis of *Aspergillus fumigatus*. *Eukaryot Cell,* 7**,** 1085-97.

CRAY, J. A., BELL, A. N., BHAGANNA, P., MSWAKA, A. Y., TIMSON, D. J. & HALLSWORTH, J. E. 2013. The biology of habitat dominance; can microbes behave as weeds? *Microb Biotechnol,* 6**,** 453-92.

CROFT, C. A., CULIBRK, L., MOORE, M. M. & TEBBUTT, S. J. 2016. Interactions of *Aspergillus fumigatus* Conidia with Airway Epithelial Cells: A Critical Review. *Front Microbiol,* 7**,** 472.

DAGENAIS, T. R. & KELLER, N. P. 2009. Pathogenesis of *Aspergillus fumigatus* in Invasive Aspergillosis. *Clin Microbiol Rev,* 22**,** 447-65.

DAGUE, E., ALSTEENS, D., LATGE, J. P. & DUFRENE, Y. F. 2008. High-resolution cell surface dynamics of germinating *Aspergillus fumigatus* conidia. *Biophys J,* 94**,** 656-60.

DE CASTRO, P. A., CHEN, C., DE ALMEIDA, R. S., FREITAS, F. Z., BERTOLINI, M. C., MORAIS, E. R., BROWN, N. A., RAMALHO, L. N., HAGIWARA, D., MITCHELL, T. K. & GOLDMAN, G. H. 2014. ChIP-seq reveals a role for CrzA in the *Aspergillus fumigatus* high-osmolarity glycerol response (HOG) signalling pathway. *Mol Microbiol,* 94**,** 655-74.

DE GROOT, P. W., BADER, O., DE BOER, A. D., WEIG, M. & CHAUHAN, N. 2013. Adhesins in human fungal pathogens: glue with plenty of stick. *Eukaryot Cell,* 12**,** 470-81.

DE VRIES, R. P., RILEY, R., WIEBENGA, A., AGUILAR-OSORIO, G., AMILLIS, S., UCHIMA, C. A., ANDERLUH, G., ASADOLLAHI, M., ASKIN, M., BARRY, K., BATTAGLIA, E., BAYRAM, O., BENOCCI, T., BRAUS-STROMEYER, S. A., CALDANA, C., CANOVAS, D., CERQUEIRA, G. C., CHEN, F., CHEN, W., CHOI, C., CLUM, A., DOS SANTOS, R. A., DAMASIO, A. R., DIALLINAS, G., EMRI, T., FEKETE, E., FLIPPHI, M., FREYBERG, S., GALLO, A., GOURNAS, C., HABGOOD, R., HAINAUT, M., HARISPE, M. L., HENRISSAT, B., HILDEN, K. S., HOPE, R., HOSSAIN, A., KARABIKA, E., KARAFFA, L., KARANYI, Z., KRASEVEC, N., KUO, A., KUSCH, H., LABUTTI, K.,

LAGENDIJK, E. L., LAPIDUS, A., LEVASSEUR, A., LINDQUIST, E., LIPZEN, A., LOGRIECO, A. F., MACCABE, A., MAKELA, M. R., MALAVAZI, I., MELIN, P., MEYER, V., MIELNICHUK, N., MISKEI, M., MOLNAR, A. P., MULE, G., NGAN, C. Y., OREJAS, M., OROSZ, E., OUEDRAOGO, J. P., OVERKAMP, K. M., PARK, H. S., PERRONE, G., PIUMI, F., PUNT, P. J., RAM, A. F., RAMON, A., RAUSCHER, S., RECORD, E., RIANO-PACHON, D. M., ROBERT, V., ROHRIG, J., RULLER, R., SALAMOV, A., SALIH, N. S., SAMSON, R. A., SANDOR, E., SANGUINETTI, M., SCHUTZE, T., SEPCIC, K., SHELEST, E., SHERLOCK, G., SOPHIANOPOULOU, V., SQUINA, F. M., SUN, H., SUSCA, A., TODD, R. B., TSANG, A., UNKLES, S. E., VAN DE WIELE, N., VAN ROSSEN-UFFINK, D., OLIVEIRA, J. V., VESTH, T. C., VISSER, J., YU, J. H., ZHOU, M., ANDERSEN, M. R., et al. 2017. Comparative genomics reveals high biological diversity and specific adaptations in the industrially and medically important fungal genus *Aspergillus*. *Genome Biol,* 18**,** 28.

DEHART, D. J., AGWU, D. E., JULIAN, N. C. & WASHBURN, R. G. 1997. Binding and germination of *Aspergillus fumigatus* conidia on cultured A549 pneumocytes. *J Infect Dis,* 175**,** 146-50.

DENNING, D. W. 1998. Invasive aspergillosis. *Clin Infect Dis,* 26**,** 781-803; quiz 804-5.

DENNING, D. W., PLEUVRY, A. & COLE, D. C. 2011. Global burden of chronic pulmonary aspergillosis as a sequel to pulmonary tuberculosis. *Bull World Health Organ,* 89**,** 864-72.

DENNING, D. W., PLEUVRY, A. & COLE, D. C. 2013. Global burden of allergic bronchopulmonary aspergillosis with asthma and its complication chronic pulmonary aspergillosis in adults. *Med Mycol,* 51**,** 361-70.

DENNING, D. W., RINIOTIS, K., DOBRASHIAN, R. & SAMBATAKOU, H. 2003. Chronic cavitary and fibrosing pulmonary and pleural aspergillosis: case series, proposed nomenclature change, and review. *Clin Infect Dis,* 37 Suppl 3**,** S265-80.

DESOUBEAUX, G., BAILLY, E. & CHANDENIER, J. 2014. Diagnosis of invasive pulmonary aspergillosis: updates and recommendations. *Med Mal Infect,* 44**,** 89-101.

DHINGRA, S., KOWLASKI, C. H., THAMMAHONG, A., BEATTIE, S. R., BULTMAN, K. M. & CRAMER, R. A. 2016. RbdB, a Rhomboid Protease Critical for SREBP Activation and Virulence in *Aspergillus fumigatus*. *mSphere,* 1.

DI-GIOVANNI, F. 1995. The variability in settling velocities of some pollen and spores.pdf. *Grana,* 34**,** 39-44.

DINAMARCO, T. M., ALMEIDA, R. S., DE CASTRO, P. A., BROWN, N. A., DOS REIS, T. F., RAMALHO, L. N., SAVOLDI, M., GOLDMAN, M. H. & GOLDMAN, G. H. 2012. Molecular characterization of the putative transcription factor SebA involved in virulence in *Aspergillus fumigatus*. *Eukaryot Cell,* 11**,** 518-31.

DYER, P. S. & O'GORMAN, C. M. 2012. Sexual development and cryptic sexuality in fungi: insights from *Aspergillus* species. *FEMS Microbiol Rev,* 36**,** 165-92.

EGGIMANN, P., CHEVROLET, J. C., STAROBINSKI, M., MAJNO, P., TOTSCH, M., CHAPUIS, B. & PITTET, D. 2006. Primary invasive aspergillosis of the digestive tract: report of two cases and review of the literature. *Infection,* 34**,** 333-8.

EICHNER, R. D., AL SALAMI, M., WOOD, P. R. & MULLBACHER, A. 1986. The effect of gliotoxin upon macrophage function. *Int J Immunopharmacol,* 8**,** 789-97.

EJZYKOWICZ, D. E., CUNHA, M. M., ROZENTAL, S., SOLIS, N. V., GRAVELAT, F. N., SHEPPARD, D. C. & FILLER, S. G. 2009. The *Aspergillus fumigatus* transcription

factor Ace2 governs pigment production, conidiation and virulence. *Mol Microbiol,* 72**,** 155-69.

EJZYKOWICZ, D. E., SOLIS, N. V., GRAVELAT, F. N., CHABOT, J., LI, X., SHEPPARD, D. C. & FILLER, S. G. 2010. Role of *Aspergillus fumigatus* DvrA in host cell interactions and virulence. *Eukaryot Cell,* 9**,** 1432-40.

ESPINOSA, V. & RIVERA, A. 2016. First Line of Defense: Innate Cell-Mediated Control of Pulmonary Aspergillosis. *Front Microbiol,* 7**,** 272.

EVANS, M. J., CABRAL, L. J., STEPHENS, R. J. & FREEMAN, G. 1975. Transformation of alveolar type 2 cells to type 1 cells following exposure to NO2. *Exp Mol Pathol,* 22**,** 142-50.

FAN, C. M. & MANIATIS, T. 1991. Generation of p50 subunit of NF-kappa B by processing of p105 through an ATP-dependent pathway. *Nature,* 354**,** 395-8.

FEKKAR, A., BALLOY, V., PIONNEAU, C., MARINACH-PATRICE, C., CHIGNARD, M. & MAZIER, D. 2012. Secretome of human bronchial epithelial cells in response to the fungal pathogen *Aspergillus fumigatus* analyzed by differential in-gel electrophoresis. *J Infect Dis,* 205**,** 1163-72.

FOSTER, K. A., AVERY, M. L., YAZDANIAN, M. & AUDUS, K. L. 2000. Characterization of the Calu-3 cell line as a tool to screen pulmonary drug delivery. *Int J Pharm,* 208**,** 1-11.

FRISVAD, J. C. & LARSEN, T. O. 2015. Extrolites of Aspergillus fumigatus and Other Pathogenic Species in *Aspergillus* Section *Fumigati*. *Front Microbiol,* 6**,** 1485.

FUKAHORI, S., MATSUSE, H., TSUCHIDA, T., KAWANO, T., NISHINO, T., FUKUSHIMA, C. & KOHNO, S. 2014. Clearance of *Aspergillus fumigatus* is impaired in the airway in allergic inflammation. *Ann Allergy Asthma Immunol,* 113**,** 180-6.

FUKUDA, T., BOECKH, M., CARTER, R. A., SANDMAIER, B. M., MARIS, M. B., MALONEY, D. G., MARTIN, P. J., STORB, R. F. & MARR, K. A. 2003. Risks and outcomes of invasive fungal infections in recipients of allogeneic hematopoietic stem cell transplants after nonmyeloablative conditioning. *Blood,* 102**,** 827-33.

GAUTAM, P., SUNDARAM, C. S., MADAN, T., GADE, W. N., SHAH, A., SIRDESHMUKH, R. & SARMA, P. U. 2007. Identification of novel allergens of *Aspergillus fumigatus* using immunoproteomics approach. *Clin Exp Allergy,* 37**,** 1239-49.

GAUTHIER, T., WANG, X., SIFUENTES DOS SANTOS, J., FYSIKOPOULOS, A., TADRIST, S., CANLET, C., ARTIGOT, M. P., LOISEAU, N., OSWALD, I. P. & PUEL, O. 2012. Trypacidin, a spore-borne toxin from *Aspergillus fumigatus*, is cytotoxic to lung cells. *PLoS One,* 7**,** e29906.

GEFTER, W. B., WEINGRAD, T. R., EPSTEIN, D. M., OCHS, R. H. & MILLER, W. T. 1981. "Semi-invasive" pulmonary aspergillosis: a new look at the spectrum of *aspergillus* infections of the lung. *Radiology,* 140**,** 313-21.

GEISSLER, A., HAUN, F., FRANK, D. O., WIELAND, K., SIMON, M. M., IDZKO, M., DAVIS, R. J., MAURER, U. & BORNER, C. 2013. Apoptosis induced by the fungal pathogen gliotoxin requires a triple phosphorylation of Bim by JNK. *Cell Death Differ,* 20**,** 1317-29.

GODET, C., PHILIPPE, B., LAURENT, F. & CADRANEL, J. 2014. Chronic pulmonary aspergillosis: an update on diagnosis and treatment. *Respiration,* 88**,** 162-74.

GOMEZ, P., HACKETT, T. L., MOORE, M. M., KNIGHT, D. A. & TEBBUTT, S. J. 2010. Functional genomics of human bronchial epithelial cells directly interacting with conidia of *Aspergillus fumigatus*. *BMC Genomics,* 11**,** 358.

GOTS, R. E., LAYTON, N. J. & PIRAGES, S. W. 2003. Indoor health: background levels of fungi. *AIHA J (Fairfax, Va),* 64**,** 427-38.

GRAVELAT, F. N., BEAUVAIS, A., LIU, H., LEE, M. J., SNARR, B. D., CHEN, D., XU, W., KRAVTSOV, I., HOAREAU, C. M., VANIER, G., URB, M., CAMPOLI, P., AL ABDALLAH, Q., LEHOUX, M., CHABOT, J. C., OUIMET, M. C., BAPTISTA, S. D., FRITZ, J. H., NIERMAN, W. C., LATGE, J. P., MITCHELL, A. P., FILLER, S. G., FONTAINE, T. & SHEPPARD, D. C. 2013. *Aspergillus* galactosaminogalactan mediates adherence to host constituents and conceals hyphal beta-glucan from the immune system. *PLoS Pathog,* 9**,** e1003575.

GRAVELAT, F. N., EJZYKOWICZ, D. E., CHIANG, L. Y., CHABOT, J. C., URB, M., MACDONALD, K. D., AL-BADER, N., FILLER, S. G. & SHEPPARD, D. C. 2010. *Aspergillus fumigatus* MedA governs adherence, host cell interactions and virulence. *Cell Microbiol,* 12**,** 473-88.

GREEN, B. J., TOVEY, E. R., SERCOMBE, J. K., BLACHERE, F. M., BEEZHOLD, D. H. & SCHMECHEL, D. 2006. Airborne fungal fragments and allergenicity. *Med Mycol,* 44 Suppl 1**,** S245-55.

GRESNIGT, M. S., BOZZA, S., BECKER, K. L., JOOSTEN, L. A., ABDOLLAHI-ROODSAZ, S., VAN DER BERG, W. B., DINARELLO, C. A., NETEA, M. G., FONTAINE, T., DE LUCA, A., MORETTI, S., ROMANI, L., LATGE, J. P. & VAN DE VEERDONK, F. L. 2014. A polysaccharide virulence factor from *Aspergillus fumigatus* elicits anti-inflammatory effects through induction of Interleukin-1 receptor antagonist. *PLoS Pathog,* 10**,** e1003936.

GROSS, O., GEWIES, A., FINGER, K., SCHAFER, M., SPARWASSER, T., PESCHEL, C., FORSTER, I. & RULAND, J. 2006. Card9 controls a non-TLR signalling pathway for innate anti-fungal immunity. *Nature,* 442**,** 651-6.

GUGNANI, H. C. 2003. Ecology and taxonomy of pathogenic *aspergilli*. *Front Biosci,* 8**,** s346-57.

GUILLOT, L., NATHAN, N., TABARY, O., THOUVENIN, G., LE ROUZIC, P., CORVOL, H., AMSELEM, S. & CLEMENT, A. 2013. Alveolar epithelial cells: master regulators of lung homeostasis. *Int J Biochem Cell Biol,* 45**,** 2568-73.

GUNZEL, D. & YU, A. S. 2013. Claudins and the modulation of tight junction permeability. *Physiol Rev,* 93**,** 525-69.

GUTIERREZ-CORREA, M., LUDENA, Y., RAMAGE, G. & VILLENA, G. K. 2012. Recent advances on filamentous fungal biofilms for industrial uses. *Appl Biochem Biotechnol,* 167**,** 1235-53.

HAN, X., YU, R., ZHEN, D., TAO, S., SCHMIDT, M. & HAN, L. 2011. beta-1,3-Glucan-induced host phospholipase D activation is involved in *Aspergillus fumigatus* internalization into type II human pneumocyte A549 cells. *PLoS One,* 6**,** e21468.

HARDISON, S. E. & BROWN, G. D. 2012. C-type lectin receptors orchestrate antifungal immunity. *Nat Immunol,* 13**,** 817-22.

HAYDEN, M. S. & GHOSH, S. 2004. Signaling to NF-kappaB. *Genes Dev,* 18**,** 2195-224.

HAYDEN, M. S. & GHOSH, S. 2011. NF-kappaB in immunobiology. *Cell Res,* 21**,** 223-44.

HAYDEN, M. S. & GHOSH, S. 2012. NF-kappaB, the first quarter-century: remarkable progress and outstanding questions. *Genes Dev,* 26**,** 203-34.

HAZEKI, K., NIGORIKAWA, K. & HAZEKI, O. 2007. Role of phosphoinositide 3-kinase in innate immunity. *Biol Pharm Bull,* 30**,** 1617-23.

HENSEL, M., ARST, H. N., JR., AUFAUVRE-BROWN, A. & HOLDEN, D. W. 1998. The role of the *Aspergillus fumigatus* areA gene in invasive pulmonary aspergillosis. *Mol Gen Genet,* 258**,** 553-7.

HERZOG, E. L., BRODY, A. R., COLBY, T. V., MASON, R. & WILLIAMS, M. C. 2008. Knowns and unknowns of the alveolus. *Proc Am Thorac Soc,* 5**,** 778-82.

HEWISON, M. 2012. An update on vitamin D and human immunity. *Clin Endocrinol (Oxf),* 76**,** 315-25.

HEYL, K. A., KLASSERT, T. E., HEINRICH, A., MULLER, M. M., KLAILE, E., DIENEMANN, H., GRUNEWALD, C., BALS, R., SINGER, B. B. & SLEVOGT, H. 2014. Dectin-1 is expressed in human lung and mediates the proinflammatory immune response to nontypeable *Haemophilus influenzae*. *MBio,* 5**,** e01492-14.

HIRAKATA, Y., YANO, H., ARAI, K., ENDO, S., KANAMORI, H., AOYAGI, T., HIROTANI, A., KITAGAWA, M., HATTA, M., YAMAMOTO, N., KUNISHIMA, H., KAWAKAMI, K. & KAKU, M. 2010. Monolayer culture systems with respiratory epithelial cells for evaluation of bacterial invasiveness. *Tohoku J Exp Med,* 220**,** 15-9.

HOHL, T. M. & FELDMESSER, M. 2007. *Aspergillus fumigatus*: principles of pathogenesis and host defense. *Eukaryot Cell,* 6**,** 1953-63.

HOPE, W. W., WALSH, T. J. & DENNING, D. W. 2005. The invasive and saprophytic syndromes due to *Aspergillus spp*. *Med Mycol,* 43 Suppl 1**,** S207-38.

HOSPENTHAL, D. R., KWON-CHUNG, K. J. & BENNETT, J. E. 1998. Concentrations of airborne *Aspergillus* compared to the incidence of invasive aspergillosis: lack of correlation. *Med Mycol,* 36**,** 165-8.

HOUSER, J., KOMAREK, J., KOSTLANOVA, N., CIOCI, G., VARROT, A., KERR, S. C., LAHMANN, M., BALLOY, V., FAHY, J. V., CHIGNARD, M., IMBERTY, A. & WIMMEROVA, M. 2013. A Soluble Fucose-Specific Lectin from *Aspergillus fumigatus* Conidia - Structure, Specificity and Possible Role in Fungal Pathogenicity. *PLoS One,* 8**,** e83077.

IOSIFIDIS, T., GARRATT, L. W., COOMBE, D. R., KNIGHT, D. A., STICK, S. M. & KICIC, A. 2016. Airway epithelial repair in health and disease: Orchestrator or simply a player? *Respirology,* 21**,** 438-48.

ITOH, M., SASAKI, H., FURUSE, M., OZAKI, H., KITA, T. & TSUKITA, S. 2001. Junctional adhesion molecule (JAM) binds to PAR-3: a possible mechanism for the recruitment of PAR-3 to tight junctions. *J Cell Biol,* 154**,** 491-7.

JOUBERT, L. M., FERREIRA, J. A., STEVENS, D. A., NAZIK, H. & CEGELSKI, L. 2017. Visualization of *Aspergillus fumigatus* biofilms with Scanning Electron Microscopy and Variable Pressure-Scanning Electron Microscopy: A comparison of processing techniques. *J Microbiol Methods,* 132**,** 46-55.

KAO, R. & DAVIES, J. 1995. Fungal ribotoxins: a family of naturally engineered targeted toxins? *Biochem Cell Biol,* 73**,** 1151-9.

KATO, A. & SCHLEIMER, R. P. 2007. Beyond inflammation: airway epithelial cells are at the interface of innate and adaptive immunity. *Curr Opin Immunol,* 19**,** 711-20.

KHOUFACHE, K., PUEL, O., LOISEAU, N., DELAFORGE, M., RIVOLLET, D., COSTE, A., CORDONNIER, C., ESCUDIER, E., BOTTEREL, F. & BRETAGNE, S. 2007.

Verruculogen associated with *Aspergillus fumigatus* hyphae and conidia modifies the electrophysiological properties of human nasal epithelial cells. *BMC Microbiol,* 7**,** 5.

KIM, E. K. & CHOI, E. J. 2015. Compromised MAPK signaling in human diseases: an update. *Arch Toxicol,* 89**,** 867-82.

KIM, Y. T., KANG, M. C., SUNG, S. W. & KIM, J. H. 2005. Good long-term outcomes after surgical treatment of simple and complex pulmonary aspergilloma. *Ann Thorac Surg,* 79**,** 294-8.

KOGAN, T. V., JADOUN, J., MITTELMAN, L., HIRSCHBERG, K. & OSHEROV, N. 2004. Involvement of secreted *Aspergillus fumigatus* proteases in disruption of the actin fiber cytoskeleton and loss of focal adhesion sites in infected A549 lung pneumocytes. *J Infect Dis,* 189**,** 1965-73.

KOSMIDIS, C. & DENNING, D. W. 2014. The clinical spectrum of pulmonary aspergillosis. *Thorax*.

KOSMIDIS, C. & DENNING, D. W. 2015. The clinical spectrum of pulmonary aspergillosis. *Thorax,* 70**,** 270-7.

KOUSHA, M., TADI, R. & SOUBANI, A. O. 2011. Pulmonary aspergillosis: a clinical review. *Eur Respir Rev,* 20**,** 156-74.

KRAPPMANN, S., BIGNELL, E. M., REICHARD, U., ROGERS, T., HAYNES, K. & BRAUS, G. H. 2004. The *Aspergillus fumigatus* transcriptional activator CpcA contributes significantly to the virulence of this fungal pathogen. *Mol Microbiol,* 52**,** 785-99.

KRAPPMANN, S. & BRAUS, G. H. 2005. Nitrogen metabolism of Aspergillus and its role in pathogenicity. *Med Mycol,* 43 Suppl 1**,** S31-40.

KRAPPMANN, S. & RAMAGE, G. 2013. A sticky situation: extracellular DNA shapes *Aspergillus fumigatus* biofilms. *Front Microbiol,* 4**,** 159.

KUMAR, H., KAWAI, T. & AKIRA, S. 2009. Pathogen recognition in the innate immune response. *Biochem J,* 420**,** 1-16.

KUNSCH, C., RUBEN, S. M. & ROSEN, C. A. 1992. Selection of optimal kappa B/Rel DNA-binding motifs: interaction of both subunits of NF-kappa B with DNA is required for transcriptional activation. *Mol Cell Biol,* 12**,** 4412-21.

KUPFAHL, C., HEINEKAMP, T., GEGINAT, G., RUPPERT, T., HARTL, A., HOF, H. & BRAKHAGE, A. A. 2006. Deletion of the gliP gene of *Aspergillus fumigatus* results in loss of gliotoxin production but has no effect on virulence of the fungus in a low-dose mouse infection model. *Mol Microbiol,* 62**,** 292-302.

KURUP, V. P. 2005. *Aspergillus* antigens: which are important? *Med Mycol,* 43 Suppl 1**,** S189-96.

KURUP, V. P., BANERJEE, B., MURALI, P. S., GREENBERGER, P. A., KRISHNAN, M., HARI, V. & FINK, J. N. 1998. Immunodominant peptide epitopes of allergen, Asp f 1 from the fungus *Aspergillus fumigatus*. *Peptides,* 19**,** 1469-77.

KURZA, O. 2014. Human Fungal Pathogens. *The Mycota,* 12**,** 19-43.

KVASNICKOVA, E., PAULICEK, V., PALDRYCHOVA, M., JEZDIK, R., MATATKOVA, O. & MASAK, J. 2016. *Aspergillus fumigatus* DBM 4057 biofilm formation is inhibited by chitosan, in contrast to baicalein and rhamnolipid. *World J Microbiol Biotechnol,* 32**,** 187.

KYRIAKIS, J. M. & AVRUCH, J. 2001. Mammalian mitogen-activated protein kinase signal transduction pathways activated by stress and inflammation. *Physiol Rev,* 81**,** 807-69.

LALE, A. M., MASON, J. D. & JONES, N. S. 1998. Mucociliary transport and its assessment: a review. *Clin Otolaryngol Allied Sci,* 23**,** 388-96.

LAMOTH, F. 2016. *Aspergillus fumigatus*-Related Species in Clinical Practice. *Front Microbiol,* 7**,** 683.

LATGE, J. P., DEBEAUPUIS, J. P., SARFATI, J., DIAQUIN, M. & PARIS, S. 1993. Cell wall antigens in *Aspergillus fumigatus*. *Arch Med Res,* 24**,** 269-74.

LATGE, J. P., MOUYNA, I., TEKAIA, F., BEAUVAIS, A., DEBEAUPUIS, J. P. & NIERMAN, W. 2005. Specific molecular features in the organization and biosynthesis of the cell wall of *Aspergillus fumigatus*. *Med Mycol,* 43 Suppl 1**,** S15-22.

LEE, M. J., LIU, H., BARKER, B. M., SNARR, B. D., GRAVELAT, F. N., AL ABDALLAH, Q., GAVINO, C., BAISTROCCHI, S. R., OSTAPSKA, H., XIAO, T., RALPH, B., SOLIS, N. V., LEHOUX, M., BAPTISTA, S. D., THAMMAHONG, A., CERONE, R. P., KAMINSKYJ, S. G., GUIOT, M. C., LATGE, J. P., FONTAINE, T., VINH, D. C., FILLER, S. G. & SHEPPARD, D. C. 2015. The Fungal Exopolysaccharide Galactosaminogalactan Mediates Virulence by Enhancing Resistance to Neutrophil Extracellular Traps. *PLoS Pathog,* 11**,** e1005187.

LEE, M. S. & KIM, Y. J. 2007. Signaling pathways downstream of pattern-recognition receptors and their cross talk. *Annu Rev Biochem,* 76**,** 447-80.

LESSING, F., KNIEMEYER, O., WOZNIOK, I., LOEFFLER, J., KURZAI, O., HAERTL, A. & BRAKHAGE, A. A. 2007. The *Aspergillus fumigatus* transcriptional regulator AfYap1 represents the major regulator for defense against reactive oxygen intermediates but is dispensable for pathogenicity in an intranasal mouse infection model. *Eukaryot Cell,* 6**,** 2290-302.

LI, J. X., FAN, L. C., LI, M. H., CAO, W. J. & XU, J. F. 2017. Beneficial effects of Omalizumab therapy in allergic bronchopulmonary aspergillosis: A synthesis review of published literature. *Respir Med,* 122**,** 33-42.

LI, X., GAO, M., HAN, X., TAO, S., ZHENG, D., CHENG, Y., YU, R., HAN, G., SCHMIDT, M. & HAN, L. 2012. Disruption of the phospholipase D gene attenuates the virulence of *Aspergillus fumigatus*. *Infect Immun,* 80**,** 429-40.

LIN, C. J., SASSE, C., GERKE, J., VALERIUS, O., IRMER, H., FRAUENDORF, H., HEINEKAMP, T., STRASSBURGER, M., TRAN, V. T., HERZOG, B., BRAUS-STROMEYER, S. A. & BRAUS, G. H. 2015. Transcription Factor SomA Is Required for Adhesion, Development and Virulence of the Human Pathogen *Aspergillus fumigatus*. *PLoS Pathog,* 11**,** e1005205.

LIN, S. J., SCHRANZ, J. & TEUTSCH, S. M. 2001. Aspergillosis case-fatality rate: systematic review of the literature. *Clin Infect Dis,* 32**,** 358-66.

LIU, H., GRAVELAT, F. N., CHIANG, L. Y., CHEN, D., VANIER, G., EJZYKOWICZ, D. E., IBRAHIM, A. S., NIERMAN, W. C., SHEPPARD, D. C. & FILLER, S. G. 2010. *Aspergillus fumigatus* AcuM regulates both iron acquisition and gluconeogenesis. *Mol Microbiol,* 78**,** 1038-54.

LIU, H., LEE, M. J., SOLIS, N. V., PHAN, Q. T., SWIDERGALL, M., RALPH, B., IBRAHIM, A. S., SHEPPARD, D. C. & FILLER, S. G. 2016. *Aspergillus fumigatus* CalA binds to integrin alpha5beta1 and mediates host cell invasion. *Nat Microbiol,* 2**,** 16211.

MARGALIT, A. & KAVANAGH, K. 2015. The innate immune response to *Aspergillus fumigatus* at the alveolar surface. *FEMS Microbiol Rev*.

MARKARYAN, A., MOROZOVA, I., YU, H. & KOLATTUKUDY, P. E. 1994. Purification and characterization of an elastinolytic metalloprotease from *Aspergillus fumigatus* and immunoelectron microscopic evidence of secretion of this enzyme by the fungus invading the murine lung. *Infect Immun,* 62**,** 2149-57.

MATTHAY, M. A., ROBRIQUET, L. & FANG, X. 2005. Alveolar epithelium: role in lung fluid balance and acute lung injury. *Proc Am Thorac Soc,* 2**,** 206-13.

MAY, M. J. & GHOSH, S. 1998. Signal transduction through NF-kappa B. *Immunol Today,* 19**,** 80-8.

MCCARTHY, M. W. & WALSH, T. J. 2017. Special Considerations for the Diagnosis and Treatment of Invasive Pulmonary Aspergillosis. *Expert Rev Respir Med*.

MCCORMICK, A., LOEFFLER, J. & EBEL, F. 2010. *Aspergillus fumigatus*: contours of an opportunistic human pathogen. *Cell Microbiol,* 12**,** 1535-43.

MCGINNIS, M. R. 2007. Indoor mould development and dispersal. *Med Mycol,* 45**,** 1-9.

MEDZHITOV, R. 2007. Recognition of microorganisms and activation of the immune response. *Nature,* 449**,** 819-26.

MERCER, R. R., RUSSELL, M. L., ROGGLI, V. L. & CRAPO, J. D. 1994. Cell number and distribution in human and rat airways. *Am J Respir Cell Mol Biol,* 10**,** 613-24.

MITCHELL, C. G., SLIGHT, J. & DONALDSON, K. 1997. Diffusible component from the spore surface of the fungus *Aspergillus fumigatus* which inhibits the macrophage oxidative burst is distinct from gliotoxin and other hyphal toxins. *Thorax,* 52**,** 796-801.

MITCHELL, S., VARGAS, J. & HOFFMANN, A. 2016. Signaling via the NFkappaB system. *Wiley Interdiscip Rev Syst Biol Med,* 8**,** 227-41.

MORENO, M. A., AMICH, J., VICENTEFRANQUEIRA, R., LEAL, F. & CALERA, J. A. 2007. Culture conditions for zinc- and pH-regulated gene expression studies in *Aspergillus fumigatus*. *Int Microbiol,* 10**,** 187-92.

MORTAZ, E., ADCOCK, I. M., TABARSI, P., DARAZAM, I. A., MOVASSAGHI, M., GARSSEN, J., JAMAATI, H. & VELAYATI, A. 2017. Pattern recognitions receptors in immunodeficiency disorders. *Eur J Pharmacol*.

MOWAT, E., BUTCHER, J., LANG, S., WILLIAMS, C. & RAMAGE, G. 2007. Development of a simple model for studying the effects of antifungal agents on multicellular communities of *Aspergillus fumigatus*. *J Med Microbiol,* 56**,** 1205-12.

MOWAT, E., RAJENDRAN, R., WILLIAMS, C., MCCULLOCH, E., JONES, B., LANG, S. & RAMAGE, G. 2010. *Pseudomonas aeruginosa* and their small diffusible extracellular molecules inhibit *Aspergillus fumigatus* biofilm formation. *FEMS Microbiol Lett,* 313**,** 96-102.

MOYES, D. L., RUNGLALL, M., MURCIANO, C., SHEN, C., NAYAR, D., THAVARAJ, S., KOHLI, A., ISLAM, A., MORA-MONTES, H., CHALLACOMBE, S. J. & NAGLIK, J. R. 2010. A biphasic innate immune MAPK response discriminates between the yeast and hyphal forms of *Candida albicans* in epithelial cells. *Cell Host Microbe,* 8**,** 225-35.

MOYES, D. L., SHEN, C., MURCIANO, C., RUNGLALL, M., RICHARDSON, J. P., ARNO, M., ALDECOA-OTALORA, E. & NAGLIK, J. R. 2014. Protection against epithelial damage during *Candida albicans* infection is mediated by PI3K/Akt and mammalian target of rapamycin signaling. *J Infect Dis,* 209**,** 1816-26.

MOYES, D. L., WILSON, D., RICHARDSON, J. P., MOGAVERO, S., TANG, S. X., WERNECKE, J., HOFS, S., GRATACAP, R. L., ROBBINS, J., RUNGLALL, M., MURCIANO, C., BLAGOJEVIC, M., THAVARAJ, S., FORSTER, T. M., HEBECKER, B., KASPER, L., VIZCAY, G., IANCU, S. I., KICHIK, N., HADER, A., KURZAI, O., LUO, T., KRUGER, T., KNIEMEYER, O., COTA, E., BADER, O., WHEELER, R. T., GUTSMANN, T., HUBE, B. & NAGLIK, J. R. 2016. Candidalysin is a fungal peptide toxin critical for mucosal infection. *Nature,* 532**,** 64-8.

NAGLIK, J. R., MOYES, D. L., WACHTLER, B. & HUBE, B. 2011. *Candida albicans* interactions with epithelial cells and mucosal immunity. *Microbes Infect,* 13**,** 963-76.

NAMVAR, S., WARN, P., FARNELL, E., BROMLEY, M., FRACZEK, M., BOWYER, P. & HERRICK, S. 2015. *Aspergillus fumigatus* proteases, Asp f 5 and Asp f 13, are essential for airway inflammation and remodelling in a murine inhalation model. *Clin Exp Allergy,* 45**,** 982-93.

NATESAN, S. K. & CHANDRASEKAR, P. H. 2016. Isavuconazole for the treatment of invasive aspergillosis and mucormycosis: current evidence, safety, efficacy, and clinical recommendations. *Infect Drug Resist,* 9**,** 291-300.

NIELSEN, S. M., KRISTENSEN, L., SONDERGAARD, A., HANDBERG, K. J., STENDERUP, J. & NORSKOV-LAURITSEN, N. 2014. Increased prevalence and altered species composition of filamentous fungi in respiratory specimens from cystic fibrosis patients. *APMIS,* 122**,** 1007-12.

O'DEA, E. & HOFFMANN, A. 2010. The regulatory logic of the NF-kappaB signaling system. *Cold Spring Harb Perspect Biol,* 2**,** a000216.

O'DEA, E. L., KEARNS, J. D. & HOFFMANN, A. 2008. UV as an amplifier rather than inducer of NF-kappaB activity. *Mol Cell,* 30**,** 632-41.

O'GORMAN, C. M., FULLER, H. & DYER, P. S. 2009. Discovery of a sexual cycle in the opportunistic fungal pathogen *Aspergillus fumigatus*. *Nature,* 457**,** 471-4.

OGUMA, T., ASANO, K., TOMOMATSU, K., KODAMA, M., FUKUNAGA, K., SHIOMI, T., OHMORI, N., UEDA, S., TAKIHARA, T., SHIRAISHI, Y., SAYAMA, K., KAGAWA, S., NATORI, Y., LILLY, C. M., SATOH, K., MAKIMURA, K. & ISHIZAKA, A. 2011. Induction of mucin and MUC5AC expression by the protease activity of *Aspergillus fumigatus* in airway epithelial cells. *J Immunol,* 187**,** 999-1005.

OSHEROV, N. 2012. Interaction of the pathogenic mold *Aspergillus fumigatus* with lung epithelial cells. *Front Microbiol,* 3**,** 346.

PALMA, A. S., FEIZI, T., ZHANG, Y., STOLL, M. S., LAWSON, A. M., DIAZ-RODRIGUEZ, E., CAMPANERO-RHODES, M. A., COSTA, J., GORDON, S., BROWN, G. D. & CHAI, W. 2006. Ligands for the beta-glucan receptor, Dectin-1, assigned using "designer" microarrays of oligosaccharide probes (neoglycolipids) generated from glucan polysaccharides. *J Biol Chem,* 281**,** 5771-9.

PANJABI, C. & SHAH, A. 2011. Allergic *Aspergillus* sinusitis and its association with allergic bronchopulmonary aspergillosis. *Asia Pac Allergy,* 1**,** 130-7.

PAPPAS, P. G., ALEXANDER, B. D., ANDES, D. R., HADLEY, S., KAUFFMAN, C. A., FREIFELD, A., ANAISSIE, E. J., BRUMBLE, L. M., HERWALDT, L., ITO, J., KONTOYIANNIS, D. P., LYON, G. M., MARR, K. A., MORRISON, V. A., PARK, B. J., PATTERSON, T. F., PERL, T. M., OSTER, R. A., SCHUSTER, M. G., WALKER, R., WALSH, T. J., WANNEMUEHLER, K. A. & CHILLER, T. M. 2010. Invasive fungal infections among organ transplant recipients: results of the Transplant-

Associated Infection Surveillance Network (TRANSNET). *Clin Infect Dis,* 50**,** 1101-11.

PARIS, S., BOISVIEUX-ULRICH, E., CRESTANI, B., HOUCINE, O., TARAMELLI, D., LOMBARDI, L. & LATGE, J. P. 1997. Internalization of *Aspergillus fumigatus* conidia by epithelial and endothelial cells. *Infect Immun,* 65**,** 1510-4.

PARIS, S., DEBEAUPUIS, J. P., CRAMERI, R., CAREY, M., CHARLES, F., PREVOST, M. C., SCHMITT, C., PHILIPPE, B. & LATGE, J. P. 2003. Conidial hydrophobins of *Aspergillus fumigatus*. *Appl Environ Microbiol,* 69**,** 1581-8.

PATTERSON, K. C. & STREK, M. E. 2014. Diagnosis and treatment of pulmonary aspergillosis syndromes. *Chest,* 146**,** 1358-68.

PAULUSSEN, C., HALLSWORTH, J. E., ALVAREZ-PEREZ, S., NIERMAN, W. C., HAMILL, P. G., BLAIN, D., REDIERS, H. & LIEVENS, B. 2017. Ecology of aspergillosis: insights into the pathogenic potency of *Aspergillus fumigatus* and some other Aspergillus species. *Microb Biotechnol,* 10**,** 296-322.

PERFECT, J. R., COX, G. M., LEE, J. Y., KAUFFMAN, C. A., DE REPENTIGNY, L., CHAPMAN, S. W., MORRISON, V. A., PAPPAS, P., HIEMENZ, J. W., STEVENS, D. A. & MYCOSES STUDY, G. 2001. The impact of culture isolation of *Aspergillus* species: a hospital-based survey of aspergillosis. *Clin Infect Dis,* 33**,** 1824-33.

POIROT, J. L., GANGNEUX, J. P., FISCHER, A., MALBERNARD, M., CHALLIER, S., LAUDINET, N. & BERGERON, V. 2007. Evaluation of a new mobile system for protecting immune-suppressed patients against airborne contamination. *Am J Infect Control,* 35**,** 460-6.

PONGPOM, M., LIU, H., XU, W., SNARR, B. D., SHEPPARD, D. C., MITCHELL, A. P. & FILLER, S. G. 2015. Divergent targets of *Aspergillus fumigatus* AcuK and AcuM transcription factors during growth in vitro versus invasive disease. *Infect Immun,* 83**,** 923-33.

PRASAD, A., AGARWAL, K., DEEPAK, D. & ATWAL, S. S. 2016. Pulmonary Aspergillosis: What CT can Offer Before it is too Late! *J Clin Diagn Res,* 10**,** TE01-5.

PRIYADARSINY, P., SWAIN, P. K. & SARMA, P. U. 2003. Expression and characterization of Asp fI, an immunodominant allergen/antigen of *A. fumigatus* in insect cell. *Mol Cell Biochem,* 252**,** 157-63.

QIAO, J., KONTOYIANNIS, D. P., CALDERONE, R., LI, D., MA, Y., WAN, Z., LI, R. & LIU, W. 2008. Afyap1, encoding a bZip transcriptional factor of *Aspergillus fumigatus*, contributes to oxidative stress response but is not essential to the virulence of this pathogen in mice immunosuppressed by cyclophosphamide and triamcinolone. *Med Mycol,* 46**,** 773-82.

RACKLEY, C. R. & STRIPP, B. R. 2012. Building and maintaining the epithelium of the lung. *J Clin Invest,* 122**,** 2724-30.

RAJENDRAN, R., MOWAT, E., MCCULLOCH, E., LAPPIN, D. F., JONES, B., LANG, S., MAJITHIYA, J. B., WARN, P., WILLIAMS, C. & RAMAGE, G. 2011. Azole resistance of *Aspergillus fumigatus* biofilms is partly associated with efflux pump activity. *Antimicrob Agents Chemother,* 55**,** 2092-7.

RAMAGE, G., RAJENDRAN, R., GUTIERREZ-CORREA, M., JONES, B. & WILLIAMS, C. 2011. *Aspergillus* biofilms: clinical and industrial significance. *FEMS Microbiol Lett,* 324**,** 89-97.

RAMOS, J. W. 2008. The regulation of extracellular signal-regulated kinase (ERK) in mammalian cells. *Int J Biochem Cell Biol,* 40**,** 2707-19.

RAJASINGHAM, R., SMITH, R. M., PARK, B. J., JARVIS, J. N., GOVENDER, N. P., CHILLER, T. M., DENNING, D. W., LOYSE, A. & BOULWARE, D. R. 2017. Global burden of disease of HIV-associated cryptococcal meningitis: an updated analysis. *Lancet Infect Dis,* 17**,** 873-881.

REICHARD, U., MONOD, M., ODDS, F. & RUCHEL, R. 1997. Virulence of an aspergillopepsin-deficient mutant of *Aspergillus fumigatus* and evidence for another aspartic proteinase linked to the fungal cell wall. *J Med Vet Mycol,* 35**,** 189-96.

REICHHARDT, C., STEVENS, D. A. & CEGELSKI, L. 2016. Fungal biofilm composition and opportunities in drug discovery. *Future Med Chem,* 8**,** 1455-68.

REMENTERIA, A., LOPEZ-MOLINA, N., LUDWIG, A., VIVANCO, A. B., BIKANDI, J., PONTON, J. & GARAIZAR, J. 2005. Genes and molecules involved in *Aspergillus fumigatus* virulence. *Rev Iberoam Micol,* 22**,** 1-23.

RICHARDSON, M. D. & PAGE, I. D. 2017. *Aspergillus* serology: Have we arrived yet? *Med Mycol,* 55**,** 48-55.

RICHIE, D. L., HARTL, L., AIMANIANDA, V., WINTERS, M. S., FULLER, K. K., MILEY, M. D., WHITE, S., MCCARTHY, J. W., LATGE, J. P., FELDMESSER, M., RHODES, J. C. & ASKEW, D. S. 2009. A role for the unfolded protein response (UPR) in virulence and antifungal susceptibility in *Aspergillus fumigatus*. *PLoS Pathog,* 5**,** e1000258.

ROCHA, M. C., FABRI, J. H., FRANCO DE GODOY, K., ALVES DE CASTRO, P., HORI, J. I., FERREIRA DA CUNHA, A., ARENTSHORST, M., RAM, A. F., VAN DEN HONDEL, C. A., GOLDMAN, G. H. & MALAVAZI, I. 2016. *Aspergillus fumigatus* MADS-Box Transcription Factor rlmA Is Required for Regulation of the Cell Wall Integrity and Virulence. *G3 (Bethesda),* 6**,** 2983-3002.

ROHDE, M., SCHWIENBACHER, M., NIKOLAUS, T., HEESEMANN, J. & EBEL, F. 2002. Detection of early phase specific surface appendages during germination of *Aspergillus fumigatus* conidia. *FEMS Microbiol Lett,* 206**,** 99-105.

ROKICKI, W., ROKICKI, M., WOJTACHA, J. & DZELJIJLI, A. 2016. The role and importance of club cells (Clara cells) in the pathogenesis of some respiratory diseases. *Kardiochir Torakochirurgia Pol,* 13**,** 26-30.

ROMANI, L. 2011. Immunity to fungal infections. *Nat Rev Immunol,* 11**,** 275-88.

ROTH, H. M., WADSWORTH, S. J., KAHN, M. & KNIGHT, D. A. 2012. The airway epithelium in asthma: developmental issues that scar the airways for life? *Pulm Pharmacol Ther,* 25**,** 420-6.

SAITOU, M., FURUSE, M., SASAKI, H., SCHULZKE, J. D., FROMM, M., TAKANO, H., NODA, T. & TSUKITA, S. 2000. Complex phenotype of mice lacking occludin, a component of tight junction strands. *Mol Biol Cell,* 11**,** 4131-42.

SAMSON, R. A., VISAGIE, C. M., HOUBRAKEN, J., HONG, S. B., HUBKA, V., KLAASSEN, C. H., PERRONE, G., SEIFERT, K. A., SUSCA, A., TANNEY, J. B., VARGA, J., KOCSUBE, S., SZIGETI, G., YAGUCHI, T. & FRISVAD, J. C. 2014. Phylogeny, identification and nomenclature of the genus *Aspergillus*. *Stud Mycol,* 78**,** 141-73.

SANGUINETTI, M. & POSTERARO, B. 2016. Diagnostic of Fungal Infections Related to Biofilms. *Adv Exp Med Biol,* 931**,** 63-82.

SCHRETTL, M., BECKMANN, N., VARGA, J., HEINEKAMP, T., JACOBSEN, I. D., JOCHL, C., MOUSSA, T. A., WANG, S., GSALLER, F., BLATZER, M., WERNER, E. R., NIERMANN, W. C., BRAKHAGE, A. A. & HAAS, H. 2010. HapX-mediated

adaption to iron starvation is crucial for virulence of *Aspergillus fumigatus*. *PLoS Pathog,* 6**,** e1001124.

SCHRETTL, M., KIM, H. S., EISENDLE, M., KRAGL, C., NIERMAN, W. C., HEINEKAMP, T., WERNER, E. R., JACOBSEN, I., ILLMER, P., YI, H., BRAKHAGE, A. A. & HAAS, H. 2008. SreA-mediated iron regulation in *Aspergillus fumigatus*. *Mol Microbiol,* 70**,** 27-43.

SCHWIENBACHER, M., WEIG, M., THIES, S., REGULA, J. T., HEESEMANN, J. & EBEL, F. 2005. Analysis of the major proteins secreted by the human opportunistic pathogen *Aspergillus fumigatus* under *in vitro* conditions. *Med Mycol,* 43**,** 623-30.

SEIDLER, M. J., SALVENMOSER, S. & MULLER, F. M. 2008. *Aspergillus fumigatus* forms biofilms with reduced antifungal drug susceptibility on bronchial epithelial cells. *Antimicrob Agents Chemother,* 52**,** 4130-6.

SETHI, P., SALUJA, R., JINDAL, N. & SINGH, V. 2012. Invasive aspergillosis in an immunocompetent host. *J Oral Maxillofac Pathol,* 16**,** 297-300.

SHAH, A. 2008. *Aspergillus*-associated hypersensitivity respiratory disorders. *Indian J Chest Dis Allied Sci,* 50**,** 117-28.

SHAH, A. & PANJABI, C. 2014. Allergic aspergillosis of the respiratory tract. *Eur Respir Rev,* 23**,** 8-29.

SHAH, A. & PANJABI, C. 2016. Allergic Bronchopulmonary Aspergillosis: A Perplexing Clinical Entity. *Allergy Asthma Immunol Res,* 8**,** 282-97.

SHARON, H., AMAR, D., LEVDANSKY, E., MIRCUS, G., SHADKCHAN, Y., SHAMIR, R. & OSHEROV, N. 2011. PrtT-regulated proteins secreted by *Aspergillus fumigatus* activate MAPK signaling in exposed A549 lung cells leading to necrotic cell death. *PLoS One,* 6**,** e17509.

SHEPPARD, D. C. 2011. Molecular mechanism of *Aspergillus fumigatus* adherence to host constituents. *Curr Opin Microbiol,* 14**,** 375-9.

SHEPPARD, D. C., DOEDT, T., CHIANG, L. Y., KIM, H. S., CHEN, D., NIERMAN, W. C. & FILLER, S. G. 2005. The *Aspergillus fumigatus* StuA protein governs the up-regulation of a discrete transcriptional program during the acquisition of developmental competence. *Mol Biol Cell,* 16**,** 5866-79.

SHERIF, R. & SEGAL, B. H. 2010. Pulmonary aspergillosis: clinical presentation, diagnostic tests, management and complications. *Curr Opin Pulm Med,* 16**,** 242-50.

SHIH, V. F., TSUI, R., CALDWELL, A. & HOFFMANN, A. 2011. A single NFkappaB system for both canonical and non-canonical signaling. *Cell Res,* 21**,** 86-102.

SHOPOVA, I., BRUNS, S., THYWISSEN, A., KNIEMEYER, O., BRAKHAGE, A. A. & HILLMANN, F. 2013. Extrinsic extracellular DNA leads to biofilm formation and colocalizes with matrix polysaccharides in the human pathogenic fungus *Aspergillus fumigatus*. *Front Microbiol,* 4**,** 141.

SMITH, G. R. 1977. *Aspergillusfumigatus* : A Possible Relationship between Spore Size and Virulence for Mice*J Gen Microbiol,* 102**,** 413-415.

SMITH, J. M., TANG, C. M., VAN NOORDEN, S. & HOLDEN, D. W. 1994. Virulence of *Aspergillus fumigatus* double mutants lacking restriction and an alkaline protease in a low-dose model of invasive pulmonary aspergillosis. *Infect Immun,* 62**,** 5247-54.

SMITH, N. L. & DENNING, D. W. 2011. Underlying conditions in chronic pulmonary aspergillosis including simple aspergilloma. *Eur Respir J,* 37**,** 865-72.

SMITH, T. D. & CALVO, A. M. 2014. The mtfA transcription factor gene controls morphogenesis, gliotoxin production, and virulence in the opportunistic human pathogen *Aspergillus fumigatus*. *Eukaryot Cell,* 13**,** 766-75.

SORCI, G., GIOVANNINI, G., RIUZZI, F., BONIFAZI, P., ZELANTE, T., ZAGARELLA, S., BISTONI, F., DONATO, R. & ROMANI, L. 2011. The danger signal S100B integrates pathogen- and danger-sensing pathways to restrain inflammation. *PLoS Pathog,* 7**,** e1001315.

SORIANI, F. M., MALAVAZI, I., DA SILVA FERREIRA, M. E., SAVOLDI, M., VON ZESKA KRESS, M. R., DE SOUZA GOLDMAN, M. H., LOSS, O., BIGNELL, E. & GOLDMAN, G. H. 2008. Functional characterization of the *Aspergillus fumigatus* CRZ1 homologue, CrzA. *Mol Microbiol,* 67**,** 1274-91.

STEFFAN, N., GRUNDMANN, A., AFIYATULLOV, S., RUAN, H. & LI, S. M. 2009. FtmOx1, a non-heme Fe(II) and alpha-ketoglutarate-dependent dioxygenase, catalyses the endoperoxide formation of verruculogen in *Aspergillus fumigatus*. *Org Biomol Chem,* 7**,** 4082-7.

SUGUI, J. A., PARDO, J., CHANG, Y. C., MULLBACHER, A., ZAREMBER, K. A., GALVEZ, E. M., BRINSTER, L., ZERFAS, P., GALLIN, J. I., SIMON, M. M. & KWON-CHUNG, K. J. 2007. Role of laeA in the Regulation of alb1, gliP, Conidial Morphology, and Virulence in *Aspergillus fumigatus*. *Eukaryot Cell,* 6**,** 1552-61.

SUN, W. K., LU, X., LI, X., SUN, Q. Y., SU, X., SONG, Y., SUN, H. M. & SHI, Y. 2012. Dectin-1 is inducible and plays a crucial role in *Aspergillus*-induced innate immune responses in human bronchial epithelial cells. *Eur J Clin Microbiol Infect Dis,* 31**,** 2755-64.

TAKAZONO, T. & SHEPPARD, D. C. 2017. *Aspergillus* in chronic lung disease: Modeling what goes on in the airways. *Med Mycol,* 55**,** 39-47.

TAYLOR, P. R., TSONI, S. V., WILLMENT, J. A., DENNEHY, K. M., ROSAS, M., FINDON, H., HAYNES, K., STEELE, C., BOTTO, M., GORDON, S. & BROWN, G. D. 2007. Dectin-1 is required for beta-glucan recognition and control of fungal infection. *Nat Immunol,* 8**,** 31-8.

TEKAIA, F. & LATGE, J. P. 2005. *Aspergillus fumigatus*: saprophyte or pathogen? *Curr Opin Microbiol,* 8**,** 385-92.

THAU, N., MONOD, M., CRESTANI, B., ROLLAND, C., TRONCHIN, G., LATGE, J. P. & PARIS, S. 1994. rodletless mutants of *Aspergillus fumigatus*. *Infect Immun,* 62**,** 4380-8.

THOMPSON, G. R., 3RD & PATTERSON, T. F. 2011. Pulmonary aspergillosis: recent advances. *Semin Respir Crit Care Med,* 32**,** 673-81.

THORLEY, A. J., GRANDOLFO, D., LIM, E., GOLDSTRAW, P., YOUNG, A. & TETLEY, T. D. 2011. Innate immune responses to bacterial ligands in the peripheral human lung--role of alveolar epithelial TLR expression and signalling. *PLoS One,* 6**,** e21827.

TILBURN, J., SARKAR, S., WIDDICK, D. A., ESPESO, E. A., OREJAS, M., MUNGROO, J., PENALVA, M. A. & ARST, H. N., JR. 1995. The *Aspergillus* PacC zinc finger transcription factor mediates regulation of both acid- and alkaline-expressed genes by ambient pH. *EMBO J,* 14**,** 779-90.

TILLEY, A. E., WALTERS, M. S., SHAYKHIEV, R. & CRYSTAL, R. G. 2015. Cilia dysfunction in lung disease. *Annu Rev Physiol,* 77**,** 379-406.

TISSOT, F., AGRAWAL, S., PAGANO, L., PETRIKKOS, G., GROLL, A. H., SKIADA, A., LASS-FLORL, C., CALANDRA, T., VISCOLI, C. & HERBRECHT, R. 2017. ECIL-6 guidelines for the treatment of invasive candidiasis, aspergillosis and mucormycosis in leukemia and hematopoietic stem cell transplant patients. *Haematologica,* 102**,** 433-444.

TOCHIGI, N., OKUBO, Y., ANDO, T., WAKAYAMA, M., SHINOZAKI, M., GOCHO, K., HATA, Y., ISHIWATARI, T., NEMOTO, T. & SHIBUYA, K. 2013. Histopathological implications of *Aspergillus* infection in lung. *Mediators Inflamm,* 2013**,** 809798.

TOMEE, J. F., WIERENGA, A. T., HIEMSTRA, P. S. & KAUFFMAN, H. K. 1997. Proteases from *Aspergillus fumigatus* induce release of proinflammatory cytokines and cell detachment in airway epithelial cell lines. *J Infect Dis,* 176**,** 300-3.

TOVEY, E. R. & GREEN, B. J. 2005. Measuring environmental fungal exposure. *Med Mycol,* 43 Suppl 1**,** S67-70.

TWUMASI-BOATENG, K., YU, Y., CHEN, D., GRAVELAT, F. N., NIERMAN, W. C. & SHEPPARD, D. C. 2009. Transcriptional profiling identifies a role for BrlA in the response to nitrogen depletion and for StuA in the regulation of secondary metabolite clusters in *Aspergillus fumigatus*. *Eukaryot Cell,* 8**,** 104-15.

VALIANTE, V., BALDIN, C., HORTSCHANSKY, P., JAIN, R., THYWISSEN, A., STRASSBURGER, M., SHELEST, E., HEINEKAMP, T. & BRAKHAGE, A. A. 2016. The *Aspergillus fumigatus* conidial melanin production is regulated by the bifunctional bHLH DevR and MADS-box RlmA transcription factors. *Mol Microbiol,* 102**,** 321-335.

VAN ITALLIE, C. M. & ANDERSON, J. M. 2014. Architecture of tight junctions and principles of molecular composition. *Semin Cell Dev Biol,* 36**,** 157-65.

VAREILLE, M., KIENINGER, E., EDWARDS, M. R. & REGAMEY, N. 2011. The airway epithelium: soldier in the fight against respiratory viruses. *Clin Microbiol Rev,* 24**,** 210-29.

VICKERS, I., REEVES, E. P., KAVANAGH, K. A. & DOYLE, S. 2007. Isolation, activity and immunological characterisation of a secreted aspartic protease, CtsD, from *Aspergillus fumigatus*. *Protein Expr Purif,* 53**,** 216-24.

WARKENTIEN, T., RODRIGUEZ, C., LLOYD, B., WELLS, J., WEINTROB, A., DUNNE, J. R., GANESAN, A., LI, P., BRADLEY, W., GASKINS, L. J., SEILLIER-MOISEIWITSCH, F., MURRAY, C. K., MILLAR, E. V., KEENAN, B., PAOLINO, K., FLEMING, M., HOSPENTHAL, D. R., WORTMANN, G. W., LANDRUM, M. L., KORTEPETER, M. G., TRIBBLE, D. R. & INFECTIOUS DISEASE CLINICAL RESEARCH PROGRAM TRAUMA INFECTIOUS DISEASE OUTCOMES STUDY, G. 2012. Invasive mold infections following combat-related injuries. *Clin Infect Dis,* 55**,** 1441-9.

WARTENBERG, D., LAPP, K., JACOBSEN, I. D., DAHSE, H. M., KNIEMEYER, O., HEINEKAMP, T. & BRAKHAGE, A. A. 2011. Secretome analysis of *Aspergillus fumigatus* reveals Asp-hemolysin as a major secreted protein. *Int J Med Microbiol,* 301**,** 602-11.

WASYLNKA, J. A., HISSEN, A. H., WAN, A. N. & MOORE, M. M. 2005. Intracellular and extracellular growth of *Aspergillus fumigatus*. *Med Mycol,* 43 Suppl 1**,** S27-30.

WASYLNKA, J. A. & MOORE, M. M. 2000. Adhesion of *Aspergillus* species to extracellular matrix proteins: evidence for involvement of negatively charged carbohydrates on the conidial surface. *Infect Immun,* 68**,** 3377-84.

WASYLNKA, J. A. & MOORE, M. M. 2002. Uptake of *Aspergillus fumigatus* Conidia by phagocytic and nonphagocytic cells *in vitro*: quantitation using strains expressing green fluorescent protein. *Infect Immun,* 70**,** 3156-63.

WASYLNKA, J. A. & MOORE, M. M. 2003. *Aspergillus fumigatus* conidia survive and germinate in acidic organelles of A549 epithelial cells. *J Cell Sci,* 116**,** 1579-87.

WASYLNKA, J. A., SIMMER, M. I. & MOORE, M. M. 2001. Differences in sialic acid density in pathogenic and non-pathogenic *Aspergillus* species. *Microbiology,* 147**,** 869-77.

WATANABE, A., KAMEI, K., SEKINE, T., WAKU, M., NISHIMURA, K., MIYAJI, M. & KURIYAMA, T. 2003. Immunosuppressive substances in *Aspergillus fumigatus* culture filtrate. *J Infect Chemother,* 9**,** 114-21.

WHITMARSH, A. J. & DAVIS, R. J. 1996. Transcription factor AP-1 regulation by mitogen-activated protein kinase signal transduction pathways. *J Mol Med (Berl),* 74**,** 589-607.

WILLGER, S. D., PUTTIKAMONKUL, S., KIM, K. H., BURRITT, J. B., GRAHL, N., METZLER, L. J., BARBUCH, R., BARD, M., LAWRENCE, C. B. & CRAMER, R. A., JR. 2008. A sterol-regulatory element binding protein is required for cell polarity, hypoxia adaptation, azole drug resistance, and virulence in *Aspergillus fumigatus*. *PLoS Pathog,* 4**,** e1000200.

WILLIAMS, C., RAJENDRAN, R. & RAMAGE, G. 2016. *Aspergillus* Biofilms in Human Disease. *Adv Exp Med Biol,* 931**,** 1-11.

WU, J., ZHANG, Y., XIN, Z. & WU, X. 2015. The crosstalk between TLR2 and NOD2 in *Aspergillus fumigatus* keratitis. *Mol Immunol,* 64**,** 235-43.

YAMAMOTO, K., FERRARI, J. D., CAO, Y., RAMIREZ, M. I., JONES, M. R., QUINTON, L. J. & MIZGERD, J. P. 2012. Type I alveolar epithelial cells mount innate immune responses during *pneumococcal pneumonia*. *J Immunol,* 189**,** 2450-9.

YAN, T., HAN, J. & YU, X. 2015. E-cadherin mediates adhesion of *Aspergillus fumigatus* to non-small cell lung cancer cells. *Tumour Biol*.

YANG, S. H., SHARROCKS, A. D. & WHITMARSH, A. J. 2003. Transcriptional regulation by the MAP kinase signaling cascades. *Gene,* 320**,** 3-21.

YANG, Z., JAECKISCH, S. M. & MITCHELL, C. G. 2000. Enhanced binding of *Aspergillus fumigatus* spores to A549 epithelial cells and extracellular matrix proteins by a component from the spore surface and inhibition by rat lung lavage fluid. *Thorax,* 55**,** 579-84.

YIN, W. B., BACCILE, J. A., BOK, J. W., CHEN, Y., KELLER, N. P. & SCHROEDER, F. C. 2013. A nonribosomal peptide synthetase-derived iron(III) complex from the pathogenic fungus *Aspergillus fumigatus*. *J Am Chem Soc,* 135**,** 2064-7.

ZHANG, H. J., QU, J. M., SHAO, C. Z., ZHANG, J., HE, L. X. & YUAN, Z. H. 2008. *Aspergillus fumigatus* conidia upregulates NOD2 protein expression both in vitro and in vivo. *Acta Pharmacol Sin,* 29**,** 1202-8.

ZHANG, Z., LIU, R., NOORDHOEK, J. A. & KAUFFMAN, H. F. 2005. Interaction of airway epithelial cells (A549) with spores and mycelium of *Aspergillus fumigatus*. *J Infect,* 51**,** 375-82.

ZMEILI, O. S. & SOUBANI, A. O. 2007. Pulmonary aspergillosis: a clinical update. *QJM,* 100**,** 317-34.

CHAPTER 2: GENERAL MATERIALS AND METHODS

2.1 General materials and equipment

2.1.1 Materials and growth conditions

Unless stated otherwise, all media components were purchased from Sigma (Sigma-Aldrich, Dorset, UK) or Gibco, UK. All chemical reagents and materials were purchased from BDH (BDH, UK), Sigma or Thermo-Scientific, UK. Fungal strains used in this study were stored as live conidia and maintained as 40% glycerol stocks at -80^{o}C.

2.1.2 Culture media

A. fumigatus strains used in this study are listed in table 2.1. Unless otherwise stated, these strains were cultivated as previously (Bertuzzi et al., 2014) on *Aspergillus* complete media (ACM) composed of adenine 0.0075% (w/v), glucose 1% (w/v), yeast extract 0.1% (w/v), bacteriological peptone 0.2% (w/v), casamino acids 0.1% (w/v), *Aspergillus* salt solution 2% (v/v) (Appendix 1A and C), vitamin solution 1% (v/v) (Appendix 1B), ammonium tartrate 1% (v/v) (from 50 mM stock), and Agar 1% (w/v). The pH of the media was adjusted to 6.5 using 10 M NaOH.

All cell lines were acquired from the American Type Culture Collection, ATCC (Rockville, MD). The A549 epithelial cells were grown and maintained in RPMI-1640 Medium with L-glutamine (Sigma-Aldrich, R0883) supplemented with 10% Fetal Bovine Serum (FBS; Gibco, UK) and 1% penicillin-streptomycin (containing 10,000 units penicillin and 10 mg streptomycin/ml) as this was optimal for *A. fumigatus* culture and growth under the experimental conditions relative to DMEM. Calu-3 cells were cultured in D-MEM-F12 (1X) (Thermo-Fisher Scientific) supplemented with 10% Fetal Bovine Serum (Sigma-Aldrich) and 1% Penicillin-Streptomycin (10,000 units penicillin and 10 mg streptomycin/ml) (Sigma-Aldrich) as recommended by the ATCC.

2.1.3 General equipment

All work involving live *A. fumigatus* was performed in Envair Bio-2 MSC Class 2 cabinet. *A. fumigatus* strains were grown in a Binder incubator at 37°C. Harvested

spores were pelleted in a Thermo-scientific Megafuge 8 centrifuge. Spores were enumerated with a NEUBAUER improved haemocytometer grid under a Nikon 014318 DBS microscope. *A. fumigatus* culture filtrate was grown in a Grant Bio or a New Brunswick Scientific Innova ES-80 orbital shaking incubator. Epithelial cells were cultured in a New Brunswick Galaxy 170S incubator with CO2, or a SANYO CO2 incubator following infection. Tissue culture plates, serological pipettes and pipette tips were sourced from Corning, USA. Tissue culture flasks and loops were sourced from Grenier Bio-One, UK. The 10 cm cell culture dishes were sourced from Biolite through Thermoscientific, UK. Fridges and -20°C freezers were supplied by LEC Medical. All autoclaving/aqueous heat sterilizations were performed in an Advantage Lab AL02-01 autoclave. TransAM samples were incubated on a Mini blot mixer from VWR. Luminex sample plates were incubated on an IKA MTS 2/4 digital shaker at 600-800 rpm and room temperature. Pipettors (P10, P20, P200, and P1000) were sourced from Gilson. MilliQ water was produced using an Alto Triple Red system. Vortexing was performed with a benchtop with VWR VV3. Eppendorf tubes were centrifuged using a JENCONS-DLS Spectrafuge 24D. Refrigerated centrifugation was performed with a U-320R BOECO centrifuge (Germany). 20 ml syringes were purchased from Eccentric. Syringe filter units (0.22 µm) were purchased from Millex-HA. Colourimetric assays were analysed using a Synergy/2 microplate reader. Falcon tubes (15 ml and 50 ml) were obtained from Thermo-Fisher scientific.

2.2 Methods

2.2.1 Cell culture procedures

2.2.1.1 Thawing of frozen A549 cells

To revive cells from a frozen stock, a 1 ml vial of cells was quickly thawed at 37^{o}C and added to 9 ml of RPMI 1640 (Sigma-Aldrich) supplemented with 10% fetal bovine serum (FBS; Gibco, UK) and 1% penicillin-streptomycin (Sigma-Aldrich). The cells were pelleted at 1200 rpm for 5 min. The cell pellet was re-suspended first in 10 ml of the culture media, and then transferred into a T-175 flask and then made up to 25 ml

with more media pre-warmed to 37^{o}C. The cells were then incubated at 37^{o}C in 5% CO_2.

2.2.1.2 Maintaining/passaging A549 cells

When cells reached about 80%-95% confluence in the T-175 tissue culture flask, the media was removed and the monolayer was washed with 10 ml of PBS (Sigma). A 4 ml of trypsin-EDTA solution (Sigma) was added to the monolayer and incubated for 5-10 min at 37^{o}C. Diluting 3 fold with 8 ml of supplemented RPMI-1640 inactivated trypsin, cells were counted and split in ratios from 1/6 to 1/2 of re-suspended cells stock to a final cell density of 2 - 6 x10^2 viable cells/ml in a total of 25 ml of supplemented RPMI-1640 in a T-175 flask.

2.2.1.3 Counting A549 cells

After trypsin inactivation, 100 µl of the cell suspension was diluted 10 fold in trypan blue solution and a 10 µl was added to the counting grid of NEUBAUER haemocytometer. Cells in the four outer squares were counted and the following equation was used to calculate the number of cells per ml of the medium:

(Total cell count ÷ 4) x 10^4 x dilution factor (10) = cells per ml of the cell suspension.

2.2.1.4 Plating/seeding A549 cells

For all experiments, cells were seeded at a density of 5x10^5 cells/ml. After enumerating the cell number in the trypsinated suspension, the following equation was used to determine the dilution factor of the stock for required cell density:

Density of suspension ÷ required density (5x10^5 cells/ml) = dilution factor

Various sizes of cell culture plates were used for different experimental procedures thereby requiring different volumes of the 5x10^5 cells/ml suspension.

Thus:

Required volume ÷ dilution factor = Volume of counted cell suspension needed.

The calculated volume of the stock suspension was then made up to the required volume with culture media. Cells were then seeded in cell culture plates (Greiner Bio-one).

2.2.1.5 Freezing down A549 cells

To freeze down cells, trypsinized cells were counted as above by diluting a small volume 10 fold in trypan blue (Sigma). Viable cell number was enumerated. Cells were pelleted at 1200 rpm for 5 min. The cell pellet was re-suspended in freezing media made up of 10% sterile dimethyl sulphoxide (DMSO) (Sigma-Aldrich) in FBS (1 ml DMSO + 9 ml FBS) at a density of at least $3x10^6$ viable cells/ml. The cells were then aliquoted in 1 ml volumes in cryovials and immediately transferred into a "Mr Frosty" (Nalgene). The Mr Frosty storage system was kept at -80^oC for 3 days and then vials were transferred to liquid nitrogen for long-term storage.

2.2.2 Microbiological procedures

2.2.2.1 Cultivation and maintenance of *A. fumigatus* strains

Clinical isolate of *A. fumigatus* was originally chosen for characterisation studies of host response to pathogenic mould. Subsequently, the mutant strains and progenitor isolates were selected based on the hypothesis arising from the characterisation. All isolates have comparable growth rate under the experimental conditions. *A. fumigatus* isolates were streaked on a microbiological petri dish containing *Aspergillus* complete media (ACM). The plate was incubated at 37^oC for 2 days. Using a loop, conidia were collected from a single colony and streaked onto solid ACM agar medium in a fresh T-25 tissue culture and incubated at 37^oC for 2-3 days. The conidia were then harvested and counted for experiments.

Table 2.1: ***A. fumigatus*** **strains used in this study**

Isolate	**Genotype**	**MFIG collection number**	**Reference/Source**
CEA10 (CBS 144-89)	Clinical isolate	MFIG15	(Monod et al., 1993)
ΔpacC^{CEA10}	[CEA10]*; pacC::ptrA*	MFIG9	(Bertuzzi et al., 2014)
ATCC46645	Clinical isolate	MFIG16	(Hearn and Mackenzie, 1980)
tdTomato^{ATCC46645}	*[ATCC46645]; his2A::Tdtomato*	MFIG12	(Lother et al., 2014)
ΔpacC^{ATCC46645}	[ATCC46645]; *pacC::ptrA*	MFIG3	(Bertuzzi et al., 2014)
ΔakuB^{KU80}	[CEA17]; *akuBKU80::A.f.pyrG*	MFIG1	(da Silva Ferreira et al., 2006)
ΔpacC^{A1160}	*[A1160; pyrG-]; ΔakuBKU80::A.f.pyrG; ΔpacC::HygB*	MFIG7	Gift from Mike Bromley
ΔprtT^{A1160}	MFIG335	MFIG335	Gift from Mike Bromley
ΔgliP ^{CEA17}	[CEA17]; *akuBKU80::A.f.pyrG; gliP::(neo-A.n.pyrG-neo)*	MFIG13	(Kupfahl et al., 2006)

2.2.2.2 Harvesting conidia

To harvest conidia, *A. fumigatus* conidial lawns were flooded with 10 ml of filtered sterile water. Spores were dispersed into the suspension using a spreader or by gentle shaking. The conidia suspension was collected in a 50 ml Falcon tube after being filtered through sterile Miracloth (Calbiochem) to remove mycelial fragments. Conidia were washed 3 times with 30 ml of sterile water and centrifuged at 4000 rpm for 5 min between washes and then counted using a haemocytometer.

2.2.2.3 Counting conidia

Harvested conidia were re-suspended in 5-10 ml of sterile water and a 10 µl aliquot of the suspension was diluted 100 or 10 fold in sterile water. A 10 µl aliquot of the suspension was added to the haemocytometer counting grid, covered with a cover slip and conidia were counted under a microscope. Five small squares in the large central square were counted and the mean was calculated. Conidia count/ml of the suspension was enumerated as :

Number of conidia counted ÷ 5 = mean of spores per 0.04 mm^2 chamber

The counting grid is 0.1 mm deep,

Thus volume counted = 0.04 mm^2 x 0.1 mm = 0.004 mm^3 (4 nl)

To calculate the count per ml:

4 nl x $2.5x10^5$ =1 ml

Total number of conidia in cfu/ml = count x dilution factor x $2.5x10^5$

2.2.2.4 Preparation of *A. fumigatus* glycerol stocks

To freeze down *A. fumigatus* strains, the conidia were harvested, counted and re-suspended at a density of at $1x10^9$ cells/ml in 40% glycerol in sterile water. The suspension was then aliquoted into 1 ml volumes in cryovials and stored at -80^oC until needed.

2.2.2.5 Preparation of *A. fumigatus* culture filtrate (CF)

Due to difficulties in handling *in vitro Aspergillus* infections for longer than 24 hours, CF from 16, 24, 48, and 72 h *A. fumigatus* cultures chosen hypothetically were prepared in order to determine the best timing and concentration with moderate impact on host cells as well as amenable to experimental modifications guided by a previous study which showed that 16 h and 48 h culture non-cytotoxic and cytotoxic to A549 cells respectively (Bertuzzi et al., 2014). For all experiments, *A. fumigatus* CF was made by inoculating freshly harvested conidia at a cell density of approximately $1x10^6$ conidia/ml in serum free RPMI-1640 medium. The suspension was incubated in an orbital incubator with shaking at 200 rpm (New Brunswick scientific, Innova 40) at 37^oC for 16 h, 24 h, 48 h, or 72 h as required. The culture suspension was filtered through sterile Miracloth (Calbiochem) and through a 0.20 µm filter to exclude all cellular fragments. The filtrate was stored at -20^oC.

2.2.3 Epithelial cell infections

2.2.3.1 Infection for damage and cytokine assays

A549 epithelial cells were suspended at a density of $5x10^5$ cells/ml after trypsination. At 48 h prior to fungal challenge, 1 ml of the suspension was added into each well of a 12 well tissue culture plate. The plates were incubated for 24 h or until the cells were 80-100% confluent. At 24 h prior to infection, the media was removed and replaced with serum free RPMI-1640 medium and incubated further for 24 h. For conidia infections, a stock concentration of $1x10^8$ conidia/ml was diluted serially in each well to give a range of MOIs (multiplicity of infections) from 10 to 0.0001. For CF, a range of dilutions of the stock filtrate, from 5 fold to 50 fold dilution was performed. Plates were incubated at 37^oC for 24 h. After incubation, supernatants were collected at indicated time points and used immediately for LDH assay or stored at -20^oC for cytokine release assay. To investigate the role of *A. fumigatus* CF in cytokine degradation, an equal volume of 24 h culture supernatant from CF-exposed A549 cells (conditioned (CDN) CF) or original naïve CF (not previously in contact with host cells) was added to an equal volume of supernatant derived at 24 h post-infection

with *A. fumigatus* spores in a fresh culture plate. The plate was further incubated for 24 h and the supernatant collected and stored as above for cytokine quantification.

2.2.3.2 Stimulation of epithelial cells prior to protein extraction

A549 epithelial cells were suspended at a density of 5 x 10^5 cells/ ml after trypsination. At 48 h prior to treatment with CF or infection with conidia, 2 ml of the suspension was added in each well of a 6 well tissue culture plate and incubated. At 24 h prior to treatments, the media was removed and replaced with serum free RPMI1640 medium and incubated for a further 24 h. For conidia infection, 200 µl of media was replaced with 1x10^8 conidia/ml stock solution added to each well (MOI of 10). Plates were incubated for 5 min, 15 min, 30 min, 1 h, 2 h, 4 h, 6 h, 8 h, and 12 h. For CF infection, 400 µl or 200 µl of media was replaced with an equal volume of CF (5 fold or 10 fold dilutions) respectively. The plates were incubated for 5 min, 15 min, 30 min, 1 h, 2 h, 3 h, 4 h, and 5 h post infection. At the end of incubation, the monolayer was washed with 1 ml of ice cold PBS and the cells lysed for protein extraction.

2.2.3.3 Stimulation of epithelial cells for transcription factor binding assays

To assay for DNA binding activity of transcription factors, 10 ml of 5x10^5 cells/ml was seeded in 100 mm (10 cm) cell culture dishes 48 h prior to infection. At 24 h prior to infection, the media was removed and replaced with serum free media and incubated for a further 24 h. For conidia infection, 1 ml of media was replaced with 1 ml of 1 x 10^8 conidia /ml spore suspension (MOI of 10). For CF challenges, 2 ml or 1 ml of media was replaced with an equal volume of CF (5 fold or 10 fold dilutions respectively). Dishes were incubated for predetermined times before the extraction of nuclear material.

2.2.4 Epithelial cell response assays

2.2.4.1 Human XL cytokine profiler

To determine the global cytokine expression from epithelial cells in response to infections with live conidia and CF, EC culture supernatants were analysed using the

HXL cytokine profile kit from R&D systems (Bio-Techne) according to the manufacturer's instructions. Briefly, a nitrocellulose membrane, pre-coated with capture antibodies against the cytokines of interest was incubated with a blocking solution on a rocking platform for 1 h. Culture supernatant from each treatment was diluted 1:3 to a final volume of 1.5 ml. The membrane was incubated with the culture supernatant overnight at 2-8^{O}C on a shaker. Membrane was washed 3x on a shaker for 10 min each and then incubated with detection antibody cocktail in specified diluents for 1 h. The membrane was washed as before and incubated with a 1:2000 dilution of streptavidin-phycoerythrin conjugate for 30 min. The membrane was washed and developed immediately using a 1:1 ratio of chemi-reagent 1 and 2 on a plastic sheet for 1 min at room temperature, protected from light. Excess reagent mix was removed and the membrane was covered with a plastic wrap and exposed to X-ray film for 1-10 min using a ChemiDoc MP imaging system (BIO-RAD). The relative amounts of cytokine were quantified by mean pixel density of the blots using ImageJ software and micro-array profile plugins (Bio-Techne) and normalized to the positive and negative control blots first and then to the PBS treated controls.

2.2.4.2 Cytokine Luminex

Quantitative assays for cytokine production were performed using the magnetic Luminex performance assay kits (Bio-Techne) according to the manufacturer's protocol. Cytokine-specific human capture antibodies were pre-coated on magnetic microparticles which were added into the wells of a 96-well microtitre plate. Samples and standard cocktails were added into pre-designated wells and incubated. After incubation, the plate was washed with 1x wash buffer and biotinylated cytokine specific detection antibodies were added and incubated. The plate was washed again. Signal was developed using streptavidin-phycoerythrin conjugate (SA-PE) to bind the detection antibody. The fluorescence signal is directly proportional to the amount of target cytokine in the supernatant and was measured using a Bioplex 200 machine (BIO-RAD). Data was analysed using Bioplex Manger 6.1 software (BioRad).

2.2.4.3 Quantitative measurement of LDH activity in culture supernatants

LDH is a stable, non-secreted cytoplasmic enzyme released by cells upon lysis and/or cell membrane damage. The activity of released LDH in the culture supernatants was measured colorimetrically with a 30 min coupled enzymatic assay that tests the conversion of tetrazolium salt (INT) into a red formazan product. To measure the lytic epithelial cell death, culture supernatants were collected after a predetermined time of incubation and assayed for LDH activity using the Cytox 96 Non-radioactive cytotoxicity assay kit (Promega) according to the manufacturer's protocol and using a recombinant porcine LDH enzyme (Sigma-Aldrich) to generate a standard curve with concentrations ranging from between 15 to 960 mU/ml. LDH activity in culture supernatants was quantified via extrapolation from the standard curve and normalized to PBS challenge.

2.2.4.4 Measurement of Trans-epithelial electrical resistance (TEER) of cultured Calu-3 monolayers

A 1 ml of A $1x10^6$/ ml Calu3 cells obtained from the ATCC (Rockville, MD) were cultured in D-MEM-F12 (1X) (Thermo-Fisher Scientific) supplemented with 10% Fetal Bovine Serum (Sigma-Aldrich) and 1% Penicillin-Streptomycin (10,000 units penicillin and 10 mg streptomycin/ml) (Sigma-Aldrich) in a trans-well insert (Scientific Laboratory Supply (SLS)). The insert was placed in a 12 well special tissue culture plate (Scientific Laboratory Supply) containing 2 mL of supplemented DMEM-F12 previously warmed to 37 °C using sterile forceps. Cells were incubated at 37°C and 5% CO_2. Media was changed every 2 days while TEER was measured every 4 days until TEER reached at least 1000 Ωcm^{-2} (~11 to 13 days) as measured with a World Precision Instrument Evom2 epithelial voltohmeter and STX-2 electrode. . To measure TEER, the probe of the voltohmeter was sterilized in 70 % ethanol followed by a rinse in sterile water. The probe was gently placed into the transwell insert such that the long arm sat in the outer well content while the shorter arm was immersed in the insert media without touching the base of the insert. To change the media, the medium in the insert was carefully aspirated with a P1000 Gilson pipette while holding the insert in a place with sterile forceps. The insert was then transferred to fresh pre-warmed

media (2 ml) in a new 12 well culture plate followed by addition of 1 ml of supplemented medium into the insert chamber. On the day of infection, the TEER (TEER 0) was measured for time zero (T 0 h) followed by challenge with 10^5 spores or a 5 fold dilution of CF (200 µl of CF in 800 µl of media in the insert). The plate was incubated for 24 h (T 24 h) and TEER was measured again (TEER 24 h). The difference between TEER 24 h and TEER 0 h was calculated as loss in TEER due to challenge (TEER 24 h-TER 0 h) and normalised to fungal viable count. The result in most cases was expressed as fold reduction in TEER relative to PBS challenge.

Viable count = number of single fungal colonies recovered out of 100 CFU plated

Normalisation coefficient = 100 ÷ viable count

ΔTEER = (TEER 24 h-TEER 0 h) × normalisation coefficient

2.2.5 Protein assays

2.2.5.1 Protein extraction

After fungal challenge of A549 cells for the predetermined time, monolayers were washed once with ice cold PBS (Sigma) on an ice tray and lysed by adding Radio immuno precipitation assay (RIPA) buffer (Appendix2) (0.05 M (50 mM) Tris-HCl pH7.5, 0.15M (150 mM) NaCl, 1% Triton X-100, 1% Sodium Deoxycholate, 0.1% SDS and 20 mM EDTA) supplemented with 10 µl/ml protease inhibitor cocktail (Thermo Scientific) and 10 µl/ml phosphatase inhibitor (Sigma). Cells were removed by scraping and collected in a microfuge tube. The lysate was incubated on ice for 30 min, centrifuged at 13000 rpm and 4^{o}C for 10 min. The supernatant containing the solubilized proteins was collected and stored at -20^{o}C.

2.2.5.2 Quantification of total protein using the Bicinchoninic Assay (BCA).

Total protein concentration was determined using the Bicinchoninic Assay (BCA) kit (Thermo Scientific) according to the manufacturer's instructions. BCA is a biochemical assay that is based on reduction of Cu^{2+} ions from copper sulphate to Cu in the reagent. The amount of Cu^{2+} reduced is proportional to the amount of protein in the

sample reflected in a colour change from green to purple. The concentration of protein was quantified by extrapolation from a standard curve with different concentrations of Bovine Serum Albumin (BSA) ranging from 31.25 and 2000 µg/ml. Briefly, whole cell or nuclear extracts were diluted 1:10 in PBS. A 25 µl of the samples and standard was mixed with 200 µl of BCA reagent and incubated at 37^{o}C for 30-45 min. Absorbance was measured at 562 nm (Synergy/2 microplate reader). Total protein concentration of lysates was calculated from the standard curve.

2.2.5.3 Detection of phosphorylated signalling protein

Detection of phosphorylated signalling proteins was carried out using the Bio-Plex Pro magnetic total/phosphoprotein detection assay kit (Bio-Rad, UK). This assay is a magnetic bead-based immunoassay for the detection of total intracellular and phosphorylated proteins from cell lysates. Briefly, capture antibodies for target proteins are pre-coated on colour-coded magnetic microspheres (beads). The beads for different signalling proteins were mixed as 1 µl/well and added into each well of a black and clear-bottomed 96 well plate (supplied in the assay kit) and washed 3x on a hand held magnetic platform (Bio-Rad). A 10 µg aliquot of total protein in each cell lysate was diluted in 50 µl of lysis buffer (Supplied) and added into duplicated wells already containing the magnetic beads. The plate was sealed, protected from light with foil and incubated on a shaker overnight (18 h) at 800 rpm and room temperature. At the end of incubation, the wells were washed three times as instructed. Biotinylated detection antibody cocktail against the phosphorylated target proteins (as detailed in Table 2.2) was added and incubated for 30 min. The plate was washed and analyte-antibody conjugate was detected by incubating with streptavidin-phycoerythrin (SA-PE) conjugate. Fluorescence was measured using a Bioplex-200 machine according to manufacturer's protocol. Data was analysed using Bioplex Manager 6.1 software. Phosphorylated protein levels were normalized to the β-actin house-keeping protein, and expressed as fold change relative to uninfected control, or expressed without normalization as a percentage of the total protein at a given time post infection.

Table 2.2: List of target signalling proteins with their respective phosphorylation form and sites

Signalling protein	Phosphorylated form/sites
Akt	Ser^{473}
Erk1/2	Thr^{202}/Tyr^{204}, Thr^{185}/Tyr^{187}
IκBα	Ser^{32}/Ser^{639}
JNK	$Thr^{183/}Tyr^{185}$
p38	Thr^{180}/Tyr^{182}

2.2.6 DNA binding assay (TransAM©)

2.2.6.1 Extraction of nuclear material from A549 epithelial cells

After infection, nuclear material was extracted from A549 cells using the nuclear extraction kit (Active Motif) according to manufacturer's instructions. In brief, monolayers were washed and scraped into ice-cold PBS supplemented with 500 µl/ml phosphatase inhibitors. Cells were pelleted at 500 rpm for 5 min at 4^{o}C. The pellet was re-suspended in hypotonic buffer to swell the cell membrane. Detergent (supplied) was added to lyse the cells, vortexed for 10 sec to release cytoplasmic contents and centrifuged at 15000 rpm for 30 sec afterwards. The supernatant containing the cytoplasmic proteins was discarded while the nuclear pellet was washed again with hypotonic buffer. The supernatant was discarded and the pellet was re-suspended in 50 µl of complete lysis buffer followed by 30 min incubation in ice on a rocking platform. After incubation, the pellet was vortexed for 30 secs and then centrifuged for 10 min at 13000 rpm. Supernatant was aliquoted and stored at -80^{o}C for future use.

2.2.6.2 Assay for activation and DNA binding ability of transcription factors

DNA binding activity of transcription factors was detected and measured using the TransAM Transcription Factor ELISA kit (Active Motif). The assays were performed in 96 strip-well plates onto which multiple copies of specific double-stranded oligonucleotide sequences (i.e transcription factor binding site sequences- 5′-GGGACTTTCC-3′ for NF-kB family transcription factors and TRE (5′-TGAGTCA-3′) for MAPKs substrates) had been immobilized. Nuclear extracts were added so that the transcription factors of interest could bind to their specific binding consensus sequences. A specific primary antibody that recognizes epitopes that are accessible only in the activated and DNA bound form of each transcription factor was added to the wells. An enzyme (horseradish peroxidase, (HRP)) linked secondary antibody to provide sensitive colourimetric readout was added. At the end of incubation, the plate was incubated with developing solution at room temperature for 2-20 min. Stop solution (2N H_2SO_4) was added and absorbance was measured at 450 nm at room temperature.

2.2.7 Microscopy

2.2.7.1 Image acquisition

Upon removal of culture media and a triple wash with PBS, *A. fumnigatus* infected monolayers were incubated with 1 ml of supplemented RPMI-1640 containing 1 µg/ml Concanavalin A conjugated to FITC (Con-A, Sigma), applied for 30 min with incubation at 37°C and 5% CO_2. Wide-field epifluorescence microscopy was performed using a Nikon Eclipse TE2000-E microscope (Nikon Instruments, Europe BV, UK) and a Nikon PlanFluor 20x/1.20 NA objective lens. Some images were acquired with a 1.5x optovar zoom lens inserted into the light path for greater magnification. A CoolLED PreciseExcite system (CoolLED, Andover, UK) was used with 470 nm and 550 nm LED arrays for FITC and tdTomato excitation, respectively. The Nikon B-2A and G-2A filter cubes were used to collect FITC and tdTomato emission, respectively. Images were captured with an ORCA-ER CCD camera (Hamamatsu, Welwyn Garden City, UK) driven by MetaMorph software v7.7.6.0 (Molecular Devices,

Sunnyvale, CA, USA). For Concanavalin-A, optical sectioning was performed with a P-721 PIFOC Z objective focusing system connected to an E-625 PZT piezo servo controller allowing rapid z-stack acquisition with 0.2 to 1 µm step size. 3D sections were background subtracted and subsequently summed using FIJI version 1.51g (https://fiji.sc/ (8/10/2017)) (Schindelin et al., 2012), to generate 2D images, which were then false coloured for clarity. Apart from basic brightness and contrast display adjustments using FIJI, no further manipulation of the raw data was used to prepare the image files for presentation. To quantify the fungal biomass at each infection time point, cumulative spore diameters and filament lengths (including branches) were measured in each infection time point image and averaged using FIJI (Schindelin et al., 2012).

2.2.7.2 Analysis of A549 monolayer integrity by detachment

Monolayers were challenged with 10^5 *A. fumigatus* spores or 5- or 10-fold diluted *A. fumigatus* CF. Following co-incubation monolayers were washed 3 times with PBS, fixed with 4% formaldehyde in PBS, and permeabilized with 0.2% Triton-X100. Nuclei of adherent A549 cells were stained with DAPI. DAPI fluorescence in adherent epithelial cells was excited with a CoolLED PreciseExcite 380 nm LED array in combination with a Nikon UV-2A filter cube, which collected the DAPI emission. Images were acquired as stated above, where at least three fields of view, per experimental well were taken. Images were then processed and quantified/enumerated using an in-house macro written for FIJI (Fig 2) (Appendix 3), where the data was exported into Prism to make graphs.

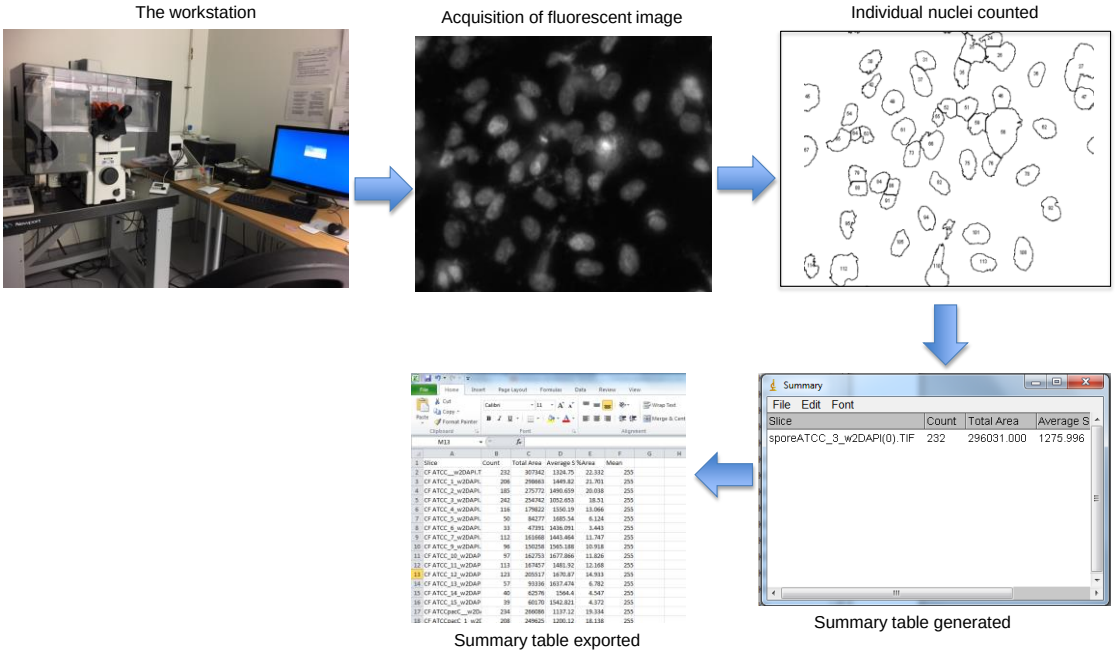

Figure 2.1: Steps in quantification of cell detachment following fungal challenge

DAPI stained adherent A549 nuclei are captured with the fluorescing microscope. The images are exported and counted with the Fiji macro, which generates a summary table of the number, size and area of each nucleus in every image counted. The summary table is then exported to excel for plotting and analysis.

2.2.8 Reverse transcription quantitative polymerase chain reaction (RT-qPCR) methods and genetic silencing

2.2.8.1 Extraction of gDNA

Genomic DNA was extracted using the QIAgen's DNeasy Blood and Tissue Kit according to the manufacturer's instruction. Monolayer of $1x10^6$ cells grown in cell culture media were detached with 200 µl of Trypsin-EDTA. Cell suspension was centrifuged for 5 mins at 300xg. Proteinase K (supplied) was added to the pellet resuspended in 200 µl of PBS followed by 200 µl of buffer AL. The suspension was mixed thoroughly by vortexing and incubated at 56^oC for 10 mins. After incubation, 200 µl of absolute ethanol was added and mixed by vortexing to a homogenous solution. The mixture was then pipetted into a DNeasy mini spin column placed in a 2 ml collection tube and spun at 8000 rpm for 1 min. The flow through and collection tube was discarded and 500 µl of AW1 buffer was added directly to the DNeasy mini

spin column placed on a new 2 ml collection tube and spun at 8000 rpm for 1 min. Again, the flow through and collection tube was discarded and the DNeasy spin column transferred to a new 2 ml collection tube. A 500 µl of AW2 buffer was added to the spin column and spun for 3 min at 13500 rpm to dry the column. The DNeasy spin column was transferred to a new 1.5 ml tube and 100 µl of AE buffer was added directly onto the DNeasy membrane. The DNeasy spin column was incubated for 1 min at room temperature and then centrifuged for 1 min at 800 rpm to elute the DNA.

2.2.8.2 Extraction of Total RNA

Total RNA was extracted from A549 cells using the QIAgen RNeasy mini plant kit according to the manufacturer's protocol for purification of total RNA from animal cells using spin technology. A monolayer of $2.5x10^5$ cells grown in cell culture medium was washed with 1 ml of PBS. A 350 µl of lysis buffer RLT containing β-mercaptoethanol (B-ME) at a concentration of 10 µl B-ME per ml of RLT was added to the washed monolayer. The cells were scraped off and transferred directly into a QIAshredder spin column placed in a 2 ml collection tube and centrifuged for 2 min at 13600 rpm to remove cellular debris. The filtration column was discarded and the filtered lysate was mixed with an equal volume of 70% ethanol by pipetting. Lysate-ethanol mixture was transferred into an RNeasy spin column placed in a 2 ml collection tube and centrifuged for 15 sec at 10000 rpm. The flow through was discarded and the RNeasy spin column was washed with 700 µl of buffer RWI by centrifuging for 15 sec at 10000 rpm. The RNeasy spin column was washed again with 500 µl of RPE buffer with 100 % ethanol by spinning for 15 sec at 10000 rpm. The filtrate was discarded and the column was washed with a further 500 µl of RPE buffer followed by centrifugation at 10000 rpm for 2 min. The RNeasy spin column was carefully removed and placed in a new 2 ml collection tube and centrifuged again for 1 min at 10000 rpm to dry the column and remove any remaining trace of ethanol. Total RNA was eluted into a new 1.5 ml collection tube with 50 µl of RNase free water and 1 min centrifugation at 13000 rpm. In some instances, 30 µl of the eluate was added back onto the spin column membrane and re-eluted for maximum RNA yield.

2.2.8.3 DNase digestion and Total RNA clean up.

To remove any trace of gDNA contamination, the total RNA was treated with QIAgen RNase-free DNase set according to manufacturer's instructions. Briefly, the total RNA (≤ 87.5 µl) in 1.5 ml microfuge bottle was mixed with 10 µl buffer RDD, 2.5 µl DNase stock solution and RNase-fee water to 100 µl and incubated on the benchtop for 10 min (20-25^{o}C).

The DNase treated RNA was cleaned using the QIAgen RNeasy mini plant kit protocol for RNA clean-up. A 100 µl of treated RNA was mixed with 350 µl of RLT (without BME). A 250 µl of absolute ethanol was added to the RNA mix and mixed by pipetting. The mixture (700 µl) was transferred to an RNeasy mini spin column placed in 2 ml collection tube and spun for 15 sec at 10000 rpm. The RNeasy mini spin column was washed twice with 500 µl of RPE buffer at 10000 rpm first for 15 s and second step for 2 min. The total DNase treated RNA was then eluted into 1.5 ml microfuge as above.

2.2.8.4 Assessing RNA quality and quantity

To confirm complete DNA digestion, 1 µl of total RNA template was amplified using the SYBR Green JumpStart Taq ReadyMix PCR mix and β-actin primers. Genomic DNA was used as positive control and RNAse free water as a negative control. A DNA free template was confirmed by no amplification with the template and negative control and positive amplification with the positive control.

The RNA concentration was measured using the Take 3 Nanodrop by Biotek and synergy plate reader at UV absorption wavelength of 260-280 nm. RNA concentration in samples was extrapolated from in built standard curve whereby optical density of 1.0 at 260 nm is equivalent to 40 µg/ml of RNA. The ratio of absorbance values at 260 nm and 280 nm was used as a measure of purity where a ratio of 1.9-2.1 is considered pure.

2.2.8.5 Reverse transcription/ synthesis of complementary DNA (cDNA)

cDNA was synthesized by reverse transcription using The Invitrogen SuperScript™ VILO cDNA Synthesis Kit from 500 ng of total RNA following the manufacturer's instruction. In brief, the reaction mix was set-up according to the following table:

Component	**Quantity**
5X VILO™Reaction Mix	4 µL
10X SuperScript™ Enzyme Mix	2 µL
Total RNA	x µl (500 ng)
RNase free-water	to 20 µL

The components were mixed gently in a 0.5 ml microfuge tube and incubated at 25°C for 10 min, 42 °C for 60 min, and then terminated at 85°C for 5 min. cDNA synthesis was confirmed by qPCR first using gDNA as a positive control and nuclease free water (NFW) as negative control. The pure and undiluted cDNA were used as template for subsequent qPCR amplifications.

2.2.8.6 Primer design

Housekeeping genes were selected based on suitability, as discerned from published information. Three genes: β-actin, (ACTB), glyceraldehyde-3-phosphate dehydrogenase (GA3PDH) and phospholipase A2 (YWHAZ) were used for qPCR optimization. Primers for these genes in addition to the target gene NF-kB inducible kinase (NIK) were designed to span the exon-exon boundaries. The genebank (NCBI) gene ID for the genes were retrieved and submitted to Primerbank with the search option set to NCBI gene ID, *Homo sapiens*. The primer sequences retrieved were ordered as desalted oligonucleotides in tube from Sigma-Aldrich website (Table 2.3) and reconstituted to 100 µM according to supplier's instruction.

Table 2.3: List of oligonucleotides used in this study

Gene	Primer sequence (5'-3')	Melting Temperature
NIK Forward	CCACCTTTTCAGAACGCATTTTC	60.8
NIK Reverse	GTAGCATGGGCCACATTGTTG	61.9
β-actin Forward	GGCTGTATTCCCCTCCATCG	61.8
β-actin Reverse	CCAGTTGGTAACAATGCCATGT	61.1
YWHAZ Forward	CCTGCATGAAGTCTGTAACTGAG	60.6
YWHAZ Reverse	GACCTACGGGCTCCTACAACA	63.0
GAPDH Forward	ACCACAGTCATGCCATCAG	60.9
GAPDH Reverse	TCCACCACCCTGTTGCTGTA	61.8

Table 2.4: Composition of qPCR reaction mix per reaction

Reagent	**Volume/reaction (µl)**
SYBR green Mix	10
Primer F1	1
Primer R1	1
DPEC/NFW	6
Total	18

2.2.8.7 Real time quantitative polymerase chain reaction (RT-qPCR)

RT-qPCR was performed using the SYBR Green JumpStart Taq ReadyMix by Sigma-Aldrich. Primers were diluted to 10 µM concentrations and PCR master mix was prepared for each primer duplex following the manufacturer's instructions for SYBR Green JumpStart Taq ReadyMix use according to the formula below:

18 µl of master mix was aliquoted into the designated wells of a PCR 96 well plate followed by 2 µl of cDNA template or gDNA positive control or RNase-free water for negative control (NTC). For each primer duplex. To generate standard curves for assessing amplification efficiency, a series of five 5-fold dilutions of gDNA were prepared ranging from 625 ng/ul to 1 ng/ul per reaction with each dilution prepared in triplicate.

qPCR thermos-cycling was performed using a 7500 Fast Real-Time PCR system with applied Biosystems software version 2.0.1 with a 2 min hot start/hold step at 94°C, followed by 40 cycles of 15 sec denaturation at 94°C, 1 min annealing and extension at 60°C. Melt curve was performed with initial denaturation step at 95°C for 15 sec followed by annealing step at 60°C for 1 min (Table 2.5). The mean Ct values for samples and controls were calculated.

Table 2.5: qPCR amplification steps and conditions

Step	**Temperature (°c)**	**Time**	**Cycles**
Initial denaturation	94	2 min	1
Denaturation	94	15 sec	30
Annealing	60	1 min	
Extension	60	1 min	
Melt curve **Initial denaturation** **Annealing**	 95 60	 15 sec 1 min	 2

For standard curve generation, the mean Ct values of each dilution were plotted (y-axis) against the concentration in a line graph. The amplification efficiency (E) was calculated as:

E= 10^(-1/m)

Where

m= slope of the line,

E= efficiency of amplification

The reaction conditions were optimized such that for each of the primer duplexes, the E values are within 10% of each other and as close as possible to 2.

To calculate the relative gene expression level, the delta-delta Ct method was used. The mean Ct values for the experimental gene were normalized to mean Ct values for house-keeping genes using the formula below:

i. Calculate Δ*C*t:

ii. $\Delta C\text{t}[\text{Control}] = C\text{t}T - C\text{t}R$ (1) *where CtT and CtR are mean Ct values for target gene(NIK) and Reference gene (B-actin, GAP3DH or* YWHAZ) respectively

iii. $\Delta C\text{t}[\text{Experimental}] = C\text{t}T - C\text{t}R$ (2)

iv. Calculate *C*t: $\Delta\Delta C\text{t} = (1) - (2)$ (3)

v. Fold change = $2^{(\Delta\Delta C\text{t})} = 2^{((3))}$

2.2.9 siRNA forward transfection

Non-canonical NF-κB signalling was inhibited by genetically silencing the upstream NF-κB inducing MAP3K14 kinase (NIK) using 10 nM stealth RNAi interference siRNA and Lipofectamine RNAimax (ThermoFisher Scientific, UK) in a forward transfection according to the manufacturer's instructions.

A day before transfection, $3x10^4$ A549 cells were seeded in 500 µl of cell culture medium without antibiotics in each well of a 24 well plate. On the day of infection, RNAi duplex-Lipofectamine RNAimax complexes were prepared as follows: 20 µM RNAi stock was diluted 10 fold to a concentration of 2 µM, 3 µl (6 pmol) of the 2 µM stock was diluted in 50 µl OptiMem reduced serum medium with gentle mixing. Lipofectamine RNAimax was gently mixed and 1 µl was diluted in 50 µl of OptiMem reduced serum Medium with gentle mixing.

The RNAi duplex and Lipofectamine RNAimax were mixed together and incubated for 10-20 min at room temperature. A 100 µl of the RNAi duplex-Lipofectamine RNAimax complexes was added to each well (30-50% confluent) giving a final concentration of 10 nM RNAi. The reaction was mixed by gentle rocking before incubation for 24 h and 48 h at 37°C with 5% CO_2. A non-targeting siRNA sequence treated exactly as the RNAi and at the same concentration was used as a negative control for non-specific or off-target effects.

Efficiency of knockdown was assessed by RT-qPCR.

2.2.10 Statistics

Summarised data were analysed using GraphPad Prism version 7 and the results expressed as mean ± SEM. The difference between treatment means was determined using one way or two way ANOVA or unpaired two-tailed student T test as specified. In all cases, $p < 0.05$ was taken as statistically significant. All experiments were performed independently at least three times each in duplicate or triplicate.

2.11 Bibliography

BERTUZZI, M., SCHRETTL, M., ALCAZAR-FUOLI, L., CAIRNS, T. C., MUNOZ, A., WALKER, L. A., HERBST, S., SAFARI, M., CHEVERTON, A. M., CHEN, D., LIU, H., SAIJO, S., FEDOROVA, N. D., ARMSTRONG-JAMES, D., MUNRO, C. A., READ, N. D., FILLER, S. G., ESPESO, E. A., NIERMAN, W. C., HAAS, H. & BIGNELL, E. M. 2014. The pH-Responsive PacC Transcription Factor of *Aspergillus fumigatus* Governs Epithelial Entry and Tissue Invasion during Pulmonary Aspergillosis. *PLoS Pathog,* 10**,** e1004413.

DA SILVA FERREIRA, M. E., KRESS, M. R., SAVOLDI, M., GOLDMAN, M. H., HARTL, A., HEINEKAMP, T., BRAKHAGE, A. A. & GOLDMAN, G. H. 2006. The akuB(KU80) mutant deficient for nonhomologous end joining is a powerful tool for analyzing pathogenicity in *Aspergillus fumigatus*. *Eukaryot Cell,* 5**,** 207-11.

HEARN, V. M. & MACKENZIE, D. W. 1980. The preparation and partial purification of fractions from mycelial fungi with antigenic activity. *Mol Immunol,* 17**,** 1097-103.

KUPFAHL, C., HEINEKAMP, T., GEGINAT, G., RUPPERT, T., HARTL, A., HOF, H. & BRAKHAGE, A. A. 2006. Deletion of the gliP gene of *Aspergillus fumigatus* results in loss of gliotoxin production but has no effect on virulence of the fungus in a low-dose mouse infection model. *Mol Microbiol,* 62**,** 292-302.

LOTHER, J., BREITSCHOPF, T., KRAPPMANN, S., MORTON, C. O., BOUZANI, M., KURZAI, O., GUNZER, M., HASENBERG, M., EINSELE, H. & LOEFFLER, J. 2014. Human dendritic cell subsets display distinct interactions with the pathogenic mould *Aspergillus fumigatus*. *Int J Med Microbiol,* 304**,** 1160-8.

MONOD, M., PARIS, S., SARFATI, J., JATON-OGAY, K., AVE, P. & LATGE, J. P. 1993. Virulence of alkaline protease-deficient mutants of *Aspergillus fumigatus*. *FEMS Microbiol Lett,* 106**,** 39-46.

SCHINDELIN, J., ARGANDA-CARRERAS, I., FRISE, E., KAYNIG, V., LONGAIR, M., PIETZSCH, T., PREIBISCH, S., RUEDEN, C., SAALFELD, S., SCHMID, B., TINEVEZ, J. Y., WHITE, D. J., HARTENSTEIN, V., ELICEIRI, K., TOMANCAK, P. & CARDONA, A. 2012. Fiji: an open-source platform for biological-image analysis. *Nat Methods,* 9**,** 676-82.

CHAPTER 3: TEMPORAL BASIS OF EPITHELIAL CELL DAMAGE IN RESPONSE TO *A. FUMIGATUS* SPORES AND CULTURE FILTRATE

3.1 Introduction

Aspergillus fumigatus is the major cause of human fungal lung disease, associated with ~200000 human fatalities on annual basis (Brown et al., 2012). Current understanding of epithelial-*A. fumigatus* interaction (Table 1.6) has been compiled from multiple, mostly single time point, studies which have used a range of different epithelial cell types and varying *A. fumigatus* morphotypes (Osherov, 2012). Bertuzzi et al (2014) previously demonstrated that *A. fumigatus*-mediated epithelial perturbations occur in two mechanistically distinct stages: early contact-dependent detachment, and late detachment due to soluble factors. To date, however, there is insufficient temporal insight into early host-mediated events, particularly for time-points relevant to study of host responses. As a result, the temporal basis of epithelial responses to *A. fumigatus* and the relative contributions of pathogen and host activities to epithelial damage remain only partially characterised. In order to determine the events occurring across the continuum of interaction with alveolar epithelial cells on a temporal and dynamic basis, the gross morphology of epithelial integrity was studied over a time series of interactions with live *A. fumigatus* spores and culture filtrate (CF). In addition, the induction of epithelial decay was also studied in more detail in order to precisely decipher the relative contribution of intact fungal cells or secreted fungal products in eliciting epithelial damage.

The airway epithelium is a tightly packed cellular barrier conferring physical protection against respiratory insults such as inhaled spores. The cilia and ciliary escalator movement in the bronchial region of the airway sweeps inhaled substances away from the airways in a backward movement (Knowles and Boucher, 2002) while the tight junctions seal adjacent epithelia cells thereby limiting the paracellular passage of particles, molecules and ions as well as restricting the movement of integral proteins between the apical and basolateral surfaces. The barrier function of airway epithelium is highly dependent on heteromeric protein complexes known as tight junctions (TJs), (Schlingmann et al., 2015). TJs maintain epithelial barriers by

connecting neighbouring epithelial cells with each other by forming a sealed interface. In humans, there are 27 claudin proteins with relative molecular weights of between 21 and 34 kDa. Of these, only claudins-1,- 3,-4,-5, 7, -8 and 18 have been confirmed to be expressed in human lung (Mitchell et al., 2011). Claudin 18 is the only member that is highly and specifically expressed by alveolar epithelium mostly by AT I cells but not by the bronchial epithelium (LaFemina et al., 2014). Claudins are also embodied with additional roles in the lung. For example, claudin-7 can interact with the human integrin beta1 receptor in the lung to suppress tumor growth in mouse lung and human cancer cells (Lu et al., 2015). Claudin-7 appears to play a role in cell detachment as re-introducing claudin-7 upregulates integrin β1 expression, increases the ability of cells to adhere to culture plates and to grow as monolayers (Lu et al., 2015).

Various models have been developed for *in vitro* study of bronchial and alveolar airway infections. Bronchial models have utilised cultured immortalized BEAS-2B and HBE (Balloy et al., 2008, Fekkar et al., 2012) or cancerous (H292 and Calu-3) human bronchial epithelial cell lines (Foster et al., 2000, Hirakata et al., 2010, Oguma et al., 2011). Models of alveolar airway infection have been limited by difficulties in isolating and culturing primary type I and II cells. To date, most of the available studies on alveolar infections have been performed using the lung carcinoma derived type II-like A549 cells (Lieber et al., 1976) which account for less than 5% of the alveolar surface. However, type II cells actually outnumber type I cells, and are responsible for multiple important functions including: first line protection against respiratory pathogens, maintenance of lung homeostasis as well as regeneration of alveolar type I cells (Guillot et al., 2013, Wong and Johnson, 2013). As a disadvantage, pro-longed passaging and co-culture of A549 could lead to changes in expression of cellular proteins especially the intracellular signalling responses as a result of mutagenesis, thereby necessitating the confirmation of results with other models (Zhang et al., 2017).

In the absence of a more stable or physiologically relevant model, and in the interest of modelling an invasive airway infection, the experimental model used in this study is the A549 epithelial cell line except for the measurement of trans-epithelial electrical resistance (TEER) assays where the Calu-3 model was used. Calu-3 (ATCC® HTB-55™) is a human bronchial adenocarcinoma epithelial cell line derived from a metastatic pleural site in a 25-year-old Caucasian male. Calu-3 is known to have the ability to secrete serous fluid and can form tight junctions in monolayers when cultured at an air-liquid interface (Hirakata et al., 2010, Foster et al., 2000). Calu-3 monolayers also exhibit features that closely mimic differentiated human airway epithelium such as cilia production and glycoprotein secretion (Grainger et al., 2006), bicarbonate secretion (Lee et al., 1998), junctional complexes and high trans-epithelial electrical resistance (Shen et al., 1994). As a result of their physiology Calu3 models are often regarded as providing a useful model for study of tight junction integrity.

Specific objectives of the work described in this chapter were to:

- Establish a dynamic model of epithelial cell interaction with different morphogenic states of *A. fumigatus*.
- Develop an automated ImageJ based macro for quantitation of epithelial cell detachment and fungal burden.
- Determine the sequence of events/processes leading to loss of epithelial barrier integrity.
- Identify the impact of different fungal morphotypes in eliciting damage events.

3. 2 Methods

3.2.1 Optimization of CF and spore dosing

Due to difficulties in handling *in vitro Aspergillus* infections for longer than 24 hours, CF from 16, 24, 48, and 72 h *A. fumigatus* cultures were made according to section (2.2.2.5) to stimulate, as well as mimic some aspects of the host-fungal interaction during late phases of infections. CF was added to epithelial cell monolayers either neat or in 5 fold, 10 fold or 50 fold dilutions in order to determine the best conditions for measuring damage reproducibly.

3.2.2 Microscopic imaging and estimation of fungal growth rate on epithelial cells

A549 monolayers were incubated with freshly harvested tdTomato *A. fumigatus* spores for different times from 0 h up to 24 h. Upon removal of culture media and a triple wash with PBS, *A. fumigatus* infected monolayers were incubated with 1 ml of supplemented RPMI-1640 containing 1 µg/ml Concanavalin A conjugated to FITC (Con-A, Sigma) for 30 min at 37°C and 5% CO_2. Wide-field epifluorescence microscopy was performed using a Nikon Eclipse TE2000-E microscope (Nikon Instruments, Europe BV, UK) and a Nikon PlanFluor 20x/0.75 NA objective lens. A CoolLED PreciseExcite system (CoolLED, Andover, UK) was used with 470 nm and 550 nm LED arrays for FITC and tdTomato excitation, respectively. Images were captured with an ORCA-ER CCD camera (Hamamatsu, Welwyn Garden City, UK) driven by MetaMorph software v7.7.6.0 (Molecular Devices, Sunnyvale, CA, USA). Fungal biomass was quantified at each infection time point, where cumulative spore diameters and filament lengths (including branches) were measured in FIJI (Schindelin et al., 2012) from representative images and averaged. At least 20 measurements were taken for each time point.

3.2.3 Measurement of trans-epithelial electrical resistance (TEER) of cultured Calu-3 monolayers

1 ml of a $1x10^6$/ ml suspension of Calu3 cells (ATCC, Rockville, MD) was cultured in D-MEM/F-12 (1X) (Thermo-Fisher Scientific) supplemented with 10% Fetal Bovine Serum (Sigma-Aldrich) and 1% Penicillin-Streptomycin (10,000 units penicillin and 10 mg streptomycin/ml, Sigma-Aldrich) in a trans-well insert (Scientific Laboratory Supplies (SLS)). The insert was placed in a 12 well special tissue culture plate (Scientific Laboratory Supplies) containing 2 mL of supplemented DMEM-F12 previously warmed to 37 °C using sterile forceps. Cells were incubated at 37°C and 5% CO_2. Media was changed every 2 days while TEER was measured every 4 days until TEER reached at least 1000 Ωcm^{-2} (~11 to 13 days) as measured with a World Precision Instrument Evom2 epithelial voltohmeter and STX-2 electrode. To measure TEER, the probe of the voltohmeter was sterilized in 70 % ethanol followed by a rinse in sterile water. The probe was gently placed into the trans-well insert such that the long arm sat in the outer well content while the shorter arm was immersed in the insert media without touching the base of the insert. To change the media, the medium in the insert was carefully aspirated with a P1000 Gilson pipette while holding the insert in place with sterile forceps. The insert was then transferred to fresh pre-warmed media (2 ml) in a new 12 well culture plate followed by addition of 1 ml of supplemented medium into the insert chamber. On the day of infection, the TEER (TEER 0) was measured for time zero (T 0 h) followed by challenge with 10^5 spores or a 5 fold dilution of CF (200 µl of CF in 800 µl of media in the insert). The plate was incubated for 24 h (T 24 h) and TEER was measured again (TEER 24 h). The difference between TEER 24 h and TEER 0 h was calculated as loss in TEER due to challenge (TEER 24 h-TER 0 h) and normalised to fungal viable count. The result in most cases was expressed as fold reduction in TEER relative to PBS challenge.

Viable count = number of single fungal colonies recovered out of 100 CFU plated

Normalisation coefficient = 100 ÷ viable count

ΔTEER = (TEER 24 h-TEER 0 h) × normalisation coefficient

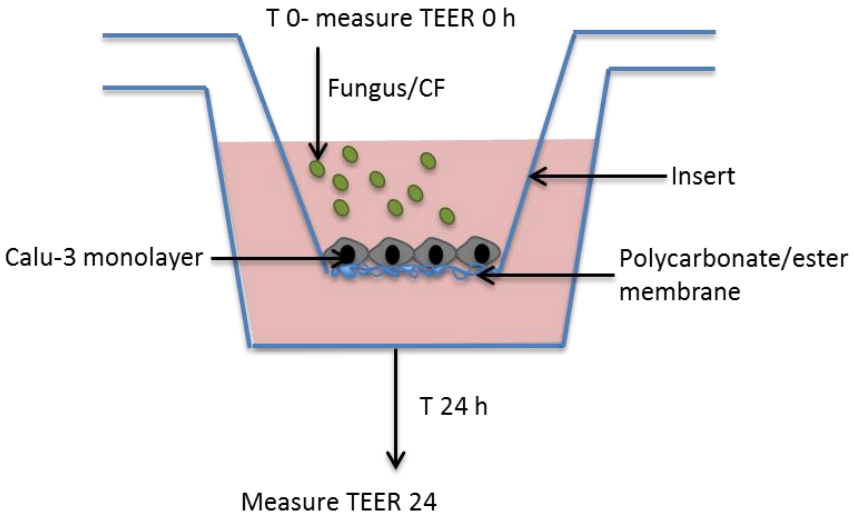

Figure 3.1 : Experimental set-up for measurement of trans-epithelial electrical resistance

TEER 0 h was recorded when TEER of cultured Calu-3 monolayers reached at least 1000 Ωcm^{-2}. For live fungal infection, 100 µl of the media in insert was discarded and replaced with 100 µl of a 10^6 spore/ml suspension. For CF challenge, 200 µl of media in the insert was discarded and replaced with an equal volume of CF[48]. The plate was covered and incubated for 24 h at 37°C and 5% CO_2. After incubation, the TEER was measured (TEER 24 h) and ΔTEER was calculated.

3.2.4 Measurement of *A. fumigatus* cytotoxicity to epithelial cells

Monolayers of A549 cells were infected with 10^3 to 10^7 *A. fumigatus* conidia or CF as indicated and incubated for different periods of time. Epithelial cell lysis was determined by measuring lactate dehydrogenase (LDH) activity in the culture supernatants after predetermined times of incubation, using the Cytox 96 Non-Radioactive Cytotoxicity Assay (Promega) according to the manufacturer's protocol and using a recombinant porcine LDH enzyme (Sigma-Aldrich) to generate a standard curve. LDH activity in culture supernatants was quantified via extrapolation from the standard curve and normalized to PBS challenge.

3.2.5 Quantitative analysis of A549 detachment

0.5 x 10^5 A549 cells were seeded in black 24 well glass bottom tissue culture plates and incubated to ≥ 90% confluency. Monolayers were challenged with 10^5 spores or a 5 fold dilution of CF (200 µl of CF in 800 µl of media). Following co-incubation, monolayers were washed 3 times with PBS, fixed with 4% formaldehyde in PBS and permeabilized with 0.2% Triton-X100. Nuclei of adherent A549 cells were stained with 300 nM DAPI. DAPI fluorescence in adherent epithelial cells was excited with a CoolLED PreciseExcite 380 nm LED array in combination with a Nikon UV-2A filter cube, which collected the DAPI emission. Adherent A549 cells were counted in at least 3 fields of view at magnifications of X20. Images were processed (Appendix 3) and quantified using an in-house "DAPI Counter" macro written for FIJI (Schindelin et al., 2012). The data was exported into Prism for graphing and analysis of significance.

3.3 Results

In order to precisely decipher the temporal basis of responses to *A. fumigatus* challenge and to distinguish the role of responses to intact fungal cells or secreted fungal products in eliciting epithelial damage, alveolar epithelial cells were challenged with either live *A. fumigatus* spores, or fungal CF derived from fungal cells cultured in shaken liquid culture for a period of up to 48 hours, and fungal cell growth rate, A549 detachment, trans-epithelial electrical resistance (TEER) or epithelial cytotoxicity (as lactate dehydrogenase release) were monitored to quantify damage during a time-series of co-incubation from 0 to 48 h. Pilot studies were done to optimise spore concentrations (10^7, 10^6, 10^5, 10^4) and time-points of morphological transitions. It was observed that the closer the spores are to each other, the slower the germination (data not shown) therefore, a 10^4 spore inoculum was chosen as optimal for the microscopy analyses.

3.3.1 Impact of *A. fumigatus* spores, germlings and hyphal morphologies on A549 epithelial monolayers

A. fumigatus spores quickly adhere to epithelial and endothelial cells which may internalize the spores. Both internalized and non-internalized spores can germinate to form hyphae (Wasylnka et al., 2005, Wasylnka and Moore, 2000, Wasylnka and Moore, 2002), ultimately leading to injury including cytoskeletal disruption, cell rounding or detachment, with proteases implicated as the major culprit (Kogan et al., 2004). To establish the relative time scales of fungal growth on epithelial cell and visible epithelial monolayer disruption, the gross appearance of epithelial monolayers infected with freshly harvested live *A. fumigatus* spores at set time-points post-infection was studied and the numbers of detaching epithelial cells quantified to measure epithelial decay. A tdTomato-expressing fluorescent *A. fumigatus* isolate and Concanavalin A-FITC stained A549 cells were used in order to differentiate between fungal cell and epithelial cells. Qualitative and quantitative analysis of fungal growth rate and epithelial monolayer architecture was performed via wide-field epifluorescence microscopy (Section 2.2.7.1). Observable changes in spore size were first seen after 4 h when most of the spores were swollen but not germinated (not

shown). Germination of *A. fumigatus* spores began at approximately 8 h (Fig. 3.2A) and was followed by a phase of rapid hyphal extension between 8 and 12 h post-infection (Fig. 3.2B). The rate of extension occurring between 16 and 24 h was not different to that occurring between 12 h and 16 h. Beyond 24 h, hyphae were too long to permit capture of entire length in a single field of view. In response to live challenge with *A. fumigatus*, gross perturbation of the monolayer architecture was first observed at 16 h post infection when the fungus is in a hyphal form (Fig 3.2A). Epithelial cell detachment from culture vessel, rounding and membrane blebbing/ruffling was evident as the interaction progressed with time to 24 h. The inter-epithelial cell outlines remained clear and intact earlier than 16 h post infection after which the cells become more rounded and difficult to separate visually from each other.

3.3.2 Impact of *A. fumigatus* secreted products on A549 epithelial monolayers

To study the effect of products secreted by the fungus beyond 24 h of growth on the epithelium, the monolayer was challenged with CF^{48} since imaging the host-fungus interaction at this stage was impractical. In contrast to challenge with live fungal spores, exposure to CF^{48} led to much more rapid epithelial decay (Fig 3.2C). The timing of epithelial decay therefore differs, according to whether challenge involves fungal spores, hyphae or secreted products. These findings concur with a previous study (Bertuzzi et al., 2014) and indicate that *A. fumigatus*-mediated epithelia decay first occurs via a contact dependent mechanism and subsequently via soluble secreted molecules.

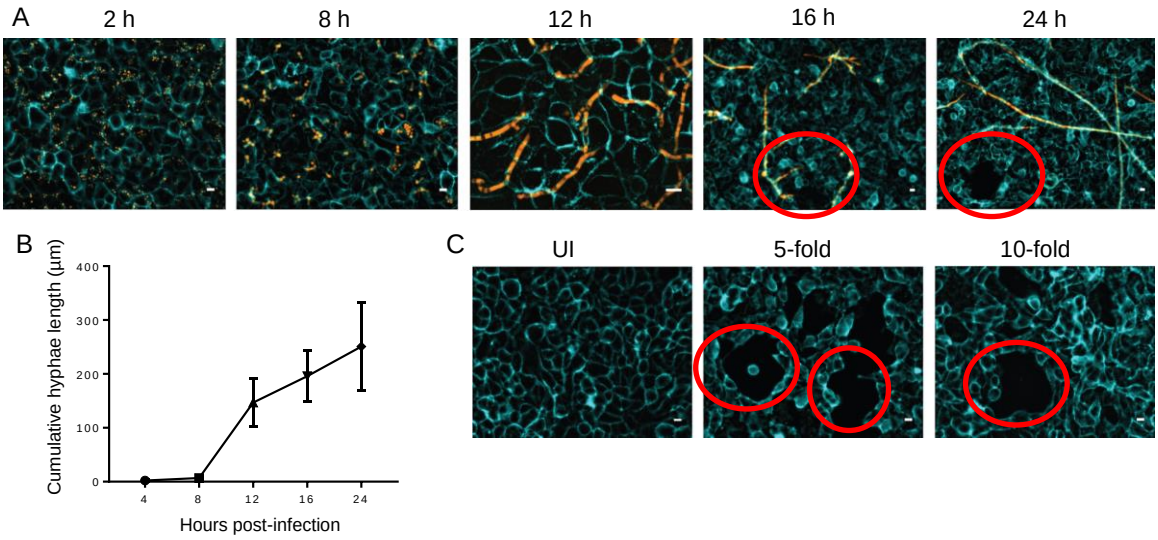

Figure 3.2: Temporal basis of epithelial decay following challenge with live *A. fumigatus* spores or CF

Concanavalin A-FITC labelled A549 cells incubated in RPMI-1640 were infected with an *A. fumigatus* tdTomato-expressing ATCC46645 isolate. (A) Growth of *A. fumigatus* spores during interaction with confluent epithelial monolayer at indicated time post-infection B) Cumulative hyphal length of tdTomato^{ATCC46645}-expressing *A. fumigatus* at different times post incubation with A549 epithelial cell C) Degradation of ConA-FITC stained A549 cells exposed to indicated concentrations of CF[48] for 4 h.

3.3.3 *A. fumigatus* spores and CF induce monolayer detachment via distinct mechanisms

Bertuzzi et al (2014) reported that *A. fumigatus* challenge resulted in extensive rounding and detachment of up to 40% of cultured A549 cells after a 16 h of co-incubation. However, a single time-point analysis offers little insight on the early events occurring during host-*A. fumigatus* interaction. Moreover, 16 h post infection may be too late to accurately capture all host responses to fungal challenge. To elaborate on events occurring from as early as 4 h post-infection, at which point the fungus is still a spore, epithelial cell detachment from the monolayer was observed in response to fungal growth, with disintegration of the monolayer being the major visual outcome of fungal challenge (red circles in Fig 3.2A). In order to quantify

epithelial cell detachment over the course of the interaction, a confluent monolayer of A549 cells challenged with *A. fumigatus* spores or CF^{48} was assessed for a series of time points and the percentage of A549 cells detached from the monolayer was calculated according to section (2.2.7.2).

In response to challenge with live *A. fumigatus* spores, significant detachment of host cells (20%) from A549 monolayers was first observed at 4 hours of co-incubation (Fig 3.3A) compared to 5% with PBS. Detachment increased as a function of time throughout the assay reaching about 50% after 16 h. Similar behaviours were observed following challenge with spores of Δ*akuB*^{KU80} strain (Fig 3.3B). To assess the impact of secreted products on epithelial detachment, confluent A549 monolayers were exposed to CF^{16} and CF^{48} representing the secretomes of young and mature hyphae respectively. In contrast to live fungal challenge at 16 h post-infection (Fig 3.3), enumeration of detached cells in response to challenge with CF^{16} revealed a failure to detach A549 cells from the monolayer (Fig 3.4A). CF^{48}, at a 5 fold dilution, elicited detachment of over 50% of cells as early as 4 h post challenge reaching over 80% after 12 h (Fig 3.4C). This response is not strain specific as similar behaviours were observed following challenge with CF^{48} derived from Δ*akuB*^{KU80}strain (Fig 3.4D). These data concur with previous findings (Bertuzzi et al., 2014) that detachment of A549 cells from monolayers in response to live spores is initially elicited via a contact-mediated process followed by propagation of damage by secreted products from mature hyphae.

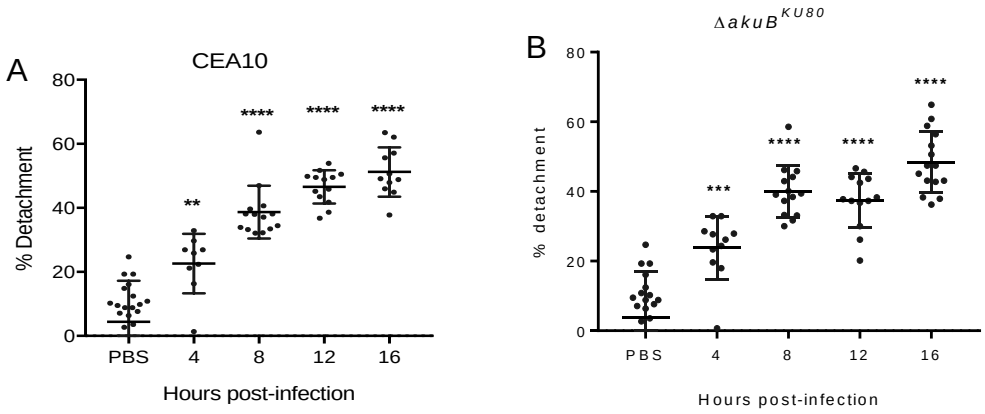

Figure 3.3: Quantitative analysis of epithelial monolayer detachment following infections with live *A. fumigatus* spores. Percentage detachment of A549 cells enumerated with ImageJ software A) challenge with 10^5 spores of *A. fumigatus* CEA10 over a 16 h time series B) Comparison of percentage detachment following infection with Δ*akuB*^{KU80} *A. fumigatus* isolate over a 16 h time series. Data represent the mean of three biological replicates (each comprised of three technical replicates). Error bars show ± SD from the mean values. Data were analysed by one-way ANOVA with Dunnett's multiple comparisons test. Significance was calculated relative to challenge with vehicle control (PBS) unless otherwise stated *, **P<0.01, ***P<0.001, ****P<0.0001.

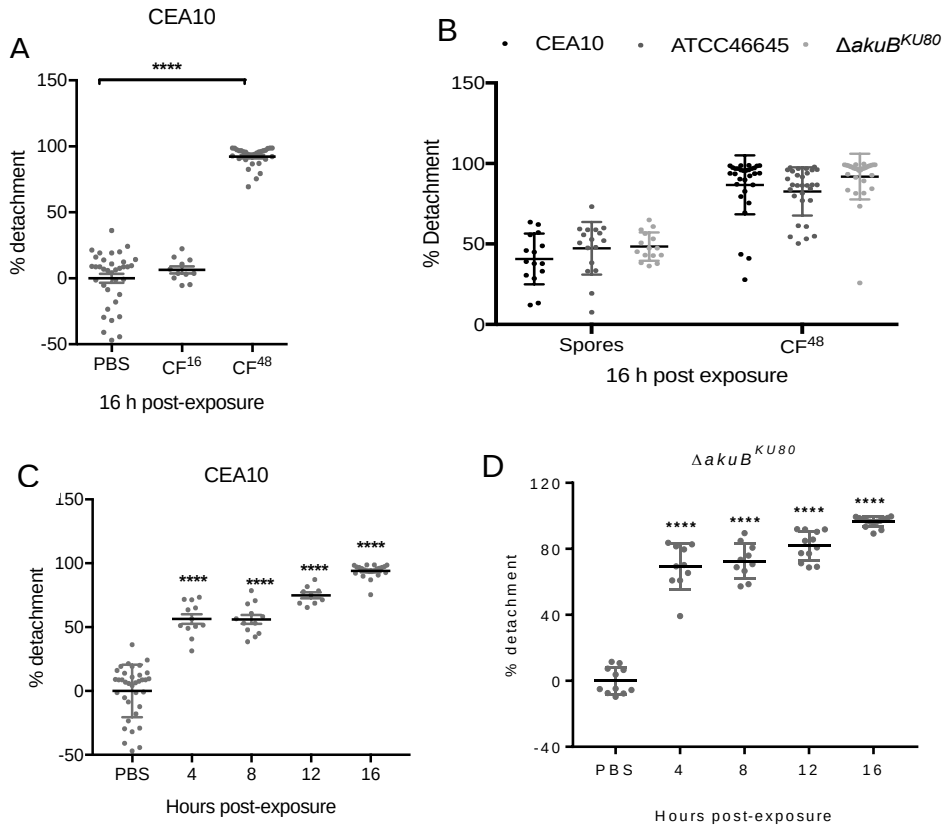

Figure 3.4: Quantitative analysis of epithelial monolayer detachment following exposure to culture filtrate (CF). Percentage detachment of A549 cells enumerated with ImageJ software following challenge with A) Fungal culture filtrate (10^6 spores/ml) grown for 16 h neat (CF^{16}) or 48 h 5 fold dilution (CF^{48}), B) Live fungal spores versus CF^{48} for three different *A. fumigatus* clinical isolates C) Time series of epithelial detachment following exposure to CEA10 CF^{48}. D) Time series of epithelial detachment following exposure to Δ*akuB*^{KU80} CF^{48}. Data represent the mean of three biological replicates (each comprised of three technical replicates). Error bars show ± SEM. Data were analysed by one-way ANOVA with Dunnett's multiple comparisons test. Significance was calculated relative to challenge with vehicle control (PBS) unless otherwise stated ***P<0.001, ****P<0.0001.

3.3.4 Induction of lytic epithelial cell damage by *A. fumigatus* spores and CF

To determine whether epithelial detachment correlated with lytic cell death, the release of lactate dehydrogenase (LDH), into the culture supernatant was measured. Triton was used as a positive control to optimize cell membrane lysis whereas fungal monoculture was as negative control during experimental optimization to ensure that LDH activity is solely as a result of fungal challenge. LDH release from A549 cells in response to live challenge with 10^6 *A. fumigatus* spores reached statistical significance at 12 h post-infection (Fig 3.5A, also expressed as fold change relative to PBS challenge in Fig 3.5B) thereby correlating with hypha development (Fig 3.2A). Epithelial damage increased with increasing fungal inoculum (Fig 3.5A and B) demonstrating dose-dependency of damage. Again, this response was observed irrespective of the strain used (Fig 3.5C and 3.5D). In contrast, exposure of A549 cells to CF^{48} prompted a rapid time- and dose-dependent increase in lytic cell death (Fig 3.6A) reaching statistical significance at 2 h post-exposure (Fig 3.6B). Notably, as with epithelial detachment, CF^{16} did not induce lytic epithelial cell death (Fig. 3.6C). Together, these data indicate that during initial infection, *A. fumigatus* spores are able to elicit epithelial cell detachment in a contact-dependent manner. However, as infection progresses, secreted products from *A. fumigatus* hyphae (as represented by CF^{48}) induce further epithelial detachment and lytic cell death, in what would appear to be a mechanistically different process.

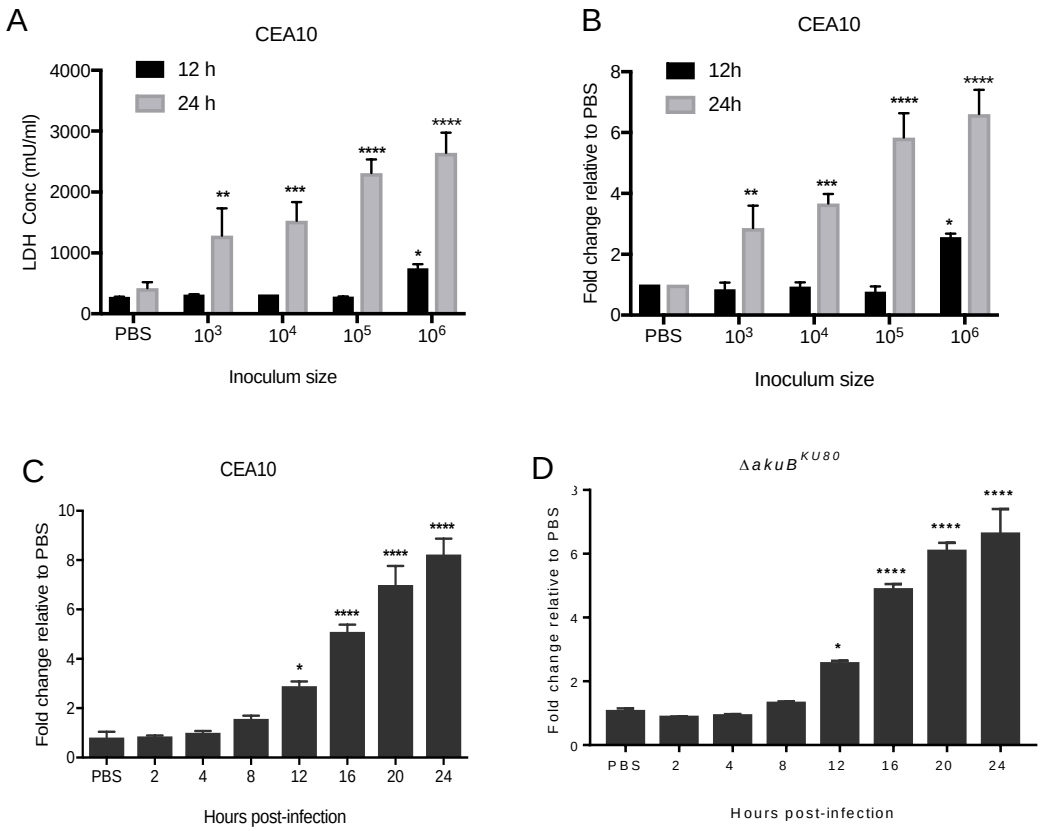

Figure 3.5: Quantification of lytic cell death in A549 epithelia in response to live *A. fumigatus* spores. Lytic cell death was quantified via lactate dehydrogenase activity in culture medium following infection of A549 cells with live *A. fumigatus* spores A) Amount of LDH activity (mU) detected 12 h and 24 h post infection with indicated spore numbers relative to PBS challenge B) Fold change in LDH released 12 h and 24 h post infection with indicated spore numbers relative to PBS challenge B) Fold change in LDH released in response to infection with 10^6 live CEA10 spores C) Fold change in LDH released in response to infection with 10^6 live CEA10 spores D) Fold change in LDH released in response to infection with 10^6 live Δ*akuB*^{KU80} spores Data represents the mean of three biological replicates (three technical data set each). Error bars show ± SEM. Data were analysed by one-way ANOVA with Dunnett's multiple comparisons test. Significance was calculated relative to challenge with vehicle control (PBS) unless otherwise stated *P<0.05, **P<0.01, ***P<0.001, ****P<0.0001.

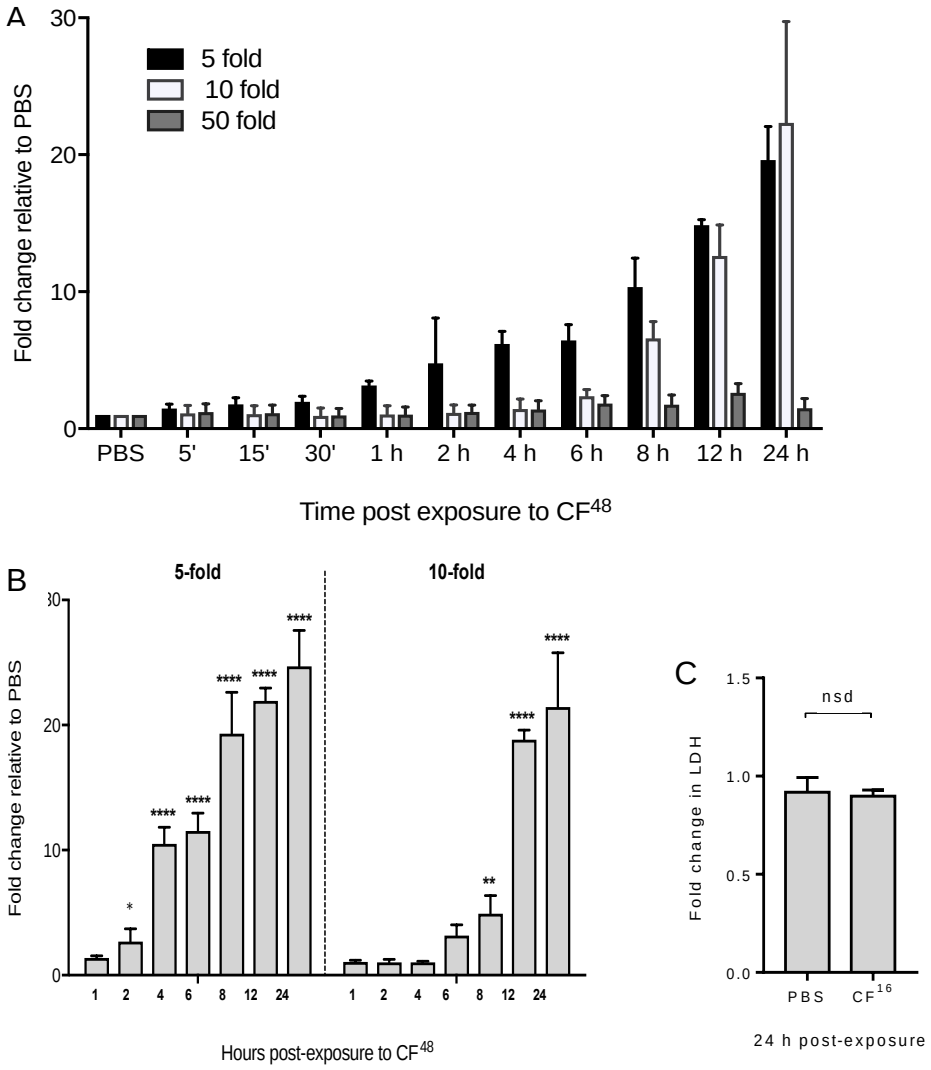

Figure 3.6: Quantification of lytic cell death in A549 epithelia in response to *A. fumigatus* culture filtrate. Lytic cell death was quantified via lactate dehydrogenase activity in culture medium following A549 cell exposure to CF from clinical *A. fumigatus* isolate CEA10. A) Lytic cell death of A549 epithelia following exposure to indicated dilutions of CF^{48} for indicated time post exposure expressed as fold change relative to PBS challenge B) Statistical analysis of fold change in lytic epithelial cell death measured 24 h post exposure to 5 fold and 10 dilution of CF^{48} relative to PBS C) Fold change in lytic cell death due to PBS challenge or CF^{16} is indistinguishable. Data represent the mean of three biological replicates (comprised of three technical replicates each). Error bars show ± SEM. Data were analysed by one-way ANOVA with Dunnett's multiple comparisons test. Significance was calculated relative to challenge with vehicle control (PBS) unless otherwise stated *P<0.05, **P<0.01, ***P<0.001, ****P<0.0001.

3.3.5 *A. fumigatus* spore or CF challenge leads to loss of trans-epithelial electrical resistance in a Calu-3 trans-well model of infection

The upper respiratory epithelial layer consists of differentiated, polarized epithelial cells joined together by tight junctions (TJs) which also exclude respiratory pathogens (Fig 1.7). To invade underlying tissues, *A. fumigatus* must penetrate this barrier. An *in vitro* assay based on culturing Calu-3 cells at an air-liquid interface has been previously optimized as a representative model of the upper airway epithelial barrier (Grainger et al., 2006) and is commonly used to study epithelial barrier integrity upon respiratory infections. The Calu-3 trans-well model has been successfully used to investigate the mechanism by which respiratory pathogens cross the epithelial barrier as exemplified in studies of the transcellular passage of *Neisseria meningitides* (Sutherland et al., 2010) whereby TEER was used as a proxy for tight junction integrity. To further characterise the epithelia barrier perturbations resulting from *A. fumigatus* infection, the integrity of Calu-3 monolayers following challenge with live *A. fumigatus* spores or CF was measured by monitoring changes in TEER at 24 h post challenge. Infection of monolayers with live fungal spores for 24 h reduced TEER by 5 fold relative to an uninfected monolayer (Fig 3.7A and B) whereas CF^{48} reduced TEER by only 2 to 3 fold relative to an uninfected monolayer (Fig 3.7C and D). This response was independent of the *A. fumigatus* strain (Fig 3.7E).

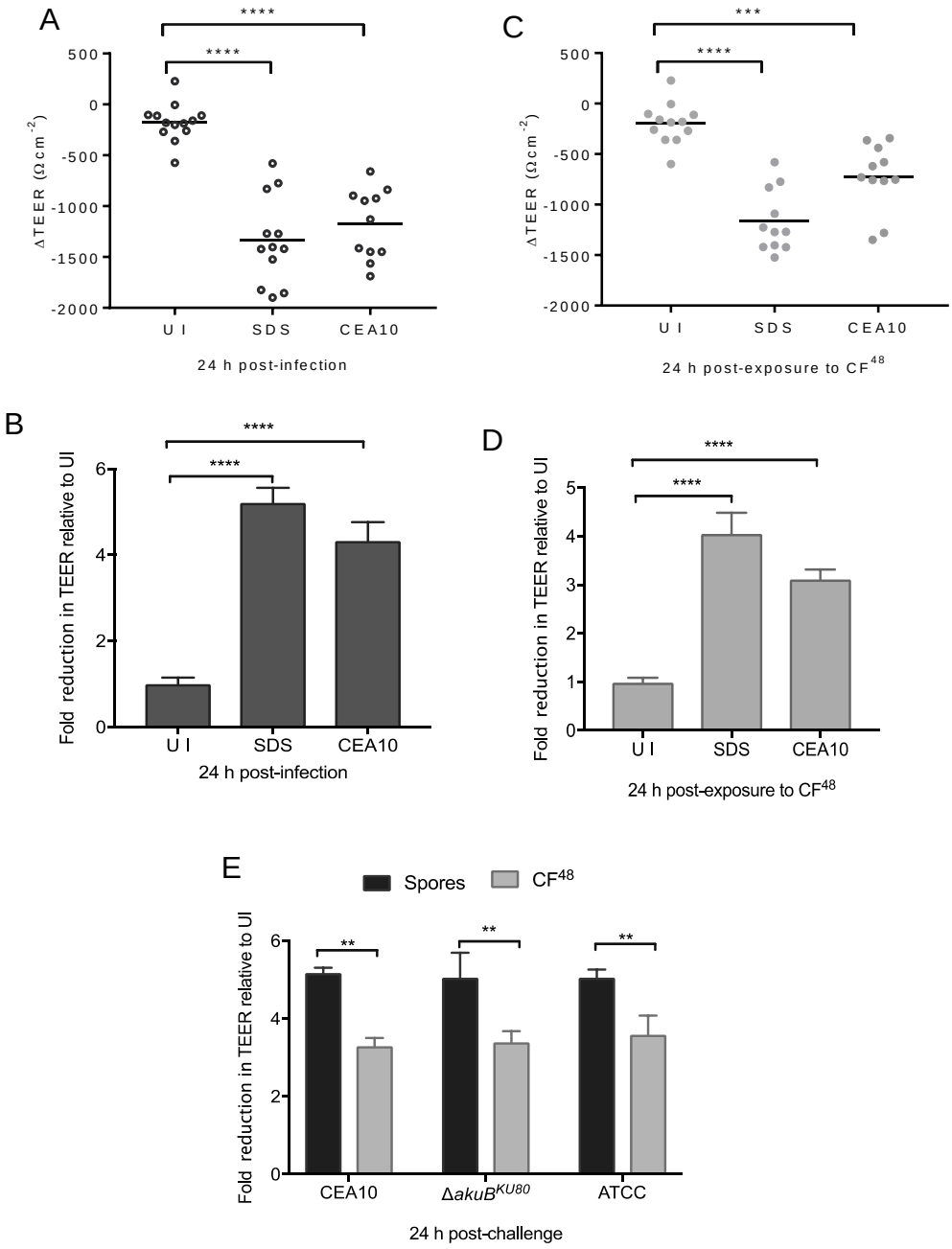

Figure 3.7: Effect of live *A. fumigatus* spore or CF challenges on trans-epithelial electrical resistance (TEER)

Calu-3 cells were grown on polycarbonate filters in a trans-well system for 11 days until TEER fell within > 1000 Ω <2000 Ωcm^{-2}. TEER was measured at 37°C before (TEER 0 h) and 24 h (TEER 24 h) following infection with 10^5 spores or a 5 fold dilution of CF for A and C) ΔTEER was calculated as (TEER 24 h-TEER 0 h) X Viable count coefficient following spore and CF challenges respectively B and D) ΔTEER expressed as fold

reduction following with 10^5 spores or a 5 fold dilution of CF relative to UI control E) Fold change in ΔTEER compared in response to 10^5 spores or a 5 fold dilution of CF in three different isolates. Shown are averages of 3 biological repeats, each performed a minimum of three times. PBS and 0.2% SDS in the media served as negative (uninfected UI) and positive controls respectively. Data represent the mean data from three biological replicates. Error bars show ± SEM. Data were analysed by one-way ANOVA with Uncorrected Fisher's LSD output. Significance was calculated relative to challenge with uninfected control (UI) ****P<0.0001.

3.4 Discussions

The integrity of the human airway epithelial barrier is essential in defining the outcome of airway epithelial cell (AEC)-*Aspergillus* interactions at the pulmonary interface. *A. fumigatus* undergoes an obligatory morphogenetic transition from inert resting spores, to antigenic germ tubes, followed by the extension of hyphae during vegetative growth. Upon contact with host cells, *A. fumigatus* adopts a phased approach to penetrate the epithelial barrier, involving: (i) Adhesion to the apical surface of epithelial cells (ii) spore internalization/endocytosis (iii) extracellular and or intracellular germination of spores on or in epithelial cells and (iv) invasion (Amitani and Kawanami, 2009). The mechanistic basis of invasion is still unclear. A previous study showed that a small proportion of internalized spores form intracellular germlings and escape from the epithelial cell phagosome through the basolateral surface into the under lying space (Wasylnka et al., 2005). Secreted products of *A. fumigatus* cause epithelial desquamation and actin depolymerisation of epithelia cells *in vitro* (Kogan et al., 2004). However, very little is known with regards to how extracellularly growing *A. fumigatus* invade the underlying tissue. Work in this chapter describes the sequence and timing of events leading to epithelial barrier decay and the relative contribution of each morphogenic state and secreted products to the process. This study is the first to conduct a fully dynamic study of morphotype-specific impacts of the host-*Aspergillus* interaction upon the airway.

Although the focus of this study was not to study the growth of *A. fumigatus*, the experimentation depicted in Fig 3.2A was necessary to guide subsequent morphotype/time dependent analyses of AEC damage and host responses. In subsequent studies, morphogenic states and/or time-points post infection were calibrated to those observed in Fig 3.2A and B, thus: 0-4 h for resting spores, 4-8 h for swollen spores, 8-12 h for germ-tubes, 12 -16 h for young hyphae, > 24 h or CF^{48} for mature hyphae or products from mature hyphae. Growth of *A. fumigatus* on epithelial cells progressed according to that expected of a classical microbial growth curve; including a lag phase, exponential phase and stationary phase (Fig 3.2B). The lag phase (time to germinate) in A549 co-culture was observed to be longer than that

previously reported for laboratory-cultured *A. fumigatus* spores. Previous reports have cited a germination efficiency of 60 % of spores at 8 h in the presence of AEC as compared to 100% germination observed in the absence of AECs (Momany and Taylor, 2000, Dague et al., 2008, Osherov and May, 2001). Various aspects of airway physiology could explain the difference between germination efficiencies in the presence or absence of AECs. For example, AECs produce antimicrobial molecules such as HBD-2 and lactoferrin both of which exhibit anti-*Aspergillus* effects (Alekseeva et al., 2009). Increase in HBD-2 mRNA and protein was induced by exposing human bronchial epithelial 16HBE cells and A549 epithelial cells to *A. fumigatus*. The biological and functional relevance of HBD-2 in *A. fumigatus* immunity was reiterated in primary culture of human respiratory cells, which upregulated HBD-2 expression in response to *A. fumigatus* (Alekseeva et al., 2009). Moreover, the population of un-germinated spores may be accountable as those internalized and possibly killed by the epithelial cells.

A549 monolayers remained visibly unaffected until about 16 h post live fungal infection or ~4 h post-exposure to CF^{48}. This finding suggests that a greater proportion of damage results from secreted fungal products than from live fungal spores. Epithelial perturbations took the form of cell rounding (Fig 3.2A) or detachment (Fig 3.2C) respectively whereby both phenotypes were demonstrable from 16 h Fig 3.2A. However, A549 detachment, as quantified using differential DAPI staining, revealed earlier epithelial disintegration with about 20% of cells detaching as early as 4 h post infection, which increased, to 50% by 16 h (Fig 3.3). Moreover, cell free CF from a 16 h culture (CF^{16}) did not induce detachment on its own. This is suggestive of a contact dependent mechanism involved in the early detachment phase. CF^{48} induced cell rounding and A549 detachment of up to 80% in less than 16 h suggesting a pivotal role for secreted products in epithelial cell detachment. These findings reiterate previous observations that *A. fumigatus* damages AECs in a biphasic manner: via initial contact dependent and subsequent secretome-mediated events (Bertuzzi et al., 2014). Importantly, this study extends the analyses previously performed by demonstrating that cell detachment is an imminent event following infection when *A. fumigatus* spores are still un-germinated suggesting the importance

of the fungal cell wall or spore-borne mycotoxins or proteins in initiating host damage following inhalation, and occurring long before germination and secretion commences. Neither resting spore, swollen spore, germ-tube nor hyphae aged 12 h or younger induced significant epithelial cell lysis relative to PBS challenge. Thus, the lysis observed between 12 h and 16 h after live fungal challenge could be derived from a contact dependent process, as CF^{16} did not induce lysis even after 24 h post exposure.

Gauthier et al identified five main spore associated toxins: tryptoquivaline F, fumiquinazoline C, questin, monomethylsulochrin and trypacidin, amongst which trypacidin was shown to be the most toxic, as evidenced by MT-mediated cytotoxicity assays and LDH quantitation in A549 and HBEC (Gauthier et al., 2012). In A549 epithelial cells, lysis was detectable as early as 1 h post exposure and was directly proportional to the dose of trypacidin used (Gauthier et al., 2012). Trypacidin triggers cell death by initiating intracellular formation of nitric oxide leading to death of the cells after about 24 h by necrosis. It will be interesting to investigate whether detachment is another mechanism of damage induced by trypacidin and whether there are other spore borne molecules involved.

Our time course analysis shows that A549 lysis increases with time suggesting that secreted products predominate as effectors of AEC death. The cell death measured by LDH is more representative of necrosis than apoptosis because of membrane lysis and loss of cytoplasmic content, just as the cell membrane lysis precedes LDH release into the supernatant (Proskuryakov et al., 2003). However, in apoptosis, the cell membrane remains intact upon division while securing the cytosolic constituents from spilling into extracellular space (Proskuryakov et al., 2003). Sharon et al (2009) showed that *A. fumigatus* secreted factors under PrtT-mediated transcriptional control are responsible, at least in part, for inducing necrotic epithelial cell death in cultured epithelia. However, the virulence of a *prtT* mutant was not attenuated in a mouse model of invasive aspergillosis suggesting that PrtT as a standalone factor is dispensable for *A. fumigatus* virulence (Sharon et al., 2009). Our findings agree with this previous observation and further confirm a central role for proteases and secreted products in lytic AEC death but implicate additional factors in *A. fumigatus*

invasiveness in whole animal model. This study extends on that performed previously by showing that soluble factors become measurably effective only after a certain threshold in hyphal maturation is crossed (occurring at or after 16 h post-infection). Another well-characterized *A. fumigatus* mycotoxin is gliotoxin, produced during hyphal growth stages (and absent from conidial extracts (Fischer et al., 2000, Gauthier et al., 2012)). Gliotoxin is well known to drive epithelial cell and macrophage rupture (Mitchell et al., 1997, Amitani et al., 1995, Eichner et al., 1986) but similar to PrtT regulated proteases, gliotoxin is not responsible for driving tissue invasion in neutropenic mouse model of invasive aspergillosis (Bertuzzi et al., 2014). *A. fumigatus* CF is likely to contain hundreds of secreted products including mycotoxins, degradative enzymes and proteases most of which are produced during hyphal growth, as evidenced by transcriptomic analyses of neutropenic mouse infection (Bertuzzi et al., 2014). Some of the cytotoxic phenotypes resulting from *A. fumigatus* CF have been characteristically linked to secreted proteases (Sharon et al., 2011, Kogan et al., 2004) or gliotoxin (Ben-Ami et al., 2009, Geissler et al., 2013). Proteases cause epithelial cell desquamation and depolymerisation of the actin cytoskeleton (Kogan et al., 2004). Cell desquamation and rounding leads to the detachment of AECs from flasks or basement membranes (Bertuzzi et al., 2014) and this study. It will now be critical to perform a thorough characterisation of all the secreted components in *A. fumigatus* CF, an objective which is being tackled in a high throughput manner currently via a library of null mutants in *A. fumigatus* secreted gene products.

There is currently little available information regarding the clinical or physiological relevance of AEC detachment and lysis in airway pathology. A previous study however, demonstrated with a CF challenge experiment that *A. fumigatus* proteases, Asp f 5 and Asp f 13 provoked strong airway inflammation and airway remodelling in an immunocopetent murine inhalation model (Namvar et al., 2015). Additionally the relevance of intestinal epithelial cell shedding and detachment within the context of various gut disorders has been studied *in vivo* (Kiesslich et al., 2012, Lai et al., 2013, Williams et al., 2013, Williams et al., 2015) to identify a direct relationship between intestinal pathology and increased epithelial cell shedding. Increases in intestinal

epithelial barrier defects were directly correlated with increased epithelial cell shedding measured by confocal endomicroscopy during inflammation in inflammatory bowel disease (IBD) patients (Kiesslich et al., 2012). The presence of gaps and microerosions in the terminal iliac surfacewas observable in the endomicroscopic images which were analysed using imageJ software (Kiesslich et al., 2012). Another study analyzed the rate of intestinal epithelial cell shedding, gap formation, and intestinal leaks in response to injected LPS in C57BL/6 mice using multiphoton microscopy (Lai et al., 2013). The result from this study demonstrated that LPS-induced epithelial cell shedding was responsible for gap formation, intestinal leaks and generalized barrier dysfunction that characterized the endotoxemia (Lai et al., 2013, Williams et al., 2013).

Our *in vitro* analysis strongly agrees with the hypothesis that detachment will enhance pathogen invasion into underlying tissues although an *in vivo* study is necessary for confirmation. Using the endomicroscopy technique, it would be possible to directly monitor bronchial or alveolar epithelial cell shedding in a mouse model following *Aspergillus* challenges. The rate and amount of AEC shedding can as well be monitored in different populations of aspergillosis patients, as the rate or amount of shedding may be different in patients with different manifestations of aspergillosis.

Our *in vitro* analyses revealed detachment of about 40% - 100% of the approximately 1 million cultured epithelial cells. Whether this number is of physiological significance when compared to the total number of alveolar cells in the human airway (about 15% of total airway cell content) or compared to the very low numbers of *A. fumigatus* spores inhaled on a daily basis, is open to discussion.

To further understand the process of hyphal invasion of sub-epithelial tissues, which was impossible with the A549 monolayer models, the integrity of Calu-3 monolayers was assessed in a trans-well model. Both infections with live *A. fumigatus* spores and CF exposure reduced the integrity of the barrier as the resistance conferred by trans-epithelial cells to movement of molecules within the two compartments was reduced. Our data shows that the impact of live fungal spores on the Calu-3-mediated

epithelial integrity is about twice that caused by CF exposure (Fig 3.7C). This finding is in line with the hypothesis that live fungal spores are involved in initiating epithelial damage, which is then further propagated by a) hyphal invasion of the epithelial layer and b) subject to effector-mediated lysis of epithelial cells. Concordant with this, the initial cell rounding and cell membrane ruffling observed prior to cell detachment may be explained by loss or decrease in expression of tight junction claudin- 7 (Lu et al., 2015). Claudin-7 appears to play a role in cell detachment as the deletion of claudin-7 in human lung cancer cells resulted in decreased integrin beta1 expression, increased cell proliferation and defects in ability to interact and adhere to the cell-matrix and culture plates (Lu et al., 2015). Re-introducing claudin-7 upregulated integrin β1 expression, increased the ability of cells to adhere to culture plates and grow as a monolayer (Lu et al., 2015), although this needs to be investigated contextually. The effect of *A. fumigatus* challenge on the expression of claudins 7 and 18 in A549 or Calu-3 cells or primary cells could be monitored by immunostaining of the proteins and microscopy or by a qPCR approach. Alternatively, the percentage of AEC detachment could be measured following knock down of specific claudins using siRNA technology. Deficiency in claudin-18 results in loss in alveolar barrier function and impaired alveologenesis in claudin-18 knockout mice and isolated lung cells (LaFemina et al., 2014). Alveolar barrier dysfunction was evidenced by significant decrease in TEER coupled with significant increase in paracellular permeability to a 0.5-kD fluorescent tracer (LaFemina et al., 2014). A paracellular permeability assay may be necessary to further characterise the alveolar epithelial barrier dysfunction following *A. fumigatus* infection.

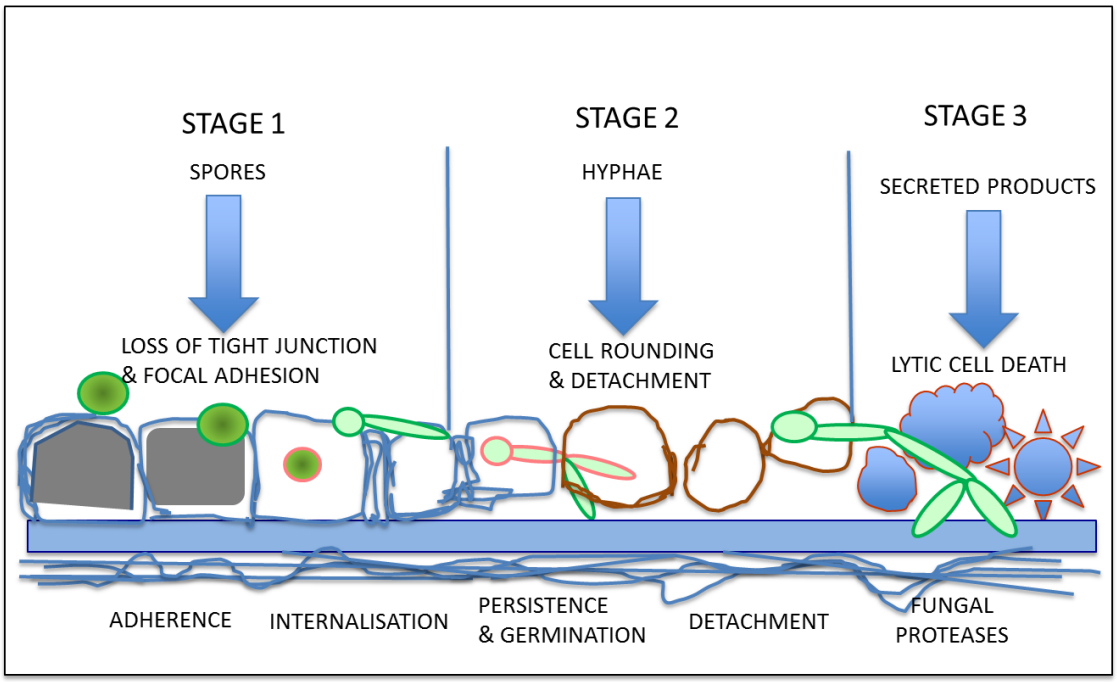

Figure 3.8: Sequence of events leading to invasion of airway epithelial barrier by *A. fumigatus*

Stage1. Fungal contact and cell wall-borne toxins initiate perturbations resulting in loss of barrier integrity and EC disaggregation leading to AEC detachment.

Stage 2. Germination of spore and exposure of epithelial cells to more varied fungal surface-associated molecules and antigens leading to complete loss of focal adhesion and rounding of individual cells. This process increases the number of detaching cells.

Stage 3. Mature growing hyphae invades the host, secrete molecules and toxins that induce more detachment and lysis of detached (suspended cells).

3.5 Bibliography

ALEKSEEVA, L., HUET, D., FEMENIA, F., MOUYNA, I., ABDELOUAHAB, M., CAGNA, A., GUERRIER, D., TICHANNE-SELTZER, V., BAEZA-SQUIBAN, A., CHERMETTE, R., LATGE, J. P. & BERKOVA, N. 2009. Inducible expression of beta defensins by human respiratory epithelial cells exposed to *Aspergillus fumigatus* organisms. *BMC Microbiol,* 9**,** 33.

AMITANI, R. & KAWANAMI, R. 2009. Interaction of *Aspergillus* with human respiratory mucosa: a study with organ culture model. *Med Mycol,* 47 Suppl 1**,** S127-31.

AMITANI, R., TAYLOR, G., ELEZIS, E. N., LLEWELLYN-JONES, C., MITCHELL, J., KUZE, F., COLE, P. J. & WILSON, R. 1995. Purification and characterization of factors produced by *Aspergillus fumigatus* which affect human ciliated respiratory epithelium. *Infect Immun,* 63**,** 3266-71.

BALLOY, V., SALLENAVE, J. M., WU, Y., TOUQUI, L., LATGE, J. P., SI-TAHAR, M. & CHIGNARD, M. 2008. *Aspergillus fumigatus*-induced interleukin-8 synthesis by respiratory epithelial cells is controlled by the phosphatidylinositol 3-kinase, p38 MAPK, and ERK1/2 pathways and not by the toll-like receptor-MyD88 pathway. *J Biol Chem,* 283**,** 30513-21.

BEN-AMI, R., LEWIS, R. E., LEVENTAKOS, K. & KONTOYIANNIS, D. P. 2009. *Aspergillus fumigatus* inhibits angiogenesis through the production of gliotoxin and other secondary metabolites. *Blood,* 114**,** 5393-9.

BERTUZZI, M., SCHRETTL, M., ALCAZAR-FUOLI, L., CAIRNS, T. C., MUNOZ, A., WALKER, L. A., HERBST, S., SAFARI, M., CHEVERTON, A. M., CHEN, D., LIU, H., SAIJO, S., FEDOROVA, N. D., ARMSTRONG-JAMES, D., MUNRO, C. A., READ, N. D., FILLER, S. G., ESPESO, E. A., NIERMAN, W. C., HAAS, H. & BIGNELL, E. M. 2014. The pH-Responsive PacC Transcription Factor of *Aspergillus fumigatus* Governs Epithelial Entry and Tissue Invasion during Pulmonary Aspergillosis. *PLoS Pathog,* 10**,** e1004413.

BROWN, G. D., DENNING, D. W., GOW, N. A., LEVITZ, S. M., NETEA, M. G. & WHITE, T. C. 2012. Hidden killers: human fungal infections. *Sci Transl Med,* 4**,** 165rv13.

DAGUE, E., ALSTEENS, D., LATGE, J. P. & DUFRENE, Y. F. 2008. High-resolution cell surface dynamics of germinating *Aspergillus fumigatus* conidia. *Biophys J,* 94**,** 656-60.

EICHNER, R. D., AL SALAMI, M., WOOD, P. R. & MULLBACHER, A. 1986. The effect of gliotoxin upon macrophage function. *Int J Immunopharmacol,* 8**,** 789-97.

FEKKAR, A., BALLOY, V., PIONNEAU, C., MARINACH-PATRICE, C., CHIGNARD, M. & MAZIER, D. 2012. Secretome of human bronchial epithelial cells in response to the fungal pathogen *Aspergillus fumigatus* analyzed by differential in-gel electrophoresis. *J Infect Dis,* 205**,** 1163-72.

FISCHER, G., MULLER, T., SCHWALBE, R., OSTROWSKI, R. & DOTT, W. 2000. Species-specific profiles of mycotoxins produced in cultures and associated with conidia of airborne fungi derived from biowaste. *Int J Hyg Environ Health,* 203**,** 105-16.

FOSTER, K. A., AVERY, M. L., YAZDANIAN, M. & AUDUS, K. L. 2000. Characterization of the Calu-3 cell line as a tool to screen pulmonary drug delivery. *Int J Pharm,* 208**,** 1-11.

GAUTHIER, T., WANG, X., SIFUENTES DOS SANTOS, J., FYSIKOPOULOS, A., TADRIST, S., CANLET, C., ARTIGOT, M. P., LOISEAU, N., OSWALD, I. P. & PUEL, O. 2012. Trypacidin, a spore-borne toxin from *Aspergillus fumigatus*, is cytotoxic to lung cells. *PLoS One,* 7**,** e29906.

GEISSLER, A., HAUN, F., FRANK, D. O., WIELAND, K., SIMON, M. M., IDZKO, M., DAVIS, R. J., MAURER, U. & BORNER, C. 2013. Apoptosis induced by the fungal pathogen gliotoxin requires a triple phosphorylation of Bim by JNK. *Cell Death Differ,* 20**,** 1317-29.

GRAINGER, C. I., GREENWELL, L. L., LOCKLEY, D. J., MARTIN, G. P. & FORBES, B. 2006. Culture of Calu-3 cells at the air interface provides a representative model of the airway epithelial barrier. *Pharm Res,* 23**,** 1482-90.

GUILLOT, L., NATHAN, N., TABARY, O., THOUVENIN, G., LE ROUZIC, P., CORVOL, H., AMSELEM, S. & CLEMENT, A. 2013. Alveolar epithelial cells: master regulators of lung homeostasis. *Int J Biochem Cell Biol,* 45**,** 2568-73.

HIRAKATA, Y., YANO, H., ARAI, K., ENDO, S., KANAMORI, H., AOYAGI, T., HIROTANI, A., KITAGAWA, M., HATTA, M., YAMAMOTO, N., KUNISHIMA, H., KAWAKAMI, K. & KAKU, M. 2010. Monolayer culture systems with respiratory epithelial cells for evaluation of bacterial invasiveness. *Tohoku J Exp Med,* 220**,** 15-9.

KIESSLICH, R., DUCKWORTH, C. A., MOUSSATA, D., GLOECKNER, A., LIM, L. G., GOETZ, M., PRITCHARD, D. M., GALLE, P. R., NEURATH, M. F. & WATSON, A. J. 2012. Local barrier dysfunction identified by confocal laser endomicroscopy predicts relapse in inflammatory bowel disease. *Gut,* 61**,** 1146-53.

KNOWLES, M. R. & BOUCHER, R. C. 2002. Mucus clearance as a primary innate defense mechanism for mammalian airways. *J Clin Invest,* 109**,** 571-7.

KOGAN, T. V., JADOUN, J., MITTELMAN, L., HIRSCHBERG, K. & OSHEROV, N. 2004. Involvement of secreted *Aspergillus fumigatus* proteases in disruption of the actin fiber cytoskeleton and loss of focal adhesion sites in infected A549 lung pneumocytes. *J Infect Dis,* 189**,** 1965-73.

LAFEMINA, M. J., SUTHERLAND, K. M., BENTLEY, T., GONZALES, L. W., ALLEN, L., CHAPIN, C. J., ROKKAM, D., SWEERUS, K. A., DOBBS, L. G., BALLARD, P. L. & FRANK, J. A. 2014. Claudin-18 deficiency results in alveolar barrier dysfunction and impaired alveologenesis in mice. *Am J Respir Cell Mol Biol,* 51**,** 550-8.

LAI, C. W., SUN, T. L., LO, W., TANG, Z. H., WU, S., CHANG, Y. J., WU, C. C., YU, S. C., DONG, C. Y. & CHEN, L. W. 2013. Shedding-induced gap formation contributes to gut barrier dysfunction in endotoxemia. *J Trauma Acute Care Surg,* 74**,** 203-13.

LEE, M. C., PENLAND, C. M., WIDDICOMBE, J. H. & WINE, J. J. 1998. Evidence that Calu-3 human airway cells secrete bicarbonate. *Am J Physiol,* 274**,** L450-3.

LIEBER, M., SMITH, B., SZAKAL, A., NELSON-REES, W. & TODARO, G. 1976. A continuous tumor-cell line from a human lung carcinoma with properties of type II alveolar epithelial cells. *Int J Cancer,* 17**,** 62-70.

LU, Z., KIM, D. H., FAN, J., LU, Q., VERBANAC, K., DING, L., RENEGAR, R. & CHEN, Y. H. 2015. A non-tight junction function of claudin-7-Interaction with integrin signaling in suppressing lung cancer cell proliferation and detachment. *Mol Cancer,* 14**,** 120.

MITCHELL, C. G., SLIGHT, J. & DONALDSON, K. 1997. Diffusible component from the spore surface of the fungus *Aspergillus fumigatus* which inhibits the

macrophage oxidative burst is distinct from gliotoxin and other hyphal toxins. *Thorax,* 52**,** 796-801.

MITCHELL, L. A., OVERGAARD, C. E., WARD, C., MARGULIES, S. S. & KOVAL, M. 2011. Differential effects of claudin-3 and claudin-4 on alveolar epithelial barrier function. *Am J Physiol Lung Cell Mol Physiol,* 301**,** L40-9.

MOMANY, M. & TAYLOR, I. 2000. Landmarks in the early duplication cycles of *Aspergillus fumigatus* and *Aspergillus nidulans*: polarity, germ tube emergence and septation. *Microbiology,* 146 Pt 12**,** 3279-84.

NAMVAR, S., WARN, P., FARNELL, E., BROMLEY, M., FRACZEK, M., BOWYER, P. & HERRICK, S. 2015. *Aspergillus fumigatus* proteases, Asp f 5 and Asp f 13, are essential for airway inflammation and remodelling in a murine inhalation model. *Clin Exp Allergy,* 45**,** 982-93.

OGUMA, T., ASANO, K., TOMOMATSU, K., KODAMA, M., FUKUNAGA, K., SHIOMI, T., OHMORI, N., UEDA, S., TAKIHARA, T., SHIRAISHI, Y., SAYAMA, K., KAGAWA, S., NATORI, Y., LILLY, C. M., SATOH, K., MAKIMURA, K. & ISHIZAKA, A. 2011. Induction of mucin and MUC5AC expression by the protease activity of *Aspergillus fumigatus* in airway epithelial cells. *J Immunol,* 187**,** 999-1005.

OSHEROV, N. 2012. Interaction of the pathogenic mold *Aspergillus fumigatus* with lung epithelial cells. *Front Microbiol,* 3**,** 346.

OSHEROV, N. & MAY, G. S. 2001. The molecular mechanisms of conidial germination. *FEMS Microbiol Lett,* 199**,** 153-60.

PROSKURYAKOV, S. Y., KONOPLYANNIKOV, A. G. & GABAI, V. L. 2003. Necrosis: a specific form of programmed cell death? *Exp Cell Res,* 283**,** 1-16.

SCHINDELIN, J., ARGANDA-CARRERAS, I., FRISE, E., KAYNIG, V., LONGAIR, M., PIETZSCH, T., PREIBISCH, S., RUEDEN, C., SAALFELD, S., SCHMID, B., TINEVEZ, J. Y., WHITE, D. J., HARTENSTEIN, V., ELICEIRI, K., TOMANCAK, P. & CARDONA, A. 2012. Fiji: an open-source platform for biological-image analysis. *Nat Methods,* 9**,** 676-82.

SCHLINGMANN, B., MOLINA, S. A. & KOVAL, M. 2015. Claudins: Gatekeepers of lung epithelial function. *Semin Cell Dev Biol,* 42**,** 47-57.

SHARON, H., AMAR, D., LEVDANSKY, E., MIRCUS, G., SHADKCHAN, Y., SHAMIR, R. & OSHEROV, N. 2011. PrtT-regulated proteins secreted by *Aspergillus fumigatus* activate MAPK signaling in exposed A549 lung cells leading to necrotic cell death. *PLoS One,* 6**,** e17509.

SHARON, H., HAGAG, S. & OSHEROV, N. 2009. Transcription factor PrtT controls expression of multiple secreted proteases in the human pathogenic mold *Aspergillus fumigatus*. *Infect Immun,* 77**,** 4051-60.

SHEN, B. Q., FINKBEINER, W. E., WINE, J. J., MRSNY, R. J. & WIDDICOMBE, J. H. 1994. Calu-3: a human airway epithelial cell line that shows cAMP-dependent Cl- secretion. *Am J Physiol,* 266**,** L493-501.

SUTHERLAND, T. C., QUATTRONI, P., EXLEY, R. M. & TANG, C. M. 2010. Transcellular passage of Neisseria meningitidis across a polarized respiratory epithelium. *Infect Immun,* 78**,** 3832-47.

WASYLNKA, J. A., HISSEN, A. H., WAN, A. N. & MOORE, M. M. 2005. Intracellular and extracellular growth of *Aspergillus fumigatus*. *Med Mycol,* 43 Suppl 1**,** S27-30.

WASYLNKA, J. A. & MOORE, M. M. 2000. Adhesion of *Aspergillus* species to extracellular matrix proteins: evidence for involvement of negatively charged carbohydrates on the conidial surface. *Infect Immun,* 68**,** 3377-84.

WASYLNKA, J. A. & MOORE, M. M. 2002. Uptake of *Aspergillus fumigatus* Conidia by phagocytic and nonphagocytic cells *in vitro*: quantitation using strains expressing green fluorescent protein. *Infect Immun,* 70**,** 3156-63.

WILLIAMS, J. M., DUCKWORTH, C. A., BURKITT, M. D., WATSON, A. J., CAMPBELL, B. J. & PRITCHARD, D. M. 2015. Epithelial cell shedding and barrier function: a matter of life and death at the small intestinal villus tip. *Vet Pathol,* 52**,** 445-55.

WILLIAMS, J. M., DUCKWORTH, C. A., WATSON, A. J., FREY, M. R., MIGUEL, J. C., BURKITT, M. D., SUTTON, R., HUGHES, K. R., HALL, L. J., CAAMANO, J. H., CAMPBELL, B. J. & PRITCHARD, D. M. 2013. A mouse model of pathological small intestinal epithelial cell apoptosis and shedding induced by systemic administration of lipopolysaccharide. *Dis Model Mech,* 6**,** 1388-99.

WONG, M. H. & JOHNSON, M. D. 2013. Differential response of primary alveolar type I and type II cells to LPS stimulation. *PLoS One,* 8**,** e55545.

ZHANG, Y. M., ZHANG, Z. M., GUAN, Q. L., LIU, Y. Q., WU, Z. W., LI, J. T., SU, Y., YAN, C. L., LUO, Y. L., QIN, J., WANG, Q. & XIE, X. D. 2017. Co-culture with lung cancer A549 cells promotes the proliferation and migration of mesenchymal stem cells derived from bone marrow. *Exp Ther Med,* 14**,** 2983-2991.

CHAPTER 4: GLOBAL EPITHELIAL CELL RESPONSES TO *A. FUMIGATUS* CHALLENGES

4.1 Introduction

Infection by *A. fumigatus* occurs primarily via inhalation of its airborne spores; thus the respiratory airway epithelium represents the first structure in the host to come into contact with *A. fumigatus.* Airway ECs (AECs) express a range of PRRs with which they recognise respiratory pathogens and are able to generate appropriate effector responses as a consequence of intracellular signalling mechanisms directed against the pathogen (Croft et al., 2016). Activation of host signalling pathways in ECs can be both destructive and protective (Osherov, 2015) and have been well documented for a few mucosal pathogens such as *Enterococcus feacalis* and *Escherichia coli* infections (Zou and Shankar, 2015), *Enterovirus* 71 infection (Shi et al., 2013, Peng et al., 2014) and the human fungal pathogen *Candida albicans* (Moyes et al., 2014, Moyes et al., 2010). However, the response of AECs to pathogenic *Aspergillus* species remains in its infancy. While *A. fumigatus* is known to interact with, and invade, airway epithelial cells the temporal basis of the host-pathogen interaction is incompletely understood because available data are sparse and fragmented. Moreover, *A. fumigatus* undergoes obligatory morphological shifts during developmental growth which effects differential immunogenic states (Latge et al., 1993, Latge et al., 2005, Dague et al., 2008). In order to understand the AEC-*Aspergillus* interaction in a manner which captures the morphogenic transitions of the pathogen in a real infection, it is necessary to elucidate the dynamic host response to the different stages of *A. fumigatus* infection. This chapter was focused on elucidating the dynamic host response to *A. fumigatus* challenge activated during interaction with epithelial cells. The study showed that airway epithelial cells orchestrate differential immune responses to distinct morphological states of *A. fumigatus* as well as to growth stage-specific secreted products of the fungus. NF-kappa B and MAPK signalling pathways were activated during early- and late-stage infections respectively, and host-derived cytokines can be modified via protease mediated degradation by the fungal secreted products as an additional immune evasion strategy. This Chapter describes a model for host signalling which differentially responds to *A. fumigatus* spores, germlings,

hyphae and secreted products thereby providing crucial new understanding which might be beneficial for devising new therapies.

Building upon the temporal interaction data reported in Chapter 3, the work described in this chapter aimed to:

1. Determine which host signalling proteins are activated by *A. fumigatus* conidia, hyphae and CFs.

2. Determine which transcription factors are activated by *A. fumigatus* conidia, hyphae and CFs.
3. Determine the epithelial cell-derived cytokines whose expression is induced by *A. fumigatus* conidia, hyphae and CFs.

4.2 Materials and Methods

4.2.1 Fungal strains and epithelial cell line

The clinical isolate CEA10 strain was used for studies in this chapter. Fungal challenges were performed using spores and CF from this strain (see section 2.2.2). A549 epithelial cells were cultured in 100 mm (10 cm), 6 well, or 12 well tissue culture plates for transcription factor, signalling protein phosphorylation or cytokine assays respectively.

4.2.2 Detection of phosphorylated signalling proteins in epithelial cells

Activation of signaling pathways was assessed by quantification of phosphorylated signalling proteins in whole cell lysate using the Bio-Plex Pro magnetic bead-based immunoassay (Bio-Rad, United Kingdom). As an indicator of MAPK-P38 pathway, MAPK-JNK pathway, MAPK ERK1/2, NF-κB pathway and PI3K pathway activation respectively, phosphorylation of -p38, Jun N-terminal protein kinase (JNK), Extracellular signal-regulated kinases 1 and 2 (ERK1/2), IκBα, and AKT was quantified. In each case a 10 μg aliquot of total protein, extracted from whole cell lysate (Section 2.2.5.1) was assayed according to the manufacturer's protocol (Section 2.2.5.3). After assembling all reagents at room temperature and planning the plate layout for

samples in duplicate wells, the amount of magnetic beads for each analyte was calculated as: 1 µl of each analyte bead per well and added in a sterile 15 ml Falcon tube protected from light. The beads were diluted in wash buffer to a final volume of 50 µl of diluted beads/well. The reaction was set-up and the samples and analyte beads were incubated with shaking overnight. After incubation, analytes were detected with antibody and streptavidine and analysed using a Bioplex plate reader using specified protocols. Phosphorylation were normalized to that of the β-actin housekeeping protein and expressed as fold change relative to the uninfected control.

4.2.3 Transcription factor DNA binding assay

DNA binding activity of selected transcription factors in nuclear extracts was assessed using the TransAM DNA binding ELISA based system (Active Motif) following A549 challenge with live fungal spores or CF (section 2.2.6). Protein content of nuclear extract was quantified by BCA assay (section 2.2.5.2). A 10 µg aliquot of protein was used for DNA binding assay (section 2.2.6.2). The amount of active and bound transcription factors is directly proportional to the colour intensity read as absorbance value at 450 nm. The final absorbance was expressed as fold change relative to uninfected epithelial cell controls.

4.2.4 Cytokine detection

To quantify cytokine secreted by A549 cells in response to *A. fumigatus* live spore or CF challenge, cell culture supernatant was collected at 24 h post challenge. A total of 25 µl of the cell culture supernatant was used to determine cytokine levels for IL-1α, IL-1β, IL-6, IL-8, G-CSF, GM-CSF , MIP-1 alpha, MIP-3 alpha, FGF-basic, and CD40 as in section 2.2.4.2. AECs stimulated with 50 ng/ml TNF-α served as a positive control of cytokine induction.

4.2.5 Statistical analysis

Summarised data were analysed using GraphPad Prism version 7 and the results were expressed as mean ± SEM. The difference between treatment means was

determined using one way ANOVA or paired student T-test. In all cases, $p < 0.05$ was taken as statistically significant. All experiments were performed independently a minimum of three times each in duplicate or triplicate.

4.3 Results

4.3.1 Activation of signalling pathways in A549 epithelial cells in response to *A. fumigatus* challenge

Exposure of human AECs to extracellular stresses or pathogenic stimuli prompts changes in the intracellular environment in order to promote appropriate host responses. Sequentially, extracellular stimuli such as pathogen recognition, or exposure to growth factors or cytokines initiates a complex program of signal transduction via specific pathways, transcriptional events and production of immunomodulators and effectors (Whitmarsh, 2007, Hill and Treisman, 1995). Mitogen activated protein kinase (MAPKs) signalling plays a critical role in the transduction of extracellular stress signals to the intracellular compartment in order to elicit the appropriate immunological responses. For example, infection of bone marrow derived macrophages by *Enterococcus feacalis* and *Escherichia coli* bacteria activates the three MAPKs ERK, JNK and p38 MAPK to drive macrophage polarization towards the M1 type and to secrete TNF-α and IL-1β (Zou and Shankar, 2015). In *Enterovirus* 71 (EV71) infection of human rhabdomyosarcoma (RD) cells, the secretion of inflammatory cytokines was induced following MAPK activation seen by upregulation of about 54 MAPK associated genes (Shi et al., 2013, Peng et al., 2014). MAPKs have demonstrated importance in recognizing and discriminating between pathogenic hyphal forms and yeast forms of the important human opportunistic fungi *C. albicans* (Moyes et al., 2011). NF-κB signalling is another crucial immune component primarily important in innate immune responses to wide range of stimuli (Oeckinghaus and Ghosh, 2009). In fact, the NF-κB transcription factor is likely the most prominent regulator of immune system development and function (Hayden and Ghosh, 2012). The PI3K/AKT/mTOR pathway is a key pathway that regulates many cellular functions such as cell growth, metabolism and apoptosis/survival (Fukao and Koyasu, 2003, Castilho et al., 2013). Little is currently known about the role of MAPK and NF-κB signalling in response to the morphogenic transition of *A. fumigatus* during A549 epithelial cell infection. In order to assess the host response to different *A. fumigatus* morphotypes and the secreted products thereof, the phosphorylation

status of three mitogen-activated protein kinases (MAPKs) p38, ERK, and JNK; of the Inhibitor of kappa-light-chain-enhancer of activated B cells (IκBα) of the NF-κB pathway; and AKT of the phosphoinositol-3-kinase (PI3K) pathway were measured over a time-series of co-incubation with live *A. fumigatus* spores, or CF[48].

4.3.1.1 Spores and hyphae stimulate mechanistically distinct host responses in A549 epithelial cells

In data presented in Chapter 3 it was shown that the transition of *A. fumigatus* from one morphogenic stage to another occurs at particular time points during vegetative growth. In order to study the AEC immune response to each morphological state, our assays of host responses utilised time-points relevant to each growth stage (Fig 3.2A). Effector: target ratio or multiplicity of infection (MOI) of 10 was chosen for signalling protein and transcription factor phosphorylation assays to ensure that each AEC is exposed to at least one fungal spore at every point in time. A. *fumigatus* did not induce phosphorylation of p38 or the PI3K/AKT pathway until 12 h post-exposure (Fig. 4.1A & B), similarly ERK1/2 phosphorylation gradually increased from 2 h post infection reaching statistical significance at 12 h (1.3 fold, $p < 0.001$) (Fig. 4.1C). JNK phosphorylation increased from 6 h post spore challenge (Fig. 4.1D), which reached significance from 6 h to 12 h (1.6 fold, $p < 0.001$). This timing is consistent with the emergence of hyphae from the germinating spore (Fig 3.2). Moreover, epithelial infection with *A. fumigatus* spores resulted in significant phosphorylation of IκBα from as early as 5 min PI (1.5 fold, $p < 0.05$), which persisted until 12 h PI (Fig.4.1E).

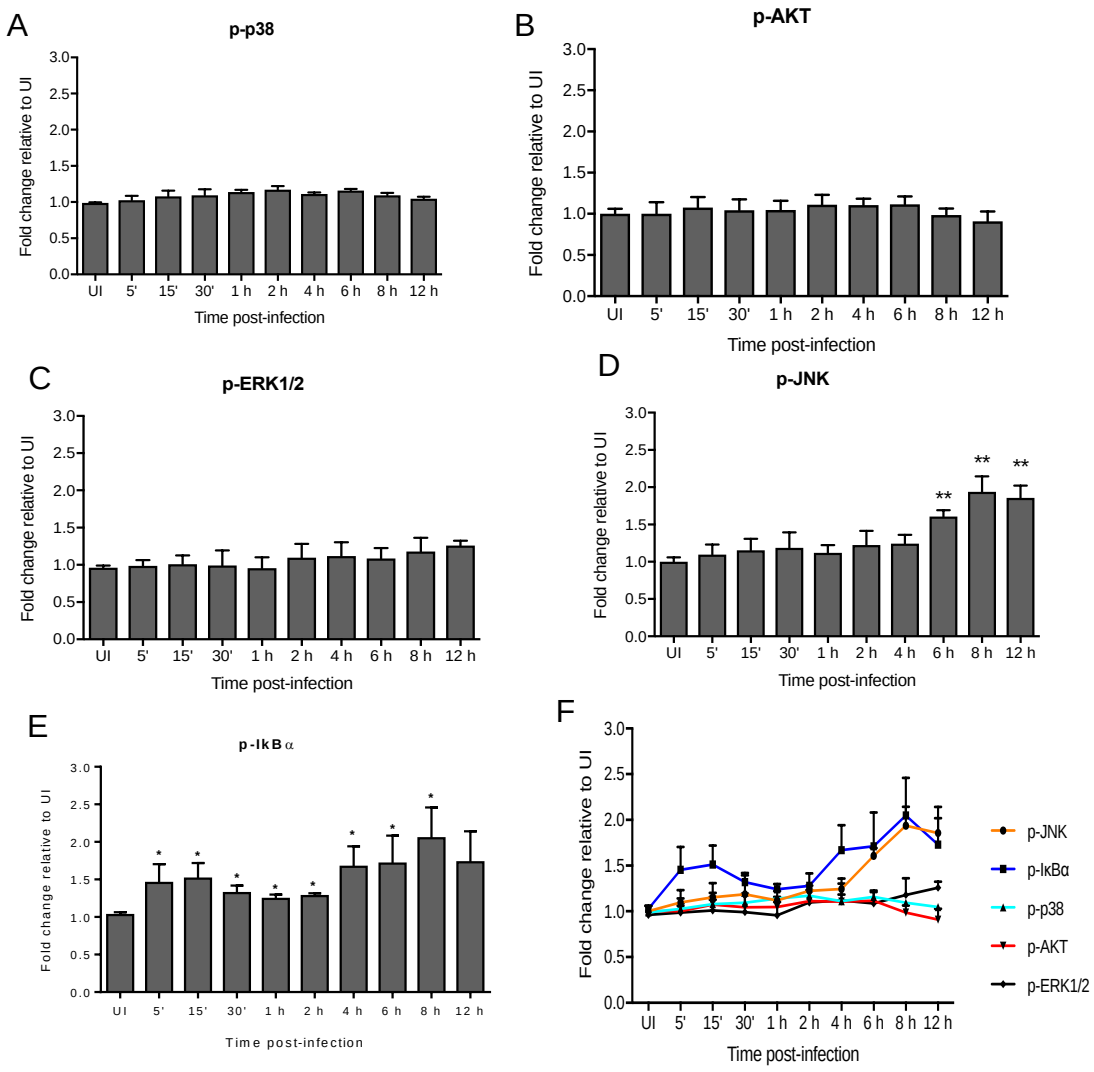

Figure 4.1: Phosphorylation of immune signalling proteins in A549 cells in response to infection with live *A. fumigatus*

Confluent monolayers of A549 epithelial cells were infected with freshly harvested *A. fumigatus* conidia (10^7) and uninfected cells (UI) were used as control. At indicated time points post infection, total intracellular proteins were harvested and analysed for phosphorylation of target proteins A) phospho-p38 B) phospho-AKT C) phospho-ERK1/2 D) phospho-JNK E) phospho- IκBα F) Composite of all signalling proteins on same axes. Data is expressed as fold change in level of phosphorylation of target proteins induced by infection relative to the level in uninfected cells and represents the average of three independent experiments; each performed in triplicate. Error bars indicate ± SEM. Significance of response due to treatment was calculated relative to UI control using unpaired student T-test. *p <0.05; **p<0.001.

4.3.1.2 Culture filtrate of *A. fumigatus* induces phosphorylation of three MAPK signalling proteins: JNK, ERK1/2 and p38 in A549 epithelial cells

A. fumigatus secretes proteases and toxins during infection, which have been shown to contribute to cellular and tissue damage during the course of infection (Bignell et al., 2016, Kothary et al., 1984). In order to investigate whether secreted molecules activate immune responses in epithelial cells in the absence of live fungus, epithelial cells were stimulated, for up to 5 h, with either 5- fold (Fig. 6 A-E) or 10-fold (Fig.7 A-E) dilutions of *A. fumigatus* CF harvested from fungal cultures grown for 48 h (CF^{48}).

AKT and IκBα (Fig 4.2A and B) showed a strikingly similar and biphasic mode of increased phosphorylation in response to a 5-fold dilution of CF. The first time-point of significantly heightened phosphorylation occurred at 30 min post exposure (1.3 fold, $p < 0.05$) followed by a return to base line from 1 h post exposure until about 4-5 h post exposure when phosphorylation increased again to 1. 5 fold that of uninfected cells ($p < 0.001$). Phosphorylation of ERK1/2, p38 and JNK increased significantly in epithelial cells from 30 min post-exposure to CF^{48} (Fig 4.2C,D and E). The phosphorylation was sustained at significantly higher levels relative to UI control throughout the 5 h of infection. Phosphorylation of p38 and JNK reached a maximum level at 3 h post-exposure (8 fold, $p <0.05$) and this was followed by a gradual decrease, although still significantly higher compared to UI cells. In contrast, ERK1/2 phosphorylation was sustained at a maximum level from 30 min post-exposure (1. 6 fold, $p < 0. 001$) to the end of 5 h time course.

A similar trend (though of lesser magnitude) was observed when challenging with a 10-fold dilution of CF (Fig 4.3A-E) compared to 5-fold diluted CF (Fig 4.2).

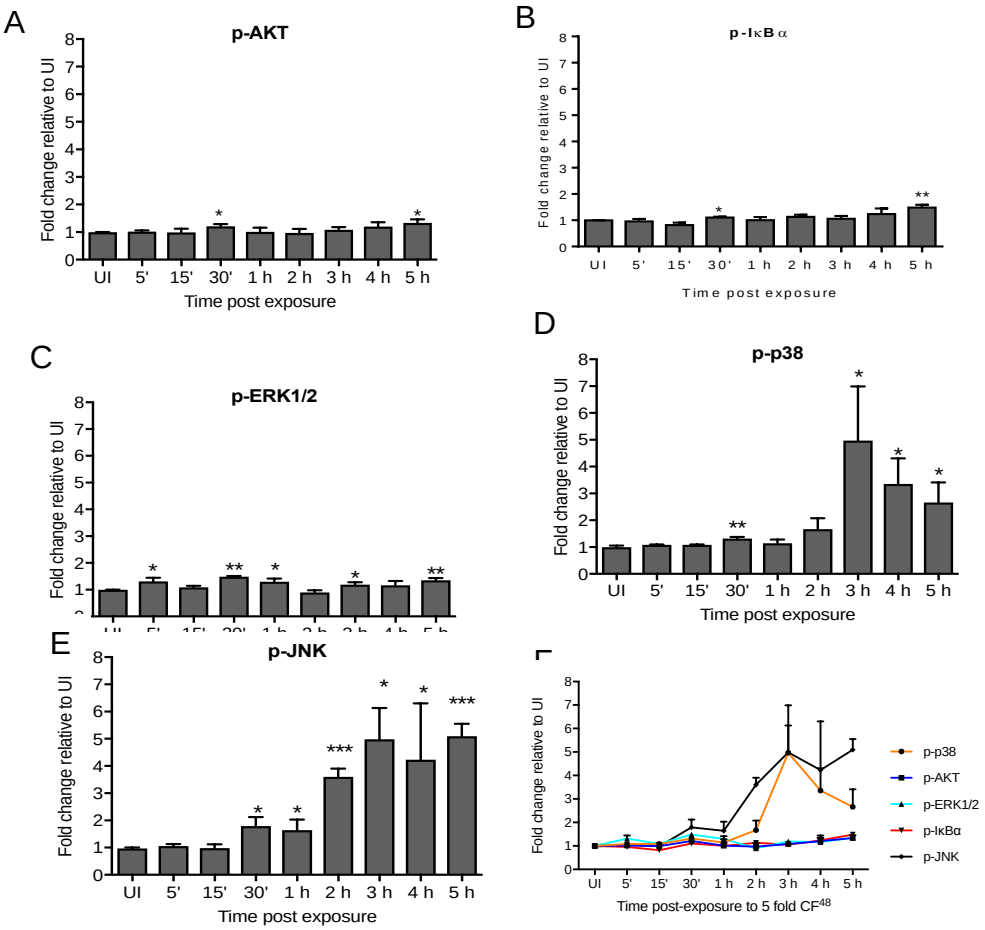

Figure 4.2: Phosphorylation of immune signalling proteins in A549 cells in response to exposure to 5 fold dilution of CF.

Confluent monolayers of A549 epithelial cells were challenged with a 5 fold dilution of CF[48] (200 µl of CF in 800 µl of media in the well) and uninfected cells (UI) were used as control. At indicated time points post infection, total intracellular proteins were harvested and analysed for phosphorylation of target proteins A) Phospho-AKT B) Phospho-IκBα C) phospho-ERK1/2 D) phospho-p38 E) Phospho-JNK F) Composite of all signalling proteins on same axes. Data is expressed as fold change in quantity of phosphorylated protein relative to that of uninfected and represents the average of three independent experiments; each performed in triplicate. Error bars indicate ± SEM. Significance of response due to treatment was calculated relative to UI control using unpaired student T-test *p <0.05; **p<0.001; ***p<0.0001.

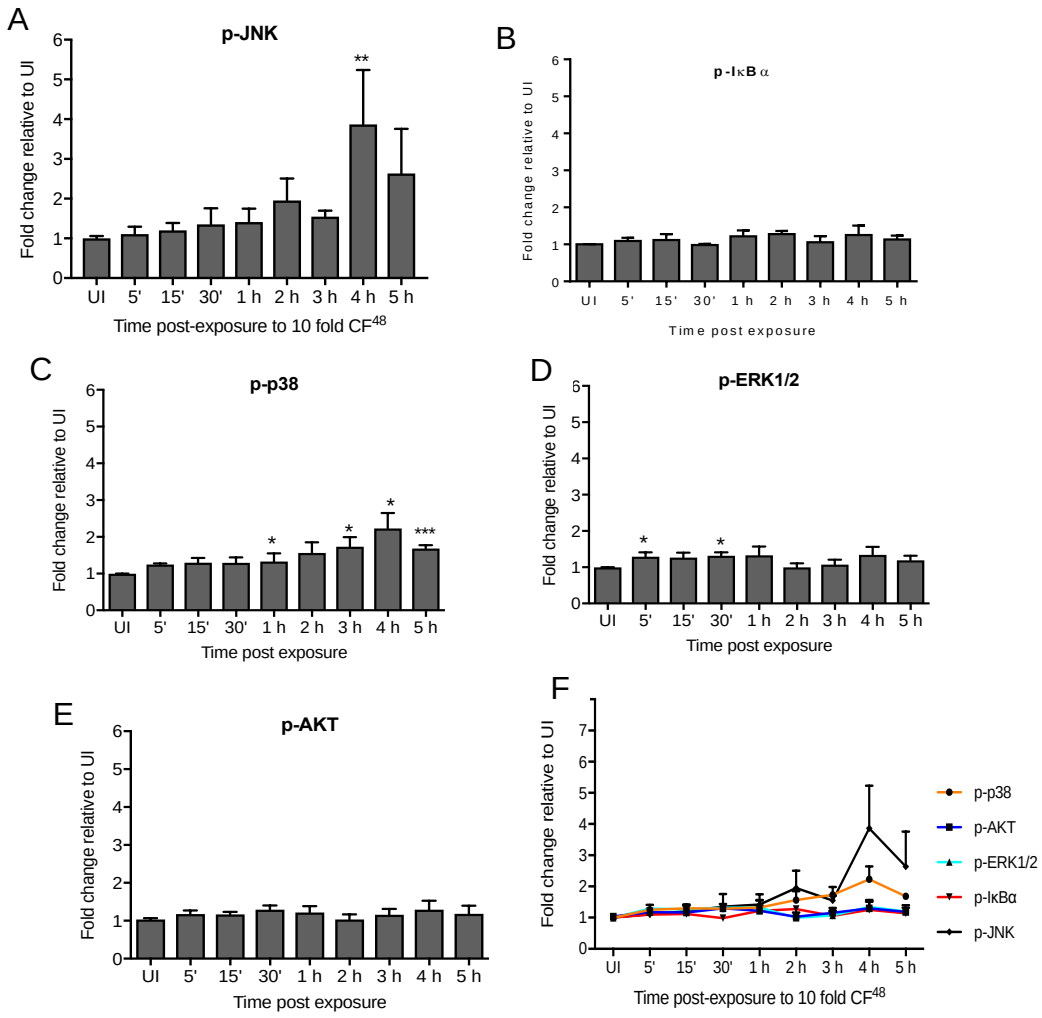

Figure 4.3 Phosphorylation of immune signalling proteins in A549 cells in response to exposure to 10 fold dilution of CF.

Confluent monolayers of A549 epithelial cells were challenged with a 10 fold dilution of CF^{48} (100 µl of CF in 900 µl of media in the well) and uninfected cells (UI) were used as control. At indicated time points post infection, total intracellular proteins were harvested and analysed for phosphorylation of target proteins A) Phospho-JNK B) Phospho-IκBα C) phospho-p38 D) phospho-ERK1/2 E) Phospho-AKT F) Composite of all signalling proteins on same axes. Data is expressed as fold change in quantity of phosphorylated protein relative to that of uninfected and represents the average of three independent experiments; each performed in triplicate. Error bars indicate ± SEM. Significance of response due to treatment was calculated relative to UI control using unpaired student T-test *p <0.05; **p<0.001; ***p<0.0001.

4.3.2 Activation of transcription factors in AECs in response to *A. fumigatus* challenges

There are a number of mammalian transcription factors which are substrates to signalling pathways activated in response to pathogens and other extracellular stresses. These include the MAPKs substrates: (ATF-2, c-Myc, STAT-1α, and MEF-2, Jun (c-Jun, Jun B, and Jun D) and Fos (c-Fos, Fos B and Fra-1)) and the NF-κB (p65 (RelA), RelB, c-Rel, p50/p105 and p52/p100) families. These transcription factors, when activated, bind to specific binding sites on DNA either as homo- and or hetero-dimers to regulate cellular processes such as differentiation, proliferation and immune responses (Whitmarsh and Davis, 1996, Oeckinghaus and Ghosh, 2009).

In principle, activation of transcription factors follows a sequence of nuclear localization, DNA binding and interaction of individual transcription factors with the basal transcription apparatus. In order to assess the activation of the above transcription factors in epithelial cells following live fungal and CF challenges, the TransAM ELISA technique (by Active Motif) which quantifies activity of transcription factors was used. Using this technique, it was possible to simultaneously measure both the nuclear localization as well as DNA binding activity of the individual transcription factors because the antibody binds to epitopes on the transcription factors which are only accessible when the transcription factor is activated and bound to its target DNA binding consensus in the nucleus (section 2.2.6).

4.3.2.1 Basal DNA binding activity of transcription factors in resting A549 epithelial cells

In resting A549 epithelial cells, a basal level of transcription factor DNA binding activity was observed for FosB, JunB, JunD, c-Jun, MEF-2 and c-Myc, but not for c-Fos, Fra-1, ATF-2 or STAT-1α (Fig 4.4A). The DNA binding activity of Jun family members, JunB and JunD, were the most constitutively present. Low level DNA binding activity was observed for all NF-κB family members in resting A549 epithelial cells compared to AP1 and MAPK members (Fig 4.4B) with p50 showing the highest level of constitutive binding.

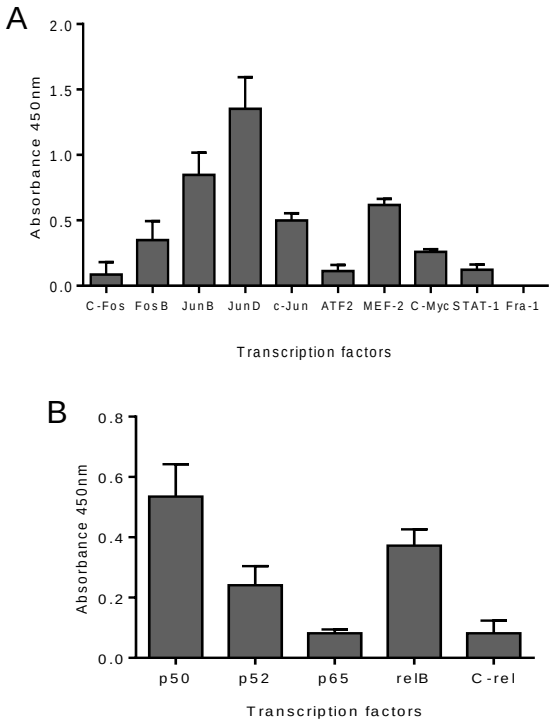

Figure 4.4: Basal DNA binding activity of Transcription factors

The DNA binding activity (absorbance values) of; A) AP-1 and MAPK- associated transcription factor family B) NF-κB family transcription factor members in resting A549 cells. A 10 µg of nuclear extract from resting/uninfected A549 cells was assayed for levels of DNA binding activity of indicated transcription factors. Data are expressed in terms of absorbance values and are representative of six (or three for STAT1, Fra 1 and C-Rel) independent experiments ± SEM.

4.3.2.2 Activation of transcription factors by live *A. fumigatus* challenge

4.3.2.2.1 Activation of MAPKs and or AP-1transcription factors by *A. fumigatus* spores

Of all MAPK/AP-1 transcription factors analysed, c-Fos binding was significantly increased following A549 infection with *A. fumigatus* spores ($p < 0.05$) (Fig 4.5A). Notably, the DNA binding activity of c-Myc was increased from 6 h PI albeit not statistically significant (fig 4.6B). The increase in c-Myc was paralleled by a significant ($p < 0.05$) decrease in the binding of MEF-2 (Fig 4.6C). There was a general repressive effect on the Jun family members JunD and c-Jun from 2 h post-infection with live fungus (Fig 4.5 D and E respectively). While the reduction in DNA binding activity of JunD was sustained at a statistically significant level (Fig 4.5D), the DNA binding activity of c-Jun returned to baseline 4 h later (Fig 4.5E). These results suggest that the Jun family members are important in modulating the host response during resting-to-swollen spore switches.

Infection of A549 cells with *A. fumigatus* for up to 8 h did not alter the DNA binding activity of the transcription factors ATF-2, STAT-1α, Fos B, Fra- 1 or JunB (Fig 4.6 A to E). Overall, the induction of these responses coincides with spore germination (Fig 3.2A) and suggests that germination of spores has a striking impact on the host response.

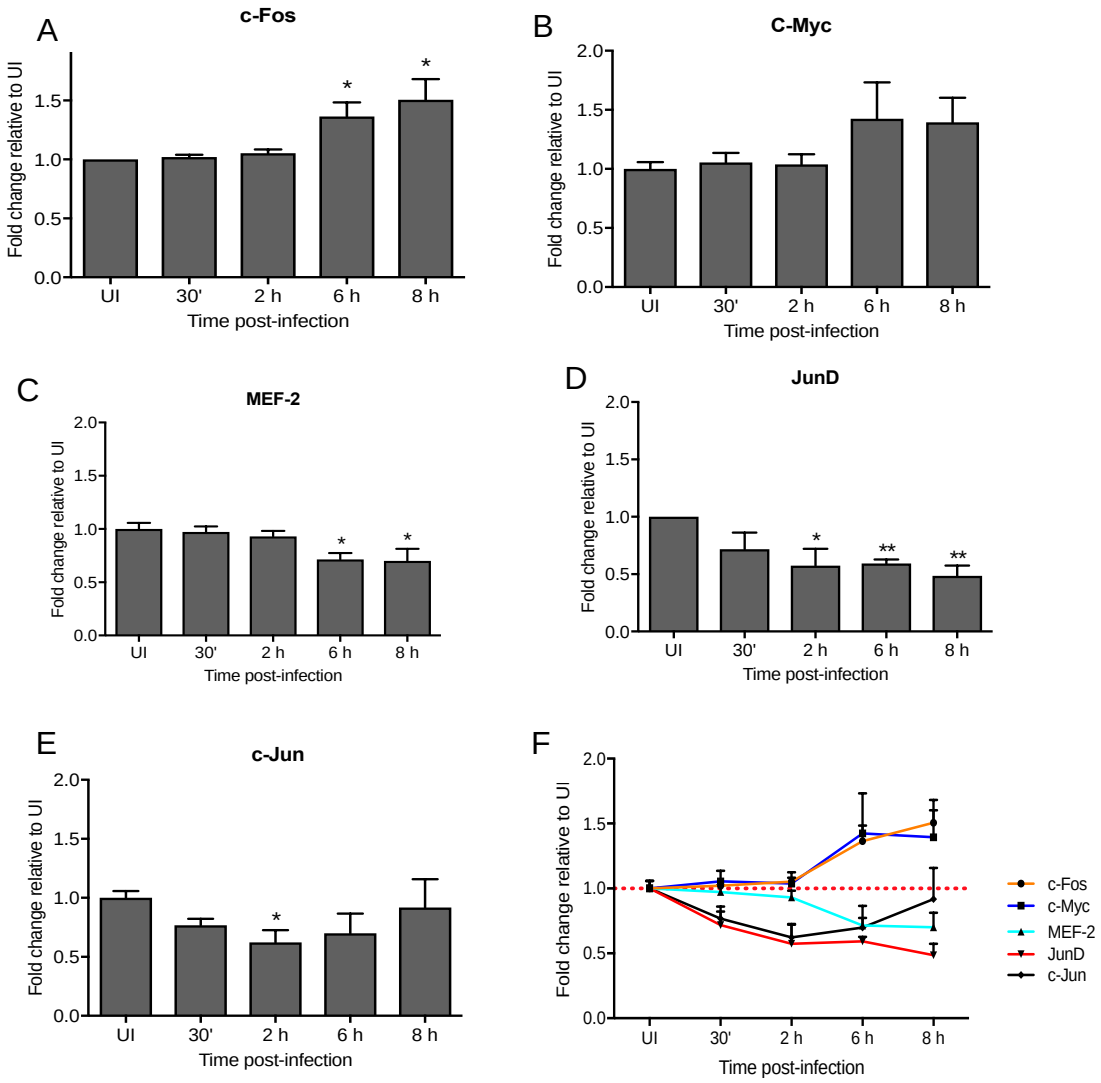

Figure 4.5: Changes in DNA binding activity of AP-1 transcription factor members in A549 cells following infection with *A. fumigatus* spores.

Confluent monolayers of A549 epithelial cells were infected with freshly harvested *A. fumigatus* conidia (MOI=10:1). At the indicated time points post infection, nuclear extracts were assayed for DNA binding activity of A) c-Fos B) c-Myc C) MEF-2 D) JunD E) c-Jun and F) Composite figure of all five transcription factors. Data are expressed as fold change in binding activity relative to uninfected cells and represent the average of three independent experiments. Error bars indicate ± SEM. Significance due to treatment was analysed with respect to uninfected controls. *p <0.05, **p<0.001.

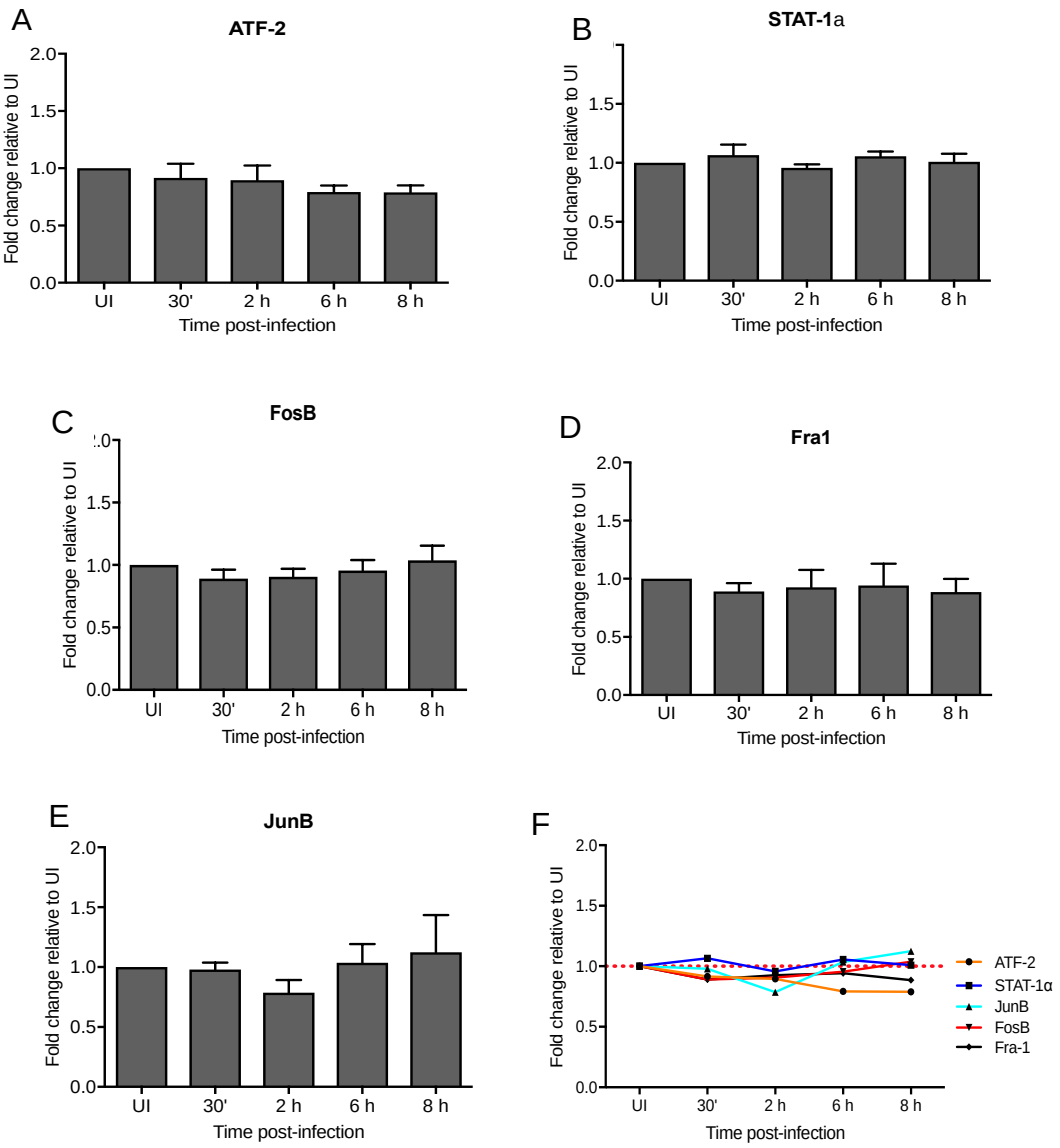

Figure 4.6: The DNA binding activity of transcription factors unchanged in A549 cells following infection with *A. fumigatus* conidia.

Confluent monolayers of A549 epithelial cells were infected with freshly harvested *A. fumigatus* conidia (MOI=10:1). At the indicated time points post infection, nuclear extracts were assayed for DNA binding activity of A) ATF-2 B) STAT-1α C) FosB D) Fra 1 E) JunB and F) Composite figure of all five transcription factors. Data are expressed as fold change in binding activity relative to uninfected cells and represent the average of three independent experiments. Error bars indicate ± SEM.

4.3.2.2.2 Activation of NF-κB transcription factors by *A. fumigatus* spores

A. fumigatus infection did not alter the DNA binding activity of p52 (Fig 4.7A) and c-Rel (Fig. 4.7B). However, RelB DNA binding decreased immediately from 30 min post-infection and continued to decrease until 8 h, resulting in ~70% reduction ($p<0.001$) (Fig 4.7C). In contrast, p50 and p65 DNA binding activity increased from 6 h post-infection, concomitant with *A. fumigatus* germination, although only the p65 was statistically significant (Fig 4.7 D and E respectively).

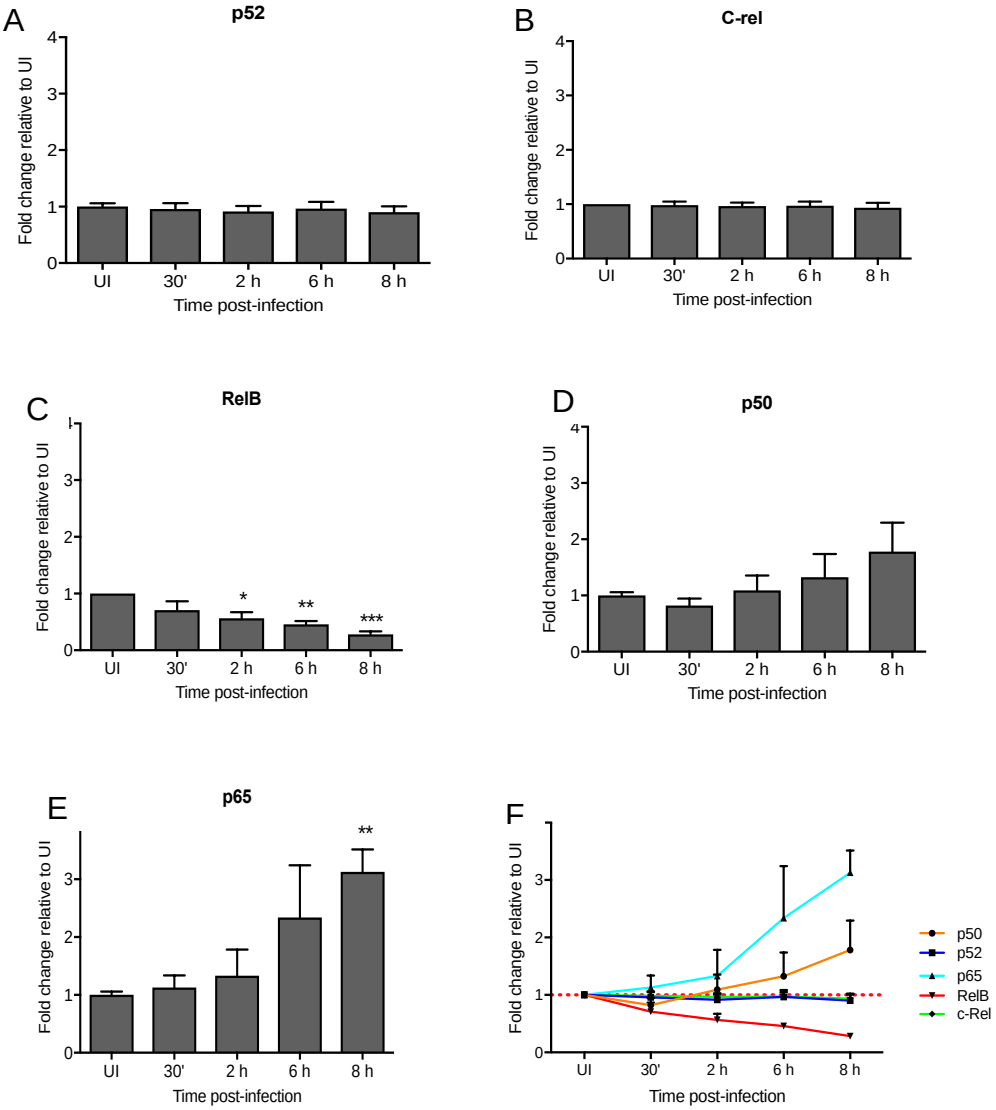

Figure 4.7: Changes in DNA binding activity of NF-κB transcription factor family in A549 cells after infection with *A. fumigatus* conidia.

Confluent monolayers of A549 epithelial cells were infected with freshly harvested *A. fumigatus* conidia (MOI 10). At the indicated time points post infection, nuclear extracts were assayed for DNA binding activity of; A) p52 **)** c-Rel C) RelB D) p65 D) p50. Data are expressed as fold change in binding activity relative to uninfected/resting cells and represent the average of three independent experiments. Error bars indicate ± SEM. *p <0.05, **p<0.001 ***p<0.0001.

4.3.2.3 Activation of Transcription factor by fungal secreted products (CF^{48})

4.3.2.3.1 Activation of MAPKs and or AP-1 transcription factors by CF^{48}

Exposure of A549 cells to 5-fold and 10-fold dilutions of *A. fumigatus* CF^{48} for up to 4 h did not alter the DNA binding activity of c-Fos, Fos B, Jun B and Jun D (Fig 4.8A-D). Binding of c-Jun was significantly ($p<0.0001$) suppressed by 10 fold CF^{48} dilution (Fig 4.8E). Similarly, the exposure of A549 cells to 10-fold and 5-fold dilutions of CF^{48} did not impact the DNA binding activity of ATF-2 and MEF-2 (Fig 4.8E and G). Interestingly, and in contrast to challenge with live *A. fumigatus* spores, 10-fold dilutions of CF^{48} induced an immediate and persistent and significant ($p<0.0001$) decrease in c-Myc DNA binding from 30 min to 4 h (Fig 4.8H).

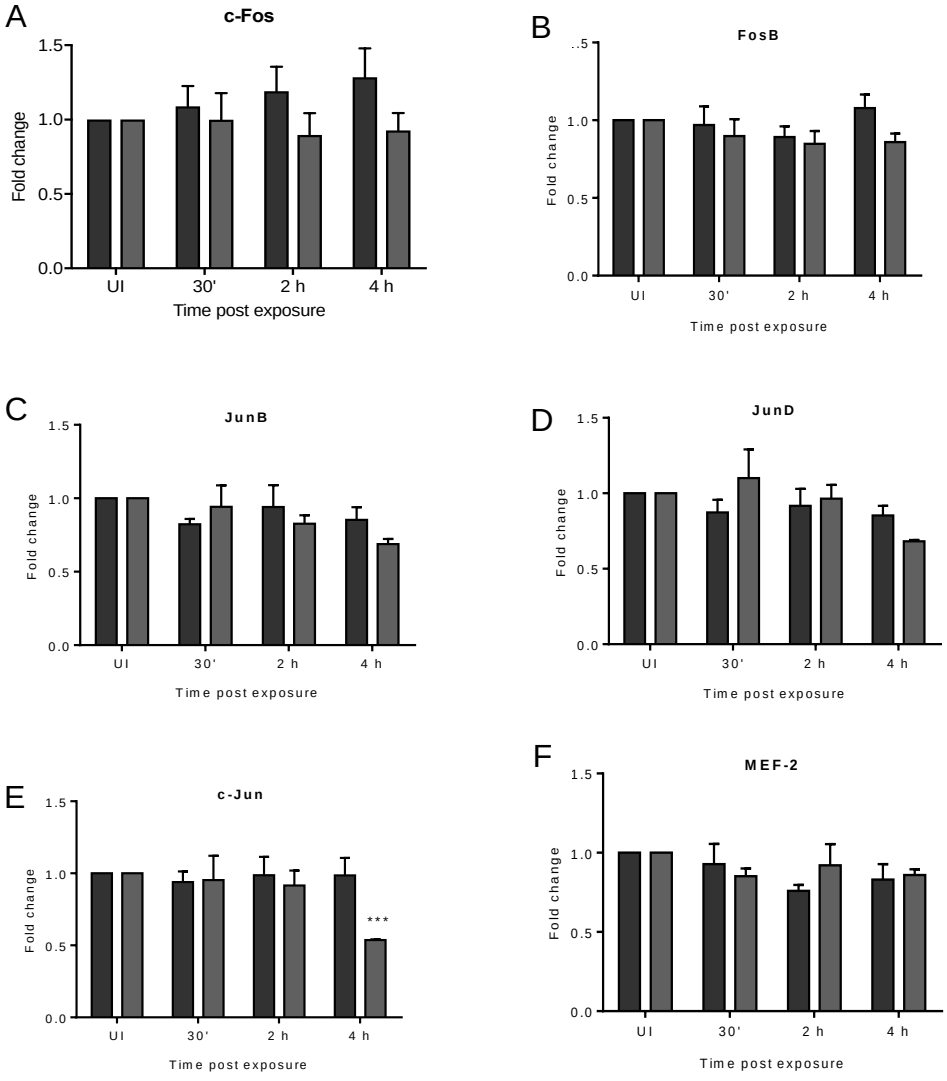

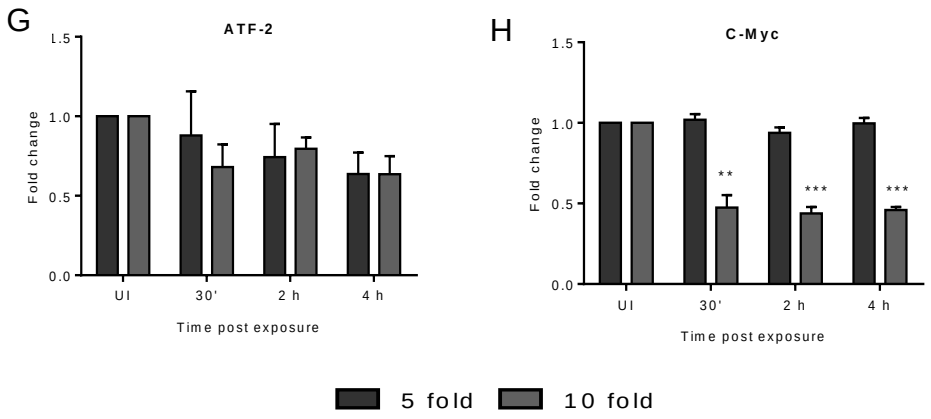

Figure 4.8: Changes in DNA binding activity of AP-1 transcription factor members in A549 cells after exposure to 5 fold and 10 fold dilutions of 48 h *A. fumigatus* culture filtrate.

A549 epithelial cells were exposed to 5 fold and 10 fold dilutions of 48 h *A. fumigatus* CF. At the indicated time points post infection, nuclear extracts were assayed for DNA binding activity of A) c-Fos, B) FosB, C) JunB, D) JunD, E) c-Jun, F) MEF-2, G) ATF-2 and H) c-Myc. Data are expressed as fold change in binding activity relative to unchallenged (UI) cells and represent the average of three independent experiments. Error bars indicate ± SEM. Significance was calculated relative to uninfected control using Two-way Anova with Fisher's LSD output ***$p<0.0001$.

4.3.2.3.2 Activation of NF-κB transcription factors by CF^{48}

Interestingly, exposure of A549 cells to 5- and 10-fold dilutions of *A. fumigatus* CF gave an effect opposite to that of live fungus. Notably, DNA binding activity of p52 and RelB was significantly ($p < 0.05$) increased from 2 h post-exposure to 5 fold CF^{48} dilution (Fig 4.9A and B), whereas p65 and p50 DNA binding were unchanged (Fig 4.9C and D).

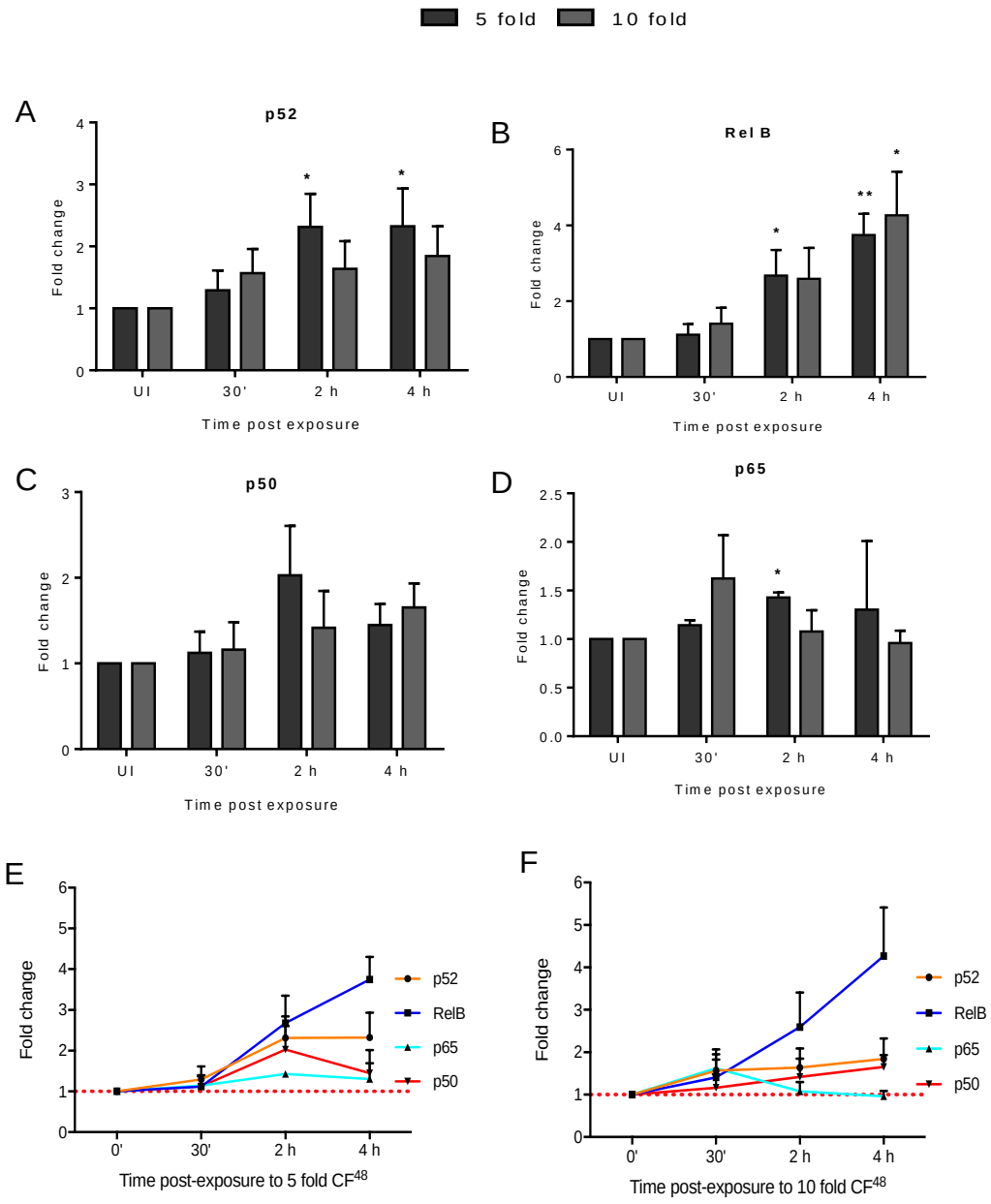

Figure 4.9: Changes in DNA binding activity of NF-κB transcription factor family in A549 cells after exposure to 5 fold and 10 fold dilutions of 48 h *A. fumigatus* CF. Confluent monolayers of A549 epithelial cells were exposed to 5 fold and 10 fold dilutions of 48 h *A. fumigatus* CF. At the indicated time points post infection, nuclear extracts were assayed for DNA binding activity of A) p50 B) p52 C) p65 D) RelB E) Composite of NF-κB transcriptional responses of A549 epithelial cells to 5 fold CF^{48} dilution F) Composite of NF-κB transcriptional responses of A549 epithelial cells to 10 fold CF^{48} dilution. Data are expressed as fold change in binding activity relative to uninfected/resting cells and represent the average of three independent experiments. Error bars indicate ± SEM. Significance was calculated relative to uninfected control*p <0.05; **p<0.001.

4.3.3 Profile of cytokines released by AECs in response to *A. fumigatus* challenges

The ultimate outcome of signalling pathway activation during innate immune responses to pathogens is the production of effector cytokines. Epithelial cells respond to *A. fumigatus* challenge via the production of proinflammatory and chemotactic cytokines thoroughly reviewed by (Osherov, 2012, Croft et al., 2016). Previous studies have investigated epithelial cell cytokine responses to single fungal morphotypes or fragments in isolation. However, none of these studies has considered the entire cohort or a temporal profile of cytokine responses to *A. fumigatus* challenge. Moreover, the impact of *A. fumigatus* secreted products on the overall cytokine profile induced by *A. fumigatus* challenge has not been previously investigated. In order to determine the epithelial cytokine profile induced by *A. fumigatus*, two independent methods for cytokine analysis were adopted. First, the global cytokine profile against the live *A. fumigatus* and its secreted products was assessed by conducting a cytokine profile array. Appendix 4 contains the raw data of two biological replicates (with two technical data sets each) and the list of all the cytokines assayed. Cytokines that showed differential expression relative to PBS control were selected for further qualitative and quantitative study using Luminex magnetic bead assay. A549 epithelial cells were challenged with live *A. fumigatus* spores and CF^{48} at different MOIs and fold-dilutions respectively for 24 h. Epithelial culture supernatants were analysed for GM-CSF, G-CSF, IL-8, IL-6, IL-1α and IL-1β (selected based previous studies) in addition to IL-2, MIP-1β, MIP-3α, MCP-1, CD40L and FGF-2 (basic) selected on the basis of differential expression from the cytokine profile array.

4.3.3.1 Induction of cytokine expression by *A. fumigatus* spores

In order to identify effector:target ratios (MOIs) yielding measurable epithelial responses, A549 cells, cultured in a standard 24 well plate, were challenged for 24 hours with a series of spore concentrations or CF dilutions. Appropriate MOIs were selected on the basis of several criteria (i) maintenance of epithelial integrity (ii) absence of gross morphological damage to epithelia (visualised under a light microscope) (iii) an appropriate generation rate of fungal biomass. At an MOI of 10

and 1 *A. fumigatus* spores to one A549 cell, hyphal growth at 24 hours was too extensive to permit recovery of culture supernatant. Therefore, the MOI of 0.1 was selected as the maximum MOI which was further reduced tenfold for subsequent fungal inoculum dependent cytokine studies.

A. fumigatus conidia did not induce significant increases in G-CSF and MIP-1β production at any of the tested MOI compared to PBS treated cells (Fig 4.10A and B), although the positive control stimulant TNF-α ($p<0.0001$) induced their production which suggests that the A549 assay is competent in production of cytokines but only in response to specific stimuli amongst which *A. fumigatus* spores are not relevant. The level of IL-6, MCP-1α, GM-CSF, Adiponectin, IL-8, FGF-basic, MIP-3α, and CD40-Ligand production detected in culture supernatant was significantly increased with MOI 0.1 ($p < 0.05$ (Fig 4.10B to J) in a dose dependent manner. Notably, A549 epithelial cells release constitutively high levels of IL-8 even in response to PBS up to 3 µg/ ml (Fig 4.10G). Both IL-1 α/β were undetectable in the assay (data not shown).

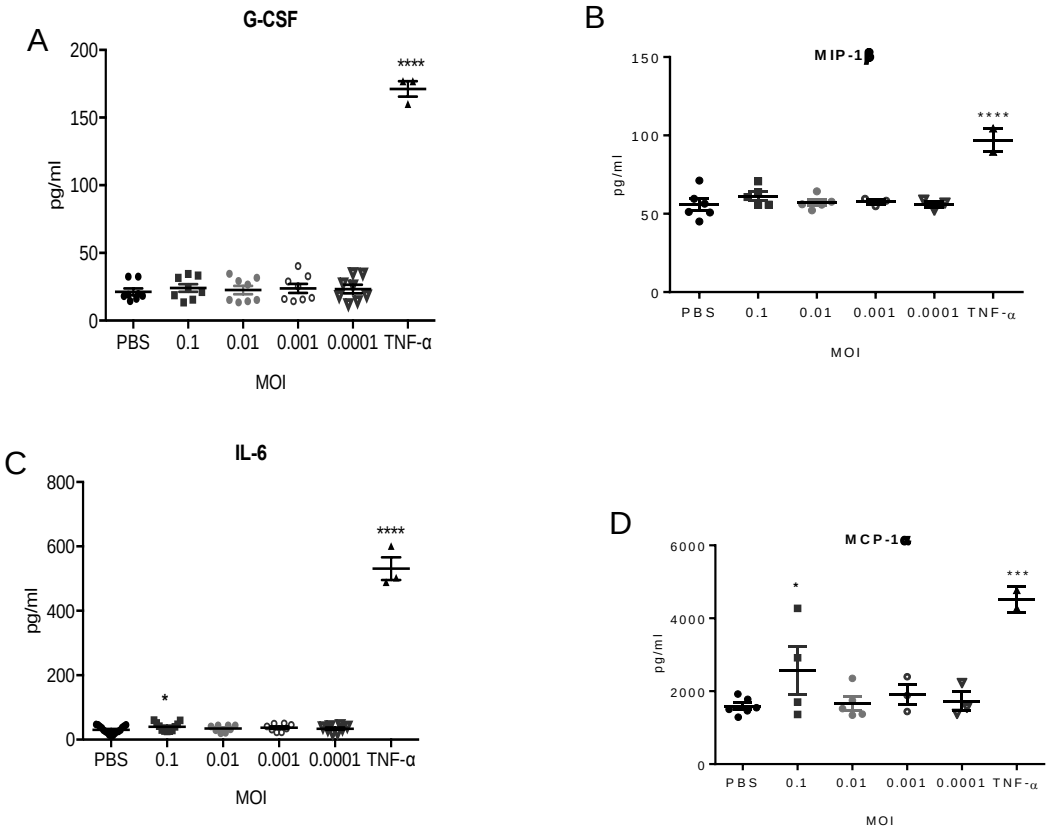

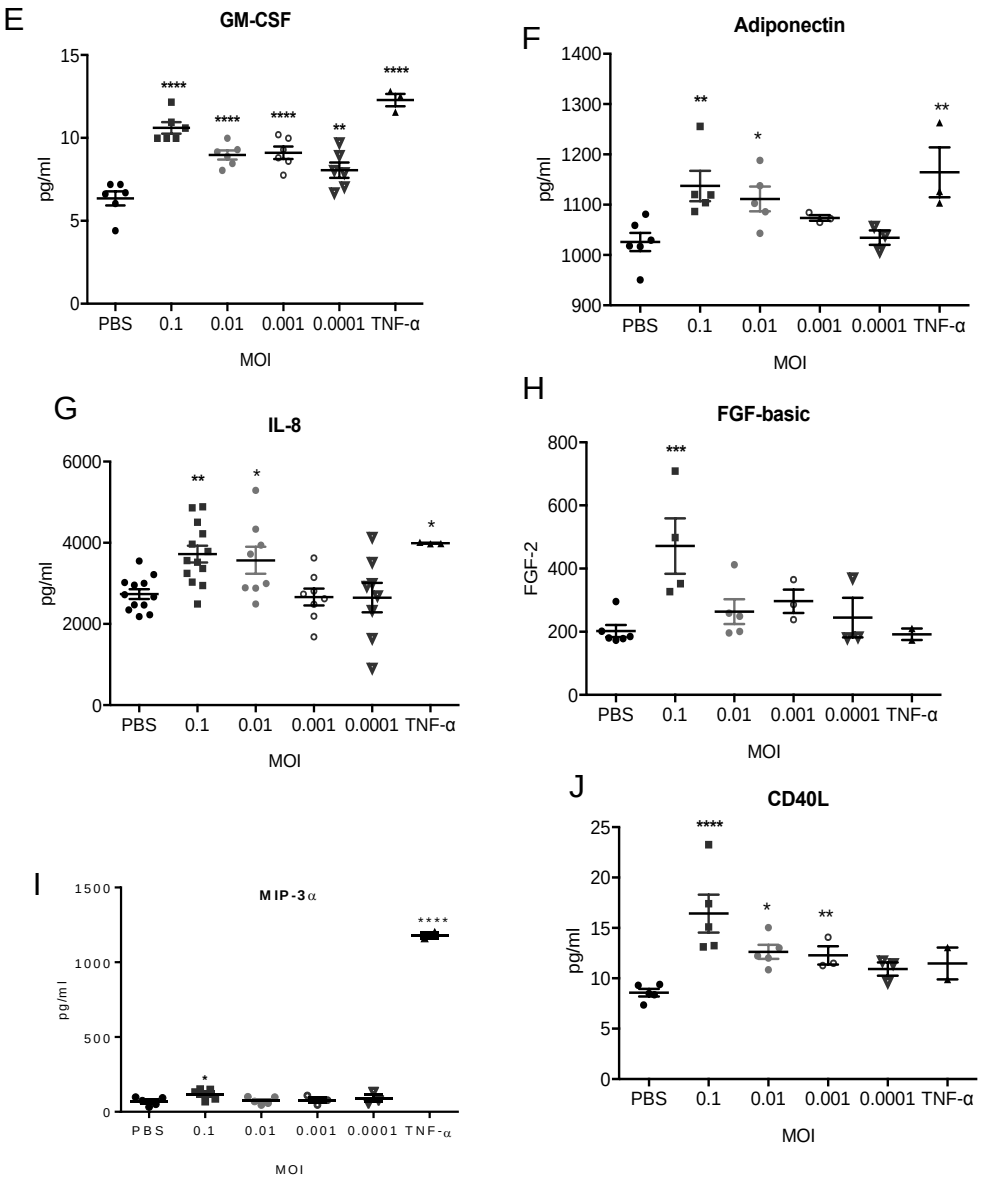

Figure 4.10: Modulation of cytokine production in A549 epithelial cells following spore challenge. Level of cytokine detected in cell culture supernatant following spore exposure for 24 h. Data represent the mean of three biological replicates. Error bars show ± SEM. Data were analysed by one-way ANOVA. Significance was calculated relative to challenge with vehicle control (PBS) with Fisher's LSD output. *P<0.05, **P<0.01, ***P<0.001, ****P<0.0001.

4.3.3.2 Induction of cytokine responses by CF^{48}

A549 epithelial cells were treated for 24 h with 5-, 10-, 20- and 50-fold dilutions of *A. fumigatus* CF and then assayed for cytokine release. The level of GM-CSF, G-CSF, IL-8, IL-6, MCP-1α, Adiponectin, IL-2 and MIP-3α detected in supernatant following CF^{48} challenge were significantly lower when compared with the PBS treated controls. Reduced cytokine level correlated directly with the concentration of CF^{48}, whereby the highest CF concentration (5 fold dilution of neat filtrate) caused a greater decrease in cytokine expression than 10 fold or 50 fold dilutions (Fig 4.11A-H). The only exception to this rule was observed with GM-CSF where cytokine concentration decreased with decreased CF^{48} concentration (Fig 4.11C). Most notably, 5-fold dilution of *A. fumigatus* CF significantly reduced IL-6, IL-8 and G-CSF expression (Fig 4.11A, B and D), an effect that was maintained for IL-8 at 10- and 20-fold dilutions also (Fig 4.11B). IL-1α and IL-1β levels were below the detectable limit of the assay. In all cases however, the positive control TNF-α induced high levels of all cytokines tested. This suggests that the A549 assay is competent in production of these host proteins but that secreted products of *A. fumigatus* are not relevant stimuli or inhibit or directly reducing their production.

Expression of FGF-basic and CD40L, was significantly increased relative to PBS treated controls (Fig 4.11I and J respectively). Again, this increase was dependent on the concentration of CF^{48} used. Although there was not statistical significance between effects of 5, 10 and 20 fold dilutions, a 50 fold dilution could not induce any significant effect on production of FGF-2 and CD40L when compared to the PBS control group.

Figure 4.13 compares the effects of live spore challenge to effects of CF^{48} exposure on cytokines that were significantly differentially expressed relative to PBS treated controls.

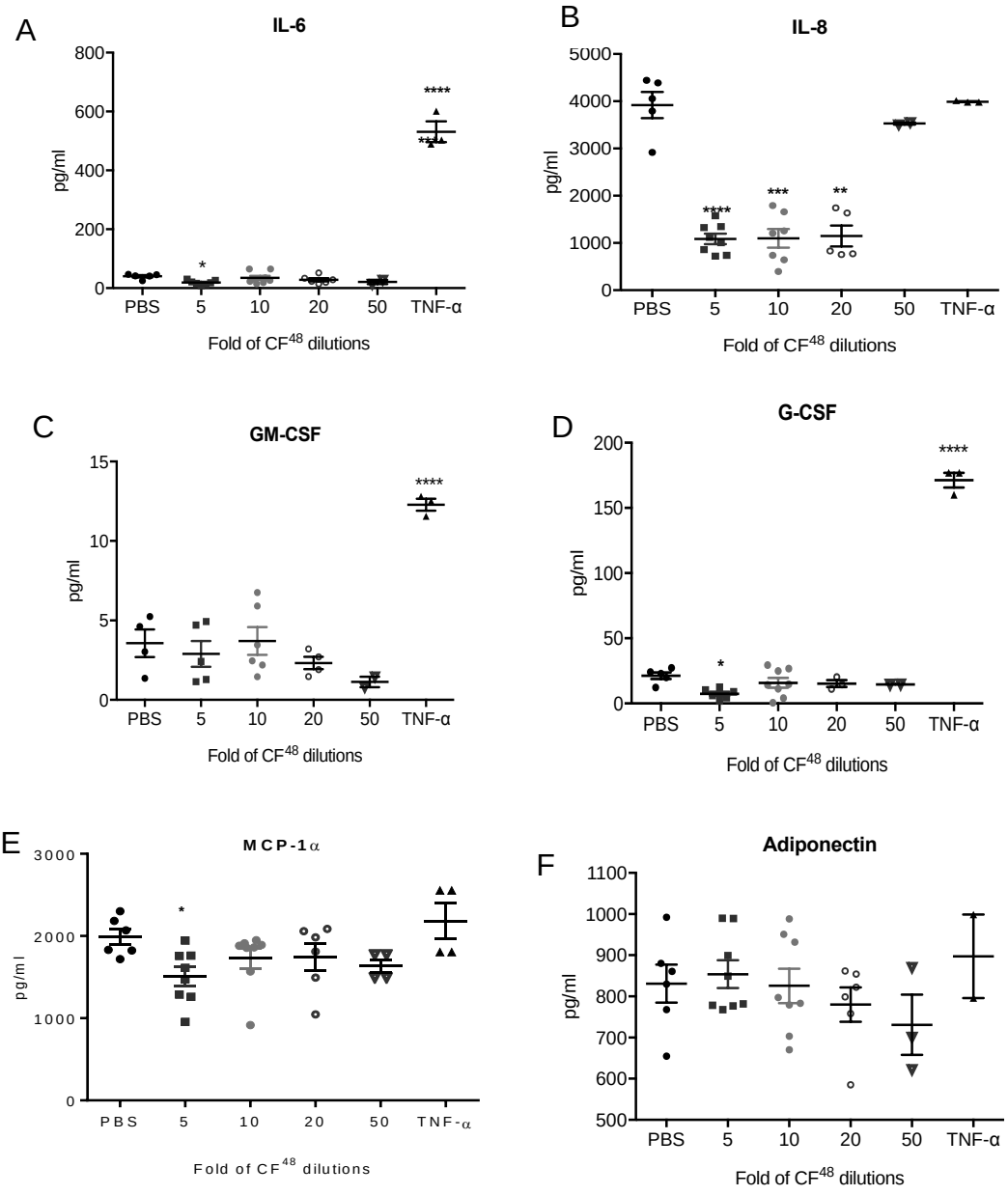
A
IL-6
pg/ml
800
600
400
200
0
****
*
PBS
5
10
20
50
TNF-α
Fold of CF48 dilutions
B
IL-8
pg/ml
5000
4000
3000
2000
1000
0
****
***
**
PBS
5
10
20
50
TNF-α
Fold of CF48 dilutions
C
GM-CSF
pg/ml
15
10
5
0
****
PBS
5
10
20
50
TNF-α
Fold of CF48 dilutions
D
G-CSF
pg/ml
200
150
100
50
0
****
*
PBS
5
10
20
50
TNF-α
Fold of CF48 dilutions
E
MCP-1α
pg/ml
3000
2000
1000
0
*
PBS
5
10
20
50
TNF-α
Fold of CF48 dilutions
F
Adiponectin
pg/ml
1100
1000
900
800
700
600
500
PBS
5
10
20
50
TNF-α
Fold of CF48 dilutions

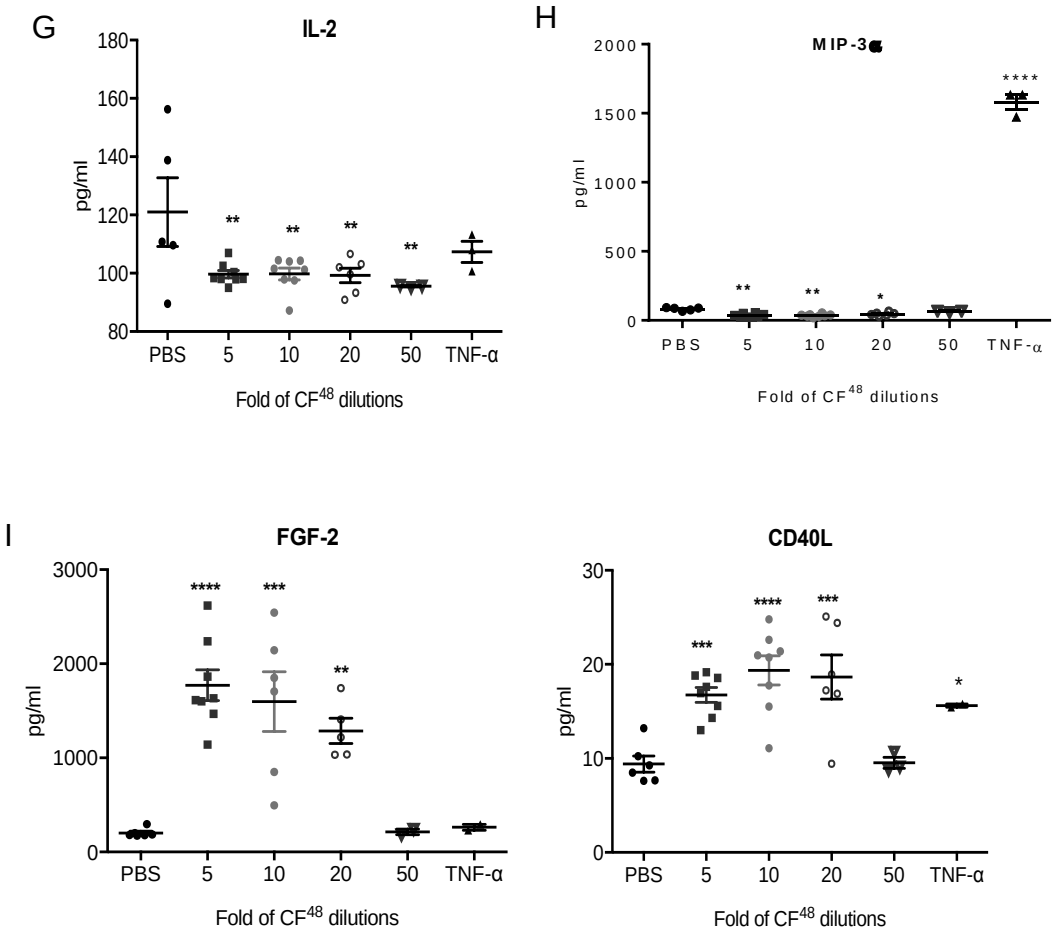

Figure 4.11: Modulation of cytokine production in A549 cells following exposure to different dilutions of CF^{48}. Quantification of cytokine detected in cell culture supernatant following exposure to CF^{48} for 24 h. Data represent the mean of three biological replicates. Error bars show ± SEM. Data were analysed by one-way ANOVA. Significance was calculated relative to challenge with vehicle control (PBS) and between each treatment as shown.*P<0.05, **P<0.01, ***P<0.001, ****P<0.0001.

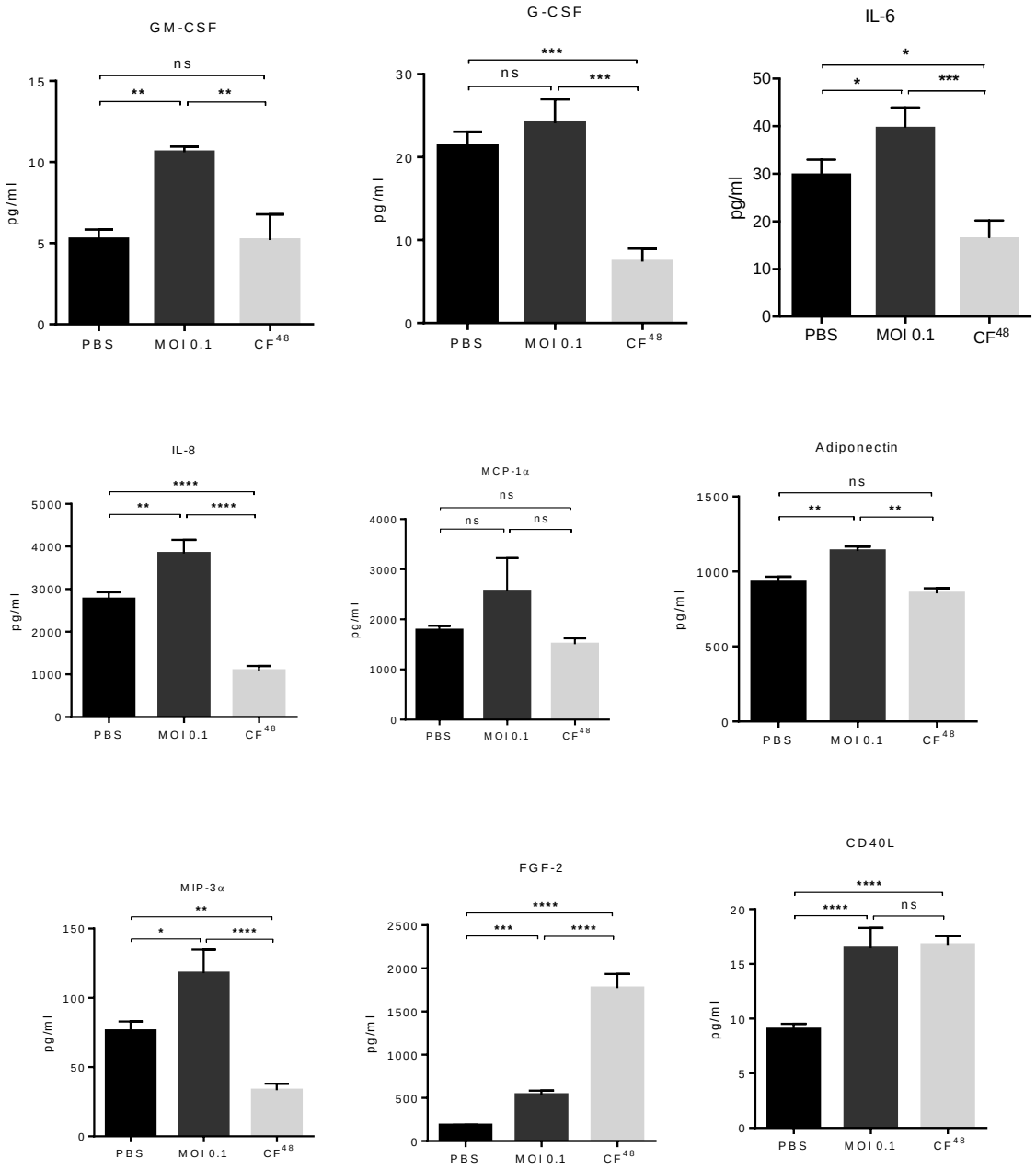

Figure 4.12: Comparative effects of live fungal spores and CF on A549 epithelial cell cytokine responses. Level of cytokines detected in cell culture supernatant following exposure to live fungal spores (MOI 0.1) or a 5 fold dilution of CF^{48} at 24 h post challenge. Data represent the mean of three biological replicates. Error bars show ± SEM. Data were analysed by one-way ANOVA. Significance was calculated relative to challenge with vehicle control (PBS) with Uncorrected Fisher's LSD output.*P<0.05, **P<0.01, ***P<0.001, ****P<0.0001.

4.4 Discussions

The pulmonary epithelium composed of AECs constitutes an important physical barrier to inhaled pathogens. The outcome of the initial interaction between AECs and *A. fumigatus* during infection is key to understanding disease initiation and progression across the spectrum of *Aspergillus* related diseases (refer to Fig 1.1). However, our understanding of the host-pathogen interaction is currently lacking with little/no knowledge of how AECs respond immunologically to dynamic growth of *A. fumigatus*. This study has demonstrated that live *A. fumigatus* and its secreted products activate differential EC immune pathways and effector responses. This is the first study to characterize the entire time line of signalling events in occurring in AECs in response to different *A. fumigatus* growth stages and the hyphal-derived secreted products.

Alveolar epithelial cells respond rapidly (15 min) to live *A. fumigatus* spores via the NF-κB pathway as seen by IκB-α phosphorylation. The IκB-α phosphorylation was sustained throughout the 12 h course of infection as long as live fungal cells were present in the interaction. In contrast, CF^{48} did not induce IκB-α phosphorylation. This suggests that NF-κB activation is an *Aspergillus* specific mucosal response at the airway dependent on fungal contact but independent of the morphological growth state of the fungus. Given the established role of NF-κB signalling in activating inflammatory responses, the prompt induction of IκB-α phosphorylation may be essential in directing subsequent and more specific host responses to clear the invading fungus. However, dysregulated NF-κB activation may lead to exaggerated airway inflammation, a primary phenotype in ABPA and SAFS (Ather et al., 2015, Edwards et al., 2009) thus, necessitating further characterisation of this pathway with respect to the AEC-*Aspergillus* interaction (As studied in Chapters 5 and 7).

Challenge with live *A. fumigatus* spores did not lead to immediate phosphorylation of JNK or ERK1/2, both of which first occur at around 6 h and 12 h respectively. Activation of the JNK pathway was sustained from 6 h post infection with live spores up to 12 h (Fig 4.1D). In contrast to the NF-κB pathway, activation of MAPK (notably the JNK pathway) signalling coincided with spore germination and hyphal growth.

Hyphae formation and maturation in *A. fumigatus* is associated with production of enzymes and proteases as well as secondary metabolites. The production of these substances by the growing hyphae is likely the trigger for the late JNK phosphorylation. CF^{48} exposure resulted in the activation of all three MAPK pathways; p38, ERK1/2 and JNK particularly the JNK and p38 pathways. In contrast to p38 and JNK pathways, ERK1/2 activation was early although without a clear trend throughout the 5 h of treatment (Fig 4.2C). The JNK and p38 phosphorylation increased from 30 min reaching a maximum at 3 h post exposure (Fig 4.2D and E). Activation of JNK-mediated signalling can be a response to host damage and/or responsible for host damage in oral and vaginal epithelial cells during *C. albicans* infection (Moyes et al, unpublished data). This inferred our hypothesis that since secreted proteases are damaging to epithelial cells, the cells maybe responding to fungus-derived secreted products via JNK activation. These hypotheses have been explored in chapter 5 by using small chemical inhibitors or siRNA to knock down JNK signalling pathway and characterise the effects on host cell damage processes.

It is notable that the peak of p38 (Fig 4.2D & Fig 4.2C) and JNK (Fig 4.2E & Fig 4.3A) phosphorylation was followed by a reduction in activation from 4 h. This could be explained by an innate negative regulation of MAPK activities mediated primarily by MAPK phosphatases (MKPs) also known as dual-specificity phosphatases (Huang et al., 2009). One of the MKPs that have been found to be upregulated in epithelial cells in response to infection is MKP-1 that also regulates the MAPK response to *C. albicans* in oral epithelial cells (Moyes et al., 2010). MKP-1 expression is initiated by the p38 pathway, but is then stabilised by ERK1/2-mediated phosphorylation, before preferentially targeting and dephosphorylating p-JNK and p-p38 (Franklin and Kraft, 1997). Since ERK1/2 activation was observed following infection (Fig 4.2C &Fig 4.3E), it is reasonable to propose that this could serve as an activating stimulus for MKP-1 activity, ultimately leading to the dephosphorylation of JNK and p38 signalling as seen in this study. Future studies will target the role of MKP-1 in regulating alveolar epithelial cell responses to *A. fumigatus* and whether a particular threshold of activation must be reached before MKP-1 is activated.

So far, there are only two studies on activation of AEC signalling pathways in response to *A. fumigatus* challenge, published by by Sharon et al (2011) who used the A549 cell line (Sharon et al., 2011) and by Balloy et al (2008) who used the bronchial BEAS-2B cell line (Balloy et al., 2008).

Our data from CF studies share similarities with the findings of Sharon et al (2011) who showed that wild type CF activated both JNK and ERK1/2 pathways in A549 cells. However, in contrast to our current study, Sharon et al did not see activation of the p38 pathway, which may be explained by the fact that they covered only a short and single time point (3 h) of exposure. To our knowledge, this constitutes the first report of p38 activation in alveolar epithelial cells in response to *A. fumigatus* CF, and provides a comprehensive overview of the MAPK signalling pathways mounted by this host cell line against *A. fumigatus*. Our findings differ more substantively from those reported by Balloy, et al 2008, who showed that infection with live *A. fumigatus* activated signalling via the PI3K, p38 and ERK1/2 pathways at 10 h post infection of humanbronchial epithelial cell line BEAS-2B (Balloy et al., 2008). This clear discrepancy between the two studies is probably a result of the use of different epithelial cell lines; alveolar versus bronchial cell lines. The bronchial region of the airway is structurally, functionally and physiologically distinct from the alveolar region. During normal life, the bronchial epithelial cells are exposed to inhaled *A. fumigatus* conidia before the alveolar cells, which may trigger a stronger or qualitatively different danger associated response. Our findings are an important addition to current knowledge and are the first to report that p38 signalling is important in *A. fumigatus* infection of the alveolar compartment. The divergent results in these two studies also suggest that the innate immune response in the lung may be site specific, whereby the bronchial epithelial cells respond differently from the alveolar epithelial cells; a subject that requires further studies.

Functional activity, measured by nuclear DNA binding, of most of the transcription factors analysed in this study were unaffected during the early time points post live spore infections: suggesting that resting spores do not induce an appreciable transcriptional response (Fig 4.5 and Fig 4.6)

Changes in the DNA binding of transcription factors: MEF-2, c-Myc, c-Fos, c-Jun, JunD, relB, p50, and p65 began at 2 h and were sustained to at least 8 h post infection except for c-Jun binding that returned to resting level about 6 h. These data suggest that the A549 epithelial cell transcriptional responses to *A. fumigatus* are driven by germination and hyphal formation. Although both Jun B and JunD show constitutive activation in resting cells (Fig 4.4A), *A. fumigatus* appears to suppress the activity of JunD (Fig 4.5D), leading to a shift towards Jun B activities during A549 *Aspergillus* infection. Exposure of A549 epithelial cells to CF^{48} had no significant impact on the DNA binding of MAPK and AP-1 transcription factors.

The NF-κB transcription factors are classed into two cohorts depending on how they are activated; the canonical NF-κB pathway that targets the p50/p65 or C-rel and the non-canonical NF-κB pathway that targets the p52/RelB complex. Studies have shown that the two NF-κB pathways are independent with regards to both activation signal and biological function. The canonical NF-κB pathway is induced mostly by PAMPs and inflammatory cytokines and is critical in inflammation and immunity (Oeckinghaus and Ghosh, 2009). Specific molecules such as TNF cytokine family members and the CD40 ligand induce the non-canonical NF-κB signalling. Rather than regulating proinflammatory responses, non-canonical NF-κB signalling regulates cellular processes such as growth, development, immunomodulation, tolerance and survival (Sun, 2012). AEC infection with live spores activated the canonical NF-κB transcription factors but suppressed the non-canonical transcription factors. CF^{48} activated the non-canonical NF-κB pathway via increased p52 and RelB translocation and binding but had no effect on the canonical pathways.

Interestingly, though, unlike *Candida* species (Moyes et al., 2012) and dermatophytes (Achterman et al., 2015), stimulation of A549 cells with live *A. fumigatus* spores did not activate p38 signalling in response to direct contact. Thus, in this instance, c-Fos is being activated by other factors, with JNK being the most likely candidate. In parallel with MAPK activation, live *A. fumigatus* also activates the canonical NF-κB signalling circuits in a contact dependent manner leading to p65/p50 activity whereas the CF^{48} could not activate this pathway. There is no activation of the PI3K circuit evident. Thus, whilst initiation of MAPK and NF-κB epithelial cell signalling circuits are

common (although with significant differences) for the three different fungal species, there are key differences, such as the lack of p38 and PI3K activity in response to live *Aspergillus* contact. These differences could be due to either differences in the epithelial cell type or the fungi and will be covered in our future studies.

Activation of canonical NF-κB signalling is a downstream effect of IκBα phosphorylation (Fig 4.1E) leading to nuclear translocation of the p50/p65(RelA) complex. Since this study investigated only IκBα phosphorylation, it is not clear at this point whether the non-canonical pathway is also activated by IκBα phosphorylation or by the IKKα/IKKα complex (Fig 1.9) which was not covered in this study. The only signalling pathway activated in response to CF[48] is MAPK p38 signalling. It will also be worth investigating whether there is cross talk between the p38 signalling and the activation of non-canonical NF-κB signalling (Chapter 7). It is evident from these data that hypha-associated products are responsible for inducing non-canonical activation although they are currently unknown. The exciting finding that CF preferentially activates non-canonical NF-κB signalling with the general lack of and or suppressive effect on MAPK transcription factors points towards a role in immunosuppression or tolerance at least at transcriptional level. Of particular interest is the role of this pathway in mediating the damaging and cytotoxic effect of the hyphal secreted products; as this study has shown that treatment of alveolar epithelial cell monolayers with *A. fumigatus* CF causes massive detachment, epithelial cell desquamation and damage soon after exposure (Chapter 3). Chapter 7 explores the role that the non- canonical NF-κB pathway and the other signalling pathways play in epithelial cell damage. Our study is the first study to report the differential activation of non-canonical NF-κB signalling in response to CF as opposed to its inhibition and canonical activation by contact with live fungi, indicating key differences between secreted products and contact-mediated stimulation of epithelial cells by *A. fumigatus*. Although our data suggests that the MAPK-associated transcription factors; ATF-2, STAT-1α, Fos B, Jun B, and Fra-1 (Fig 4.5 and Fig 4.6) are not activated during an epithelial response to *A. fumigatus*, the possibility that other MAPK-associated transcription factors not captured in this study, such as Elk-1, Elk-2 and

Fra-2, etc. may be of importance during *A. fumigatus* infection cannot be overemphasized.

The ultimate outcome of signalling pathway and transcriptional activation during an immune response to pathogens is the production of effector molecules, most importantly inflammatory cytokines. Given the differences in signalling circuits observed in response to live *A. fumigatus* spores and *A. fumigatus* CF^{48}, it is unsurprising that cytokine profiles in response to these challenges differs. The presence of live fungal spores activated production of all the cytokines investigated. In stark contrast, challenge with CF^{48} prompted a significant drop in proinflammatory cytokines and chemokines (IL-6 and IL-8) and pro-inflammatory MIP-3α with no increase above the baseline level of GM-CSF, Adiponectin and MCP-1 (Fig 4.12). This strongly suggests that components of the *A. fumigatus* secretome can lead to differential remodelling of host immune responses by altering cytokine profiles in the infection milieu. One possible mechanism by which cytokine depletion occurs is via proteolytic degradation of cytokines by secreted fungal products. As will be seen inChapter 5, not all host proteins are susceptible to proteolytic degradation as FGF-2 and CD40L were significantly increased in response to CF^{48} challenge (Fig 12I and J). Therefore, *A. fumigatus* secreted products act in a target-specific manner to remodel the local cytokine environment during infection. Recently, Sterkel et al discovered a fungal mimicry strategy used by *Blastomyces dermatitidis* to disable the host immune system (Sterkel et al., 2016). The pathogenic yeast uses dipeptidyl peptidase (DppIV), a fungal homolog of human aminopeptidase, to cleave the active site of cytokines and GM-CSF in a C-C and CXCL target specific manner (Lorenzini et al., 2017, Sterkel et al., 2016). As covered in Chapter 5, most of the cytokines degraded by CF have either conserved C-C or CXCL motifs. GM-CSF is essential in antifungal defence against *A. fumigatus* (Kasahara et al., 2016), however, the net effect from live spore and CF challenge GM-CSF production and its implications for *Aspergillus* clearance remains as yet unanswered. Protease mediated cytokine degradation has also been shown previously where the bacterium *Porphorymonas gingivalis* uses gingipains to proteolytically degrade IL-8 post secretion. Immunomodulation elicited by the *A. fumigatus* secretome was first evident at transcriptional level via suppression of

canonical NF-κB and MAPK transcription factors leaving us with no option but further characterise the details of the mechanism involved in this interesting result. CD40L is generally expressed under inflammatory conditions (Elgueta et al., 2009) and has been shown to be important in resolution of *A. fumigatus* infection (Stuehler et al., 2015). Concordant with our finding that CD40L was significantly increased following CF challenge, Rodland et al (2010) previously showed that only mature *A. fumigatus* hyphae induced CD40L production in THP-1 monocytes which was essential for IL-8 production (Rodland et al., 2010). Exercise induced CD40L upregulation leads to heightened inflammation in asthmatics (Zietkowski et al., 2008). FGF-2 potentiates in situ angiogenesis, survival rates and enhanced antifungal drug activities in a murine model of invasive aspergillosis as reviewed in (Ben-Ami, 2013, Ben-Ami et al., 2013). Overall, these results highly suggest that an intact airway epithelium may be indispensable during immunosuppression for mounting adequate anti-*Aspergillus* protection against inhaled fungal spores.

Similar to studies on signalling pathways, only a few studies have investigated cytokine responses of human epithelial cell lines in response to *A. fumigatus* either at the transcript or protein level. Reports from these studies still suffer from a lack of standardisation of experimental conditions and cell lines. While some groups have studied the cytokine response in the type II alveolar cell line (A549) (Bellanger et al., 2009, Zhang et al., 2005, Borger et al., 1999, Kauffman et al., 2000, Tomee et al., 1997), others have investigated various bronchial epithelial cell lines (Beisswenger et al., 2012, Sun et al., 2012, Balloy et al., 2008). In addition, cytokine levels have been reported both as transcript and protein outputs and stimuli vary from single live morphotypes (Bellanger et al., 2009, Balloy et al., 2008), or heat- or UV-killed hyphal fragments (Beisswenger et al., 2012, Sun et al., 2012, Zhang et al., 2005) or different types of cell extracts (Borger et al., 1999, Kauffman et al., 2000, Tomee et al., 1997). In all, IL-8 production appears to be a consistent response to fungal contact, which is consistent with our findings. Similarly, high concentrations of culture extract lead to reductions in cytokine level and increased epithelial cell desquamation (Kauffman et al., 2000, Tomee et al., 1997). Putting these results together, a conclusion is reached that *A. fumigatus* challenge stimulates several mechanistically distinct host

responses, via both contact-mediated and diffusible mechanisms, and that secreted fungal products are capable of significant remodelling of the host immune response.

In conclusion, it is evident that epithelial cell responses to *A. fumigatus* are dynamic, varying with the growth stage of the fungus. With these findings, a model of the dynamic responses of epithelial cells to both live *A. fumigatus* spores and secreted products which fall into four broad categories is hereby proposed (Fig 4.13). First is the immediate response to the fungal spores, which results in an instant activation of the NF-κB signaling circuit. This is followed by an early response, during which the spores swell and expose further cell wall components. This leads to activation of MAPK signaling (JNK) and changes in the AP-1 heterodimer profile and activity (decreased JunD and c-Jun). As the spores germinate to generate hyphae, the intermediate fungal growth phase elicits further alterations in the MAPK signaling circuit, with activation of c-Fos, and potentially c-Myc, alongside a subsequent decrease in MEF2 activity. Finally, in the late phase, hyphal-secreted components drive modulation of MAPK signaling circuits, with an increase in both JNK and p38 signalling, with increase in DNA binding of RelB and p50. Follow-up studies shall continue to link these events to the host damages occurring in response to *A. fumigatus* infection, gathering a clear picture of the molecular mechanisms involved which will lead us to the identification of future therapeutic targets.

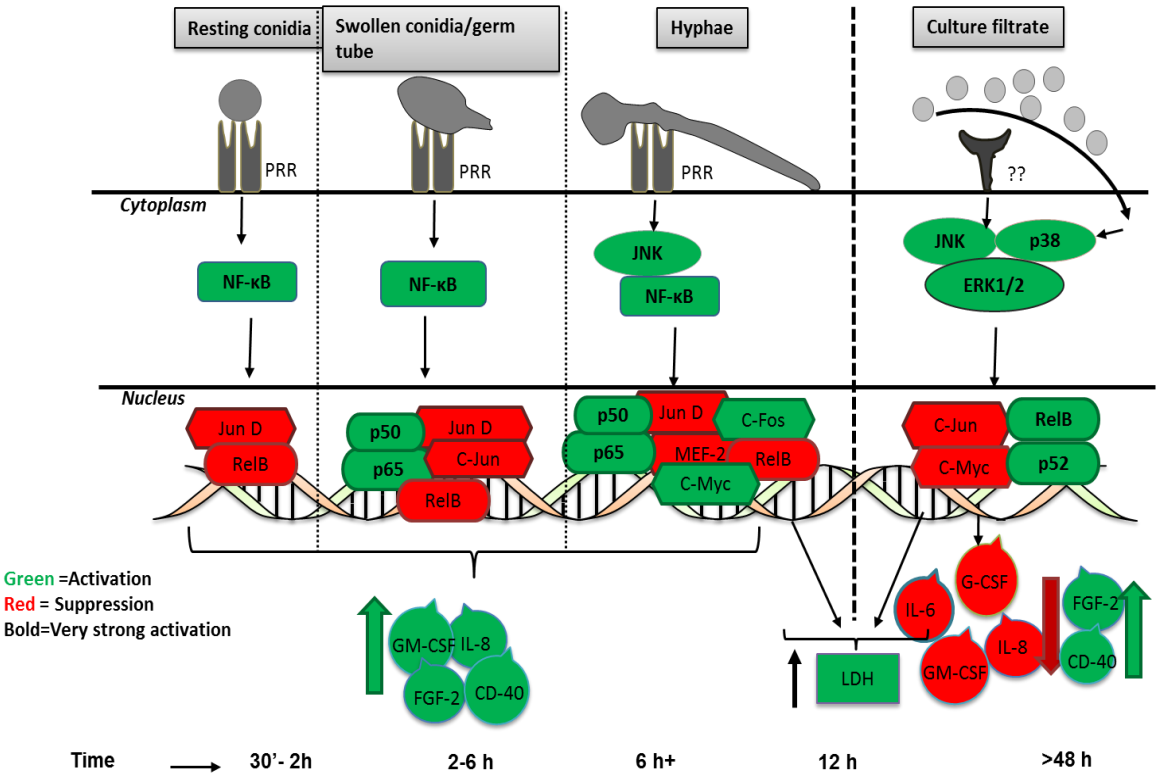

Figure 4.14: Innate immune response of alveolar epithelial cells against *A. fumigatus.*

A. fumigatus conidia interact with epithelial cells activating the canonical (p50/p65) NF-κB pathway and JNK/c-Fos or c-Myc signalling specifically during hyphal growth leading to IL-8 and GM-CSF synthesis. Culture filtrate interacts with epithelial cells and activates three MAPK pathways – JNK, p38 and ERK1/2 and the non-canonical (RelB and p52) NF-κB transcription factors, with a resultant decrease in cytokine. In all cases, LDH release (cellular damage) shows an increase. Green and red colours indicate activation and suppression respectively. Bold lettering indicates strong responses.

4.5 Bibliography

ACHTERMAN, R. R., MOYES, D. L., THAVARAJ, S., SMITH, A. R., BLAIR, K. M., WHITE, T. C. & NAGLIK, J. R. 2015. Dermatophytes activate skin keratinocytes via mitogen-activated protein kinase signaling and induce immune responses. *Infect Immun,* 83**,** 1705-14.

ATHER, J. L., FOLEY, K. L., SURATT, B. T., BOYSON, J. E. & POYNTER, M. E. 2015. Airway epithelial NF-kappaB activation promotes the ability to overcome inhalational antigen tolerance. *Clin Exp Allergy,* 45**,** 1245-58.

BALLOY, V., SALLENAVE, J. M., WU, Y., TOUQUI, L., LATGE, J. P., SI-TAHAR, M. & CHIGNARD, M. 2008. *Aspergillus fumigatus*-induced interleukin-8 synthesis by respiratory epithelial cells is controlled by the phosphatidylinositol 3-kinase, p38 MAPK, and ERK1/2 pathways and not by the toll-like receptor-MyD88 pathway. *J Biol Chem,* 283**,** 30513-21.

BEISSWENGER, C., HESS, C. & BALS, R. 2012. *Aspergillus fumigatus* conidia induce interferon-beta signalling in respiratory epithelial cells. *Eur Respir J,* 39**,** 411-8.

BELLANGER, A. P., MILLON, L., KHOUFACHE, K., RIVOLLET, D., BIECHE, I., LAURENDEAU, I., VIDAUD, M., BOTTEREL, F. & BRETAGNE, S. 2009. *Aspergillus fumigatus* germ tube growth and not conidia ingestion induces expression of inflammatory mediator genes in the human lung epithelial cell line A549. *J Med Microbiol,* 58**,** 174-9.

BEN-AMI, R. 2013. Angiogenesis at the mold-host interface: a potential key to understanding and treating invasive aspergillosis. *Future Microbiol,* 8**,** 1453-62.

BEN-AMI, R., ALBERT, N. D., LEWIS, R. E. & KONTOYIANNIS, D. P. 2013. Proangiogenic growth factors potentiate in situ angiogenesis and enhance antifungal drug activity in murine invasive aspergillosis. *J Infect Dis,* 207**,** 1066-74.

BIGNELL, E., CAIRNS, T. C., THROCKMORTON, K., NIERMAN, W. C. & KELLER, N. P. 2016. Secondary metabolite arsenal of an opportunistic pathogenic fungus. *Philos Trans R Soc Lond B Biol Sci,* 371.

BORGER, P., KOETER, G. H., TIMMERMAN, J. A., VELLENGA, E., TOMEE, J. F. & KAUFFMAN, H. F. 1999. Proteases from *Aspergillus fumigatus* induce interleukin (IL)-6 and IL-8 production in airway epithelial cell lines by transcriptional mechanisms. *J Infect Dis,* 180**,** 1267-74.

CASTILHO, R. M., SQUARIZE, C. H. & GUTKIND, J. S. 2013. Exploiting PI3K/mTOR signaling to accelerate epithelial wound healing. *Oral Diseases,* 19**,** 551-558.

CROFT, C. A., CULIBRK, L., MOORE, M. M. & TEBBUTT, S. J. 2016. Interactions of *Aspergillus fumigatus* Conidia with Airway Epithelial Cells: A Critical Review. *Front Microbiol,* 7**,** 472.

DAGUE, E., ALSTEENS, D., LATGE, J. P. & DUFRENE, Y. F. 2008. High-resolution cell surface dynamics of germinating *Aspergillus fumigatus* conidia. *Biophys J,* 94**,** 656-60.

EDWARDS, M. R., BARTLETT, N. W., CLARKE, D., BIRRELL, M., BELVISI, M. & JOHNSTON, S. L. 2009. Targeting the NF-kappaB pathway in asthma and chronic obstructive pulmonary disease. *Pharmacol Ther,* 121**,** 1-13.

ELGUETA, R., BENSON, M. J., DE VRIES, V. C., WASIUK, A., GUO, Y. & NOELLE, R. J. 2009. Molecular mechanism and function of CD40/CD40L engagement in the immune system. *Immunol Rev,* 229**,** 152-72.

FRANKLIN, C. C. & KRAFT, A. S. 1997. Conditional expression of the mitogen-activated protein kinase (MAPK) phosphatase MKP-1 preferentially inhibits p38 MAPK and stress-activated protein kinase in U937 cells. *J Biol Chem,* 272**,** 16917-23.

FUKAO, T. & KOYASU, S. 2003. PI3K and negative regulation of TLR signaling. *Trends Immunol,* 24**,** 358-63.

HAYDEN, M. S. & GHOSH, S. 2012. NF-kappaB, the first quarter-century: remarkable progress and outstanding questions. *Genes Dev,* 26**,** 203-34.

HILL, C. S. & TREISMAN, R. 1995. Transcriptional regulation by extracellular signals: mechanisms and specificity. *Cell,* 80**,** 199-211.

HUANG, G., SHI, L. Z. & CHI, H. 2009. Regulation of JNK and p38 MAPK in the immune system: signal integration, propagation and termination. *Cytokine,* 48**,** 161-9.

KASAHARA, S., JHINGRAN, A., DHINGRA, S., SALEM, A., CRAMER, R. A. & HOHL, T. M. 2016. Role of Granulocyte-Macrophage Colony-Stimulating Factor Signaling in Regulating Neutrophil Antifungal Activity and the Oxidative Burst During Respiratory Fungal Challenge. *J Infect Dis,* 213**,** 1289-98.

KAUFFMAN, H. F., TOMEE, J. F., VAN DE RIET, M. A., TIMMERMAN, A. J. & BORGER, P. 2000. Protease-dependent activation of epithelial cells by fungal allergens leads to morphologic changes and cytokine production. *J Allergy Clin Immunol,* 105**,** 1185-93.

LATGE, J. P., DEBEAUPUIS, J. P., SARFATI, J., DIAQUIN, M. & PARIS, S. 1993. Cell wall antigens in *Aspergillus fumigatus*. *Arch Med Res,* 24**,** 269-74.

LATGE, J. P., MOUYNA, I., TEKAIA, F., BEAUVAIS, A., DEBEAUPUIS, J. P. & NIERMAN, W. 2005. Specific molecular features in the organization and biosynthesis of the cell wall of *Aspergillus fumigatus*. *Med Mycol,* 43 Suppl 1**,** S15-22.

MOYES, D. L., MURCIANO, C., RUNGLALL, M., ISLAM, A., THAVARAJ, S. & NAGLIK, J. R. 2011. *Candida albicans* yeast and hyphae are discriminated by MAPK signaling in vaginal epithelial cells. *PLoS One,* 6**,** e26580.

MOYES, D. L., MURCIANO, C., RUNGLALL, M., KOHLI, A., ISLAM, A. & NAGLIK, J. R. 2012. Activation of MAPK/c-Fos induced responses in oral epithelial cells is specific to *Candida albicans* and *Candida dubliniensis* hyphae. *Med Microbiol Immunol,* 201**,** 93-101.

MOYES, D. L., RUNGLALL, M., MURCIANO, C., SHEN, C., NAYAR, D., THAVARAJ, S., KOHLI, A., ISLAM, A., MORA-MONTES, H., CHALLACOMBE, S. J. & NAGLIK, J. R. 2010. A biphasic innate immune MAPK response discriminates between the yeast and hyphal forms of *Candida albicans* in epithelial cells. *Cell Host Microbe,* 8**,** 225-35.

MOYES, D. L., SHEN, C., MURCIANO, C., RUNGLALL, M., RICHARDSON, J. P., ARNO, M., ALDECOA-OTALORA, E. & NAGLIK, J. R. 2014. Protection against epithelial damage during *Candida albicans* infection is mediated by PI3K/Akt and mammalian target of rapamycin signaling. *J Infect Dis,* 209**,** 1816-26.

OECKINGHAUS, A. & GHOSH, S. 2009. The NF-kappaB family of transcription factors and its regulation. *Cold Spring Harb Perspect Biol,* 1**,** a000034.

OSHEROV, N. 2012. Interaction of the pathogenic mold *Aspergillus fumigatus* with lung epithelial cells. *Front Microbiol,* 3**,** 346.

OSHEROV, N. 2015. Modulation of host-cell MAPkinase signaling during fungal infection. *MAP Kinase,* 4.

PENG, H., SHI, M., ZHANG, L., LI, Y., SUN, J., ZHANG, L., WANG, X., XU, X., ZHANG, X., MAO, Y., JI, Y., JIANG, J. & SHI, W. 2014. Activation of JNK1/2 and p38 MAPK signaling pathways promotes *enterovirus* 71 infection in immature dendritic cells. *BMC Microbiol,* 14**,** 147.

RODLAND, E. K., UELAND, T., PEDERSEN, T. M., HALVORSEN, B., MULLER, F., AUKRUST, P. & FROLAND, S. S. 2010. Activation of platelets by *Aspergillus fumigatus* and potential role of platelets in the immunopathogenesis of Aspergillosis. *Infect Immun,* 78**,** 1269-75.

SHARON, H., AMAR, D., LEVDANSKY, E., MIRCUS, G., SHADKCHAN, Y., SHAMIR, R. & OSHEROV, N. 2011. PrtT-regulated proteins secreted by *Aspergillus fumigatus* activate MAPK signaling in exposed A549 lung cells leading to necrotic cell death. *PLoS One,* 6**,** e17509.

SHI, W., HOU, X., LI, X., PENG, H., SHI, M., JIANG, Q., LIU, X., JI, Y., YAO, Y., HE, C. & LEI, X. 2013. Differential gene expressions of the MAPK signaling pathway in *enterovirus* 71-infected rhabdomyosarcoma cells. *Braz J Infect Dis,* 17**,** 410-7.

STERKEL, A. K., LORENZINI, J. L., FITES, J. S., SUBRAMANIAN VIGNESH, K., SULLIVAN, T. D., WUTHRICH, M., BRANDHORST, T., HERNANDEZ-SANTOS, N., DEEPE, G. S., JR. & KLEIN, B. S. 2016. Fungal Mimicry of a Mammalian Aminopeptidase Disables Innate Immunity and Promotes Pathogenicity. *Cell Host Microbe,* 19**,** 361-74.

STUEHLER, C., NOWAKOWSKA, J., BERNARDINI, C., TOPP, M. S., BATTEGAY, M., PASSWEG, J. & KHANNA, N. 2015. Multispecific *Aspergillus* T cells selected by CD137 or CD154 induce protective immune responses against the most relevant mold infections. *J Infect Dis,* 211**,** 1251-61.

SUN, S. C. 2012. The noncanonical NF-kappaB pathway. *Immunol Rev,* 246**,** 125-40.

SUN, W. K., LU, X., LI, X., SUN, Q. Y., SU, X., SONG, Y., SUN, H. M. & SHI, Y. 2012. Dectin-1 is inducible and plays a crucial role in *Aspergillus*-induced innate immune responses in human bronchial epithelial cells. *Eur J Clin Microbiol Infect Dis,* 31**,** 2755-64.

TOMEE, J. F., WIERENGA, A. T., HIEMSTRA, P. S. & KAUFFMAN, H. K. 1997. Proteases from *Aspergillus fumigatus* induce release of proinflammatory cytokines and cell detachment in airway epithelial cell lines. *J Infect Dis,* 176**,** 300-3.

WHITMARSH, A. J. 2007. Regulation of gene transcription by mitogen-activated protein kinase signaling pathways. *Biochim Biophys Acta,* 1773**,** 1285-98.

WHITMARSH, A. J. & DAVIS, R. J. 1996. Transcription factor AP-1 regulation by mitogen-activated protein kinase signal transduction pathways. *J Mol Med (Berl),* 74**,** 589-607.

ZHANG, Z., LIU, R., NOORDHOEK, J. A. & KAUFFMAN, H. F. 2005. Interaction of airway epithelial cells (A549) with spores and mycelium of *Aspergillus fumigatus*. *J Infect,* 51**,** 375-82.

ZIETKOWSKI, Z., SKIEPKO, R., TOMASIAK, M. M. & BODZENTA-LUKASZYK, A. 2008. Soluble CD40 ligand and soluble P-selectin in allergic asthma patients during exercise-induced bronchoconstriction. *J Investig Allergol Clin Immunol,* 18**,** 272-8.

ZOU, J. & SHANKAR, N. 2015. Roles of TLR/MyD88/MAPK/NF-kappaB Signaling Pathways in the Regulation of Phagocytosis and Proinflammatory Cytokine Expression in Response to *E. faecalis* Infection. *PLoS One,* 10**,** e0136947.

CHAPTER 5: MECHANISTIC BASIS OF EPITHELIAL DAMAGE DURING *A. FUMIGATUS* INFECTION; HOST CONTRIBUTION

5.1 Introduction

Over the time course of A*spergillus* infections, the lung epithelium must interact with and eliminate various fungal products including: inhaled spores, which germinate to produce hyphae, as well as fungal proteins and toxins which are secreted from mature hyphae. The outcome of this interaction, is mediated by both host and fungal activities, and is a critical determinant of disease prognosis leading ultimately to neutralization of pathogen threat or establishment of infection and associated tissue damage.

The studies documented in chapter 4 demonstrated clearly that airway epithelial cells (AECs) respond in a dynamic manner to various morphotypes and secreted products of *A. fumigatus* via NF-κB and MAPK signalling. NF-κB signalling is central to the proinflammatory immune response, thus, aberrant /uncontrolled activation can lead to dysregulated inflammation. This is usually the case in ABPA and SAFs patients (Edwards et al., 2009). In addition to inducing inflammatory host tissue damage, activation of signalling pathways in AECs has been linked to other forms of host tissue damage. Protease-induced ERK/JNK MAPK signalling in *A. fumigatus*-infected A549 cells caused epithelial cell peeling and death by necrosis, a phenotype that was negated by heat inactivation of CF (Sharon et al., 2011). Geissler et al also reported that gliotoxin induced apoptosis in different cell types, which was mediated through JNK phosphorylation (Geissler et al., 2013). These studies so far looked at only the impact of secreted products on host signalling and damage, but the contact-mediated response to intact fungal cells has been largely overlooked.

Bertuzzi et al (2014) previously discovered an *A. fumigatus* PacC null mutant which exhibited significant dysregulation of multiple genes encoding secreted gene products and which was less efficiently internalized by epithelial cells. Consequently, PacC null mutants are unable to damage airway epithelium in *in vitro* culture or to invade lung tissues during murine infection (Bertuzzi et al., 2014). A recent study has shown that uptake of *A. fumigatus* spores is dependent on the interaction between the fungal

CalA protein with the human α5β1 integrin on host epithelia cells (Liu et al., 2016). It was also shown that a Δ*CalA* mutant was attenuated for virulence and tissue invasion in a corticosteroid treated murine model of invasive aspergillosis (Liu et al., 2016). Taken together, these data suggest that epithelial entry by spores maybe an added strategy by which the fungus damages the host cells.

A previous study found that *A. fumigatus* elicited epithelial cell damage via two mechanistically distinct events: the first being contact dependent and the second, later event mediated by secreted products (Bertuzzi et al., 2014). The same study showed that both damage processes were deficient in PacC null mutants. The study in the present chapter was aimed at furthering the investigation of early and late phases of epithelial damage in order to identify the underlying mechanisms. To this end the role, in epithelial decay, of host-mediated signalling (chapter 4) and fungal uptake (chapter 3) was characterised using chemical or genetic inhibitors. It was found that although the fungus secretes damaging molecules, it is the host response to such products, and not the gene products themselves, which exerts the greater degree of host damage.

5.2 Methods

5.2.1 Chemical inhibition of signalling pathways

At 1 h prior to fungal challenge, confluent epithelial cell monolayers were treated with inhibitors for target signalling pathways at concentrations previously determined (Moyes et al., 2010) as shown in table 5.1. Epithelial cells were then challenged with either live fungal spores or CF^{48}, and LDH (section 2.2.4.3), TEER (section 2.2.4.4) and detachment (section 2.2.7.2) were measured.

Table 5.1: Signalling pathway inhibitors and concentrations used in this study

Signalling pathway	Inhibitor	Conc.	Reference	Supplier
MAPK-JNK (Primary target: JNK1, JNK2, JNK3)	SP600125	10 μM	(Bennett et al., 2001)	Calbiochem
MAPK-p38 (Primary target: p38 of MAPK pathway)	SB203580	10 μM	(Cuenda et al., 1995)	Calbiochem
NF-κB (Primary target: IκB-α of canonical pathway)	BAY11-7082	2 μM	(Pierce et al., 1997, Mori et al., 2002)	Calbiochem

5.2.2 Inhibition of internalisation/actin polymerization

To block fungal internalization into A549 cells, monolayers were pre-incubated with Cytochalasin D (CytD), an inhibitor of actin polymerization (CytD, 0.2 μM) at 1 h before challenging with live fungal spores. Phosphorylation of signalling proteins was measured according to section 2.2.5.

5.2.3 Measurement of trans-epithelial electrical resistance (TEER) of cultured Calu-3 monolayer

Trans-epithelial electrical resistance was measured following infection of A549 epithelial monolayers pre-treated with 0.2 μM Cytochalasin D, or signalling pathway inhibitors for 1 h according to section 2.2.4.4. On the day of infection, the TEER (TEER 0) was measured for time zero (T 0 h) followed by monolayer pre-treatment with 0.2

µM Cytochalasin D, or signalling pathway inhibitors for 1 h and then fungal challenge with 10^5 spores or a 5 fold dilution of CF (200 µl of CF in 800 µl of media in the insert). The plate was incubated for 24 h (T 24 h) and TEER was measured again (TEER 24 h). The difference between TEER 24 h and TEER 0 h was calculated as loss in TEER due to challenge (TEER 24 h-TER 0 h) and normalised to fungal viable count. The result in most cases was expressed as fold reduction in TEER relative to PBS challenge.

Viable count = number of single fungal colonies recovered out of 100 CFU plated

Normalisation coefficient = 100 ÷ viable count

ΔTEER = (TEER 24 h-TEER 0 h) × normalisation coefficient

5.2.4 Quantitative analysis of A549 detachment

$0.5x10^5$ A549 cells were seeded in black 24 well glass bottom tissue culture plates and incubated to ≥ 90% confluency. Monolayers were treated with signaling pathway inhibitors for 1 h prior to challenge with 10^5 spores or 5 fold dilution of CF (200 µl of CF in 800 µl of media). Following co-incubation monolayers were washed 3 times with PBS, fixed with 4% formaldehyde in PBS and permeabilized with 0.2% Triton-X100. Nuclei of adherent A549 cells were stained with 300 nM DAPI. DAPI fluorescence in adherent epithelial cells was excited with a CoolLED PreciseExcite 380 nm LED array in combination with a Nikon UV-2A filter cube, which collected the DAPI emission. Adherent A549 cells were counted in at least 3 fields of view at magnifications of X20. Images were then processed and quantified using an in-house “DAPI Counter” macro (Appendix 3) written for FIJI (Schindelin et al., 2012) and data were exported into Prism for plotting and analysis of significance.

5.3 Results

5.3.1 Role of JNK and NF-κB signalling pathways in epithelial cell damage

In work described in Chapter 4, it was discovered that A549 epithelial cells respond to *A. fumigatus* spores and secreted products via NF-κB, JNK and p38 signalling. In order to investigate the contribution of host-mediated signalling in A549 cells in response to fungal challenge, the extent of epithelial damage in the presence of NF-κB-, JNK-, and p38-specific small chemical inhibitors was assessed.

5.3.1.1 Role of JNK, p38 and NF-κB signalling pathways in epithelial cell lysis

Inhibition of JNK signalling led to greater than a 60% decrease in lytic cell damage induced by live fungal spore and CF challenges (Fig 5.1A). p38 inhibitor decreased lytic cell death due to secreted products by about 40% but had no effect on spore induced lysis (Fig 5.1B). IκBα inhibitor led to a significant decrease, about 30% and 60% respectively in spore-induced and CF-induced epithelial cell lysis (Fig 5.1C). Simultaneous inhibition of JNK and NF-κB pathways conferred no additional protection over that incurred by JNK pathway inhibition alone. Inhibition of JNK and NF-κB either singly or simultaneously prior to epithelial challenge with CF led to over 50% reduction in lytic epithelial cell death (Fig 5.1D). When compared, ECs challenged with clinical isolate CEA10 or laboratory isolate Δ*akuB*^{KU80}, mounted similar responses (Fig 5.1E and F).

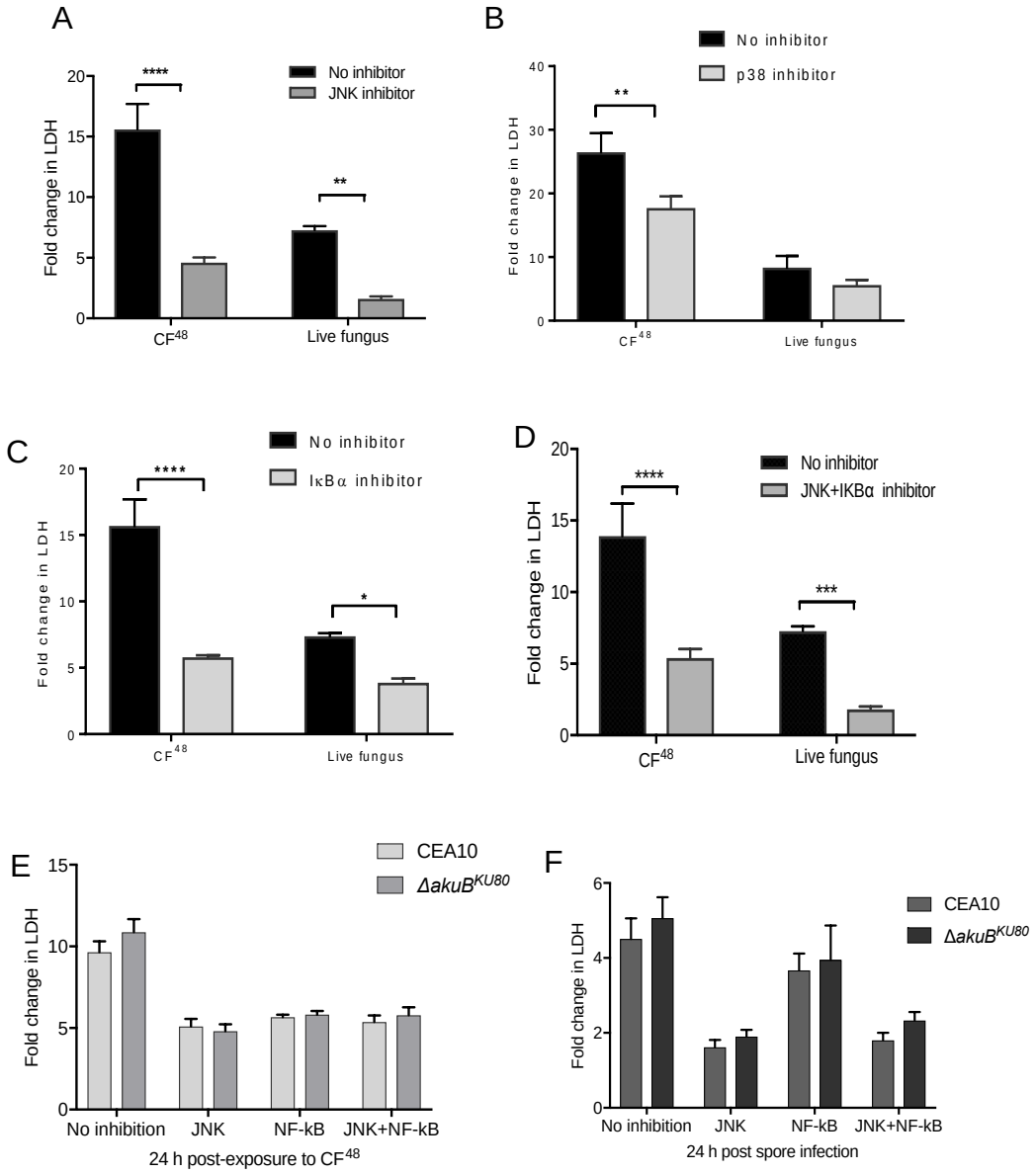

Figure 5.1: JNK and NF-κB activation in response to *A. fumigatus* challenge plays a role in epithelial cell damage

A549 cells were challenged with CF and live spores derived from *A. fumigatus* clinical isolate CEA10 following treatment with small chemical inhibitors. Phosphorylation of specified signalling proteins was quantified in the presence and absence of inhibitors and LDH activity was measured relative to PBS challenged cells A) Effect of JNK inhibition B) Effect of p38 inhibition C) Effect of IκBα inhibition D) Effect of simultaneous inhibition of JNK and IκBα phosphorylation on epithelial cell damage quantified by LDH release 24 h post infection E) Comparison of effect of inhibitor following exposure to CF^{48} from two different *A. fumigatus* genetic backgrounds F) Comparison of effect of the inhibitors following challenge with *A. fumigatus* spores

from two different genetic backgrounds. Data represent the mean of three biological replicates (each performed as three technical replicates). Error bars show ± SEM. Data were analyzed by one way or two-ways (E and F) ANOVA. Significance was calculated relative to challenge with vehicle control (PBS) with Sidak's multiple comparisons test, ***P<0.001, ****P<0.0001.

5.3.1.2 Role of JNK and NF-κB signaling pathways in epithelial cell detachment and loss in TEER

Live *A. fumigatus* spores induced detachment of about 50% of cultured pneumocytes compared to PBS treated controls. Pre-treatment of pneumocytes with JNK inhibitor before live fungal challenge moderately, but significantly, reduced this detachment (Fig 5.2A). However, NF-κB inhibitor did not confer any significant protection to the epithelial cells against detachment (Fig 5.2A).

Over 80% of epithelial cells detached after 16 h of exposure to CF^{48} (Fig 3.4B) with over 15 fold increase in LDH after 24 h relative to PBS treated controls (Fig 3.6A). Although JNK and NF-κB inhibitors protected from the lytic cell death measured by LDH release (Fig 5.1A and C), these inhibitors had no significant effect on detachment induced by CF exposure (Fig 5.2A). JNK and NF-κB inhibitors protected cultured pneumocytes from loss of TEER following both live fungal and CF^{48} challenge (Fig 5.2B).

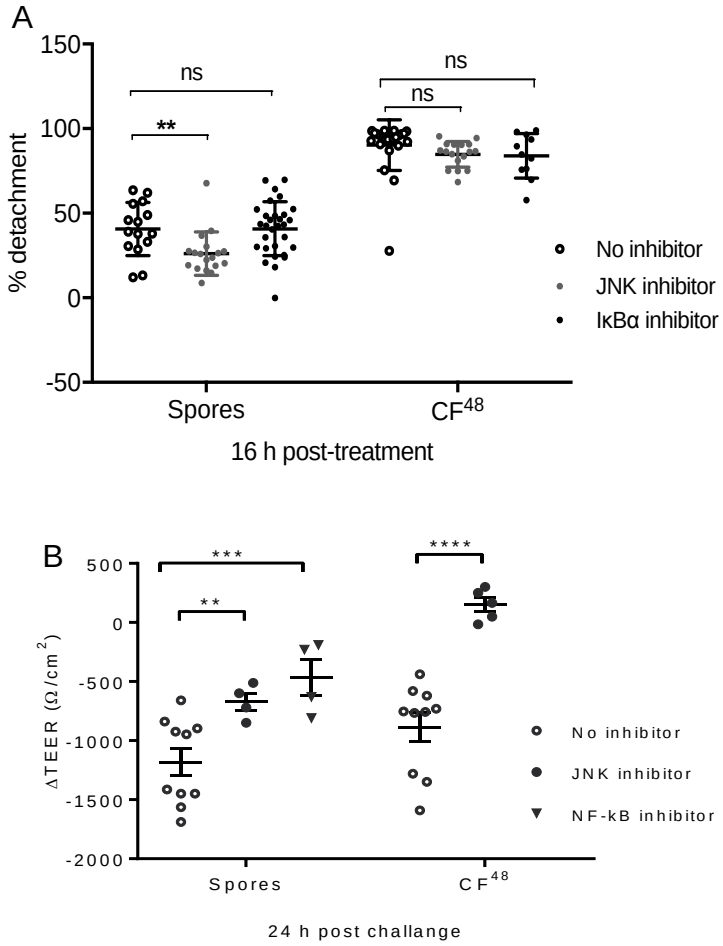

Figure 5.2: JNK or NF-κB inhibition leads to reduction in detachment and loss in TEER

Inhibition of JNK and IκBα signalling induction in A549 cells exposed to *A. fumigatus* spores or CF^{48} from the CEA10 clinical isolate A) Effect of JNK or IκBα inhibition on epithelial cell detachment B) Effect of the inhibitors on trans-epithelial electrical resistance relative to uninfected control. Data represent the mean of three biological replicates (each performed in three technical replicates. Error bars show ± SEM. Data were analysed by two-way Anova. Significance was calculated relative to no inhibitor treatment with Sidak's multiple comparisons test, ***P<0.001, ****P<0.0001.

5.3.2 Role of spore uptake by A549 epithelial cells damage via detachment and loss of TEER

A previous study by Bertuzzi et al (2014) showed that spore internalization by epithelial cells contributes significantly to epithelial monolayer destruction, thus the role of fungal internalization in activation of epithelial cell signalling responses to *A. fumigatus* and in inducing damage events was investigated. AEC-mediated internalization of *A. fumigatus* spores is an actin polymer dependent process that can be blocked using an actin polymerization inhibitor, Cytochalasin D 2 µM (CytD). Blocking fungal internalization and other actin dependent processes in epithelial cells significantly but incompletely improved epithelial integrity as measured in a trans-well assay (Fig 5.3A). Also, CytD treatment before spore infection partly but significantly reduced cell detachment (Fig 5.3B).

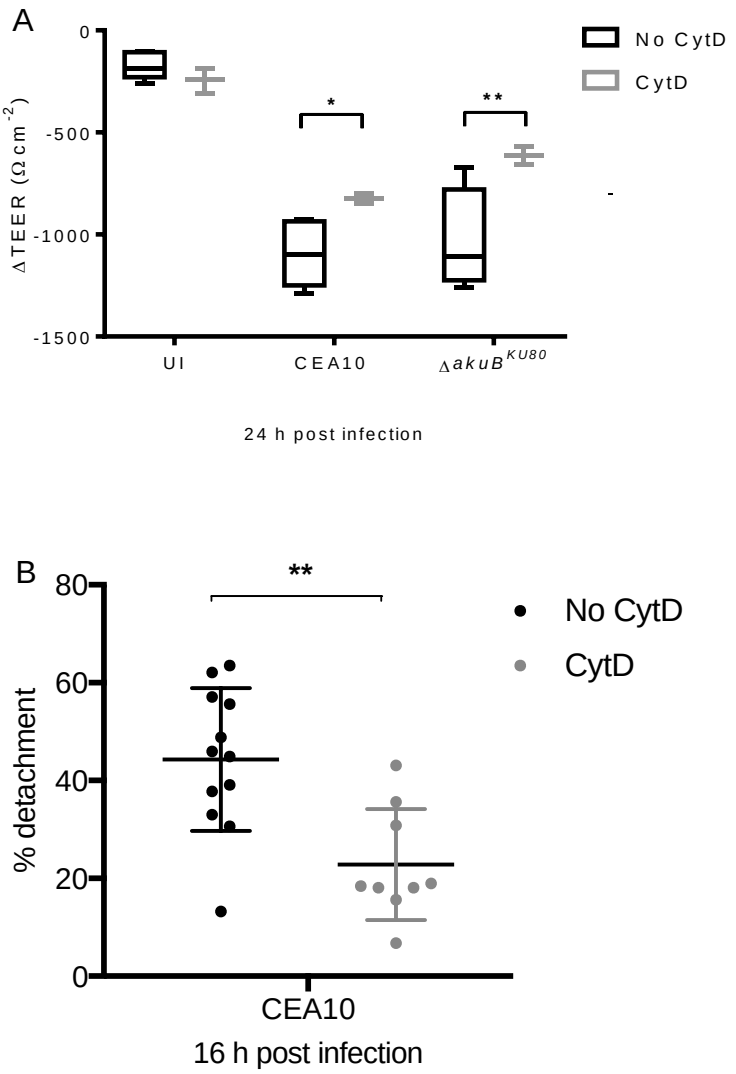

Figure 5.3: Pre-treatment of A549 epithelial cells leads to reduction in detachment and loss of TEER

A549 cells infected with *A. fumigatus* spores following 1 h pre-exposure to 0.2 µM Cytochalasin D (CytD) A) Loss in trans-epithelial electrical resistance (TEER) 24 h post infection with two genetically different strains B) Epithelial cell detachment 16 h post infection. Data represent the mean of three biological replicates (each performed in three technical replicates. Error bars show ± SEM. Data were analysed by two-way (A) or oneway (B) ANOVA. Significance was calculated relative to treatments with Sidak's multiple comparisons test. ***P<0.001, ****P<0.0001.

5.3.3 Activation of host JNK and NF-κB signalling is dependent on fungal viability but independent of spore uptake by A549 epithelial cells.

Activation of JNK or NF-κB signalling pathway occurs independently of actin polymerisation as pre-treatment of host cells with CytD did not alter the timing, or magnitude, of pJNK or IKBα phosphorylation. (Fig 5.4A). This result also demonstrates that actin polymerisation is not important for activation of host signalling, which in turn suggests that uptake of spores is also not important for signalling. There was no difference between a clinical and a laboratory isolate with respect to signalling in the presence of CytD (Fig 5.4B).

To understand whether the induction of host signalling in response to contact with fungal cells is dependent upon fungal viability or a morphotype-specific heat labile fungal cell surface moiety, A549 monolayers were challenged with heat killed (HK) pre-grown fungal morphotypes. Interestingly, viable fungal cells are required for signal activation (Fig 5.4C).

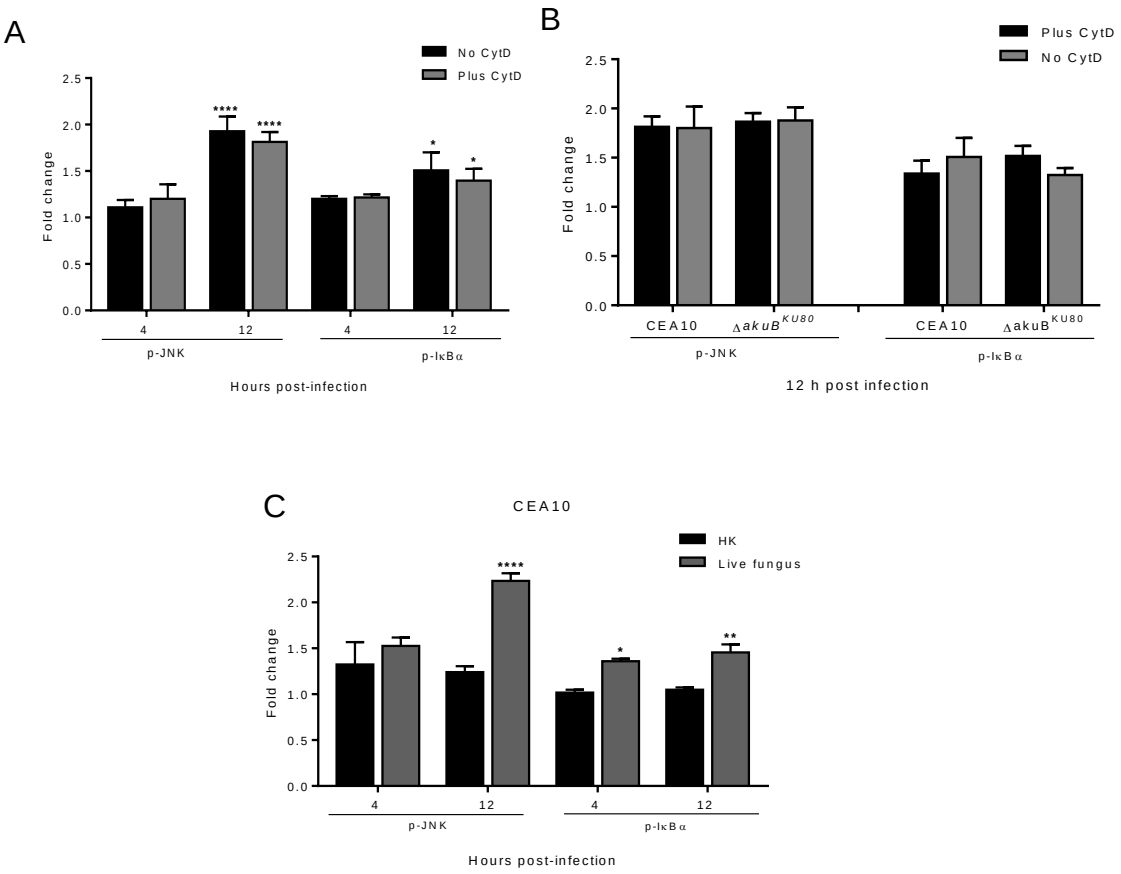

Figure 5.4: Signalling activation occurs independently of actin polymerisation but requires fungal viability A) Quantity of phosphorylated p-JNK and IκBα in A549 cells infected with spore (4 h) or hyphal (12 h) morphotypes of an *A. fumigatus* CEA10 isolate following pre-incubation with Cytochalasin D (CytD, 0.2 µM) B) Behaviours of different wild type strains after 12 h of infection C) Quantity of JNK and IκBα phosphorylation in A549 cells following 4 h incubation with live and heat killed (HK 90 degree for 45 min) morphotypes of *A. fumigatus*. Data represent the mean of three biological replicates (performed as three technical replicates each). Error bars show ± SEM. Data were analysed by Two-way ANOVA. Significance was calculated relative to no CytD treatments with Sidak's multiple comparisons test. *P<0.05, ****P<0.0001.

5.3.4: Soluble factor(s) from *A. fumigatus* degrade host cytokines but not growth factors

In chapter 4, epithelial challenge with *A. fumigatus* spores for 24 h significantly increased the secretion of GM-CSF, IL-8, IL-6, TNF-α and FGF-2, relative to the vehicle control. In stark contrast, challenge with CF^{48} for 24 h prompted a significant drop in levels of all but FGF-2 which was significantly increased in response to CF^{48} challenge (Section 4.3.3). To determine whether the reductions in cytokine expression following CF challenge were an artefact of rapid epithelial decay, or the result of direct protease-mediated cytokine degradation, a "prime and challenge" experiment was performed whereby cell free supernatants recovered at 24 hours after spore challenge were harvested and then directly exposed to CF^{48}. This revealed that IL-8, IL-6, and TNF-α (Fig 5.5A-C) are susceptible to direct degradation by CF^{48} while the growth factor, FGF-2 is resistant to such degradation (Fig 5.5D).

To ascertain whether any host factors are required for this process, the supernatants recovered from live spore infection were exposed to culture supernatant recovered from 24 h exposure of epithelial cells to CF, called conditioned CF (CDN). There was no significant difference between effects of CF and CDN upon cytokine level. It was therefore concluded that *A. fumigatus* secreted products act in a target-specific manner to remodel the local cytokine and extracellular matrix environment during infection and that host-derived factors make little or no contribution to this process.

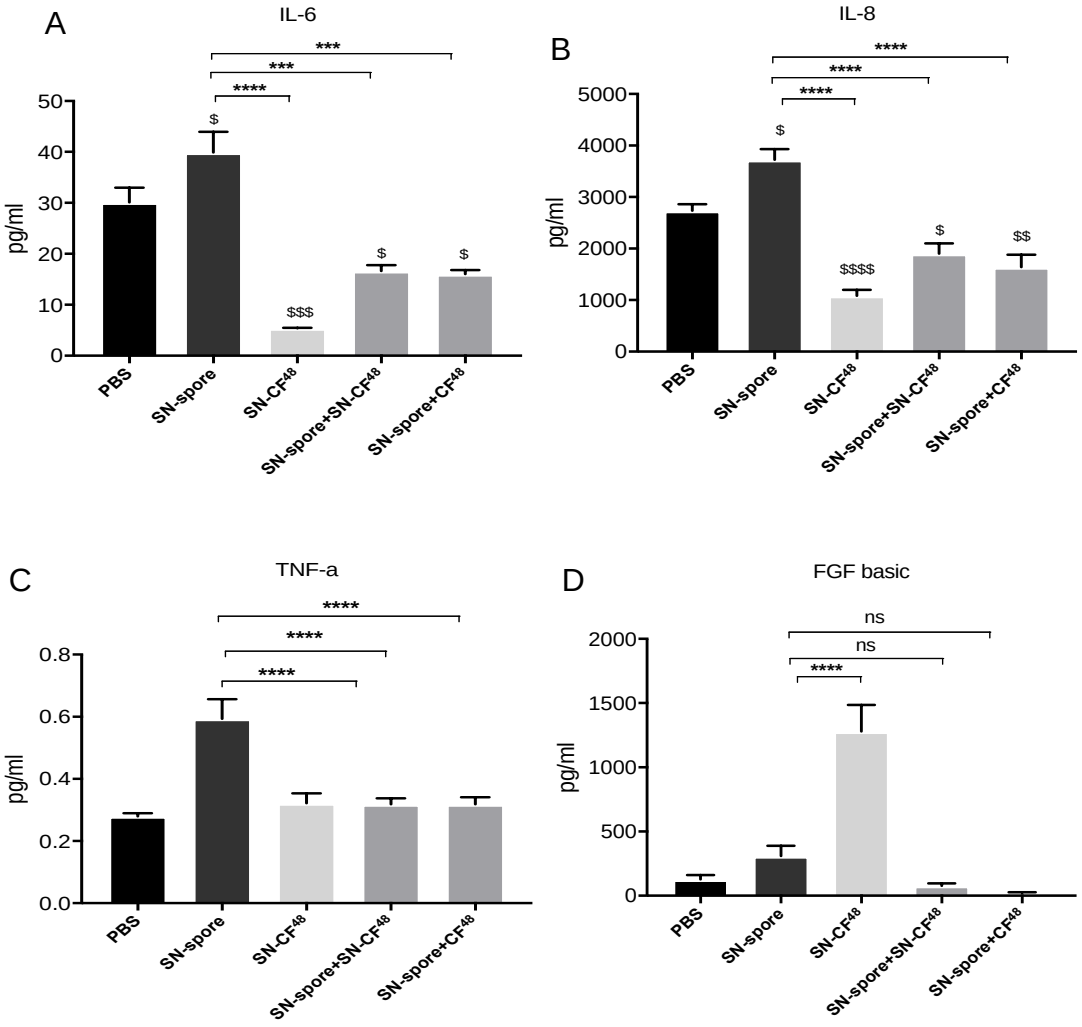

Figure 5.5: Degradation of host cytokines and ECM components by *A. fumigatus* secreted products

A549 epithelial cells were cultured in 24 well tissue culture plates and challenged with 10^5 spores (spores) or 200 µl of CF^{48} added to 800 µl of media (5 fold dilution) and incubated at 37°C and 5% CO_2 for 24 h. Supernatant (SN) from each challenge, SN-spore or SN-CF^{48} was analysed for cytokine content. SN-spore was then mixed with an equal volume of SN-CF^{48} or neat CF^{48} and incubated for a further 24 h at which point cytokine/FGF-2 expression was quantified again. Data represent the average of three biological experiments ± SEM and significance was calculated between treatment and PBS challenge ($) or SN-spore (*). *P<0.05, **P<0.01, ***P<0.001, ****P<0.0001.

5.4 Discussions

Activation of host signalling pathways in ECs is one host response that has been identified as a contributing factor to epithelial damage in response to *A. fumigatus*. Protease-induced ERK/JNK MAPK signalling in A549 cells caused *in vitro* lung cell peeling and death by necrosis, and heat inactivation of the CF neutralized its ability to peel the cells (Sharon et al., 2011). Specifically, intracellular host signalling pathways activated in response to pathogens do have some additional effects on the activated host cells. A notable example is PI3K signalling in myeloid cells which can positively and negatively regulate PRR responses, particularly, TLR-mediated proinflammatory responses (Hazeki et al., 2007). Excessive production of pro-inflammatory cytokines in airways resulting from activation of intracellular signalling pathways can lead to tissue damage as seen in ABPA patients (Fukahori et al., 2014).

The aim of the work reported in this chapter was to understand how host responses to fungal challenge perturb epithelial integrity. The role of various host cell responses to different *A. fumigatus* morphotypes and secreted products, including fungal spore uptake, activation of signalling, cytokine release, loss of TEER and epithelial cell detachment were investigated. To verify whether contact dependent NF-κB signalling seen during early infection (Fig. 4.1E and F) drives loss of TEER and lytic epithelial cell death, canonical NF-κB signalling was blocked at the level of IκBα phosphorylation using Bay11-7082 (Table 5.1). Bay11-7082 has been shown to act as a potent inhibitor of canonical NF-κB signalling with a strong inhibitory effect towards p65 DNA binding (Kwon et al., 2016, Sharma et al., 2015). TEER reduction was significantly reduced by Bay11-7082 during early infection as represented in this study by live fungal spore challenges (Fig 5.2B). Similarly, lytic epithelial cell death was partially, but significantly blocked following Bay11-7082 pre-treatment (Fig 5.1C). Contact-mediated epithelial cell detachment was however, found to occur independently of NF-κB signalling (Fig 5.2A). It remains to be seen whether the specificity of Bay11-7082 for inhibition of canonical NF-κB signalling is confounded by off target effects. A previous study showed that Bay11-7082 was able to effectively block both canonical and non-canonical NF-κB signalling induced by adeno-associated virus in HeLa cells, although the exact mechanism was not demonstrated

(Jayandharan et al., 2011). If non-canonical signalling activated during late infection (as shown by response to CF^{48} challenge, Fig 4.9 E and F) is effectively blocked by Bay11-7082, our result would imply that loss in TEER and epithelial cell detachment induced by CF^{48} occurred independently of canonical and non-canonical NF-κB signalling (Fig 5.2A and B). Continuation of this work has included functional analysis of non-canonical NF-κB signalling by genetic silencing of NIK (Chapter 7).

A previous study by Sharon et al (2011) demonstrated that p-JNK phosphorylation induced by *A. fumigatus* secreted products was partially responsible for losses of cell viability, desquamation and necrosis in A549 human alveolar carcinoma cells, as shown by inhibiting JNK activities prior to challenge with CF (Sharon et al., 2011). Inhibition of JNK and p38 signalling in our study prior to live spore challenge protected A549 cells from lytic cell death (Fig 5.1A and B), reduction in TEER (Fig 5.2B) and epithelial cell detachment (Fig 5.2A). Inhibiting p38 signalling did not protect epithelial cells from lysis during early infections (Fig 5.1B). (Fig 5.2A). Although more physiologically relevant to real time infection compared to CF challenge experiments, the exact mechanism by which fungal contact improves the protective effects of JNK inhibitor is not clear. One potential hypothesis is that fungal cells induce a stronger protective immune response at both transcriptional and protein levels due to receptor ligand interaction or multiple ligand binding. This is in contrast to CF^{48} challenge that exhibited suppressive effects on the initial NF-κB response.

Similar to the effect of JNK inhibition, blocking fungal spore uptake by A549 cells protected the epithelial cells from loss of TEER and epithelial cell detachment (Fig 5.4). The establishment of tightly interconnected cells and epithelial cell detachment from culture vessels involves a level of cell membrane dynamics or blebbing, both of which requires the formation and polymerization of a contractile cortex of myosin II decorated actin filaments (Charras et al., 2006). It was not surprising therefore, that an inhibitor of actin processes will reduce these cellular perturbations. Interestingly, this effect is not directly related to the possible role of actin processes in JNK activation, as inhibition of actin did not affect hyphal-induced JNK activation (Fig 5.5). This finding implies that a membrane-resident non-endocytosed receptor is active in JNK and NF-κB activation. Membrane bound receptors such as TLR2 and 4 as well as Dectin-1 have been shown to be important in activating signalling pathways in

professional and non-professional immune cells in response to *Aspergillus* infections (Chai et al., 2009, Meier et al., 2003, Liu et al., 2015, Herbst et al., 2015). In order to transduce intracellular signals resulting from an extracellular bound ligand, these receptors recruit the functions of intracellular adaptors rather than undergo endocytosis as a receptor-ligand complex (Romani, 2011, Lee and Kim, 2007). Protection derived from inhibition of fungal spore uptake can thus be linked to blocking of different cellular events that can be detrimental to the host perhaps including: intracellular housing of *A. fumigatus* spores, or cell rounding which could lead to detachment or apoptosis and loss of focal adhesion thereby reducing TEER (Wasylnka and Moore, 2003, Desouza et al., 2012, Charras et al., 2006).

It was discovered that components of the *A. fumigatus* secretome can lead to differential remodelling of host immune responses via TNF-α, IL-8 and IL-6 degradation (Fig 5.5A-C). Cytokine depletion occurs in targeted manner as certain other secreted host products, such as FGF-2, were unaffected by fungal secreted products, possibly due to conservation of a cleavage site in the cytokines prone to degradation. It is likely, based upon these data, that *A. fumigatus* secreted products act in a target-specific manner to remodel the local cytokine environment. GM-CSF is essential in antifungal defence against *A. fumigatus* (Kasahara et al., 2016), however, the net effect from spore and CF challenge on the level of this cytokine in the human infection milieu and its impact on *Aspergillus* clearance remains as yet unanswered. Recently, Liu et al described a mechanism whereby *Blastomyces dermatitidis* disables innate immunity to a great extent by mimicking the Mammalian Aminopeptidase homologue, serine protease dipeptidyl peptidase IVA (DppIVA) in a C-C target specific manner (Sterkel et al., 2016, Lorenzini et al., 2017). By cleaving C-C chemokines and GM-CSF, the yeast DppIVA halted monocyte recruitment and differentiation, prevented phagocyte activation and maturation and decreased production of ROS (Sterkel et al., 2016). The most recent study by the same group has shown a broader target for DppIVA to include the CXCL group of cytokines (Lorenzini et al., 2017). Interestingly, expression of the DPPIV homologue in *A. fumigatus* is under PacC-mediated regulation in murine a model of invasive aspergillosis (Bertuzzi et al., 2014) a factor which might contribute to target-specific modulation of host responses. Taken together our results suggest that *A. fumigatus* challenge stimulates several

mechanistically distinct host responses, via both contact-mediated and diffusible mechanisms, and that secreted fungal products are capable of significant remodelling of the host immune response.

5.5 Bibliography

BENNETT, B. L., SASAKI, D. T., MURRAY, B. W., O'LEARY, E. C., SAKATA, S. T., XU, W., LEISTEN, J. C., MOTIWALA, A., PIERCE, S., SATOH, Y., BHAGWAT, S. S., MANNING, A. M. & ANDERSON, D. W. 2001. SP600125, an anthrapyrazolone inhibitor of Jun N-terminal kinase. *Proc Natl Acad Sci U S A,* 98**,** 13681-6.

BERTUZZI, M., SCHRETTL, M., ALCAZAR-FUOLI, L., CAIRNS, T. C., MUNOZ, A., WALKER, L. A., HERBST, S., SAFARI, M., CHEVERTON, A. M., CHEN, D., LIU, H., SAIJO, S., FEDOROVA, N. D., ARMSTRONG-JAMES, D., MUNRO, C. A., READ, N. D., FILLER, S. G., ESPESO, E. A., NIERMAN, W. C., HAAS, H. & BIGNELL, E. M. 2014. The pH-Responsive PacC Transcription Factor of *Aspergillus fumigatus* Governs Epithelial Entry and Tissue Invasion during Pulmonary Aspergillosis. *PLoS Pathog,* 10**,** e1004413.

CHAI, L. Y., KULLBERG, B. J., VONK, A. G., WARRIS, A., CAMBI, A., LATGE, J. P., JOOSTEN, L. A., VAN DER MEER, J. W. & NETEA, M. G. 2009. Modulation of Toll-like receptor 2 (TLR2) and TLR4 responses by *Aspergillus fumigatus*. *Infect Immun,* 77**,** 2184-92.

CHARRAS, G. T., HU, C. K., COUGHLIN, M. & MITCHISON, T. J. 2006. Reassembly of contractile actin cortex in cell blebs. *J Cell Biol,* 175**,** 477-90.

CUENDA, A., ROUSE, J., DOZA, Y. N., MEIER, R., COHEN, P., GALLAGHER, T. F., YOUNG, P. R. & LEE, J. C. 1995. SB 203580 is a specific inhibitor of a MAP kinase homologue which is stimulated by cellular stresses and interleukin-1. *FEBS Lett,* 364**,** 229-33.

DESOUZA, M., GUNNING, P. W. & STEHN, J. R. 2012. The actin cytoskeleton as a sensor and mediator of apoptosis. *Bioarchitecture,* 2**,** 75-87.

EDWARDS, M. R., BARTLETT, N. W., CLARKE, D., BIRRELL, M., BELVISI, M. & JOHNSTON, S. L. 2009. Targeting the NF-kappaB pathway in asthma and chronic obstructive pulmonary disease. *Pharmacol Ther,* 121**,** 1-13.

GEISSLER, A., HAUN, F., FRANK, D. O., WIELAND, K., SIMON, M. M., IDZKO, M., DAVIS, R. J., MAURER, U. & BORNER, C. 2013. Apoptosis induced by the fungal pathogen gliotoxin requires a triple phosphorylation of Bim by JNK. *Cell Death Differ,* 20**,** 1317-29.

HERBST, S., SHAH, A., MAZON MOYA, M., MARZOLA, V., JENSEN, B., REED, A., BIRRELL, M. A., SAIJO, S., MOSTOWY, S., SHAUNAK, S. & ARMSTRONG-JAMES, D. 2015. Phagocytosis-dependent activation of a TLR9-BTK-calcineurin-NFAT pathway co-ordinates innate immunity to Aspergillus fumigatus. *EMBO Mol Med,* 7**,** 240-58.

JAYANDHARAN, G. R., ASLANIDI, G., MARTINO, A. T., JAHN, S. C., PERRIN, G. Q., HERZOG, R. W. & SRIVASTAVA, A. 2011. Activation of the NF-kappaB pathway by adeno-associated virus (AAV) vectors and its implications in immune response and gene therapy. *Proc Natl Acad Sci U S A,* 108**,** 3743-8.

KASAHARA, S., JHINGRAN, A., DHINGRA, S., SALEM, A., CRAMER, R. A. & HOHL, T. M. 2016. Role of Granulocyte-Macrophage Colony-Stimulating Factor Signaling in Regulating Neutrophil Antifungal Activity and the Oxidative Burst During Respiratory Fungal Challenge. *J Infect Dis,* 213**,** 1289-98.

KWON, H. J., CHOI, G. E., RYU, S., KWON, S. J., KIM, S. C., BOOTH, C., NICHOLS, K. E. & KIM, H. S. 2016. Stepwise phosphorylation of p65 promotes NF-kappaB

activation and NK cell responses during target cell recognition. *Nat Commun,* 7**,** 11686.

LEE, M. S. & KIM, Y. J. 2007. Signaling pathways downstream of pattern-recognition receptors and their cross talk. *Annu Rev Biochem,* 76**,** 447-80.

LIU, H., LEE, M. J., SOLIS, N. V., PHAN, Q. T., SWIDERGALL, M., RALPH, B., IBRAHIM, A. S., SHEPPARD, D. C. & FILLER, S. G. 2016. *Aspergillus fumigatus* CalA binds to integrin alpha5beta1 and mediates host cell invasion. *Nat Microbiol,* 2**,** 16211.

LIU, Z. C., WANG, M., SUN, W. K., XIA, D., TAN, M. M., DING, Y., QIAN, Q., SU, X. & SHI, Y. 2015. Up-regulation of Dectin-1 in airway epithelial cells promotes mice defense against invasive pulmonary aspergillosis. *Int J Clin Exp Med,* 8**,** 17489-97.

LORENZINI, J., SCOTT FITES, J., NETT, J. & KLEIN, B. S. 2017. *Blastomyces dermatitidis* serine protease dipeptidyl peptidase IVA (DppIVA) cleaves ELR+ CXC chemokines altering their effects on neutrophils. *Cell Microbiol,* 19.

MEIER, A., KIRSCHNING, C. J., NIKOLAUS, T., WAGNER, H., HEESEMANN, J. & EBEL, F. 2003. Toll-like receptor (TLR) 2 and TLR4 are essential for *Aspergillus*-induced activation of murine macrophages. *Cell Microbiol,* 5**,** 561-70.

MORI, N., YAMADA, Y., IKEDA, S., YAMASAKI, Y., TSUKASAKI, K., TANAKA, Y., TOMONAGA, M., YAMAMOTO, N. & FUJII, M. 2002. Bay 11-7082 inhibits transcription factor NF-kappaB and induces apoptosis of HTLV-I-infected T-cell lines and primary adult T-cell leukemia cells. *Blood,* 100**,** 1828-34.

MOYES, D. L., RUNGLALL, M., MURCIANO, C., SHEN, C., NAYAR, D., THAVARAJ, S., KOHLI, A., ISLAM, A., MORA-MONTES, H., CHALLACOMBE, S. J. & NAGLIK, J. R. 2010. A biphasic innate immune MAPK response discriminates between the yeast and hyphal forms of *Candida albicans* in epithelial cells. *Cell Host Microbe,* 8**,** 225-35.

PIERCE, J. W., SCHOENLEBER, R., JESMOK, G., BEST, J., MOORE, S. A., COLLINS, T. & GERRITSEN, M. E. 1997. Novel inhibitors of cytokine-induced IkappaBalpha phosphorylation and endothelial cell adhesion molecule expression show anti-inflammatory effects in vivo. *J Biol Chem,* 272**,** 21096-103.

ROMANI, L. 2011. Immunity to fungal infections. *Nat Rev Immunol,* 11**,** 275-88.

SCHINDELIN, J., ARGANDA-CARRERAS, I., FRISE, E., KAYNIG, V., LONGAIR, M., PIETZSCH, T., PREIBISCH, S., RUEDEN, C., SAALFELD, S., SCHMID, B., TINEVEZ, J. Y., WHITE, D. J., HARTENSTEIN, V., ELICEIRI, K., TOMANCAK, P. & CARDONA, A. 2012. Fiji: an open-source platform for biological-image analysis. *Nat Methods,* 9**,** 676-82.

SHARMA, V., JORDAN, J. J., CIRIBILLI, Y., RESNICK, M. A., BISIO, A. & INGA, A. 2015. Quantitative Analysis of NF-kappaB Transactivation Specificity Using a Yeast-Based Functional Assay. *PLoS One,* 10**,** e0130170.

SHARON, H., AMAR, D., LEVDANSKY, E., MIRCUS, G., SHADKCHAN, Y., SHAMIR, R. & OSHEROV, N. 2011. PrtT-regulated proteins secreted by *Aspergillus fumigatus* activate MAPK signaling in exposed A549 lung cells leading to necrotic cell

STERKEL, A. K., LORENZINI, J. L., FITES, J. S., SUBRAMANIAN VIGNESH, K., SULLIVAN, T. D., WUTHRICH, M., BRANDHORST, T., HERNANDEZ-SANTOS, N., DEEPE, G. S., JR. & KLEIN, B. S. 2016. Fungal Mimicry of a Mammalian Aminopeptidase Disables Innate Immunity and Promotes Pathogenicity. *Cell Host Microbe,* 19**,** 361-74.

WASYLNKA, J. A. & MOORE, M. M. 2003. *Aspergillus fumigatus* conidia survive and germinate in acidic organelles of A549 epithelial cells. *J Cell Sci,* 116**,** 1579-87.

CHAPTER 6: ROLE OF *A. FUMIGATUS* VIRULENCE FACTORS IN EPITHELIAL CELL RESPONSES AND DAMAGE

6.1 Introduction

The success of *A. fumigatus* as an opportunistic pathogen can be explained by a range of pathogen related traits as well as host related factors, with the major host factor being the immune status. On the other hand, pathogenic behaviour of *A. fumigatus* can be attributed to a range of characteristics including: morphological features, stress tolerance, secondary metabolism and ability to source energy from the host (Paulussen et al., 2017). A unique combination of these factors is important in the virulent behaviour exhibited by *A. fumigatus*. For example, the rodlet layer of *A. fumigatus* spores prevents immune recognition and this may promote infection in the host (Aimanianda et al., 2009). Moreover, fungal toxins, enzymes and secondary metabolites greatly influence the outcome of the interaction between the host and *A. fumigatus* in favour of the fungus. A number of *A. fumigatus* spore- and hypha-borne toxins have been described with gliotoxin being the most-well-studied and clinically relevant. Gliotoxin supresses neutrophil responses, inhibits phagocytosis and induces apoptosis of host cells (Geissler et al., 2013).

A. fumigatus also secretes a variety of enzymes exerting proteolytic activities upon host cells or proteins (Bertuzzi et al., 2014) including many enzymes that presumably enable the fungus to degrade and utilize organic matter. Functional genomic studies by Bertuzzi et al showed that the pH sensing regulator, PacC, governed pathogenicity and invasive growth in mice (Bertuzzi et al., 2014). This study identified over 250 secreted proteins in addition to gliotoxin and other cell wall associated genes differentially expressed in Δ*PacC* compared to WT during invasive aspergillosis in a murine model.

The rationale for this study was to challenge the model of *A. fumigatus*- epithelial interaction, already well-characterised in work described in Chapters 3, 4 and 5, with strains lacking known virulence determinants: PacC, GliP or PrtT – in order to; a) gain some insight into the mechanistic basis of the reduced virulence and whether reduced virulence correlates with any specific alteration in host response b) to

optimise the model for screening of individual PacC-dependent gene products that govern virulence.

6.2 Methods

6.2.1 Epithelial cell damage assays

To study epithelial cell damage in response to challenge with different *A. fumigatus* mutant strains, the following events/processes were assessed following fungal spore or CF challenge: trans-epithelial electrical resistance using a trans-well assay (see Section 2.2.4.4), A549 cell detachment (see Section 2.2.7.2) and epithelial cell lysis by quantitation of LDH (see Section 2.2.4.3).

6.2.2 Measurement of phosphorylated signalling proteins

Activation of signalling responses in AECs following infection by different *A. fumigatus* mutant strains was determined by measuring the phosphorylation status of specific signalling proteins in whole cell lysates (as described in Section 2.2.5).

6.2.3 Activation of transcription factor DNA binding

Following AEC challenge with spores or CF from *A. fumigatus* mutant strains, nuclear protein was extracted and tested for DNA binding of transcription factors using TransAM ELISA (see section 2.2.6 for details).

6.2.4 Cytokine response

To quantify cytokine production in response to challenge with different *A. fumigatus* isolates, culture supernatant was collected at 24 h post-challenge with spores or CF and tested using the high performance luminex cytokine assay (as described in Section 2.2.4.2).

6.3 Results

6.3.1 *A. fumigatus* Δ*pacC*, Δ*glip* and Δ*prtT* mutants are unable to induce epithelial cell damage in response to spore or CF[48] challenge

Live spores or CF derived from mutants lacking the PacC transcription factor did not induce epithelial cell lysis (Fig 6.1A and B). A Δ*gliP* mutant induced significantly higher LDH release than the uninfected control following both live spore and CF challenges but the quantity of LDH produced was significantly lower than that elicited by challenge with progenitor isolate (PgI) (Fig 6.1A and B). Challenge with Δ*prtT* spores led to an approximately 2.5 fold increase in LDH (Fig 6.1A) relative to PBS challenge which did not achieve statistical significance (p = 0.077) In contrast Δ*prtT* CF induced significantly more lysis than PBS challenge but drastically reduced relative to that elicited by CF from the progenitor isolate (Fig 6.1B).

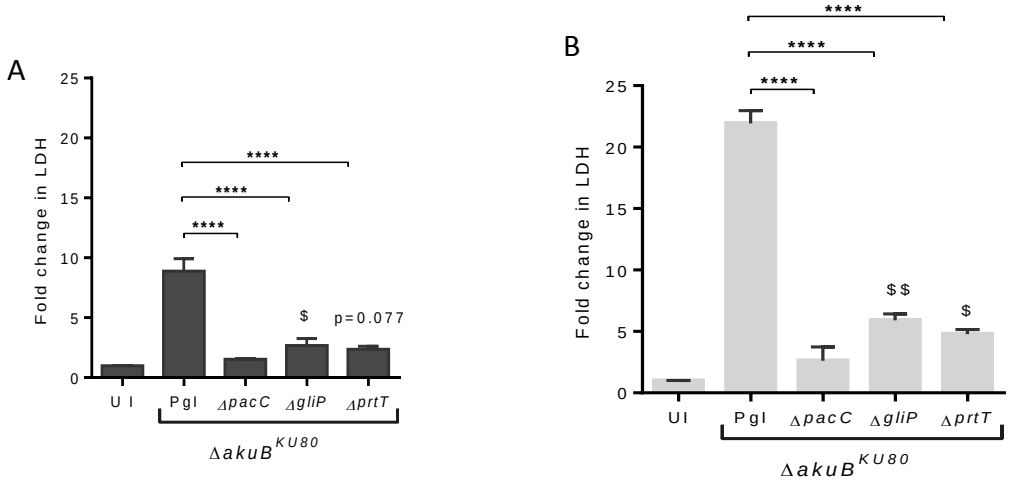

Figure 6.1: Lytic cell death of A549 cells in response to *A. fumigatus* spores or CF[48]
Monolayers of A549 epithelial cells were incubated with A) spores at an MOI of 0.1 or B) 5 fold dilution of CF[48] from mutants or progenitor isolates of *A. fumigatus* for 24 h. At indicated time points post-infection, culture supernatant was collected and LDH was quantified. Data represent the average of three independent experiments ± SEM. Statistical significance was calculated relative to uninfected (PBS treated) control ($) or wild type (*) by one-way ANOVA using Fishers LSD output. For * or $ p <0.05; **/$$ p<0.001 ***p<0.0001.

6.3.2 Spores and CF[48] of Δ*pacC*, Δg*liP* and Δ*prtT A. fumigatus* mutants induce significantly less A549 cell detachment than respective progenitor isolate

Regardless of whether epithelial monolayers were challenged with live spores or with CF, a *ΔpacC* mutant failed to induce significant epithelial cell detachment (Fig 6.2A and B). Live fungal spores from a Δ*gliP* mutant induced a similar level of cell detachment compared to that induced by the progenitor isolate (Fig 6.2A). CF from a Δ*gliP* mutant caused significantly less detachment than the progenitor isolate but significantly more than an isogenic *ΔpacC* mutant (Fig 6.2B). For both live spore and CF challenges, a Δ*prtT* mutant induced significantly more detachment than *ΔpacC* but significantly less than that elicited by the wild type progenitor isolate (Fig 6.2A and B). Similar to what was shown in Fig 5.3B, A549 detachment was significantly reduced by pre-treating epithelial cell monolayers with 0.2 µM Cytochalasin D (CytD) for 1 h prior to live fungal spore challenge (Fig 6.2C).

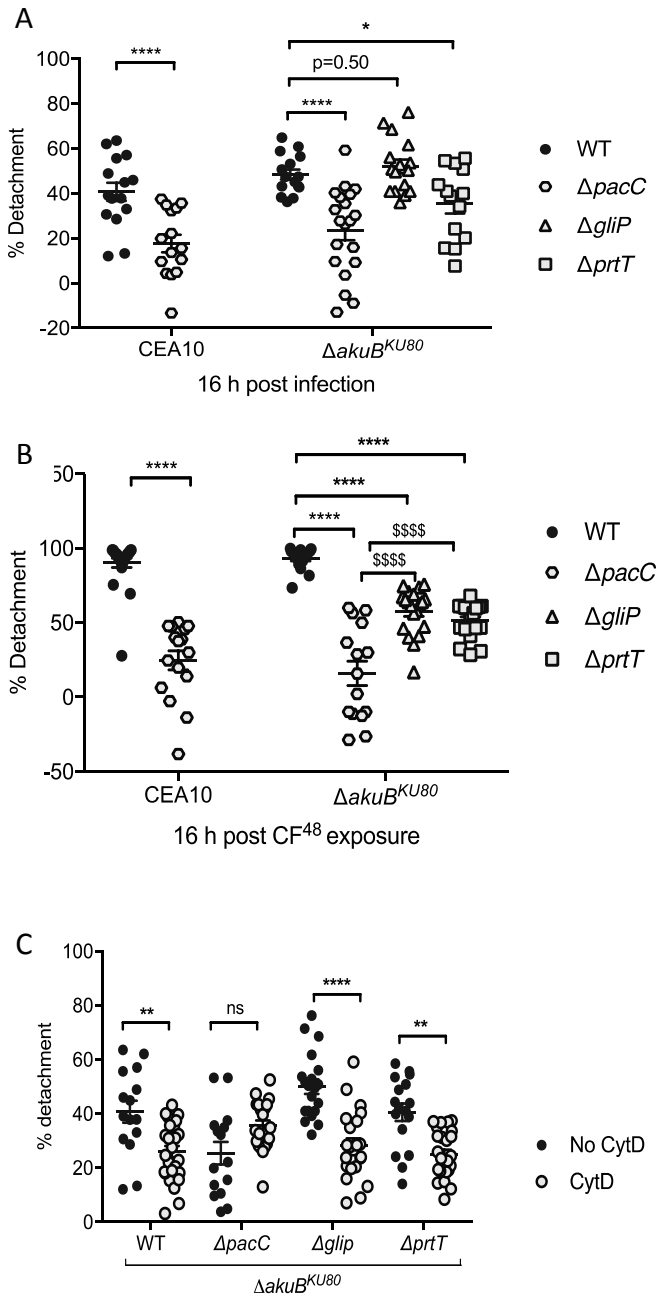

Figure 6.2: Quantitative analysis of epithelial monolayer detachment following challenge. (A) fungal spores or (B) culture filtrate (C) 0.2 µM Cytochalasin D (CytD) prior to fungal challenge. Percentage detachment induced by spores or CF of mutants or progenitor isolates of *A. fumigatus*. Data represent the mean of three biological replicates (three technical data set each). Error bars show ± SEM. Data were analysed by one-way ANOVA. Significance was calculated relative to progenitor isolates (*), and PacC from the same progenitor isolate ($) with Fisher's LSD output. *P<0.05, ****P<0.0001.

6.3.3 Spores and CF[48] of Δ*pacC*, Δ*glip* and Δ*prtT A. fumigatus* mutants are deficient in eliciting loss of transepithelial electrical resistance (TEER)

ΔpacC and Δ*prtT* spores and CF induced significantly less reduction in TEER than the progenitor isolate (Fig 6.3A and B). Challenge with spores of Δ*gliP* led to a similar extent of TEER reduction as that resulting from challenge with wild type spores (Fig 6.3A). However, reduction in TEER caused by CF from Δ*gliP* mutant was significantly less than the progenitor isolate (Fig 6.3B).

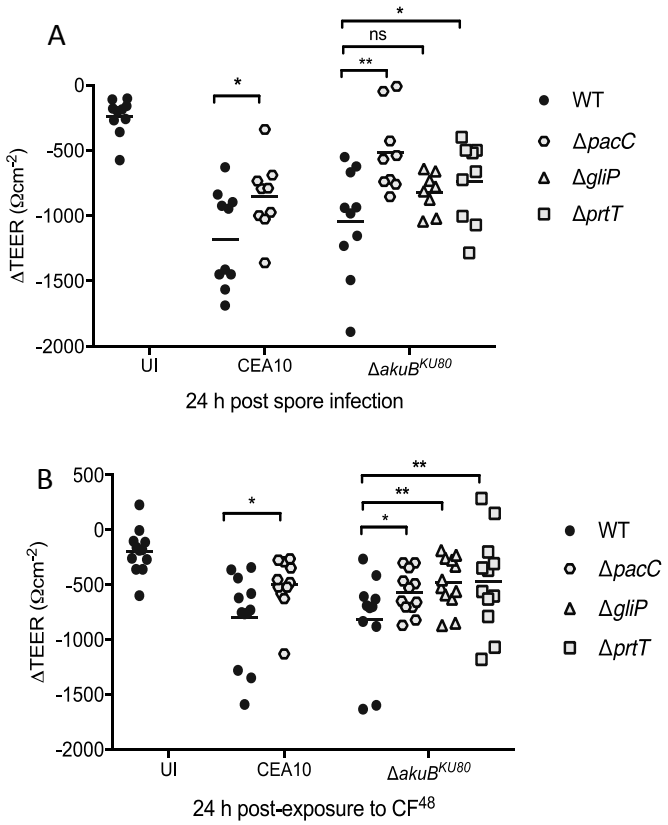

Figure 6.3: Effect of spore and CF challenge on trans-epithelial electrical resistance (TEER). Calu-3 cells were grown on a polycarbonate filter in a trans-well system for 11 days until TEER was > 1000 Ω. TEER was first measured before challenge with 10^5 spores or CF from mutants or progenitor isolates of *A. fumigatus* for 24 h. The loss in TEER was calculated. Shown are averages of 3 biological repeats each performed in triplicate wells. Data represent the mean of three biological replicates (three technical data sets each). Error bars show ± SEM. Data were analysed by one-way ANOVA. Significance was calculated relative to progenitor isolates with Fisher's LSD output. *P<0.05, **P<0.01, ***P<0.001, ****P<0.0001.

6.3.4 Activation of NF-κB and MAPK signalling

6.3.4.1 Requirement for PacC, GliP or PrtT for activating MAPK and NF-κB signalling in A549 epithelial cells following *A. fumigatus* spore challenge

A. fumigatus mutant strains lacking PacC*,* GliP or PrtT transcription factors were unable to activate IκBα phosphorylation unlike their respective progenitor isolate (PgI) (Fig 6.4A). A Δ*gliP* mutant significantly induced JNK phosphorylation more than uninfected cells, although the magnitude of activation was lower than that of the wild type strain (Fig 6.4B). Δ*pacC* and Δ*prtT* mutants were unable to induce phosphorylation of JNK in cultured A549 epithelia cells (Fig 6.4B). Like their respective parent strains, neither of the mutants induced p38 phosphorylation in epithelial cells (Fig 6.4C).

These results suggest that none of the transcription factors PacC, GliP or PrtT or the gene products under their regulation are critical for inducing canonical NF-κB-mediated signalling in epithelial cells in response to *A. fumigatus* challenge. However, unlike p*acC* and p*rtT*, g*liP* (gliotoxin) is not required or at least not the sole requirement for ability of *A. fumigatus* to activate JNK signalling in epithelial cells.

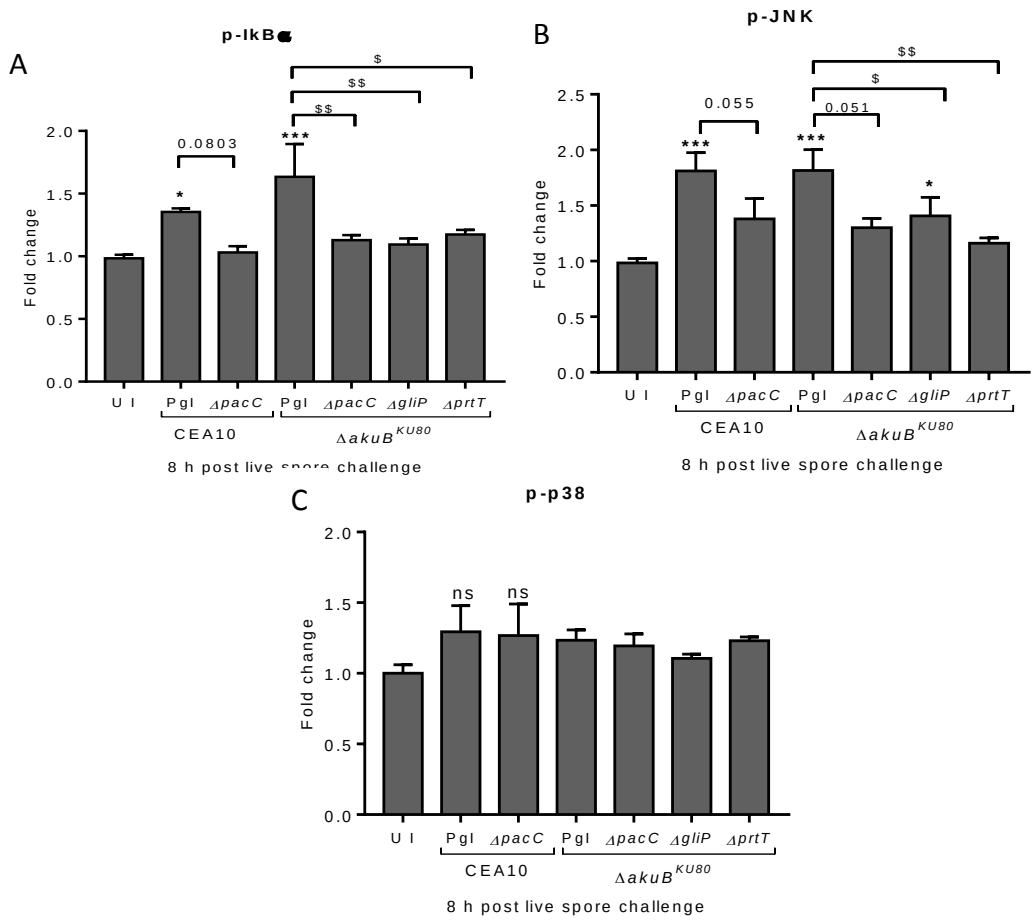

Figure 6.4: Phosphorylation of host signalling proteins in A549 epithelial cells by live *A. fumigatus* spore challenge

Phosphorylation of IκBα, p38 and JNK as measured at 8 h post-infection of A549 cells with spores of *A. fumigatus* mutant strains and respective progenitors. Data is expressed as fold change in quantity of phosphorylated protein relative to the uninfected (UI) control (*) and progenitor strain ($) and represents the average of three independent experiments; each performed in triplicate. Error bars indicate ± SEM. Data were analysed by one-way ANOVA and significance was calculated relative to UI (*) or progenitor isolates ($) with Fisher's LSD output. *p <0.05, **p<0.01, ***<0.001.

6.3.4.2 Requirement for PacC, GliP or PrtT for activating MAPK and NF-κB signalling in A549 epithelial cells following exposure to CF^{48}

Similar to EC response to challenge with CF^{48} of progenitor isolates, the impact of CF^{48} from a Δ*pacC* mutant was not significantly different from that caused by CF^{48} of the progenitor isolate with regards to IκBα phosphorylation after 4 h of exposure (Fig 6.5A). Intriguingly, CF from mutants lacking *gliP* or *prtT* induced a significant increase in IκBα phosphorylation compared to their progenitor isolate (Fig 6.5A). Secreted products under *pacC* or g*liP* or *prtT* regulation are partially responsible for JNK and p38 activation as the mutants lacking these genes were unable to induce phosphorylation of p38 and JNK when compared to their progenitor strains (Fig 6.5B and C). These results suggest that secreted products under *pacC*, g*liP* or *prtT* control are important factors for MAPK activation during late infection and that inhibition of IκBα phosphorylation following CF exposure is mediated by g*liP* or *prtT* regulated factors.

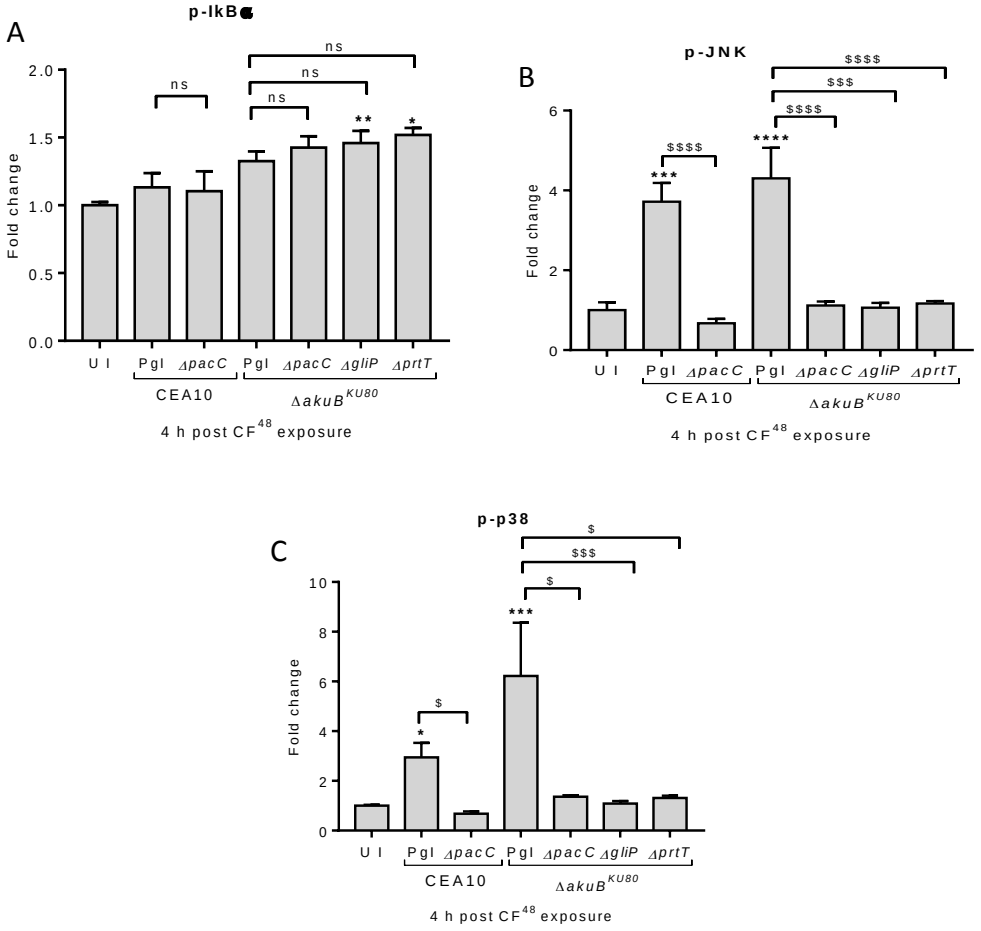

Figure 6.5: Phosphorylation of host signalling proteins in A549 epithelial cells by CF^{48}

Phosphorylation of IκBα, p38 and JNK at 4 h post-exposure of A549 AEC line to CF^{48} from *A. fumigatus* mutant strains and progenitor isolates. Data is expressed as fold change in quantity of phosphorylated protein relative to the uninfected (UI) control (*) and parent strain ($) and represents the average of three independent experiments; each performed in triplicate. Error bars indicate ± SEM and significance was calculated relative to UI (*) or progenitor isolates ($) with Fisher's LSD output. *p <0.05, **p<0.01, ***p<0.001, ****p<0.0001.

6.3.5 Requirement for PacC, GliP and PrtT for activation of A549 transcription factors

6.3.5.1 Requirement for PacC, Glip and PrtT in activation of A549 transcription factors following challenge with live *A. fumigatus* spores

The DNA binding activities of host transcription factors in response to challenge with wild type strains was compared to that of cells challenged with mutant strains lacking *pacC* or g*liP* or *prtT* with specific emphasis upon transcription factors significantly affected by live fungal or CF challenges as deduced from Chapter 4. Relative to challenge with spores of a progenitor isolate, DNA binding activity of p65 and c-Fos (Fig 6.6C) was significantly reduced following challenge with live fungal spores from a *ΔpacC* mutant. Deletion of g*liP* significantly reduced p65 DNA binding activity compared to the progenitor strain (Fig 6.6A) but did not affect the DNA binding activity of c-Fos (Fig 6.6C). Live fungal spore challenge with a *ΔprtT* mutant reduced the DNA binding of both p65 (Fig 6.6A) and c-Fos (Fig 6.6C) although was only statistically significant for C-Fos DNA binding.

In stark contrast, neither the suppression of RelB (Fig 6.6B) nor JunD (Fig 6.6D) following live fungal challenge was significantly dependent on *pacC* or g*liP* or *prtT* as there was no statistical difference between the mutant strains and their progenitor isolates.

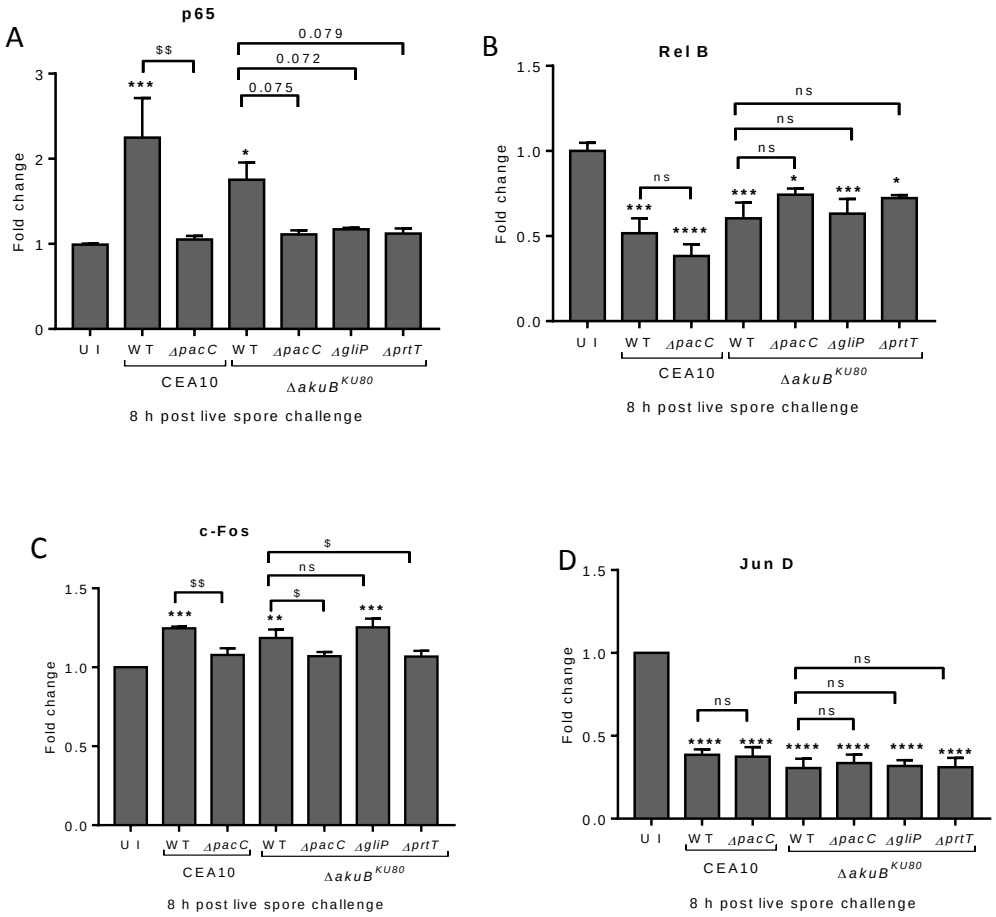

Figure 6.6: Changes in DNA binding activity of p65, RelB, c-Fos and JunD transcription factors in A549 cells in response to *A. fumigatus* spore challenge

DNA binding activity of p65, RelB, c-Fos and JunD at 8 h post-infection of A549 AEC line with spores of *A. fumigatus* mutant strains or progenitor isolates. Data is expressed as fold change in quantity of phosphorylated protein relative to the uninfected (UI) control and represents the average of three independent experiments; each performed in triplicate. Error bars indicate ± SEM and significance was calculated relative to UI (*) or progenitor isolates ($) with Fisher's LSD output. *p <0.05, **p<0.01, ***<0.001, ****p<0.0001.

6.3.5.2 Requirement for PacC, GliP or PrtT for activation of A549 epithelial transcription factors following challenge with *A. fumigatus* CF[48]

Contrary to live fungal challenge, an increase in DNA binding of RelB and p52 in response to CF[48] exposure was significantly dependent on secreted soluble factors under the control of *pacC* or g*liP* as neither the *ΔpacC* nor *Δgli*P was able induce DNA binding activity relative to progenitor isolate (Fig 6.7A and B). CF from a *ΔprtT* mutant led to significant reduction in DNA binding of RelB (Fig 6.7A) but not p52 (Fig 6.7B). DNA binding activity of p65 was significantly less when A549 epithelial cells were challenged with CF from *ΔpacC* or *ΔprtT* mutants but not a *Δgli*P mutant relative to their progenitor isolate (Fig 6.7C). These results highlight the existence of distinct mechanisms by which fungal contact and secreted products impact host response during *A. fumigatus* infections, which extend to modulation of host cell transcription.

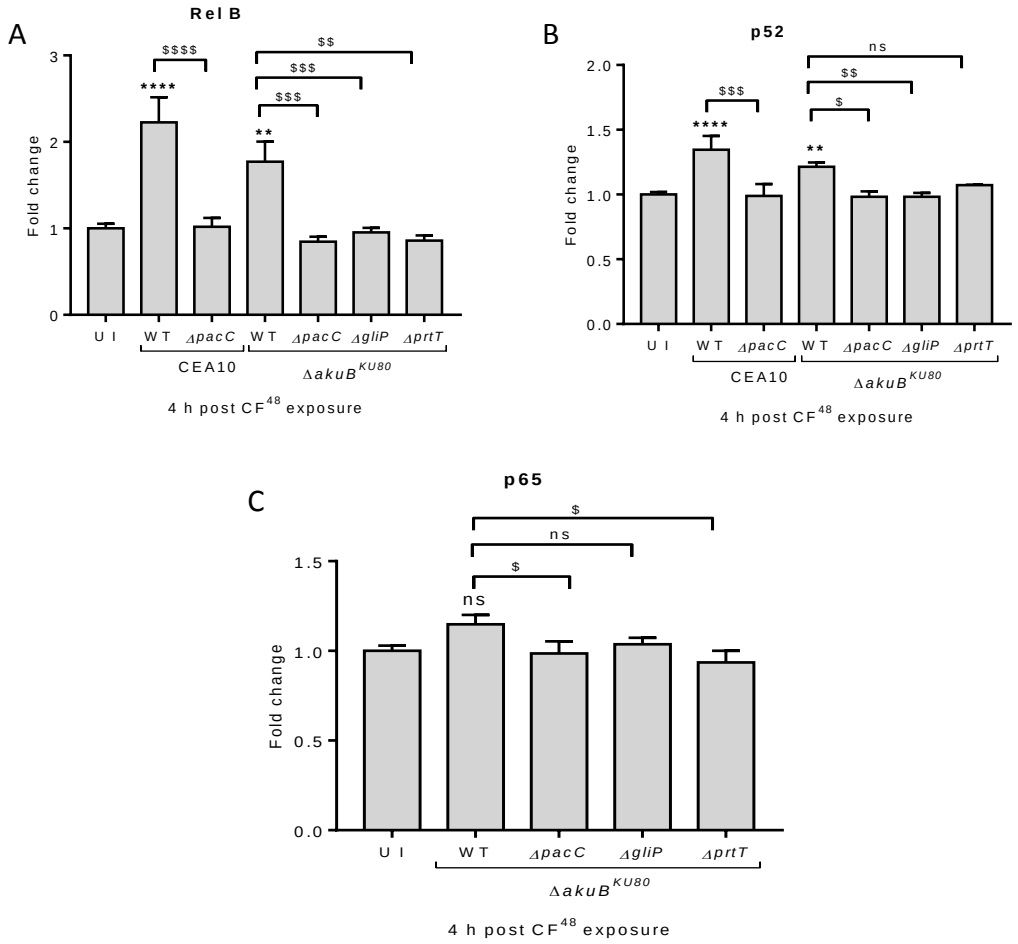

Figure 6.7: Changes in DNA binding activity of NF-κB transcription factors in A549 cells in response to *A. fumigatus* CF^{48}

DNA binding of RelB, p52 and p65 at 4 h post-exposure of A549 cells to CF^{48} from *A. fumigatus* mutant strains and progenitor isolates. Data is expressed as fold change in quantity of phosphorylated protein relative to the uninfected (UI) control and represents the average of three independent experiments; each performed in triplicate. Error bars indicate ± SEM and significance was calculated relative to UI (*) or progenitor isolates ($) with Fisher's LSD output. *p <0.05, **p<0.01, ***<0.001, ****p<0.0001.

6.3.6 Role of PacC, Glip and PrtT in induction of cytokine production following A549 challenge with live fungal spores

Secretion of IL-8 was dependent on PacC and GliP but not PrtT integrity (Fig 6.8A). In stark contrast, GM-CSF secretion was dependent on PrtT regulated factors but independent of PacC or GliP (Fig 6.8C). FGF-basic secretion is also dependent on factors controlled by PacC or GliP (Fig 6.8D). There was no statistical difference between IL-6 protein levels in response to live fungal spores of *ΔpacC*, *ΔgliP* or *ΔprtT* mutants compared to their progenitor isolate.

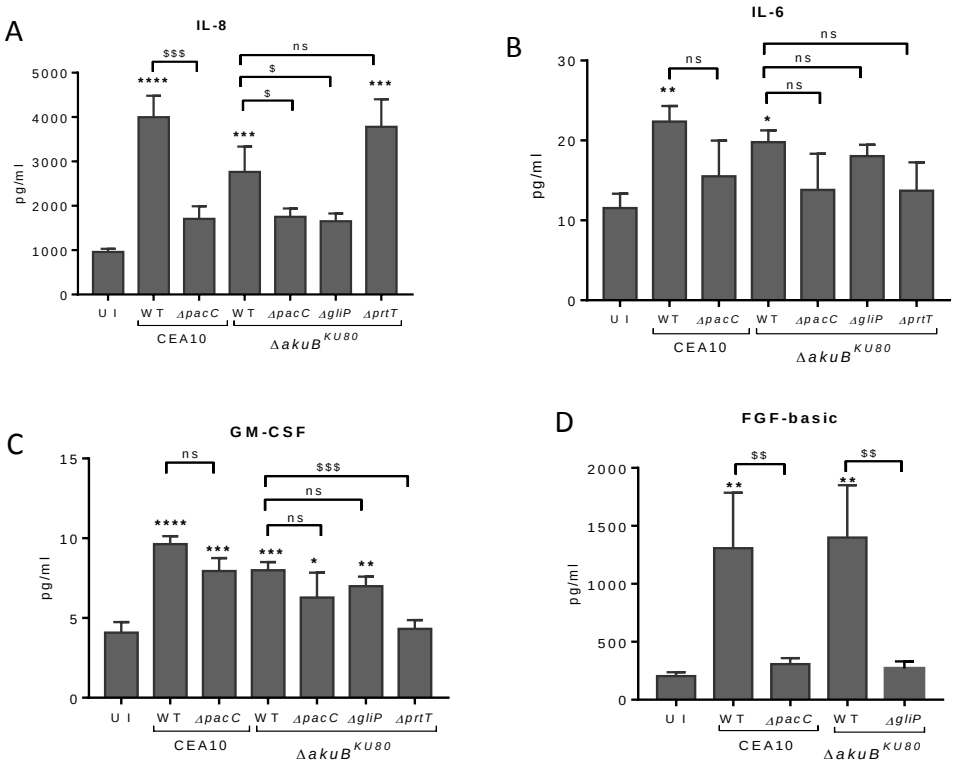

Figure 6.8: Cytokine release by A549 AECs in response to *A. fumigatus* infection.
Monolayers of A549 epithelial cells were infected with conidia from mutant strains of *A. fumigatus* and relevant progenitor isolates. IL-8, IL-6, GM-CSF and FGF-basic in culture supernatant were quantified at 24 h post-infection. Data represent the average of three independent experiments each performed in duplicate. Error bars indicate ± SEM and statistical significance was calculated relative to uninfected (*)

control or respective wild type ($) by one-way ANOVA using Fishers LSD output. *p <0.05,**p0.001***p<0.0001.

6.4 Discussions

A conserved regulatory pathway in fungi that acts via the PacC/Rim101 transcriptional signalling plays an important role in environmental adaptation and pH-dependent regulation of secreted proteins (Bertuzzi et al., 2014). It has been previously demonstrated that *A. fumigatus* mutants lacking PacC are attenuated for virulence *in vitro* as well as *in vivo* (Bertuzzi et al., 2014). From transcriptomic data, it was shown that Δ*pacC* mutants exhibited dysregulated expression of genes encoding many different secreted molecules, including cell wall biosynthetic enzymes and genes involved in gliotoxin biosynthesis, during invasive growth in a leukopenic mammalian lung relative to wild type isolates (Bertuzzi et al., 2014).

A characterisation of airway epithelial cell immunological and damage responses to *A. fumigatus* clinical isolates CEA10 or laboratory isolate *ΔakuB*^{KU80} strains has been reproducibly established (Chapters 3 and 4) and the possible mechanistic basis of cell damage has been probed (Chapter 5). Collectively the results, from Chapter 5 in particular, indicate that *Aspergillus* secreted factors in all or at least in most parts comprise an important arsenal used by *A. fumigatus* during lung invasion either directly as lytic agents or toxins, or indirectly by inducing harmful intracellular responses in host cells. Here, the involvement of the master transcriptional regulator of virulence and invasive growth, PacC was investigated using a *ΔpacC* null mutant in order to identify the single gene products that are responsible for host damage. In order to narrow down the relevant cohorts of genes under *pacC* regulatory control, the phenotypes of a protease (Δp*rtT*) and a gliotoxin (Δg*liP*) deficient mutant were also investigated. The *prtT* (AFUA_4G10120) gene encodes a putative zinc finger-containing transcription factor (Zn2Cys6) with the main function of controlling the expression of multiple secreted products and extracellular proteolytic activity in *Aspergillus* species (Sharon et al., 2009). Gliotoxin is one of the most studied *A. fumigatus* virulence factors (Chen et al., 2015, Comera et al., 2007, Eichner et al., 1986, Tsunawaki et al., 2004) and genes important in gliotoxin biosynthesis were also universally down regulated in a PacC null mutant showing that gliotoxin biosynthesis is under the control of the PacC transcription factor during murine infection (Bertuzzi

et al., 2014). Of 12 gene clusters involved in the gliotoxin synthetic pathway (Gardiner and Howlett, 2005), Glip is the only gene in the gliotoxin biosynthetic cluster that has been characterized as indispensable for gliotoxin production (Kupfahl et al., 2006).

Δ*pacC* null mutants constructed in two different genetic backgrounds were studied and the phenotypes were all comparable. However, only Δp*rtT* and Δ*gliP* nulls constructed in the *ΔakuB*^{KU80} genetic background were available at the time of this study.

Activation of both NF-κB and MAPK signalling by both live fungal cells and secreted products were dependent on PacC regulated factors. Although it has been shown in the previous Chapters 3, 4 and 5 that live fungus and secreted products induced responses in mechanistically distinct manners, these findings were not surprising because the PacC transcription factor regulates both cell wall associated and secreted protein-encoding genes during infection of mammalian lung (Bertuzzi et al., 2014). This is the first study to report the role of PacC in activation of intracellular signalling pathways during *Aspergillus* infection *in vitro*. A Δ*prtT* mutant was, in a similar way unable to activate host signalling. A previous study by Sharon et al (2009) identified at least 6 individual *A. fumigatus* protease genes whose expression was significantly decreased in a Δ*prtT* mutant when grown on skimmed milk medium (Sharon et al., 2009). All of the 6 proteases ALP, MEP, CpdS, Dpp4, and two uncharacterized proteases (AFUA_2G17330 and AFUA_7G06220), contained signal peptide motifs (Sharon et al., 2009, Hagag et al., 2012). Of the 6 proteases, the expression of the extracellular (secreted) dipeptidyl peptidase 4 (DPP4) was also downregulated during Δ*pacC*-mediated infection in mice (Bertuzzi et al., 2014). Thus, although the two experiments were conducted in different model systems with disparity in kinetics of experimentation, the *dpp4* was down regulated thus, making it an important protease of interest for further studies. Further studies using different knockout and Tetracycline regulatable DPP4 strains to clearly understand the exact role of this secreted protease in *Aspergillus* pathology are currently ongoing in our group.

An interesting observation is the cooperativity and redundancy of the secreted proteases in MAPK activation as deletion of one (as with Δ*gliP*) or all (as in Δ*pacC* or

Δ*prtT*) of them lead to no JNK or p38 activation. Gliotoxin is not important for spore-induced JNK activation but is important for JNK activation by secreted products. A previous study showed that gliotoxin mediates apoptosis of cells through JNK mediated phosphorylation of major splice variant of Bcl-2-interacting mediator of cell death (BIM) known as BIMEL at three amino acid residues (S100, T112 and S114) in mouse fibroblasts, human bronchial and mouse alveolar epithelial cells (Geissler et al., 2013). This observation is in line with our finding since CF from a Δ*gliP* mutant was unable to induce JNK activation. However, whether the absence of g*liP* or inhibition of JNK has a role in apoptosis of A549 epithelial cells was not accommodated in the current study but will form part of future work.

A different study demonstrated that apoptosis induced by gliotoxin is mediated through suppression of anti-apoptotic NF-κB signaling in colorectal cancer cells (Chen et al., 2015). This is interesting as challenge with a *Δgli*P mutant led to a significant increase in canonical NF-κB activation following CF challenge compared to wild type (Fig 6.5A). However, this was not the case with live fungal challenge where NF-κB activation is dependent on GliP (Fig 6.4A). The mechanistic basis of NF-κB suppression by gliotoxin has not been clearly described, especially in tissue resident cells such as epithelial and endothelial cells. Recently, Sakamoto et al (2015) unraveled a novel mechanism of NF-κB suppression by gliotoxin, which is mediated through inhibition of a linear ubiquitin chain assembly complex (LUBAC) on the NF-κB essential modulator (NEMO) of the NF-κB transduction pathway (Sakamoto et al., 2015). The inhibition of the enzymatic activity of LUBAC was preceded by the activation of TNF receptor signalling complex (TNFRSC) upstream of the IKK complex. In the context of CF challenge in our study, these data suggest that either gliotoxin in the CF could serve as a PAMP capable of activating a TNFR and initiating NF-κB signalling (See Fig 1.10 to refresh on components of NF-κB pathway). The exact host receptor(s) through which gliotoxin activates host responses are yet to be investigated.

Investigation of the role of PacC, GliP and PrtT on host transcriptional regulation showed that these fungal factors are involved in transcriptional induction but not suppression because only the transcription factors activated by wild type challenges were defective in the mutants (Fig 6.6A and C and Fig 6.7A and B). Repression of RelB

and JunD following spore challenge was not mediated by factors or processes under pacC, gliP or prtT regulation (Fig 6.6B and D). This is the first study implicating *A. fumigatus* PacC or associated secreted products in transcriptional activation of alveolar epithelial cell genes during *in vitro* infection studies. A previous study did demonstrate that pretreatment of cells of the human bronchial epithelial cell line BEAS-2B with *A. fumigatus* extract suppressed the IFN-beta induced epithelial signal transducer and activator of transcription 1 (STAT-1) activation (Bhushan et al., 2015). However, the effect of the *A. fumigatus* extracts alone on STAT 1 activation was not assessed. Suffice it to say that activation of STAT 1 by *A. fumigatus* spores and CF has been investigated in the current study (Chapter 4, Fig 4.6B), but no change was observed in response to the challenges. Interestingly, the inhibitory effect of gliotoxin on IκBα-NF-κB signaling was not evident at the level of nuclear DNA binding of the RelA (p65) transcription factor. This could be due to either or both of two possibilities: First, the process of inhibiting LUBAC activity of the NEMO complex may dynamically be so slow that at the time of measuring DNA binding, negligible quantities of already translocated p65 are present in the nuclear compartment. Alternatively, another component of the CF may be inducing an opposing but positive signal through the same or a different pathway in a crosstalk manner. Mutants of the individual secreted gene products under PacC regulation are currently being generated. These mutants shall be screened for roles in canonical and non-canonical NF-κB and MAPK signaling activation.

Effects of deletion of p*acC*, *gliP* or p*rtT* on the cytokine profile of wild type *A. fumigatus* were highly variable and highly dependent on the specific cytokine under investigation. IL-8, IL-6 and FGF-2 were clearly more abundantly present in culture supernatants from progenitor isolates relative to culture supernatants from *ΔpacC* or *ΔgliP* challenges (Fig 6.8A, B and D), as such these gene products are likely required to mount the necessary immune response in epithelial cells that will lead to transcription and production of these cytokines. IL-8 production in response to a PrtT null mutant challenge was equivalent to that induced by the progenitor isolate (Fig 6.8A) thus excluding the proteases ALP, MEP, CpdS, and Dpp4 as possible effectors for IL-8 production. In other words, there's clearly a PrtT-dependent, PacC-independent

factor that is driving IL8 cleavage and the most likely culprit is DPP4. A recent study demonstrated the ability of the pathogenic yeast of *Blastomyces dermatitidis* to down play host immune responses by elaborating the activities of dipeptidyl-peptidase IVA (DppIVA), a close mimic of the mammalian ectopeptidase CD26 (Sterkel et al., 2016). It was shown that DppIVA cleaved human chemokine in a C-C (Sterkel et al., 2016) and C-X-C (Lorenzini et al., 2017) targeted manner. IL-8 chemokine ((C-X-C motif) ligand 8, CXCL8) is a known CXC type chemokine produced by many immune cells including epithelial cells and serves as a major neutrophil chemoattractant (Harada et al., 1994). The role of *A. fumigatus* Dpp4 in fungal mediated cytokine degradation using a Dpp4 mutant is currently under investigation. Contrary to p*acC* or g*liP*, p*rtT* regulated proteases important for GM-CSF induction in cultured airway epithelial cells (Fig 6.8C). The aberrant regulation of cytokine expression by PacC or PrtT-dependent factors could be explained by several different hypotheses: First, a component under their control might act as a PAMP or alternatively might cleave, for example, a group of protease activated receptor (PAR). PARs are a group of G protein-coupled receptors cleaved and activated by proteolysis. There are four well described PAR members: PAR1-4 (Soh et al., 2010). Expression of PARs in mammalian lung is well documented *in vitro* (Asokananthan et al., 2002, Asokananthan et al., 2015) and *in vivo* (Lan et al., 2004). Asokanathan et al previously showed that stimulation of PAR-1 and PAR-2 with an agonist peptide induced the release of IL-6 and IL-8 cytokines from A549, BEAS-2B, and HBECs airway epithelial cells (Asokananthan et al., 2002) and recently from human lung fibroblasts (Asokananthan et al., 2015). To the best of our knowledge, no study has looked at PAR mediated induction of IL-6 and IL-8 cytokines from epithelial cells following *A. fumigatus* infections. However, a very recent study by Homma et al has shown, using extracts that *A. fumigatus* can activate PAR-2 leading to expression of both CXCL10 (IP-10) mRNA and protein from NHBE epithelia cells (Homma et al., 2016). Upon identifying the individual secreted products driving cytokine expressions, the specific receptors involved shall also be investigated using a simple receptor knockdown technique or chemical inhibition including other possible non-PAR mediated mechanisms of induction.

Lastly, assessment of lytic epithelial cell death (Fig 6.1), detachment (Fig 6.2) and loss of TEER (Fig 6.3) demonstrates an overall reduction in virulence of the mutants compared to their respective wild type strains. Live fungal spore challenge with Δ*gliP* mutant had no significant impact on epithelial cell detachment compared to the progenitor isolate and in contrast to the *ΔprtT* mutant (Fig 6.2A). It has been shown in the previous chapter (Chapter 5) that a relationship exists between fungal spore uptake into A549 epithelial cells and epithelial cell detachment as pre-treatment of epithelial cell monolayers significantly reduced detachment (Fig 5.3B) and (Fig 6.2C). It becomes imperative thus to speculate that the indifference in detachment phenotype observed between the Δ*gliP* mutant and its progenitor isolate is a result of lack of difference in their uptake by the A549 epithelial cells. Very recent studies have demonstrated the ability of fungal gliotoxin to interfere with various processes of cell membrane actin dynamics (Jia et al., 2014, Schlam et al., 2016). However, the impact of the interference on the overall cellular functions and physiology appears to be cell type specific. Gliotoxin impaired the ability of macrophages to phagocytose targets in immortalized RAW 264.7 and J774 murine macrophage cell line (Jia et al., 2014, Schlam et al., 2016). Gliotoxin induced inhibition of phagocytosis in macrophages was mediated via decrease in the plasma membrane concentrations of phosphoinositides (PtdIns) PtdIns(4,5)P_2 and PtdIns(3,4,5)P_3, the key players in the phosphoinositides 3 kinases (PI3K) signalling during actin polymerizations (Schlam et al., 2016). This effect was shown to be concentration dependent (Jia et al., 2014). Contrary to the effect on macrophages actin dynamics, gliotoxin has been shown to improve fungal spore uptake (phagocytosis) by A549 epithelial cells as fungal uptake was significantly suppressed in Δ*gliP* mutant (Jia et al., 2014). Unlike the PtdIns (3,4,5)P_3 target on macrophages, the effect of gliotoxin on A549 cells acts via increase in phospholipase D (PLD) activity, which has been previously shown to be important for spore uptake by epithelial cells (Han et al., 2011). Challenge with spores from a Δ*gliP* mutant in this study did not appear to reduce detachment relative to the progenitor. It was therefore assumed that uptake of a Δ*gliP* by A549 cells is comparable to that of the progenitor isolate and can be significantly reduced by pretreatment with 2 µM of cytochalasin D (CytD) (Fig 6.2C). Our findings thus appear to be slightly different and opposing from the previous finding which suggests that Δ*gliP* mutant should cause

more detachment as a result of more uptake, although this is just a speculation as the actual spore uptake was not measured. It could also be true that uptake of Δ*gliP* mutant was increased as seen from the high significance level achieved with CytD treatment (Fig 6.2C). It is also possible that gliotoxin mediates epithelial cell detachment and fungal spore uptake via an independent mechanisms. Some of the discrepancies may have resulted from the differences in experimental and technical systems from fungal strains (*A. fumigatus* B5233 versus Δ*akuB*^{KU80}), fungal growth media, which greatly impact fungal metabolism (ACM versus peptone agar) or the cell culture media (RPMI versus DMEM), to mention but a few (Jia et al., 2014).

The molecular mechanism of redundancy of function between gliotoxin and PrtT for JNK activation cannot be sufficiently explained by our current findings. Potentially, these proteins might be interacting with the same receptor or with different receptors probably requiring co-operation at the level of intracellular adaptor to mediate an effect and the absence of either of the factors interrupts the interaction and the downstream effect. This mechanism has been described in natural killer cells whereby the sole engagement of either of individual receptors NKG2D (CD314), 2B4 (CD244) or DNAM-1 (CD226) is insufficient for NF-κB activation in response to different stimuli (Kwon et al., 2016). Translocation of NF-κB p65 was monitored by microscopy and the result showed significant increase in nuclear translocation of p65 in a conjugated human NK cell line (NKL cells) following co-stimulation of both NKG2D and 2B4 simultaneously in contrast to little and non-significant translocation seen following stimulation with NKG2D or 2B4 alone (Kwon et al., 2016). More detailed scrutiny shows that damage resulting from challenge with a *ΔprtT* mutant in all the assays was significantly reduced compared to the Δ*gliP* mutant. It is therefore reasonable to speculate on this basis that although a level of redundancy exists across *A. fumigatus* secretome, prtT regulated secreted proteases are more important for inducing epithelial cell damages and lysis during *in vitro* infections than gliotoxin.

6.5 Bibliography

AIMANIANDA, V., BAYRY, J., BOZZA, S., KNIEMEYER, O., PERRUCCIO, K., ELLURU, S. R., CLAVAUD, C., PARIS, S., BRAKHAGE, A. A., KAVERI, S. V., ROMANI, L. & LATGE, J. P. 2009. Surface hydrophobin prevents immune recognition of airborne fungal spores. *Nature,* 460**,** 1117-21.

ASOKANANTHAN, N., GRAHAM, P. T., FINK, J., KNIGHT, D. A., BAKKER, A. J., MCWILLIAM, A. S., THOMPSON, P. J. & STEWART, G. A. 2002. Activation of protease-activated receptor (PAR)-1, PAR-2, and PAR-4 stimulates IL-6, IL-8, and prostaglandin E2 release from human respiratory epithelial cells. *J Immunol,* 168**,** 3577-85.

ASOKANANTHAN, N., LAN, R. S., GRAHAM, P. T., BAKKER, A. J., TOKANOVIC, A. & STEWART, G. A. 2015. Activation of protease-activated receptors (PARs)-1 and -2 promotes alpha-smooth muscle actin expression and release of cytokines from human lung fibroblasts. *Physiol Rep,* 3.

BERTUZZI, M., SCHRETTL, M., ALCAZAR-FUOLI, L., CAIRNS, T. C., MUNOZ, A., WALKER, L. A., HERBST, S., SAFARI, M., CHEVERTON, A. M., CHEN, D., LIU, H., SAIJO, S., FEDOROVA, N. D., ARMSTRONG-JAMES, D., MUNRO, C. A., READ, N. D., FILLER, S. G., ESPESO, E. A., NIERMAN, W. C., HAAS, H. & BIGNELL, E. M. 2014. The pH-Responsive PacC Transcription Factor of *Aspergillus fumigatus* Governs Epithelial Entry and Tissue Invasion during Pulmonary Aspergillosis. *PLoS Pathog,* 10**,** e1004413.

BHUSHAN, B., HOMMA, T., NORTON, J. E., SHA, Q., SIEBERT, J., GUPTA, D. S., SCHROEDER, J. W., JR. & SCHLEIMER, R. P. 2015. Suppression of epithelial signal transducer and activator of transcription 1 activation by extracts of *Aspergillus fumigatus*. *Am J Respir Cell Mol Biol,* 53**,** 87-95.

BIGNELL, E., CAIRNS, T. C., THROCKMORTON, K., NIERMAN, W. C. & KELLER, N. P. 2016. Secondary metabolite arsenal of an opportunistic pathogenic fungus. *Philos Trans R Soc Lond B Biol Sci,* 371.

CHEN, J., WANG, C., LAN, W., HUANG, C., LIN, M., WANG, Z., LIANG, W., IWAMOTO, A., YANG, X. & LIU, H. 2015. Gliotoxin Inhibits Proliferation and Induces Apoptosis in Colorectal Cancer Cells. *Mar Drugs,* 13**,** 6259-73.

COMERA, C., ANDRE, K., LAFFITTE, J., COLLET, X., GALTIER, P. & MARIDONNEAU-PARINI, I. 2007. Gliotoxin from *Aspergillus fumigatus* affects phagocytosis and the organization of the actin cytoskeleton by distinct signalling pathways in human neutrophils. *Microbes Infect,* 9**,** 47-54.

EICHNER, R. D., AL SALAMI, M., WOOD, P. R. & MULLBACHER, A. 1986. The effect of gliotoxin upon macrophage function. *Int J Immunopharmacol,* 8**,** 789-97.

GARDINER, D. M. & HOWLETT, B. J. 2005. Bioinformatic and expression analysis of the putative gliotoxin biosynthetic gene cluster of *Aspergillus fumigatus*. *FEMS Microbiol Lett,* 248**,** 241-8.

GEISSLER, A., HAUN, F., FRANK, D. O., WIELAND, K., SIMON, M. M., IDZKO, M., DAVIS, R. J., MAURER, U. & BORNER, C. 2013. Apoptosis induced by the fungal pathogen gliotoxin requires a triple phosphorylation of Bim by JNK. *Cell Death Differ,* 20**,** 1317-29.

HAGAG, S., KUBITSCHEK-BARREIRA, P., NEVES, G. W., AMAR, D., NIERMAN, W., SHALIT, I., SHAMIR, R., LOPES-BEZERRA, L. & OSHEROV, N. 2012.

Transcriptional and proteomic analysis of the *Aspergillus fumigatus* Delta prtT protease-deficient mutant. *PLoS One,* 7**,** e33604.

HAN, X., YU, R., ZHEN, D., TAO, S., SCHMIDT, M. & HAN, L. 2011. beta-1,3-Glucan-induced host phospholipase D activation is involved in *Aspergillus fumigatus* internalization into type II human pneumocyte A549 cells. *PLoS One,* 6**,** e21468.

HARADA, A., SEKIDO, N., AKAHOSHI, T., WADA, T., MUKAIDA, N. & MATSUSHIMA, K. 1994. Essential involvement of interleukin-8 (IL-8) in acute inflammation. *J Leukoc Biol,* 56**,** 559-64.

HOMMA, T., KATO, A., BHUSHAN, B., NORTON, J. E., SUH, L. A., CARTER, R. G., GUPTA, D. S. & SCHLEIMER, R. P. 2016. Role of *Aspergillus fumigatus* in Triggering Protease-Activated Receptor-2 in Airway Epithelial Cells and Skewing the Cells toward a T-helper 2 Bias. *Am J Respir Cell Mol Biol,* 54**,** 60-70.

JIA, X., CHEN, F., PAN, W., YU, R., TIAN, S., HAN, G., FANG, H., WANG, S., ZHAO, J., LI, X., ZHENG, D., TAO, S., LIAO, W., HAN, X. & HAN, L. 2014. Gliotoxin promotes *Aspergillus fumigatus* internalization into type II human pneumocyte A549 cells by inducing host phospholipase D activation. *Microbes Infect,* 16**,** 491-501.

KUPFAHL, C., HEINEKAMP, T., GEGINAT, G., RUPPERT, T., HARTL, A., HOF, H. & BRAKHAGE, A. A. 2006. Deletion of the gliP gene of *Aspergillus fumigatus* results in loss of gliotoxin production but has no effect on virulence of the fungus in a low-dose mouse infection model. *Mol Microbiol,* 62**,** 292-302.

KWON, H. J., CHOI, G. E., RYU, S., KWON, S. J., KIM, S. C., BOOTH, C., NICHOLS, K. E. & KIM, H. S. 2016. Stepwise phosphorylation of p65 promotes NF-kappaB activation and NK cell responses during target cell recognition. *Nat Commun,* 7**,** 11686.

LAN, R. S., STEWART, G. A., GOLDIE, R. G. & HENRY, P. J. 2004. Altered expression and in vivo lung function of protease-activated receptors during *influenza* A virus infection in mice. *Am J Physiol Lung Cell Mol Physiol,* 286**,** L388-98.

LORENZINI, J., SCOTT FITES, J., NETT, J. & KLEIN, B. S. 2017. *Blastomyces dermatitidis* serine protease dipeptidyl peptidase IVA (DppIVA) cleaves ELR+ CXC chemokines altering their effects on neutrophils. *Cell Microbiol,* 19.

PAULUSSEN, C., HALLSWORTH, J. E., ALVAREZ-PEREZ, S., NIERMAN, W. C., HAMILL, P. G., BLAIN, D., REDIERS, H. & LIEVENS, B. 2017. Ecology of aspergillosis: insights into the pathogenic potency of *Aspergillus fumigatus* and some other *Aspergillus species*. *Microb Biotechnol,* 10**,** 296-322.

SAKAMOTO, H., EGASHIRA, S., SAITO, N., KIRISAKO, T., MILLER, S., SASAKI, Y., MATSUMOTO, T., SHIMONISHI, M., KOMATSU, T., TERAI, T., UENO, T., HANAOKA, K., KOJIMA, H., OKABE, T., WAKATSUKI, S., IWAI, K. & NAGANO, T. 2015. Gliotoxin suppresses NF-kappaB activation by selectively inhibiting linear ubiquitin chain assembly complex (LUBAC). *ACS Chem Biol,* 10**,** 675-81.

SCHLAM, D., CANTON, J., CARRENO, M., KOPINSKI, H., FREEMAN, S. A., GRINSTEIN, S. & FAIRN, G. D. 2016. Gliotoxin Suppresses Macrophage Immune Function by Subverting Phosphatidylinositol 3,4,5-Trisphosphate Homeostasis. *MBio,* 7**,** e02242.

SHARON, H., HAGAG, S. & OSHEROV, N. 2009. Transcription factor PrtT controls expression of multiple secreted proteases in the human pathogenic mold *Aspergillus fumigatus*. *Infect Immun,* 77**,** 4051-60.

SOH, U. J., DORES, M. R., CHEN, B. & TREJO, J. 2010. Signal transduction by protease-activated receptors. *Br J Pharmacol,* 160**,** 191-203.

STERKEL, A. K., LORENZINI, J. L., FITES, J. S., SUBRAMANIAN VIGNESH, K., SULLIVAN, T. D., WUTHRICH, M., BRANDHORST, T., HERNANDEZ-SANTOS, N., DEEPE, G. S., JR. & KLEIN, B. S. 2016. Fungal Mimicry of a Mammalian Aminopeptidase Disables Innate Immunity and Promotes Pathogenicity. *Cell Host Microbe,* 19**,** 361-74.

TSUNAWAKI, S., YOSHIDA, L. S., NISHIDA, S., KOBAYASHI, T. & SHIMOYAMA, T. 2004. Fungal metabolite gliotoxin inhibits assembly of the human respiratory burst NADPH oxidase. *Infect Immun,* 72**,** 3373-82.

CHAPTER 7: CHARACTERIZING THE ROLE OF NF-KB SIGNALLING IN EPITHELIAL CELL RESPONSES TO *A. FUMIGATUS*

7.1 Introduction

The non-canonical nuclear factor kappa-light-chain-enhancer of activated B cells (NF-κB) pathway was discovered in the earliest part of the twenty first century as an alternative pathway to NF-κB activation (Senftleben et al., 2001). Non-canonical NF-κB signalling can be activated via stimulation of specific members of the TNF-receptor subfamily such as the lymphotoxin β (LTβ) receptor (LTβR), B cell activating factor (BAFF), CD40, as well the receptor activator of NF-κB (RANK) by specific ligands. Ligand mediated activation of non-canonical signalling, is highly dependent on the synthesis and steady state regulation of NF-κB inducing kinase (NIK), which appears to be the most important kinase of the non-canonical pathway. Unlike the canonical pathway that involves the IKKβ and NF-κB essential modulator (NEMO), complete activation of the non-canonical pathway by NIK involves a downstream target, IKKα. Phosphorylation of IKKα by NIK leads to phosphorylation (serines 866 and 870) and activation of p100 (NF-kB2) leading to proteasome-mediated partial degradation to p52. p100 acts in a similar manner to the IκB-like molecule of the canonical pathway, to sequester and retain itself and the RelB in the cytoplasm pending activation by an appropriate signal (Zarnegar et al., 2008). Signal induced processing of p100 leads to the formation and nuclear translocation of the non-canonical NF-κB complex RelB–p52. Binding of RelB–p52 to κB site leads to activation of target gene transcription. In non-stimulated conditions, NIK proteins are continuously degraded to maintain a low basal level. This process is mediated by the intracellular adaptor NF receptor-associated factor 3 (TRAF3) which recruits the NIK protein to a second adaptor TRAF2 leading to ubiquitination and proteasomal degradation of NIK (Cildir et al., 2016). The low level of NIK in unstimulated cells ensures that the non-canonical NF-κB transcription factor complexes (RelB–p50) are held in an inactive state in the cytoplasm. Following signal induced activation of non-canonical signalling, TRAF3 is marked for degradation leading to stabilization of newly synthesized NIK and subsequent accumulation. Accumulation of NIK ultimately leads to p100 processing

and full activation of the non-canonical NF-κB pathway. Unlike the canonical NF-κB pathway, which, acting independently of *de novo* protein synthesis, occurs rapidly, the kinetics of non-canonical pathway activation are slow, inducible and dependent on *de novo* protein synthesis (Sun, 2017). Compared to the vast amount of mechanistic information on canonical NF-κB signalling, the molecular basis, and the role of, non-canonical NF-κB signalling in human health and diseases is not completely known. Various functions of non-canonical NF-κB signalling have been studied in mammalian cells types and a few *in vivo* mouse models especially alymphoplasia (aly/aly) mice having a point mutation in the gene encoding NIK (Shinkura et al., 1999, Cildir et al., 2016). The most well-characterised function of non-canonical NF-κB signalling is in immune regulation especially with regards to lymphoid development, B-cell maturation and survival, DC maturation and germinal centre (GC) formation (Sun, 2017). Thus far, it is evident that the non-canonical NF-κB signalling is central in regulation of the development, maturation and functions of innate and adaptive immune cells (Cildir et al., 2016, Sun, 2017). Similar to the canonical pathway, important roles of non-canonical NF-κB pathway in inflammation and cancer have been demonstrated (Maijer et al., 2015, Noort et al., 2014, Noort et al., 2015). Constitutive and uncontrolled NF-κB2 activation leads to fibrotic lung inflammation and alveolar damage in mice (Yang et al., 2010). However, the role of non-canonical NF-κB signalling during normal function of epithelial cells as non-professional immune cells remains unclear. The following studies were prompted by the highly evident inability of CF^{48} from a non-invasive *A. fumigatus* mutant to perturb non-canonical NF-κB signalling (Fig 6.7A and B). The aim was therefore to understand the important role of non-canonical NF-κB signalling in epithelial homeostasis, our initial hypothesis being that activation of the non-canonical signalling mechanism would be detrimental to epithelial integrity.

7.2 Methods

7.2.1 RT-qPCR methods

Total genomic DNA (gDNA) and RNA was extracted from A549 monolayers (comprised of approximately $1x10^6$ cells) according to sections 2.2.8.1 and 2.2.8.2 respectively. The total RNA was column-purified (section 2.2.8.3), amplified by PCR to ascertain purity using gDNA as a positive control (section 2.2.8.4) and then reverse transcribed to cDNA (section 2.2.8.5). PCR conditions were optimized for maximal amplification of the NIK, B-actin, YWHAZ and GAP3DH using a range of arbitrary gDNA concentrations (e.g 300, 200, 100, 50, 10, 1) by qPCR (Section 2.2.8.7) and using the relevant primer pair (Table 7.1). The cycle threshold (Ct) values were plotted as a function of gDNA concentration and the amplification efficiency for each primer pair (E-value) was calculated as in section 2.2.8.7 (Pfaffl, 2001). Amplification conditions that gave an E-value between 1.8 to 2.2 for all the genes tested was selected as the optimal amplification protocol (Table 2. 4). β-actin and NIK open reading frames were amplified from cDNA derived from 500 ng of total RNA and gDNA was used as template to generate a standard curve (concentrations in ng: 625, 125, 25, 5,1). The concentrations of β-actin and NIK amplicons were extrapolated from the standard curve. Transcript abundance for the gene of interest (GOI) was normalised to that of the β-actin reference gene and expressed as relative copy number NIK/β-actin. To calculate the relative gene expression level following treatments, the delta-delta Ct method was adopted (Section 2.2.8.7). Monolayers treated with OptiMem reduced serum media served as vehicle control for siRNA-treated monolayers (section 2.2.9). All experiments were done only when the NIK mRNA knockdown efficiency was at least 70%.

Table 7.1: Lists of the oligonucleotides used in this study

Oligonucleotide	Primer sequence (5'-3')	Melting Temperature (°C)
NIK Forward	CCACCTTTTCAGAACGCATTTTC	60.8
NIK Reverse	GTAGCATGGGCCACATTGTTG	61.9
B-actin Forward	GGCTGTATTCCCCTCCATCG	61.8
B-actin Reverse	CCAGTTGGTAACAATGCCATGT	61.1
YWHAZ Forward	CCTGCATGAAGTCTGTAACTGAG	60.6
YWHAZ Reverse	GACCTACGGGCTCCTACAACA	63.0
GAPDH Forward	ACCACAGTCATGCCATCAG	60.9
GAPDH Reverse	TCCACCACCCTGTTGCTGTA	61.8

7.2.2 RNA interference

Non-canonical NF-κB signalling was inhibited by genetically silencing the upstream NF-κB inducing MAP3K14 kinase (NIK) using 10 nM stealth RNAi interference siRNA (Table 5.2) and non-targeting siRNA as a negative control (Section 2.2.9). $1x10^6$ A549 cells were seeded in 10 cm sized tissue culture plates in 10 ml of antibiotic-free cell culture media (see section 2.2.1.2). RNAi duplexes were prepared by diluting 6 µl of RNAi 20 µM stock (i.e 120 pmol RNAi) with 994 µl of OptiMem reduced serum medium (total volume = 1 ml). Lipofectamine RNAiMAX was prepared by diluting 20 µl Lipofectamine with 980 µl of OptiMem reduced serum medium (Total volume =1 ml). The RNAi duplex mix was added to the Lipofectamine-RNAiMAX mix to form the RNAi duplex-Lipofectamine RNAiMAX complexes. The mixture was incubated at room temperature for 20 min and added to the 10 cm dish containing 10 ml of media (total volume = 12 ml). This resulted in a final RNAi concentration of 10 nM.

To prepare a 120 pmol challenge of negative siRNA control sequence (non-targeting scrambled sequences), 2.4 µl of a 50 µM stock concentration was diluted in 998 µl of OptiMem reduced serum medium (total volume = 1 ml). 20 µl of Lipofectamine RNAiMAX was diluted in 980 µl OptiMem reduced serum medium. The RNAi duplex-Lipofectamine RNAiMAX complex was formed as described above.

A549 epithelial cells were incubated with RNAi for 24 h. For NIK inhibited phenotypes, the cells were lysed and processed for transcription factor assays as in section 2.2.6 or treated with fungal spores or CF before lysis for investigation of fungal inducible effects on transcription factors or for LDH release. If Bay11-7082 treatment was required, transfected cells were treated with Bay11-7082 inhibitor (Table 5.1) for 1 h before fungal challenges or nuclear lysis.

Table 3: Table 7.2: Stealth small interference RNA (RNAi) targeting the MAP3K14 gene (NIK)

Primer Name	RNA Sequence 5' to 3'	length	Cat.no	purity
MAP3K14VHS40827 (NIK)	F1: GCCAGUCCGAGAGUCUUGAUCAGAU R1: AUCUGAUCAAGACUCUCGGACUGGC	25 25	10620318 10620319	Desalt Desalt

7.2.3 LDH assay

Lytic epithelial cell death was assessed by quantifying lactate dehydrogenase activity in cell culture supernatant following infections (see section 2.2.4.3).

7.2.4 Measurement of DNA binding activities of NF-κB transcription factors

The DNA binding activity of NF-κB transcription factors in nuclear extracts was assessed using the TransAM DNA binding ELISA based system (Active Motif) following A549 challenge with live fungal spores or CF (section 2.2.6). DNA binding activity of nuclear extract was quantified in 10 µg of protein aliquots (section 2.2.5.2 and 2.2.6.2). Absorbance value of the protein samples at 450 nm was blanked to the optical density measured from no protein control wells. The final absorbance was expressed as fold change value relative to uninfected epithelial cell controls.

7.3 Results

7.3.1 The NF-κB inducing kinase (NIK) is as abundant as β-actin in resting epithelial cells and down regulated following NIK RNAi treatment

In order to study the role of non-canonical NF-κB signalling in *A. fumigatus*-mediated AEC damage, RNA interference technology was used to inhibit the expression of NF-κB inducing kinase (NIK). NIK is the major anchor of non-canonical signalling activation and essential for phosphorylation of downstream IKKα to trigger inducible processing of p100 (Fig 1.9). It was appreciated however, that the effect of NIK silencing may go beyond impacting on RelB activity only and may have other off-target effects.

Prior to genetic silencing of NIK synthesis, the basal level of expression in resting A549 cells was measured using the human β-actin (ACTB) gene (NCBI gene ID: 60) as a reference. Fig 7.1A shows that the mRNA of NIK could be detected, and was as abundant in resting A549 cells as β-actin transcript.

The expression of NIK in A549 epithelial cells was significantly down regulated using NIK RNAi from 24 h post transfection (Fig 7.1B). The down regulation of NIK expression was sustained after 48 h (Fig 7.1C) ensuring down regulation during the period of fungal challenge.

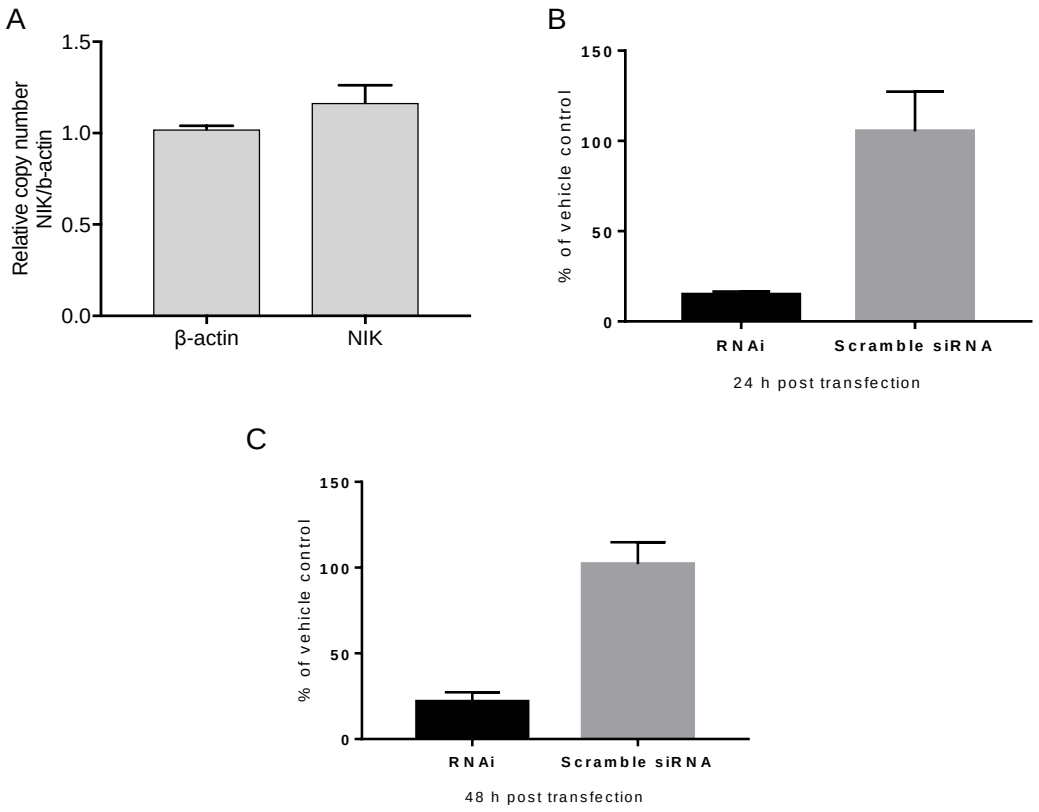

Figure 7.1: Basal and RNAi-treated expression of NIK gene in unstimulated A549 epithelial cells

Total RNA was extracted from confluent monolayers of A549 cells (10^6 cells), reverse transcribed and amplified in a quantitative real time polymerase chain reaction (RT-qPCR) using gDNA from the cell lines as positive control for amplification A) Basal expression of NIK relative to β-actin in resting A549 monolayers B) Expression level of NIK mRNA at 24 h post transfection following anti-NIK RNAi treatment C) Expression level of NIK at 48 h post transfection following anti-NIK RNAi treatment. Negative siRNA control was monolayer treated with scrambled non-targeting sequences at exactly the same concentration as the targeting siRNA. OptiMem reduced serum medium was used as the experimental vehicle control.

7.3.2 Effect of NIK silencing on steady state/basal DNA binding activity of p65 and RelB transcription factors

The effect of inhibiting non-canonical NF-κB signalling on the basal expression level of the RelA(p65) transcription factor of the canonical pathway and RelB of the non-canonical pathway was investigated.

Interestingly, NIK silencing specifically and significantly reduced the basal level of RelB DNA binding to about 50% of that detectable in untreated monolayers (Fig 7.2A) but had no cross effect on the basal level of RelA (p65) (Fig 7.2B).

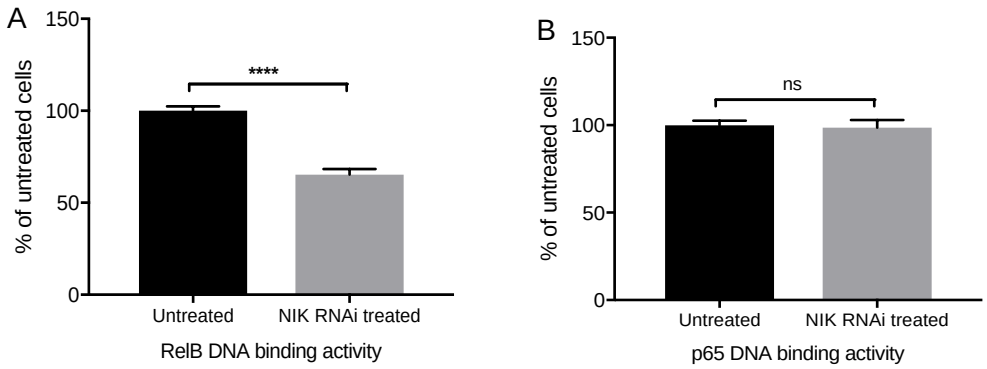

Figure 7.2: Effect of inhibition of NIK inhibition on DNA binding activity of p65 (RelA) and RelB

Measurement of DNA binding activities of p65 and RelB at 24 h post-transfection of A549 epithelial monolayers with anti-NIK siRNA A) DNA binding activity of RelB in untreated versus anti-NIK RNAi-treated A549 epithelial cell monolayers B) DNA binding activity of p65 in untreated versus anti-NIK RNAi-treated A549 epithelial cell monolayers. Data is expressed a percentage of DNA binding activity in the untreated group. Treatment was compared to untreated monolayer for significance. Data represent the mean of three biological replicates. Error bars show ± SEM. Data were analysed by unpaired, two-tailed student T test. ****P<0.0001.

7.3.3 Effect of NIK silencing on inducible DNA binding of p65 and RelB transcription factors

RNAi-mediated silencing of NIK significantly reduced the inducible DNA binding activity of RelB in response to CF^{48} exposure (Fig 7.3A) but had no effect on the DNA binding activity of RelB in response to spore challenge. DNA binding activity of p65 in response to live fungal spore challenge was reduced although not significant (p=0.0519). There was no change in the binding activity of p65 in response to CF (Fig 7.3B).

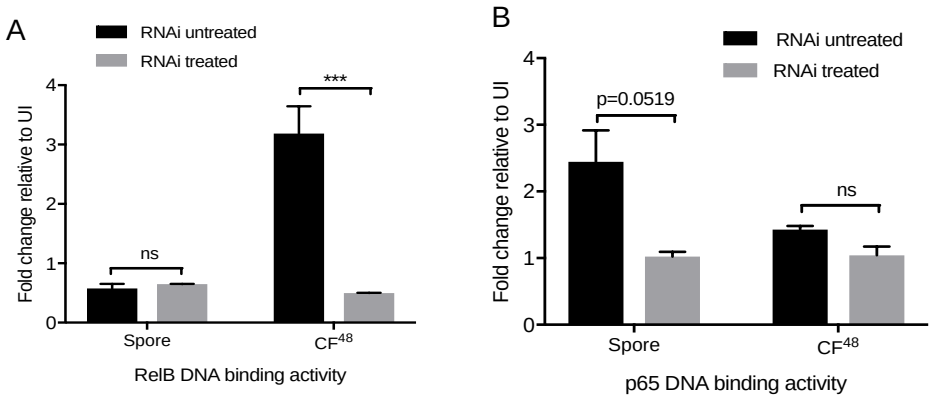

Figure 7.3: Quantitation of inducible level of RelB and p65 DNA binding activity in the presence of anti-NIK RNAi

A549 epithelial cell monolayers were treated with anti-NIK RNAi for 24 h and then challenged with $1x10^7$ *A. fumigatus* spores for 8 h, or a 5 fold dilution of CF^{48} for 4 h. A) DNA binding activity of RelB following spore or CF^{48} challenge B) DNA binding activity of p65 following spore or CF^{48} challenge. Comparison was between RNAi treated versus untreated epithelial cell monolayer. Data represent the mean of three biological replicates. Error bars show ± SEM. Data were analysed by one-way ANOVA with uncorrected Fisher LSD output. ***P<0.001.

7.3.4 Combinatorial impact of NIK and IκBα inhibition on basal DNA binding activity of p65 and RelB transcription factors

Treatment of A549 monolayers with IκBα inhibitor had no impact on the basal DNA binding activity of RelB (Fig 7.4A). Intriguingly, IκBα inhibitor moderately but significantly increased the basal DNA binding of p65 in A549 epithelial cells (7.4B). Very interestingly, it was observed that sequential inhibition of both pathways with NIK RNAi preceding IκBα inhibitor decreased the basal level of both RelA and RelB (Fig 7.4 C and D).

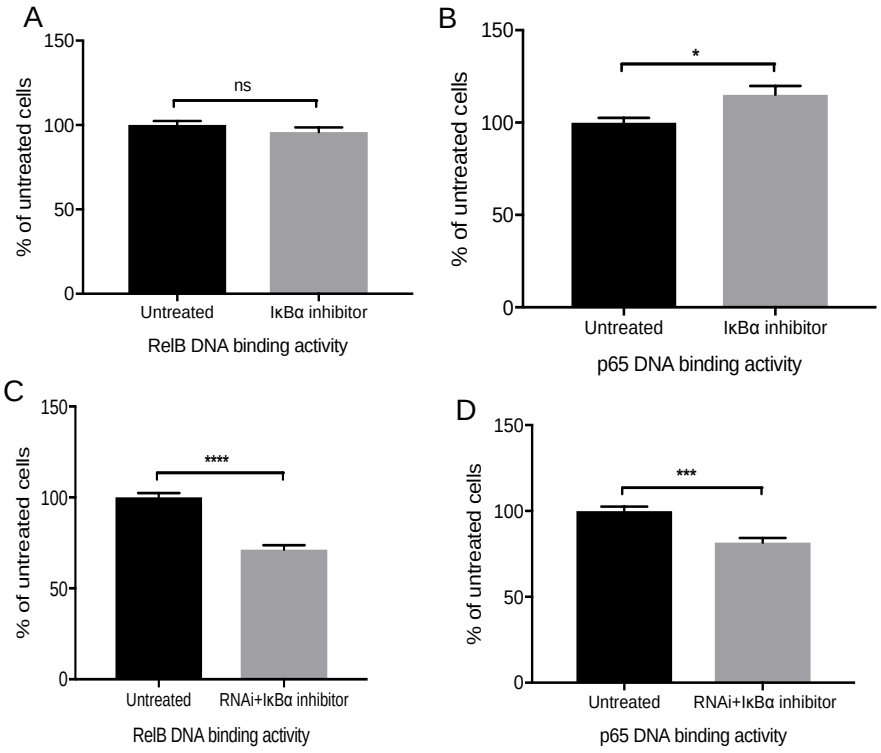

Figure 7.4: Effect of IκBα inhibition alone, or in combination with anti-NIK RNAi on DNA binding activity of p65 (RelA) and RelB

DNA binding activities of p65 and RelB in A549 epithelial cell monolayers A) DNA binding of RelB following incubation of monolayer with IκBα phosphorylation inhibitor for 1 h B) DNA binding of p65 following incubation of monolayer with IκBα phosphorylation inhibitor for 1 h C) DNA binding activity of RelB following treatment of monolayer first with anti-NIK RNAi for 24 h plus further treatment with IκBα phosphorylation inhibitor for 1 h D) DNA binding activity of p65 following treatment of monolayer first with anti-NIK RNAi for 24 h plus further treatment with IκBα phosphorylation inhibitor for 1 h. All treatment was compared to untreated

monolayer for significance. Data represent the mean of three biological replicates. Error bars show ± SEM. Data were analysed by unpaired, two-tailed student T test. *P<0.05, ***P<0.001, ****P<0.0001.

7.3.5 NIK has a role in maintaining epithelial cell viability/integrity

When compared with untreated epithelial cell monolayers, it was found that LDH activity was significantly higher in uninfected A549 monolayers following anti-NIK RNAi treatment (Fig 7.5A). Combined anti-NIK and IκBα inhibitor treatments also lead to a moderate increase in LDH activity although this did not reach significance. Monolayers pre-treated with anti-NIK RNAi before live fungal spore or CF^{48} challenge were significantly more susceptible to lytic cell death compared to cells not treated with RNAi (Fig 7.5B). Interestingly, lysis resulting from anti-NIK RNAi treatment was reversed by concomitant IκBα inhibition for 1 h prior to live spore or CF^{48} and, moreover, proffered additional protection (Fig 7.5B).

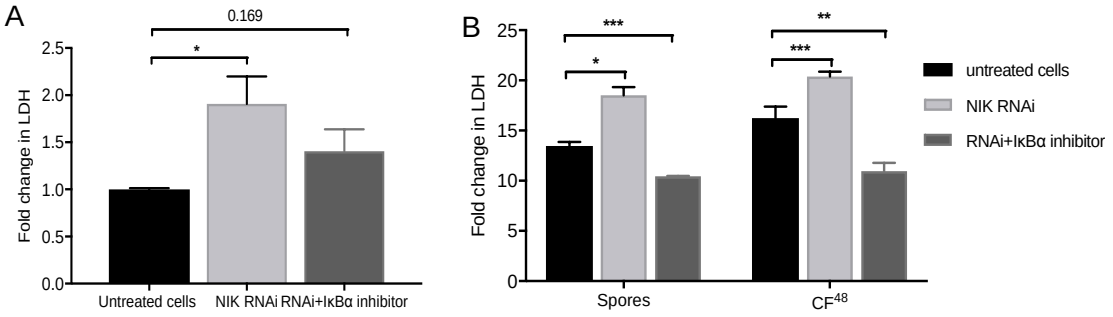

Figure 7.5: Role of NIK in modulating lytic epithelial cell death during *A. fumigatus* challenge

Quantification of LDH activity released by A549 epithelial cell monolayer in culture supernatant after 24 h A) LDH activity from monolayer treated with anti-NIK RNAi for 24 h or anti-NIK RNAi followed by treatment with IκBα inhibitor B) When monolayers in A above were challenged with live fungal spores or CF^{48}. Data represent the mean of three biological replicates. Error bars show ± SEM. Data were analysed by two-way ANOVA with multiple comparison and uncorrected Fisher's LSD output. Significance was calculated relative to no RNAi treatment groups *p<0.05, **P<0.01, ***P<0.001.

7.3.6 Activation of RelB and p65 DNA binding in epithelia cell during fungal challenge is independent of MAPK phosphorylation

DNA binding of non-canonical NF-κB transcription factors RelB and p52 was significantly activated in response to fungal CF^{48} exposure (Fig 4.9) an effect which was not observed following challenge with CF^{48} obtained from a PacC null mutant (Fig 6.7A). Similarly, JNK- and p38-mediated signalling was significantly activated in response to CF^{48} obtained from wild type isolates (Fig 4.2D and E) but not in response to CF^{48} obtained from a PacC null mutant (Fig 6.5B and C). To investigate the relevance of JNK- and p38-mediated signalling in activation of non-canonical NF-κB activation, RelB and p65 DNA binding, in the presence and absence of chemical inhibitors of JNK and p38 phosphorylation, was assessed. The experiment detected no dependency of RelB (Fig 5.6A and B) or p65 (Fig 5.6C and D) on activation of JNK or p38 signalling during epithelial cell responses to fungal challenge.

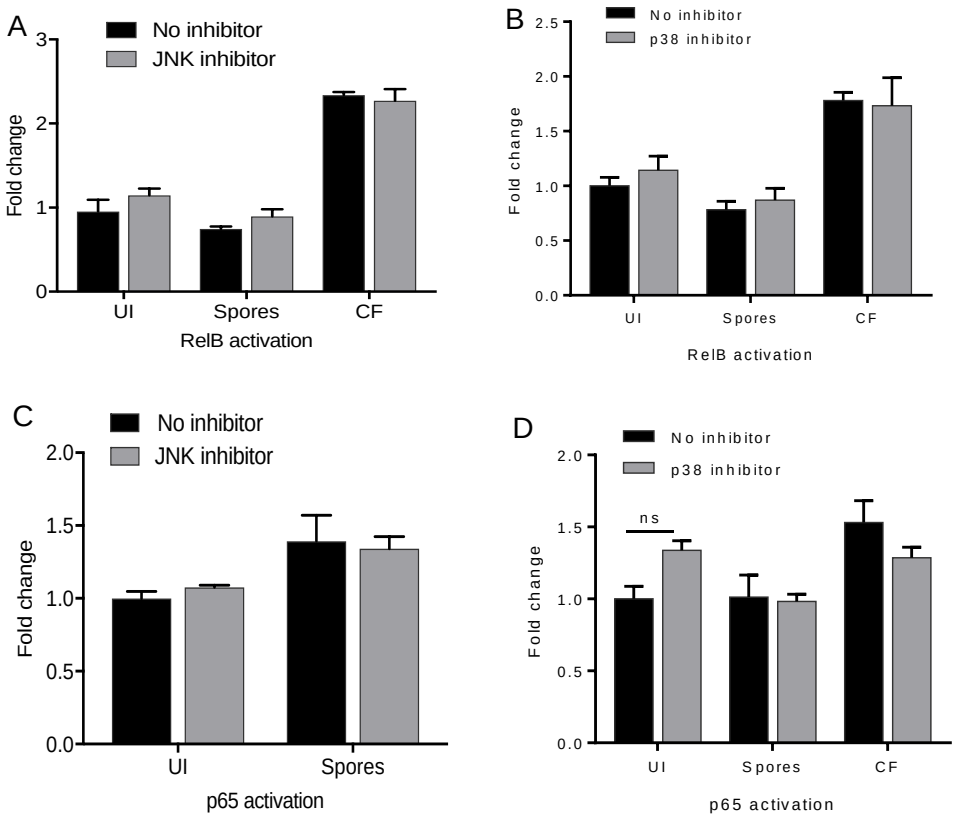

Figure 7.6: Inhibition of p38 or JNK signalling does not affect the DNA binding activity of RelB or p65 in A549 epithelial cells during *A. fumigatus* infection.

Effect of JNK and p38 inhibitor following exposure to spore and CF[48] on A and B) RelB DNA binding activity C and D) p65 DNA binding activity. Data represent the mean of three biological replicates. Error bars show ± SEM. Data were analysed by Two-way ANOVA. Significance was calculated relative to no inhibitor treatments with Sidak's multiple comparisons test. ns= non-significant.

7.4 Discussions

NIK is the upstream activator of the non-canonical subunits of NF-κB (Fig 1.9). At the transcriptional level, NIK transcript is stably expressed in unstimulated type II alveolar A549 cells at a 1:1 ratio with that of the house keeping cytoskeletal β-actin gene (Fig 7.1A). The human β-actin (ACTB) gene encodes a highly conserved protein involved in maintaining cell structure, motility and integrity (https://www.ncbi.nlm.nih.gov/gene/60 (5/10/2017)). Currently, the current physiological function of human NIK (MAP3K14) is limited to its role as a kinase involved in NF-κB signalling, and little is known of its prevalence in different cell types although a previous study has reported its relative abundance in human B cell and embryonic kidney cell lines (Qing et al., 2005). As a highly expressed epithelial protein (Fig 7.1A) and (Qing et al., 2005), it was not unreasonable to speculate a role for NIK in maintaining epithelial integrity. This hypothesis was verified by knocking down the expression of NIK using RNA interference (RNAi). Epithelial cell lysis was significantly increased in response to live spore and CF^{48} challenge (Fig 7.5) when NIK expression was reduced by 80%. The lytic effect of NIK silencing did not result from wholesale silencing of NF-κB signalling but rather from selective silencing of non-canonical transcription factors because only the basal level of RelB, but not p65, was changed (Fig 7.2).

NIK knockdown did not affect the steady state level of p65 DNA binding activity (Fig 7.2B) but reduced its activation in response to fungal challenge (Fig 7.3A and B). The damage induced by canonical NF-κB signalling, which could be inhibited using the Bay11-7082 IκBα inhibitor (Fig 5.2C), is likely due to excessive inflammation in response to the presence of the fungal spores. The canonical heterodimer (RelA/p50) is efficiently constrained to the cytosol by IκB proteins but nuclear translocation and DNA binding of RelA/p50 is highly inducible by stimuli such as TNFα and IL-1 receptor signals (Birbach et al., 2002). This explains the low basal level of nuclear RelA(p65) compared to that induced by live fungal spore challenge (Fig 4.7E).

Basal RelB activity (the non-canonical pathway) was significantly reduced by anti-NIK RNA interference without affecting the RelA level, thus verifying the silencing strategy to be a good option for studying RelB functionality or non-canonical NF-κB activity in cases where direct RelB knockdown is lethal or impossible. RelB has both activator and repressor roles in regulating NF-κB-dependent gene expression whereby heterodimeric complexes of RelB and p50 or p52 positively regulate NF-κB-dependent gene expression. However, RelB represses NF-κB activity by direct complexation with RelA thereby inhibiting RelA DNA binding.

RelA/RelB heterodimers are unable to bind κB binding sites (Marienfeld et al., 2003). It is unclear which factors determine whether RelB will complex with p50/p52 (activator) or RelA (repressor). Moreover, despite having a transactivation domain RelB does not bind κB sites either as a monomer or a homodimer (Marienfeld et al., 2003). The transcription of both RelB and p52 is RelA-regulated (Bren et al., 2001), which might explain why, initially, the quantity of nuclear-localised RelB remains low during early fungal challenge until newly synthesized RelB and p100 are translated in the cytosol. This process may take a similar amount of time to that needed for hyphal formation and production of secreted products (Fig 4.7 and 4.10). Alternatively, induction of RelB function may depend on a direct activation by a secreted product from mature fungal hyphae, thus the reason for a rapid increase in nuclear level following exposure to CF^{48} (Fig 4.9). The secreted component/(s) responsible for activation of non-canonical signalling might act via binding to the TNFR or other non-canonical receptors leading to p100 processing and eventual RelB translocation into the nucleus (and possible feed-back attenuation of p65 dependent signalling). In RelB knockout fibroblasts, there was an increase in release of proinflammatory cytokines and chemokines which corresponded with increased p50 and RelA activity (Xia et al., 1997). In contrast, RelB knockdown in monocyte-derived macrophages reduced the inflammatory activity compared to wild type macrophages (Xia et al., 1997). The immune-modulatory role of RelB in fibroblasts might also be relevant in epithelial cells since, contrary to the hematopoietic cells which have very brief lifespans after an inflammatory attack, resident tissue cells such as fibroblasts and ECs must develop a mechanism to dampen inflammatory signaling to maintain tissue homeostasis, plausibly through RelB activation. In this respect, it would interest researchers in the field to investigate the modulatory role of NIK in airway damage progression and whether there is a possible mutation in the NIK from diseased lungs compared to healthy lung.

Due to the similarities in the types of stressor/stimuli involved in their activation, multiple occurrences of crosstalk between NF-κB transcription factors and other signalling pathways are likely. Further, the presence of multiple phosphorylation sites present on NF-κB subunits as well as their susceptibility to post translational modifications increases the chances of activation of NF-κB transcription factors by other interactors and signalling pathways (Oeckinghaus et al., 2011, Oeckinghaus and Ghosh, 2009). The crosstalk occurring between NF-κB and MAPK-mediated signalling, predominantly JNK and p38, has been documented since nearly two decades ago (Schulze-Osthoff et al., 1997). Activation of canonical NF-κB subunits is predominantly achieved via phosphorylation of IκBα inhibitor by appropriate

stimuli (Fig 1.9). However, signalling crosstalk allows co-activation of this pathway by other kinases. An example is the activation of p65 transcription factors by MAPK p38 kinase leading to transcription of NF-κB dependent gene expressions (Vermeulen et al., 2003). Inhibition of p38 signalling using the chemical inhibitor SB203580 abrogated TNF-mediated p65 transcriptional activities in L929sA and HEK293 mouse fibroblast cells (Vermeulen et al., 2003). Contrary to these findings, the potent p38 inhibitor, SB203580 had no effect on either live spore- or CF^{48}-induced p65 activation or on CF^{48}-induced non-canonical RelB activation (Fig 7.6B and D). The discrepancy between data reported in the previous study and those obtained from this study might be due to trivial methodological effects ranging from cell type differences to experimental set-up. Moreover, NF-κB activity is cell type, stimulus and micro-environment specific (Xia et al., 1997).

Similarly, inhibition of JNK 1 and 2 using JNK inhibitor II had no effect on the canonical NF-κB subunits activated by live fungal challenge or the non-canonical response induced by CF^{48} challenge (Fig 7.6 A and C). Previous studies showed that the protective activity NF-κB activation is mediated by inhibiting pro-apoptotic JNK signalling in NIH/3T3 Fibroblasts (Papa et al., 2004, De Smaele et al., 2001). Thus if NF-κB inhibits JNK activities, JNK-mediated activation of NF-κB will be very unlikely to occur.

Interestingly, this was not so in the case of epithelial cell responses to *A. fumigatus* challenge. Our current finding is interesting as it clearly shows that activation of NF-κB following CF^{48} challenge occurs independently of JNK- or p38-mediated signalling. Thus, it can be inferred that the presence of a TNF receptor like ligand in the CF^{48} of *A. fumigatus* is capable of directly activating NIK phosphorylation. A cohort of secreted product mutants shall further be exploited through high throughput screening in order to uncover the secreted molecule of *A. fumigatus* involved in activating non-canonical NF-κB signalling.

Onward hypotheses regarding mechanism

Inhibition of IκBα phosphorylation with Bay11-7082 reduced lytic cell death possibly by inhibiting further NF-κB activity induced by the persistent fungal presence on the epithelial cell signal.

Increase in the nuclear level of p65 in the presence of Bay11-7082 is likely due to reduced export from the nucleus mediated by IκBα, which might lead to unattenuated (consititutive) activation of an inflammatory state. On the contrary, lytic cell death is reduced possibly because the bound p65, in the absence of more input from the bound stimulus, produces just

enough inflammatory molecules to combat the fungus and protect the host (Fig 7.7). This may perhaps explains why it has a global protection on both the spore and CF induced epithelial cell damage.

To verify this hypothesis, reduced cytokine production should be observed in the presence of BAay11-7082 (or at least slightly lower level than in the absence of Bay11-7082 but higher than resting level). Also, more inflammatory cytokine production would be expected in the absence of NIK compared to presence of NIK (RelB).

Blocking IκBα following NIK silencing protects the monolayer, leading to less death as measured by LDH. This indicates that NIK/RelB is important in maintaining normal inflammation in the tissue resident cells like epithelia cells. This result in addition suggests that NIK protection is mediated via anti-inflammatory effect and as such, blocking canonical signalling following NIK silencing abrogates the excessive inflammation that would have resulted to cell death. If this hypothesis is verified, then, an overexpression of NIK or RelB activity may be beneficial in auto-immune inflammatory disease states. Also, the fungus through secreted products may just be manipulating this anti-inflammatory function to its favour as could be seen by the magnitude of increase induced by CF.

A second possibility is that in the absence of fungal challange, the canonical pathway is not activated and thus, no immune/protective response is activated for the host cells, rather, the non-canonical pathway, which is anti-inflammatory is activated. This leads to increased susceptibility of the epithelial cells to CF^{48} components and death. The rapidity of activation by CF^{48} also suggests that it may contain a substance capable of activating the specific TNF receptor for the non-canonical pathway (Fig 7.8). These results show that there is a level of co-operativity between the two arms of NF-κB signalling, with the absence of either of the pathways resulting in more lytic cell death although the sequence of activation or inhibition of the pathways could be manipulated for improved epithelial protection during *A. fumigatus* infection.

NIK genetic silencing does affect only the steady state and inducible nuclear level of RelB but not p65. This suggests that NIK inhibition can be used as an alternative target when studying the non-canonical NF-κB pathway. Of importance going forward is the inclusion of scramble siRNA controls tested simultaneously with the targeted RNAi at treatment time points to rule out the effects of effects of transfection especially the lipofectamine carrier on cell function.

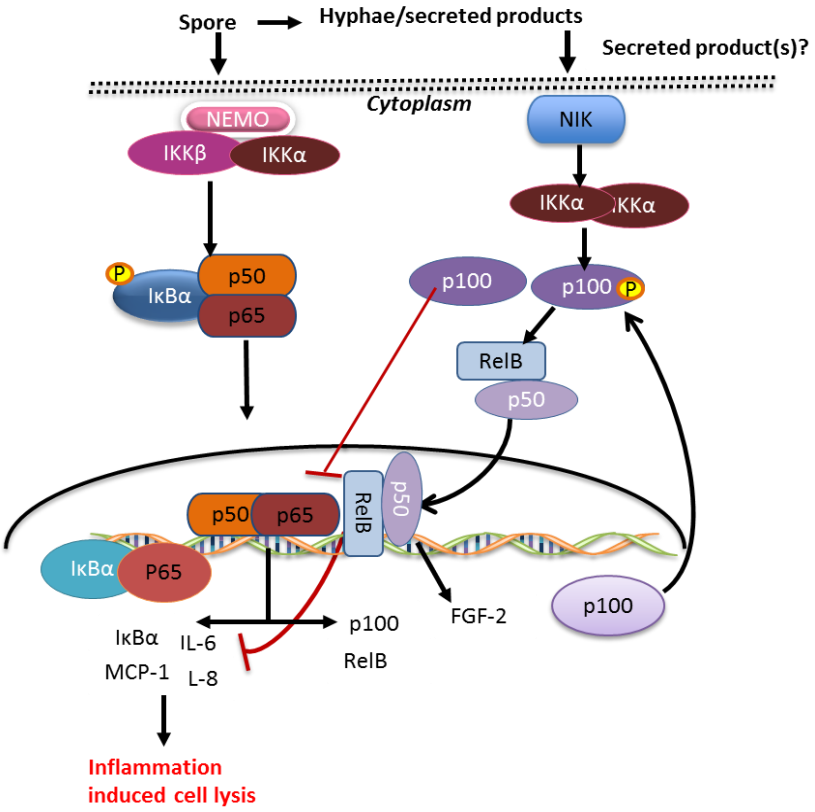

Figure 7.7: Proposed model of NF-κB signalling in AECs during airway anti-*Aspergillus* response

Spore exposure triggers the phosphorylation and ubiquitination of IkBα and nuclear translocation of the active p50 and p65 dimer. Binding of p50/p65 dimer to κB sites triggers the transcription of pro-inflammatory genes as well as IkBα, p100 genes. The inflammatory response initiates a protective antifungal response. The newly synthesized IkBα, together with p65 are exported back into the cytosol and this acts negatively to repress p65 activity. Newly synthesized p52 is translated and modified in the cytosol awaiting a phosphorylation-mediated signal, also resident are very low levels of RelB or p52 (the processed form of p100). As the fungal spore germinates to form a hypha, soluble products are secreted. One or more of the secreted products binds to a potential TNFR leading to the phosphorylation of NIK and subsequent activation of p100 processing and nuclear translocation of RelB. RelB in the nucleus binds to p65 preventing further inflammatory gene transcription. Also some of the unprocessed p100 subunits oligomerize into higher molecular weight complexes IkBσ

that are capable of binding and inhibiting p65 activity. The exaggerated inflammation leads to epithelial cell death.

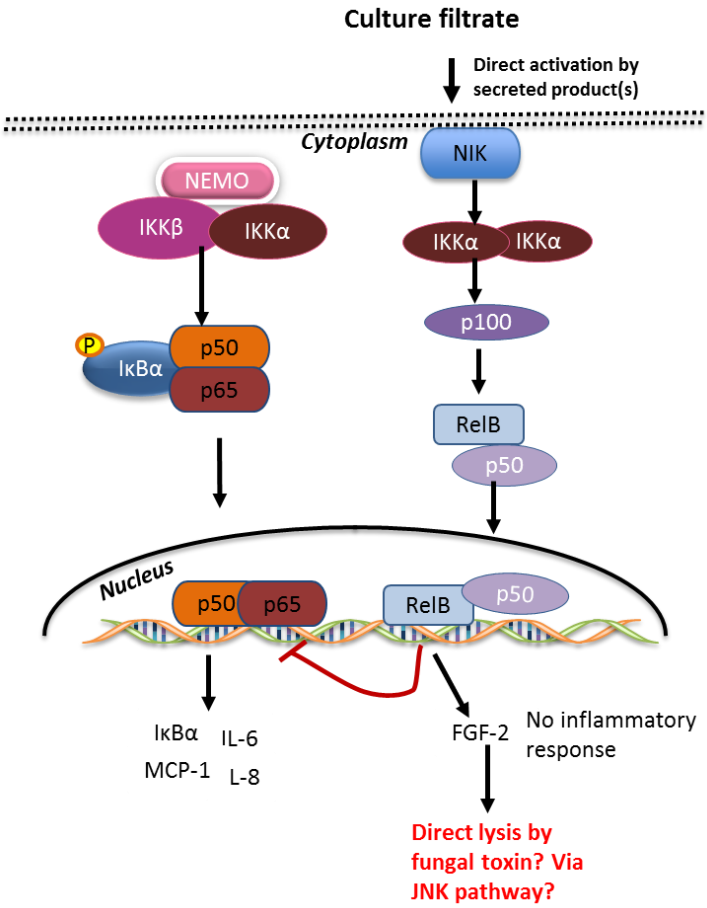

Figure 7.8: *A. fumigatus* secreted product(s) are capable of activation non-canonical NF-κB signalling directly.

During CF[48] challenge, prior spore-mediated activation of canonical NF-κB signalling has not occurred rather, the anti-inflammatory non-canonical pathway is activated in isolation. This leads to increased susceptibility of the epithelial cells to CF due either to a lack of immune protection, or direct cytotoxicity of the filtrate, or both.

7.5 Bibliography

BIRBACH, A., GOLD, P., BINDER, B. R., HOFER, E., DE MARTIN, R. & SCHMID, J. A. 2002. Signaling molecules of the NF-kappa B pathway shuttle constitutively between cytoplasm and nucleus. *J Biol Chem,* 277**,** 10842-51.

BREN, G. D., SOLAN, N. J., MIYOSHI, H., PENNINGTON, K. N., POBST, L. J. & PAYA, C. V. 2001. Transcription of the RelB gene is regulated by NF-kappaB. *Oncogene,* 20**,** 7722-33.

CILDIR, G., LOW, K. C. & TERGAONKAR, V. 2016. Noncanonical NF-kappaB Signaling in Health and Disease. *Trends Mol Med,* 22**,** 414-29.

DE SMAELE, E., ZAZZERONI, F., PAPA, S., NGUYEN, D. U., JIN, R., JONES, J., CONG, R. & FRANZOSO, G. 2001. Induction of gadd45beta by NF-kappaB downregulates pro-apoptotic JNK signalling. *Nature,* 414**,** 308-13.

MAIJER, K. I., NOORT, A. R., DE HAIR, M. J., VAN DER LEIJ, C., VAN ZOEST, K. P., CHOI, I. Y., GERLAG, D. M., MAAS, M., TAK, P. P. & TAS, S. W. 2015. Nuclear Factor-kappaB-inducing Kinase Is Expressed in Synovial Endothelial Cells in Patients with Early Arthritis and Correlates with Markers of Inflammation: A Prospective Cohort Study. *J Rheumatol,* 42**,** 1573-81.

MARIENFELD, R., MAY, M. J., BERBERICH, I., SERFLING, E., GHOSH, S. & NEUMANN, M. 2003. RelB forms transcriptionally inactive complexes with RelA/p65. *J Biol Chem,* 278**,** 19852-60.

NOORT, A. R., TAK, P. P. & TAS, S. W. 2015. Non-canonical NF-kappaB signaling in rheumatoid arthritis: Dr Jekyll and Mr Hyde? *Arthritis Res Ther,* 17**,** 15.

NOORT, A. R., VAN ZOEST, K. P., WEIJERS, E. M., KOOLWIJK, P., MARACLE, C. X., NOVACK, D. V., SIEMERINK, M. J., SCHLINGEMANN, R. O., TAK, P. P. & TAS, S. W. 2014. NF-kappaB-inducing kinase is a key regulator of inflammation-induced and tumour-associated angiogenesis. *J Pathol,* 234**,** 375-85.

OECKINGHAUS, A. & GHOSH, S. 2009. The NF-kappaB family of transcription factors and its regulation. *Cold Spring Harb Perspect Biol,* 1**,** a000034.

OECKINGHAUS, A., HAYDEN, M. S. & GHOSH, S. 2011. Crosstalk in NF-kappaB signaling pathways. *Nat Immunol,* 12**,** 695-708.

PAPA, S., ZAZZERONI, F., BUBICI, C., JAYAWARDENA, S., ALVAREZ, K., MATSUDA, S., NGUYEN, D. U., PHAM, C. G., NELSBACH, A. H., MELIS, T., DE SMAELE, E., TANG, W. J., D'ADAMIO, L. & FRANZOSO, G. 2004. Gadd45 beta mediates the NF-kappa B suppression of JNK signalling by targeting MKK7/JNKK2. *Nat Cell Biol,* 6**,** 146-53.

PFAFFL, M. W. 2001. A new mathematical model for relative quantification in real-time RT-PCR. *Nucleic Acids Res,* 29**,** e45.

QING, G., QU, Z. & XIAO, G. 2005. Stabilization of basally translated NF-kappaB-inducing kinase (NIK) protein functions as a molecular switch of processing of NF-kappaB2 p100. *J Biol Chem,* 280**,** 40578-82.

SCHULZE-OSTHOFF, K., FERRARI, D., RIEHEMANN, K. & WESSELBORG, S. 1997. Regulation of NF-kappa B activation by MAP kinase cascades. *Immunobiology,* 198**,** 35-49.

SENFTLEBEN, U., CAO, Y., XIAO, G., GRETEN, F. R., KRAHN, G., BONIZZI, G., CHEN, Y., HU, Y., FONG, A., SUN, S. C. & KARIN, M. 2001. Activation by IKKalpha of a

second, evolutionary conserved, NF-kappa B signaling pathway. *Science,* 293**,** 1495-9.

SHINKURA, R., KITADA, K., MATSUDA, F., TASHIRO, K., IKUTA, K., SUZUKI, M., KOGISHI, K., SERIKAWA, T. & HONJO, T. 1999. Alymphoplasia is caused by a point mutation in the mouse gene encoding Nf-kappa b-inducing kinase. *Nat Genet,* 22**,** 74-7.

SUN, S. C. 2017. The non-canonical NF-kappaB pathway in immunity and inflammation. *Nat Rev Immunol,* 17**,** 545-558.

VERMEULEN, L., DE WILDE, G., VAN DAMME, P., VANDEN BERGHE, W. & HAEGEMAN, G. 2003. Transcriptional activation of the NF-kappaB p65 subunit by mitogen- and stress-activated protein kinase-1 (MSK1). *EMBO J,* 22**,** 1313-24.

XIA, Y., PAUZA, M. E., FENG, L. & LO, D. 1997. RelB regulation of chemokine expression modulates local inflammation. *Am J Pathol,* 151**,** 375-87.

YANG, L., CUI, H., WANG, Z., ZHANG, B., DING, J., LIU, L. & DING, H. F. 2010. Loss of negative feedback control of nuclear factor-kappaB2 activity in lymphocytes leads to fatal lung inflammation. *Am J Pathol,* 176**,** 2646-57.

ZARNEGAR, B., YAMAZAKI, S., HE, J. Q. & CHENG, G. 2008. Control of canonical NF-kappaB activation through the NIK-IKK complex pathway. *Proc Natl Acad Sci U S A,* 105**,** 3503-8.

CHAPTER 8: GENERAL DISCUSSIONS AND SUMMARY

Invasive aspergillosis (IA) is one of the top four most fatal fungal diseases of humans, accounting for over 90% of death due to invasive mould infections. Incidence of IA is currently estimated at 200,000 cases per annum with an unacceptably high mortality rate of 50-95%. Incidence of IA is likely to be underestimated due to difficulties with accurate diagnosis and lack of national surveillance programmes. IA is a disease of the immune-compromised mostly affecting patients with haematological malignancies, stem cell transplantees, and neutropenic individuals. In the light of the severe immuno deficiency associated with chemotherapy and transplant procedures the integrity of the upper and lower respiratory epithelium, which is the first point of contact for inhaled microorganisms, is crucial to prevent the germination of fungal spores and subsequent growth into underlying tissues to cause invasive disease. In addition to offering a physical barrier against inhaled conidia, the respiratory epithelium has been shown to phagocytose fungal spores, inhibit spore germination and secrete anti-microbial components via activation of an immune response to fungal components (Escobar et al., 2016).

In IA inhaled spores of *A. fumigatus* breach the respiratory epithelium and invade underlying tissues. The mechanistic basis of invasion is poorly understood but destruction of epithelial integrity and angioinvasion are key pathological events and drivers of patient mortality. The work presented in this thesis describes the establishment of a dynamic *in vitro* model with which to study both host and pathogen components of the host-pathogen interaction, and in particular the response of the alveolar epithelium to different morphotypes of *A. fumigatus*. Critically, given the morphogenic programme underlying the fungal insult, the timescales of host responses have been studied in order to identify the temporal basis of host responses to distinct fungal structures.

The obligatory morphological transition of *A. fumigatus* across the respiratory epithelium exposes epithelial cells to a wide range of fungal antigens and toxins during infection. The outcome of *A. fumigatus*-epithelial interactions, and the

consequent impact upon other immune responses, is a critical driver of differential disease outcomes and a more thorough understanding of the process will undoubtedly improve targeted therapies and more efficient diagnoses.

8.1 Mechanism of epithelial damage and invasion by *A. fumigatus*

This study reports a previously unappreciated degree of mechanistic complexity occurring in three sequential phases and involving: contact-mediated perturbation; physical invasion of the epithelial stratum by *A. fumigatus* germlings, and hyphae and lytic activity of soluble effectors (Chapter 3). Contact-mediated damage occurs as an immediate response to spore challenge and prompts epithelial cell detachment as early as 4 h post infection (Fig 3.3). Analysis of epithelial viability using LDH assay confirmed an intermediate phase of lytic cell death coinciding with the initiation of hyphae formation (Fig 3.2A and 3.5A-D). The intermediate lytic event is independent of a secreted/soluble factor as demonstrated by the inability of an early phase culture filtrate (CF^{16}) to induce either detachment or lytic cell death (3.4A and 3.6C). Interestingly, data from a Calu-3 tight junction model revealed a potential explanation to be physical invasion, as relative to challenge with CF from mature fungal culture (CF^{48}), the reduction in TEER at 24 h post fungal challenge was significantly higher, being almost doubled (Fig 3.7E). This finding suggests that that certain secreted factors may be required to assist physical invasion, whilst others are important for driving lytic cell death. A similar mechanism has been demonstrated for invasive *C. albicans* infections whereby physical force exerted by the growing hyphae on the epithelium is complemented by several secreted proteases and proteinases such as Als3 and Sap5 which help in digesting and degrading epithelial basement membrane and tight junction proteins especially E-cadherin (Villar et al., 2007, Filler and Sheppard, 2006, Swidergall and Filler, 2017). In the case of *A. fumigatus* invasion, proteases such as elastases may be degrading the collagen and or other host proteins; and or lytic enzymes/proteases may be digesting the AECs thereby enhancing the impact of physical penetrative force from the hyphae (Kothary et al., 1984) and (this study).

The latest phase of events is mechanistically driven by soluble factors secreted from mature hyphae and causing cellular damage mostly via cell detachment and lytic cell death (Fig 3.4A and C) and (Fig 3.6A and B). These results also demonstrate a certain degree of co-operativity between physical fungal invasion and input from soluble effectors in achieving the overall extent of damage to the host. The data support the hypothesis that physical invasion of fungal hyphae is important in reducing the interepithelial adhesion (TEER) thereby initiating cell detachment whereas soluble products are required for inducing lytic cell death as seen by the rapidity of epithelial cell lysis and detachment following exposure to CF^{48}, a response which could not be achieved from soluble factors from 16 h CF (Chapter 3).

To successfully invade the human lung, *A. fumigatus* must efficiently adapt or counter the variety of suboptimal conditions in the lung such as hypoxia, high temperature, nutrient deficiency as well as the slightly alkaline pH. The PacC/Rim101 regulatory pathway, which is conserved across the fungal kingdom plays an important role in environmental adaptation to alkaline pH and pH-dependent regulation of secreted proteins (Penalva et al., 2008). In addition to pH regulation, the role of the transcription factor PacC in virulence during invasive aspergillosis has been demonstrated for *A. nidulans* and *A. fumigatus* (Bignell et al., 2005, Bertuzzi et al., 2014). *A. fumigatus ΔpacC* mutants differentially express many genes commonly associated with invasive growth during initiation of a murine infection including genes involved in gliotoxin or cell wall biosynthesis or encoding secreted proteases (Bertuzzi et al., 2014). The events identified from this study as leading to epithelial cell decay appear to be mechanistically due to a combination of factors under the *A. fumigatus* master regulator PacC (Chapter 6). Although the cohort of PacC regulated factors mediating the damage events differ, it appears that fungal proteases and gliotoxin might act additively to bring about epithelial cell lysis and detachment following hyphal maturation (Fig 6.1B and 6.2B). This is in contrast to the contact-mediated events occurring earlier which are mediated by a fungal protein but not gliotoxin (Fig 6.2A and 6.3A). These observations are broadly consistent with transcriptional findings presented by Bertuzzi et al which showed that specific cell wall proteins and secreted product genes can be significantly upregulated during both early and late

phases of infection whereas genes involved in secondary metabolism including gliotoxin synthesis genes are expressed during late infection and invasive growth only (Bertuzzi et al., 2014). Although some mycotoxins and secondary metabolites such as Fumigaclavine C, tryptoquivaline, and trypacidin have been extracted from *A. fumigatus* spores, gliotoxin has been consistently undetectable from a spore extract (Fischer et al., 2000, Gauthier et al., 2012), reinforcing the role of a cell wall associated entity rather than gliotoxin in initiating the process of host decay.

8.2 Morphotype-specific epithelial cell responses

Concordant with observational analysis of the sequential and mechanistically distinct modes of epithelial decay (Chapter 3), the present study provides new evidence that airway epithelial cells respond in a distinctive and dynamic manner to *A. fumigatus* infection during the early (conidia), intermediate (germlings/immature hyphae) and late (mature hyphae/secreted effector) phases of infection (Chapter 4). The presence of *A. fumigatus* conidia triggers an immediate and sustained activation of the canonical NF-κB signaling circuit (Fig 4.1F) and corresponding increase in DNA binding of p50 and p65 and decrease in DNA binding of RelB transcription factors (Fig 4.7F). The DNA binding activity of JunD and c-Jun are also simultaneously decreased in response to early spore contact. This is followed by an intermediate response to swollen conidia and early germ tube formation from about 4 h post infection via activation of JNK signalling in addition to NF-κB signalling and corresponding alterations in the DNA binding of the AP-1family of transcription factors (increase in DNA binding of c-Fos and c-Myc and decrease in DNA binding activity of MEF-2 and JunD simultaneously) (Fig 4.5F). During the late phase of *A. fumigatus* infection, hyphae and hyphal-secreted soluble effectors drive the activation of MAPK JNK, p38 (Fig 4.2F) and a concurrent increase in DNA binding of non-canonical NF-κB dimers RelB and p50 (Fig 4.9E and F). This is the first and only study to the best of our knowledge, to synthesize the global response of airway epithelial cells to the different morphogenetic transitions of *A. fumigatus* in an *in vitro* infection model. Our result on NF-κB mediated responses to conidia and germ-tubes are in line with the only previous study which investigated the role of NF-κB signalling in airway *Aspergillus*

infection. However, only a single time point of 15 h (germlings/immature hyphae) was investigated previously (Balloy et al., 2008).

To further reinforce that early responses and early perturbations are mechanistically dependent, it was found that activation of canonical NF-κB signalling was via a contact-dependent mechanism as this activation was absent in response to challenge with soluble hyphal secreted products (Fig 4.2F). Interestingly, the early NF-κB response, although driven by physical fungal contact, requires fungal viability or a heat sensitive entity as heat-killing of the fungus prior to challenge abolished the early responses including the early JNK activation (Chapter 5, Fig 5.4C). *A. fumigatus* germlings induce IL-8 synthesis in bronchial epithelial cells via canonical NF-κB signalling (Balloy et al., 2008), and heat inactivation of fungal fragments abolishes IL-8 production (Zhang et al., 2005). Our finding forms a bridge between these two previous findings and suggests that a heat labile fungal element is important for inducing the IL-8 response in epithelial cells via NF-κB signalling. This finding is an interesting addition to the current understanding of canonical NF-κB responses in airway defences against *Aspergillus.* Furthermore, this result suggests that β-glucan, which is one of the best-studied cell wall-associated antigens in *A. fumigatus* immunity (Fontaine et al., 2000, Arana et al., 2009, van de Veerdonk et al., 2008), is unlikely to be the major PAMP inducing canonical NF-κB -mediated signalling in airways. As with most carbohydrates, heating at temperatures up to 160 degree Celsius has been shown to change the conformation and branching of β-glucan (Xu et al., 2013). However, the immunogenicity of fungal cell wall β-glucan is not always dependent on branching or conformation as short fragments (2 -8 μm) fungal cell wall β-glucan are sufficient to induce macrophage activation and immune signalling (McCann et al., 2005) as well as platelet activation (Vancraeyneste et al., 2016). Moreover, the extraction of cell wall β-glucan for various studies is usually done under high temperature conditions (Aimanianda et al., 2009). The absence of canonical NF-κB signalling following challenge with CF^{48} suggests that the ligands or the effectors inducing NF-κB signalling are not secreted proteases or soluble factors in the CF^{48}. Thus, the early contact-mediated canonical NF-κB signalling may likely

therefore; to be mediated by one of the vast groups of *A. fumigatus* glycophosphatidylinositol (GPI) anchored cell wall proteins or other cell wall entities.

GPI-anchored proteins are proteins which are attached to the cell wall by a glycolipid known as glycophosphatidylinositol attached to the C-terminal signal sequence of the protein (Fontaine et al., 2003). GPI anchoring of proteins is encountered in all eukaryotes including humans. Fungal GPI anchored proteins (GPI-AP) include antigens, receptors, enzymes, and protective cell surface components which may be involved in cell wall organisation, synthesis or stability (Vaknin et al., 2014), as well as in virulence *in vivo* (Li et al., 2007, Liu et al., 2016). Some of the plasma membrane associated GPI-APs include the β-glucanase , β-glucanosyltransferase encoded by *GEL* 4 in *A. fumigatus*, aspartyl protease, superoxide dismutase, and phospholipase (Richard and Plaine, 2007). The core of the GPI anchor is synthesized in the endoplasmic reticulum and consists of a lipid group, an inositol group, a phosphoethanolamine group and a stepwise addition of sugars such as an *N*-acetylglucosamine and mannose groups (Pittet and Conzelmann, 2007). During the early steps of GPI synthesis in *C. albicans*, the inositol group is acylated enabling the addition of a terminal ethanolamine group needed for protein linkage to the GPI anchor. After protein attachment, the acyl chain is removed by the action of inositol deacylase. The yeast homolog of the human inositol deacylase encoded by *BST1* has been shown to play a role in host invasion by *C. albicans* (Liu et al., 2016). Deletion of BST1 led to poor GPI-APs attachment to the host and a resultant decrease in invasion. Interesting, deacylation of GPI-APs resulted in increased inflammatory responses via NF-κB signalling and nuclear translocation of p65, and enhanced JNK, p38 and ERK1/2 signalling in macrophages (Liu et al., 2016). Although not demonstrated in the study, the mechanism by which deacylation resulted in stronger inflammatory responses maybe due to the release of the anchored proteins from the cell wall thereby reducing their ability to adhere properly to host cell.

The bone marrow stromal antigen-2 (Tetherin) is a GPI-AP encoded in humans by the BST2 gene. Tetherin is an interferon inducible anti-viral protein with dual functions of trapping new virion envelops and inducing activation of proinflammatory responses (Blasius et al., 2006). BST2 has been shown to improve anti-HIV immunity by

activating NF-κB signalling as the major inflammatory response to either sensing of viral particles or tethering of new virions (Galao et al., 2012, Tokarev et al., 2013). BST2 induced NF-κB signalling occurred predominantly via the canonical signalling pathway as a mutant lacking IKKβ was unable to induce activation even in response to the maximum dose of viral protein achievable in the human embryonic HEK293T cell line (Tokarev et al., 2013). By using an Ebola virus-like particle (VLP) model based on the matrix protein (VP40), a recent study found a co-operation between BST2 and the viral GPI-AP like glycoprotein amplifies the NF-κB inflammatory response (Rizk et al., 2017).

Furthermore, PbPga1, a GPI-AP protein located on the surface of *Paracoccidioides brasiliensis*, the leading cause of paracoccidioidomycosis (PCM) was shown to induce NF-κB transcription factors in the Raw 264.7 macrophage cell line as early as 2 h into co-incubation (Valim et al., 2015). Recombinant PbPga1 (r PbPga1) also induced NF-κB activation in mast cells leading to IL-6 and TNF-a expression. Overall, these findings suggest that GPI-APs can act as either a receptor or a ligand/antigen to induce pro-inflammatory responses via NF-κB signalling and also demonstrate beyond doubt that fungal GPI-APs are important in initial contact with the host and can modulate the host pathogen interaction through immune activation.

Our data shows that the entities inducing canonical NF-κB signalling during early infection are under PacC regulation and appears to be related to gliotoxin and PrtT protease (Fig 6.4A). Perhaps, there is a certain level of gliotoxin borne in the conidia that is below the detectable limits of the HPLC, MS etc used in the studies that previously reported that gliotoxin is not produced by conidia (Fischer et al., 2000, Gauthier et al., 2012). However, complete deletion of the *gliP* gene completely eradicates even the smallest molecule of gliotoxin present and any potential effect it has on the phenotype.

Our data on MAPK activation during late infection concur with the only one previous study which shows that PrtT regulated proteases from *A. fumigatus* are responsible for activation of JNK and ERK1/2 signalling in airway epithelial cells (Sharon et al., 2011). Concordantly, analysis of CF from PacC and PrtT null mutants showed that

activation of the MAPK signalling were PacC and PrtT dependent (Fig 6.5B and C). Also, this finding points in the direction of involvement of protease activated receptors (PARs) in mediating the observed MAPK responses. There are four well described PAR members: PAR1-4 (Soh et al., 2010) whose expression in mammalian lung has been well demonstrated *in vitro* (Asokananthan et al., 2002, Asokananthan et al., 2015) and *in vivo* (Lan et al., 2004). PARs are protein receptors generalized in recognizing unique peptide sequences with PAR-1 and PAR-2 being the best studied in relation to lung inflammation and diseases (Dulon et al., 2003, Asokananthan et al., 2002, Asokananthan et al., 2015, Driesbaugh et al., 2015). Proteases are primarily known for their potential as degradative enzymes prior to the discovery that they can also specifically modulate host cell responses by cleaving and activating members of the PAR family of receptors. To activate PAR, the protease binds and cleaves the PAR at a specific peptide bond within the extracellular amino terminal exodomain thereby exposing a new amino terminal. The new amino terminal acts as a tethered ligand, binds and activates the cleaved receptor via the interaction of a unique six amino acid sequence (SLIGKV for PAR-2) of the tethered ligand domain with specific extracellular and transmembrane domains of the cleaved receptor (Dery et al., 1998, Dulon et al., 2003). Activation of MAPK ERK1/2 signalling through stimulation of PAR-2 receptor on A549 epithelial cell with a PAR-2 agonist leads to increase in IL-8 expression, a response which is completely abrogated using an ERK1/2 inhibitor (Moriyuki et al., 2008). Also, *A. fumigatus* allergen extracts activate PAR-2 leading to expression of both CXCL10 (IP-10) mRNA and protein from NHBE epithelial cells (Homma et al., 2016). In addition to activating PARs, proteases also modulate the relative expression of PAR-2 in neutrophils *in vitro* and *in vivo* in a TLR4 dependent manner, whereby activation of TLR4 leads to downregulation of PAR-2 and inhibition of the canonical NF-κB inflammatory response (Moretti et al., 2008). Inhibition of PAR-2 was mediated by proteases as treatment of *A. fumigatus* culture supernatant with protease inhibitors abolished the ability of the extract to deactivate PAR-2. Interestingly, an opposing phenotype was observed with culture supernatant from *C. albicans* which upregulates PAR-1 expression in a manner independent of proteases leading to increased ERK1/2 and NF-κB inflammatory responses in activated neutrophils (Moretti et al., 2008). It appears however, that deactivation of PAR-2 is

mediated by a neutrophil derived protease triggered in response to the fungal challenge. A previous study implicated the neutrophil-derived serine proteases elastase and cathepsin G in deactivation of PAR-2 activation through proteolytic cleavage of the extracellular domain of the tethered ligand domain leaving the unmodified SLIGKV which is unable to induce a response (Dulon et al., 2003). Modulation of PAR activity by fungus-induced host proteases was significantly different in response to challenge with different fungal morphotypes, as hyphal challenge led to more inflammatory response than conidia (Moretti et al., 2008). It appears thus far that *A. fumigatus* induces production of an anti-PAR-2 protease from the host to block initial host inflammatory response via p38 inactivation after which the build-up of fungal secreted proteases during late infection increases PAR-1 and PAR-2 inflammatory response via the p38 activation leading to increased inflammatory host damage.

8.3 Epithelial cell damage is driven by host responses to fungal morphotypes

The three mechanistically distinct events leading to epithelial perturbations can easily be synchronized with the three major phases of the dynamic host responses, which directly or indirectly could be driving the epithelial cell damage/perturbations. The inhibition of canonical NF-κB signalling significantly reduces epithelial cell lysis and fungal invasiveness (as measured by TEER) resulting from early infection but had no significant effect on detachment (Chapter 5). As reported previously, acylation of GPI anchors improves the ability of the cell wall GPI-APs of pathogenic *C. albican* to attach more firmly and invade the host tissues (Liu et al., 2016). The exact mechanism of invasion is not clear but the role of GPI-APs in NF-κB activation (Liu et al., 2016, Valim et al., 2015) appears to be the most viable explanation such that strong attachment of GPI-APs to host activates persistent NF-κB signalling which could lead to huge cellular stress and reduced TEER. Accordingly, lytic epithelial cell death and cell detachment during both early and late infection was maximally reduced following inhibition of MAPK JNK and p38 signalling. Accordingly, if adhesion is crucial for GPI-AP mediated detachment and loss of TEER, a fungal mutant deficient in adhesion and binding would be unable to induce cell detachment, such as Δ*rodA* mutant lacking the

cell wall hydrophobic rodlets (Thau et al., 1994). Moreso, a Δ*cspA* lacking the glycophosphatidylinositol (GPI)-anchored cell wall protein should be unable to induce detachment (Levdansky et al., 2010, Levdansky et al., 2007).

8.4 Modulation of epithelial cell transcriptional activities and gene expression by *A. fumigatus*

The ultimate goal of activating the host's signalling events in response to *A. fumigatus* is to increase the expression of immune effectors including cytokines, chemokines and growth factors. Activation of signalling pathways in epithelial cells in response to different *A. fumigatus* morphotypes ultimately leads to expression and secretion of cytokines. Consistent with previous studies, activation of host signalling in response to early *A. fumigatus* infection resulted in significant increases in cytokines such as GM-CSF, IL-8, IL-6 (Fig 6.8A-) and TNF-a (Fig 5.5C) (Bellanger et al., 2009, Sun et al., 2012). This study appears to be the first to report an increase in FGF-2(basic) release from airway epithelial cells in response to early *Aspergillus* infection (Fig 5.5D and Fig 6.8D). Interestingly, and in agreement with some previous studies, exposure of epithelial cells to CF alone leads to significant reduction in cytokine expression and production (Fig 5.5A-D) in a concentration dependent manner (Fig 4.14 A-D), suggesting the role of a soluble factor in degrading these cytokines (Borger et al., 1999, Kauffman et al., 2000, Tomee et al., 1997). The degradation in cytokine levels is likely mediated by proteases and possibly in a target specific manner as some host-derived signalling factors, such as FGF-2, were resistant to degradation even following exposure to mature CF (Fig 4.11I and Fig 5.5D). By incubating supernatants from fungal spore challenge with CF previously incubated with (SN-spore+SN-CF48) or without (SN-spore+CF48) host cells, it was found that cytokine degradation was not impacted upon by any secreted host factor (Fig 5.5A-D). GM-CSF degradation appears to be under a non-PrtT PacC regulated protease (Fig 6.8C) whereas IL-8 degradation appears to be mediated by a PrtT regulated protease (Fig 6.8A). This finding is supported by findings from a recent study which demonstrated the ability of the pathogenic yeast of *Blastomyces dermatitidis* to down play host immune responses by elaborating the activities of dipeptidyl-peptidase IVA (DppIVA), a close mimic of

the mammalian ectopeptidase CD26. It was shown that DppIVA cleaved human chemokine in a C-C (Sterkel et al., 2016) and C-X-C (Lorenzini et al., 2017) targeted manner.

A. fumigatus hyphal maturation occurring during the late infection leads to the production of soluble factors such as proteases and degradative enzymes to assist in degrading the mammalian lung tissues highly composed of collagen and elastin (Bertuzzi et al., 2014). As a result, a large proportion of studies of the role of protease in pathogenesis of invasive aspergillosis have focused on elastases and one such study directly correlated elastase production with virulence in non-neutropenic mice. All mice exposed to high protease producing strains of *A. fumigatus* died at most 4 days post exposure with an increased fungal burden and complete tissue necrosis post mortem (Kothary et al., 1984). A significant level of functional redundancy has been demonstrated amongst *A. fumigatus* proteases. As such, deletion of a master regulator of secreted protease did not attenuate virulence, increasing the difficulties in exploring the role of an individual protease (Bergmann et al., 2009, Sharon et al., 2009).

Prior to this study, the transcription factors involved in cytokine gene expression following activation of signalling pathways in response to *A. fumigatus* infection of the airway remained largely unstudied (Table 1.6). This study is the first to investigate the dynamic changes in the DNA binding activities of three relevant transcription factor families, namely canonical and non-canonical NF-κB, AP-1 and other MAPK-related family members and concomitant intracellular signalling in response to morphogenetic changes of *A. fumigatus* (Chapter 4) (Whitmarsh and Davis, 1996). In tandem with activation of intracellular host signalling pathways, changes in DNA binding activities of transcription factors occurred in three distinct patterns. Early and intermediate infection increases the transcriptional activity of p65 and p50 via IkBα phosphorylation while reducing the binding activity of the AP-1 heterodimer.

8.5 Integrity of non-canonical NF-kB signalling is critical for epithelial viability

Most literature evidence supports a role for p65 in inflammation (Ather et al., 2015, Noort et al., 2014, Durand and Baldwin, 2017), and RelB in cell growth and development and anti-inflammation (Weih et al., 1996, Yoza et al., 2006, Zhu et al., 2012a). Regardless of this, the function of RelB as regards inflammation is cell type- and stimulus-specific and the majority of studies have been conducted in professional immune cells such as macrophages, B-cells and dendritic cells. Although epithelial cells are the first line of contact and defence against inhaled agents as well as a non-professional innate immune cell, only a single study has investigated the role of RelB (non-canonical NF-κB signalling) in airway inflammatory responses to inhaled stressors (Tully et al., 2012). Stimulation of primary murine tracheal epithelial cells (MTECs) or spontaneously transformed Type II murine lung alveolar epithelial cell line (C10) with different agonists including LPS, Poly IC, TNF-a, CD40L, IL-17 and lipotechoic acid resulted in activation of both p65 and RelB DNA binding (Tully et al., 2012). Nuclear accumulation of RelA protein in response to LPS was observed and occurred by 30 min post challenge but returned to base line by 2 h whereas accumulation of RelB protein was slower but sustained up to 48 h post challenge (Tully et al., 2012). This is similar to our finding that showed increase in p65 binding with decreased RelB binding in early infection (Fig 4.7F). RelB binding activity increases during CF^{48} exposure, at which time the p65 activity has returned to baseline (Fig 4.9 E and F). By using siRNA targeted at p65 and RelB, it was previously found [48] that both canonical and non-canonical NFkB signalling impacted on production of CCL-20, RANTES, keratinocyte-derived chemokine (KC) and IL-6 in response to LPS. Interestingly, knock-down of RelB resulted in a roughly 3 fold increase in IL-6 production. This observation argues in favour of the anti-inflammatory role for RelB for two reasons. Firstly, IL-6 can function as either a pro- or anti-inflammatory cytokine depending on the stimulus (Scheller et al., 2011) and LPS is known to be an inflammatory stimulus (Wong and Johnson, 2013, Zhong et al., 2012). Secondly, an increase in the expression of pro-inflammatory IL-6 following RelB knockdown suggests a role for RelB in modulating inflammation via reduction of the IL-6 level in response to LPS challenge.

Therapeutic agents targeted against the inflammatory role of canonical NF-κB signalling such as Bortezomib (Velcade/PS-341; Millennium Pharmaceuticals), a reversible 26S proteasome inhibitor that prevents IkBα degradation thus preventing activation of canonical signalling (Baud and Karin, 2009, Gupta et al., 2010) suggest that an anti-inflammatory role of RelB could be protective in a specified context. It is not clear at this point if the protective role of the non-canonical signalling observed in NIK knockdown A549 epithelial cell model used in this is as a result of inflammatory modulation. Another possible mechanism by which RelB could be protective is through down-regulation of apoptosis. A recent study showed that RelB knockdown suppressed the growth of human prostate cancer cell line DU145 by promoting the rate of apoptosis (Wang et al., 2016) which occurred via reduction in the expression of the pro-survival (anti-apoptotic) BCL-2 gene (Wang et al., 2016). Knockdown of RelB did not affect the expression and functions of other NF-κB subunits. This is interesting and very similar to our finding that NIK knockdown affected only RelB but not p65 basal activity (Fig 7.2). Another study also showed that the ability of RelB to increase the invasiveness of breast cancer was mediated via its activity on the BCL-2 promoter (Wang et al., 2007a). It is thus clear that RelB mediated increase in BCL-2 activity may play a role in cancer progression. However, whether the BCL-2 has a role in airway epithelial cell integrity during airway infections is unclear.

Activation of non-canonical (nc) NF-κB signalling is primarily mediated by activation of NIK through ligand-receptor interaction between a distinct group of receptors such as the lymphotoxin β (LTβ) receptor (LTβR), B cell activating factor (BAFF), CD40, as well the receptor activator of NF-κB (RANK). Activated NIK in turn activates IKKα leading to direct phosphorylation of p100 (Sun, 2017). Studies have shown that IKKα is receptive to a wider range of stimuli including the inducers of the canonical NF-κB signalling (Sun, 2017). However, signals that subvert NIK and activate only IKKα are insufficient in activating the non-canonical NF-κB signalling possibly because NIK may be required to facilitate IKKα binding to p100 or perhaps activating an additional factor which is functionally required to co-operate with IKKα for full non canonical activation (Sun, 2017).

Non-canonical NF-κB signalling predominantly activates p52/RelB heterodimer as the main effector. However, the NF-κB protein that dimerizes with RelB appears to be dependent on both stimuli and cell type involved. Unlike in mouse embryonic fibroblasts (MEFs) where RelB is found only in association with p52, immunoprecipitation of whole cell lysate from bone marrow derived dendritic cells (BMDCs) showed that in addition to the expected RelB/p52 dimmer, RelB was also found associated with IκBα and IκBε inhibitors and p50 of the canonical pathway, although RelB/p50 complexes were primarily found in the cytoplasmic lysate (Shih et al., 2012). Binding of IkBα with RelB served to downregulate RelB activity leading to immaturity of DCs and poor antigen presentation. IkBα deficiency in knockout DCs resulted in increased nuclear RelB/P50 complex over the typical RelB/p52 and a resultant inappropriate and spontaneous increase in DC maturation phenotypes, all of which were dependent on RelB as a compound deletion of the *Relb* gene completely reversed the phenotypes (Shih et al., 2012). Thus, the association of RelB with other NF-κB proteins largely affects not only its cellular localization but most importantly its functionality both qualitatively and quantitatively. These findings show broad similarity to most of our data as seen with increase in DNA binding of p52 and p50 (Fig 4.9A and C) associated with increase in RelB binding (Fig 4.9B) following CF^{48} challenge (although p50 increase did not reach statistical significance). There was no increase in nuclear binding of RelB following IkBα inhibition (Fig 7.4A), and the fact that IkBα is important in down regulating RelB activity by complexing it into inactive RelB/IkBα complex could explain the drastic decrease in lytic cell death induced by CF^{48} challenge following IkBα inhibition (Fig 5.1C) which was unlikely due to canonical NF-κB activity (not induced by CF^{48} challenge Chapter 4). This is because, inhibiting IkBα phosphorylation and its release from the NEMO complex make it unavailable for RelB binding and inactivation thereby increasing the availability of RelB protein and its protective effect as shown in Chapter 7. A prevoious study has shown that activation of RelB in association with p50 or IkBα is dependent on TLR 2, 4 or 9 mediated canonical NF-κB signalling by appropriate stimuli in BMDC as early as 30 min post challenge but occurred at late time points in MEFs (Shih et al., 2012). RelB activation in A549 cells in response to *A. fumigatus* challenge occurred late and only in response to secreted products and is thus similar to RelB regulation in MEFs. In

contrast however, it is very unlikely that stimuli activating canonical NF-κB in epithelial cells are responsible for non-canonical or RelB signalling. *A. fumigatus* spore challenge activated canonical NF-κB signalling but not non canonical signalling in a contact dependent manner. However, CF challenge presumably is devoid of the stimuli activating canonical signalling as there are no fungal particles present. How then does an *A. fumigatus* secreted product (or CF) activate NIK *vis a vis* non-canonical signalling in epithelial cells? Some studies have shown that various pathogens such as HIV virus, Influenza virus and *Helicobacter pylori*,and pathogen-derived proteins such as LegK1 *Legionella pneumophila* protein can directly activate non-canonical NF-κB signalling (Sun, 2017). Activation of non-canonical NF-κB signalling by effector proteins such as LegK1 suggests strongly the possibility of direct activation of non-canonical signalling by an *A. fumigatus* secreted protein (Ge et al., 2009). This can be verified by challenging the current A549 model with mutants lacking the various secreted product genes especially the cohort under the master regulator PacC and examining the pattern of NF-κB activation.

8.6 Study limitations and recommendations for further studies

8.6.1 Improvements to study model

Although the work presented in this study used an *in vitro* model of alveolar carcinoma cells, it provides a robust and reproducible model for the study of the global and temporal basis of airway epithelial cell responses to *A. fumigatus*. However, validation of these observations in other cell lines and using differentiated primary airway epithelial cells where feasible is necessary. Airway epithelial cells are physiologically built in a 3-dimensional tissue structure (Rackley and Stripp, 2012), therefore, dissociation and propagating epithelial cells as 2 dimensional monolayers results in aberrant and physiologically dissociated phenotypes as a result of dedifferentiation, loss of specialized features and mutagenesis. The transmembrane integrins found on the basal axis *in vivo* are lost by culturing epithelial cells on plastic surfaces *in vitro*. These limitations have led to development of *in vitro* 3D models that better preserve the properties of the airway epithelium for the study of host pathogen interaction at the pulmonary interface. A 3D model of A549 epithelial cells

has been developed for the study of host responses to respiratory pathogens (Carterson et al., 2005, Berube et al., 2010), and could be exploited to study epithelial cell responses to *A. fumigatus* and mechanisms of epithelial damage. Using an *in vitro* 3D model with multicellular compartments would be necessary to gain more understanding of the way in which airway epithelial responses play a role in shaping other immune components and in orchestrating other immune cells such as dendritic cells and neutrophils by providing an additional platform for cell-cell interaction such as in tumor-immune system *in vitro* 3D models (Hirt et al., 2014). Although cell lines and primary cell culture models allow for study of cellular interaction, the conditions and outcomes are not necessarily similar to those found *in vivo*. As such the studies on host responses to *A. fumigatus* challenge should be replicated *ex vivo* and *in vivo* using human tissues from patients with the different forms of aspergillosis or animal models of the different forms of aspergillosis respectively. This study was conducted with a planktonic culture of *A. fumigatus*. However, recent advancement in lung microbiome studies has revealed the important role of microbial communities in the lung in human lung and airway pathogenesis (Shukla et al., 2017, Gomez and Chanez, 2016, Dickson et al., 2013b, Dickson et al., 2013a, Dickson and Huffnagle, 2015). The need to investigate the impact of a mixed/polymicrobial culture on the epithelial cell response model is therefore evident. Similar to most of the previous studies investigating the interaction of *A. fumigatus* with epithelial cells, this study made use of the culture filtrate as an imperfect mimic of the invasive phase of *Aspergillus* infection which is rather unfeasible to accommodate in an *in vitro* culture condition (Daly et al., 1999, Sharon et al., 2011, Sharon et al., 2009). Culture filtrate contains only soluble secreted factors and excludes the contribution of other aspects of the fungus that impacts the outcome of interaction such as cell-cell contact, carbohydrate antigens and receptors. In addition, the human lung can express some endogenous proteases and protease inhibitors. Therefore, the actual concentration of the different secreted proteases in the CF available physiologically in the lung environment during a real infection may vary from the amount the epithelial cell monolayers are exposed to *in vitro*.

8.6.2 Transmigration assay

In a monoculture system, such as the *in vitro* epithelial cell culture model used in this study, clearance of inhaled fungal conidia is absolutely dependent on the integrity of the epithelial cells. In response to inhaled conidia, epithelial cells initiated protective barrier actions, one of which is a previously described as spore uptake (Paris et al., 1997, Wasylnka and Moore, 2002). Spore uptake by airway epithelial cells has been shown to create safe house for a small proportion of spores and might lead to reinfection (Wasylnka et al., 2005, Wasylnka and Moore, 2003). Internalized spores may cross into the basolateral surface through the transcellular route involving adhesion on to the apical surface, receptor mediated endocytosis, and exocytosis or directional growth through the basolateral surface (Sutherland et al., 2010).

In Chapter 3, it was shown that cell wall borne toxins on the extracellular conidia quickly initiate cellular stress and perturbations which could lead to loss of epithelial tight junction integrity and paracellular barrier function as measured by TEER (Srinivasan et al., 2015). Although not investigated in this study, epithelial cell detachment may potentially facilitate the migration of some of the unphagocytosed conidia, via the paracellular route (interepithelial junction) into the underlying compartment prior to their germination because cell detachment exposes more surface area for further binding of more spores (DeHart et al., 1997).

In a previous study, the paracellular passage of bacteria into the basolateral chamber was monitored by measuring the amount of bacteria crossing the transwell into the basolateral chamber by plating the basolateral fluid on a culture media (Hirakata et al., 2010, Miller et al., 2013) and correlating it with increase in paracellular passage of a moderately sized radio tracer molecule whose apical-to-basolateral passage is limited only to regions where the tight junction network has been compromised (Coureuil et al., 2012, Miller et al., 2013). The most commonly available paracellular tracers include the Texas Red-labelled 70,000-molecular weight dextran (Invitrogen) (Sutherland et al., 2010) and the 0.5 kDa tracer pyranine (Sigma) (LaFemina et al., 2010). These salts have been added to the apical chamber of the transwell culture system prior to challenge with *N. meningitidis* and the fluorescence intensity of the

media in the basolateral chamber monitored over 24 h. This study and the currently available literature suggest that *A. fumigatus* could overcome the epithelial barrier to invade underlying tissues through both the paracellular and the transcellular routes. For example, the intestinal commensal bacteria, *Campylobacter jejuni* migrates across the intestinal epithelium via both the paracellular and transcellular route (Backert and Hofreuter, 2013).

8.6.3 Tight Junction assays

Whilst cell surface receptors are important for endocytosis and transcellular migration, the tight junction claudins are the major regulators of paracellular transmigration of pathogens and solutes (Schlingmann et al., 2015, Backert and Hofreuter, 2013) of which claudin-18 appears to be most important for optimal alveolar epithelial barrier functioning (LaFemina et al., 2014). Secondly, the rearrangement of actin cytoskeleton involved in the process of spore uptake does not only facilitate transmigration by reducing the TEER, but also results in loss of focal adhesion to the basal matrix, cell rounding and detachment (Chapter 3) and as seen by reduction in detachment following AECs treatment with cytochalasin D inhibitor for actin polymerization (Chapter 5). The detachment of epithelial cells exposes the underlying tissues to further adhesion and invasion by fungus as exposed ECM is more susceptible to fungal invasion (Coulot et al., 1994). Interestingly, a role for yet another claudin-7 in initial cell rounding and cell membrane ruffling observed prior to cell detachment has been demonstrated by deleting claudin-7 using lentivirus shRNA or by targeted-gene deletion in human lung cancer cells (Lu et al., 2015). Deletion of claudin-7 resulted in cells which were rounded, growing on each other and unable to adhere to the matrix (Lu et al., 2015). These studies provide sufficient evidence in support of the role of claudins in airway barrier function as well as a pointer to the hidden possibilities of claudin dysregulation in the pathogenesis of invasive and semi-invasive aspergillosis.

8.7 Implications and translational applications of this study

Invasive aspergillosis is a disease of immunocompromised individuals and therapies or preventive measures independent of the host immune system if possible will be gold standards. Findings from this study have elaborated on the role of the airway epithelial barrier/function in host defence against aspergillosis in the absence of other arms of the immune systems. It has therefore given further insights into the different ways in which the barrier function of the epithelium can be preserved/enhanced in order to prevent or at the least delay the invasion of inhaled fungus into the underlying tissues.

It could be inferred from this study that the process of invasive growth is a complex event involving the host and the pathogen whereby the majority of the damage to epithelium occurs as a result of epithelial intracellular responses to the fungus and fungal secreted products. Given the contributions of the AECs, therapeutic strategies targeted at the detrimental epithelial response axis might influence the outcome of invasive disease development. The JNK signalling which drives early and late damage via detachment, loss in TEER and lytic cell death appears to be a potential target for development of an immunomodulator against invasive aspergillosis (Davies and Tournier, 2012). Previous study showed that *C. albicans* hyphae express an invasion Als3 which drove epithelial invasion through the epidermal growth factor (EGF) signalling pathway. Conconcordantly, blocking the EGF receptor (EGFR) with small molecule inhibitors in a mouse model of oropharyngeal candidiasis (OPC) inhibited epithelial invasion and reduced the severity of OPC (Zhu et al., 2012b, Phan et al., 2007). Activation of JNK signalling appears to be driven via the Dectin-1 receptor on alveolar epithelial cells. Although not covered in the current study, a previous study showed that anti-Dectin-1 antibody completely protected A549 pneumocytes from detachment *in vitro*. However an anti-Dectin-1- mice significantly increased lytic cell death in a leukopenic mouse model of IPA suggesting multiple roles for the Dectin-1 receptor in protecting against *Aspergillus* infection *in vivo* (Bertuzzi et al., 2014). The antagonistic roles of JNK activation in mediating apoptosis and cell death as well as regulation of cell proliferation necessitate an adequate precaution when targeting JNK as a therapeutic option. Interestingly, studies have demonstrated that transient

JNK activation is important for cell survival whereas prolonged and persistent activation is destructive to host cells (Ventura et al., 2006). JNK activation in response to *A. fumigatus* challenge in this study persisted from spore challenge and through challenge with secreted product, further reiterating its potential as a pharmaceutical target. The two main activators of JNK in the MAPK axis, MKK4 and MKK7 (Fig 1.11) also function in a non-redundant manner although their preference for phosphorylation site is different for tyrosine and threonine residues respectively (Wang et al., 2007b). Interestingly, kinases have shown increased amenability as drug targets. Many therapeutic peptides such as SP600125 and AS601245 have been developed which target the JNK protein itself but with numerous adverse effects of suppression of basal JNK activity (Wang et al., 2004, Gaillard et al., 2005). As a result, attention has been redirected from targeting JNK activity to targeting JNK activation by specifically inhibiting MKK4 and or MKK7. RASSF7 is a protein that binds to MKK7 thereby disrupting its interaction with upstream MAP3K and down stream JNK (Takahashi et al., 2011). Therefore, directly inhibiting the JNK axis of MAPK would be a preferred approach, but only after an *in vivo* study with these inhibitors is reproduced in leukopenic or other mouse models of IPA with a high benefit to risk ratio.

Although the mechanistic basis of epithelial cell protection conferred by non-canonical NF-κB signalling is as yet incompletely known, improving the action of this pathway may also be considered in therapy development. This can be achieved by pre-treating epithelial cells (or high risk patients) with any of the known members of the TNF superfamily of cytokines important in non-canonical NF-κB signalling such as CD40 ligand, the B-cell activating factor (BAFF) or tumor necrosis factor-like weak inducer of apoptosis (TWEAK). TWEAK was shown to activate non-canonical NF-κB signalling and RelB activity *in vitro* in cultured murine tubular epithelial cells and *in vivo* with no significant adverse effects such as tubular injury, increased creatinine level or cell death in healthy control mice (Sanz et al., 2010).

Since JNK activation as well as epithelial lysis is driven by a secreted soluble factor of *A. fumigatus*, identifying and characterizing the pathologic mechanisms of protein(s)

involved (such as with *C. albicans* Als3p (Sui et al., 2017)) can lead to development of a vaccine against invasive pulmonary aspergillosis.

8.8 Concluding remarks

Continued research is advancing the current understanding of the complexities involved in the pathogenesis of invasive aspergillosis. In the course of this study, an *in vitro* model of dynamic and temporal epithelial cell responses to *A. fumigatus* infections was successfully established. This study has successfully demonstrated that airway epithelial cells differentially recognize the different morphotypes of *Aspergillus* by mounting distinct and effective immune responses, further reinforcing the fact that the airway epithelium is functionally crucial in anti-*Aspergillus* immunity. Furthermore, this study has demonstrated that during the course of interaction with *A. fumigatus*, the epithelial cell responses activated could be either destructive or protective and in most cases, the destructive responses are driven in response to fungal secreted factors. Table 8.1 contains an update on our understanding of the outcome of AECs-*A. fumigatus* interaction as derived from data gathered from this study.

Table 8.1: Update on the outcome of AECs-*A. fumigatus* interaction *in vitro*

Fungal morphotypes	Epithelial cell type	Signal protein phosphorylated	Transcription factor activated	Transcription factors repressed	Cytokine expression (experimental approach)	Effect of interaction on host	References
Conidia	A549	IκBα (NF-κB)	Canonical NF-κB (p65 and p50),	Non canonical NF-κB (RelB), JunD, c-Jun, MEF-2	hBD2 and hBD9 (RT-qPCR) IL-8, TNF-α, IL-6, GM-CSF, FGF-basic (high performance cytokine Luminex)	Epithelial cell deaggregation	(Alekseeva et al., 2009)
	HBECs	?	NF-κB		IFN-β, IP-10, TNFα, GM-CSF, IL8, hBD2 and hBD9 (RT-qPCR)	?	(Beisswenger et al., 2012)
Hyphae	A549	IκBα (NF-κB), JNK	c-Fos, c-Myc, canonical NF-κB (p65 and p50)	Non canonical NF-κB (RelB)	IL-6 and IL-8 (ELISA) TNF-alpha, IL-8, IL-6 and GM-CSF (RT-PCR) TNF-α, and FGF-basic (high performance cytokine Luminex)	Epithelial cell detachment, loss of TEER and epithelial cell lytic cell death	(Zhang et al., 2005, Bellanger et al., 2009, Borger et al., 1999)
	HBECs	?	?		TNF-α, IL-6, IP-10, MCP- 1, MIP- 2 (Luminex multiplex technology)	?	(Chaudhary et al., 2012)
	BEAS-2B	Phosphatidylinositol 3-kinase, p38 MAPK, and ERK1/2	NF-κB		IL-8 (RT-qPCR)	?	(Balloy et al., 2008)
Culture filtrate	A549	P38 and JNK	Non canonical NF-κB (RelB and p52)	c-Myc	FGF-basic and CD40 ligand (high performance cytokine Luminex)	Disruption of the actin fiber cytoskeleton and loss of focal adhesion sites, necrosis, Lytic cell death and epithelial cell detachment, host cytokine degradation	(Kogan et al., 2004, Sharon et al., 2011)

Footnote: **Data in grey are from this study, data in green are previous data reproduced during this study**. HBECs: Human bronchial epithelial cells, IFN: interferon gamma, TNF: Tumour necrosis factor, IL: interleukin, IP: IFN-gamma-inducible protein, HBD: human beta defensin, MCP: monocyte chemotactic protein, MIP: Macrophage inflammatory protein, GM-CSF: Granulocyte-macrophage colony stimulating factor, BEAS-2B: Transformed human bronchial epithelial cell, A549: carcinomic human alveolar basal epithelial cell.

8.9 Bibliography

AIMANIANDA, V., CLAVAUD, C., SIMENEL, C., FONTAINE, T., DELEPIERRE, M. & LATGE, J. P. 2009. Cell wall beta-(1,6)-glucan of *Saccharomyces cerevisiae*: structural characterization and in situ synthesis. *J Biol Chem,* 284**,** 13401-12.

ALEKSEEVA, L., HUET, D., FEMENIA, F., MOUYNA, I., ABDELOUAHAB, M., CAGNA, A., GUERRIER, D., TICHANNE-SELTZER, V., BAEZA-SQUIBAN, A., CHERMETTE, R., LATGE, J. P. & BERKOVA, N. 2009. Inducible expression of beta defensins by human respiratory epithelial cells exposed to *Aspergillus fumigatus* organisms. *BMC Microbiol,* 9**,** 33.

ARANA, D. M., PRIETO, D., ROMAN, E., NOMBELA, C., ALONSO-MONGE, R. & PLA, J. 2009. The role of the cell wall in fungal pathogenesis. *Microb Biotechnol,* 2**,** 308-20.

ASOKANANTHAN, N., GRAHAM, P. T., FINK, J., KNIGHT, D. A., BAKKER, A. J., MCWILLIAM, A. S., THOMPSON, P. J. & STEWART, G. A. 2002. Activation of protease-activated receptor (PAR)-1, PAR-2, and PAR-4 stimulates IL-6, IL-8, and prostaglandin E2 release from human respiratory epithelial cells. *J Immunol,* 168**,** 3577-85.

ASOKANANTHAN, N., LAN, R. S., GRAHAM, P. T., BAKKER, A. J., TOKANOVIC, A. & STEWART, G. A. 2015. Activation of protease-activated receptors (PARs)-1 and -2 promotes alpha-smooth muscle actin expression and release of cytokines from human lung fibroblasts. *Physiol Rep,* 3.

ATHER, J. L., FOLEY, K. L., SURATT, B. T., BOYSON, J. E. & POYNTER, M. E. 2015. Airway epithelial NF-kappaB activation promotes the ability to overcome inhalational antigen tolerance. *Clin Exp Allergy,* 45**,** 1245-58.

BACKERT, S. & HOFREUTER, D. 2013. Molecular methods to investigate adhesion, transmigration, invasion and intracellular survival of the foodborne pathogen Campylobacter jejuni. *J Microbiol Methods,* 95**,** 8-23.

BALLOY, V., SALLENAVE, J. M., WU, Y., TOUQUI, L., LATGE, J. P., SI-TAHAR, M. & CHIGNARD, M. 2008. *Aspergillus fumigatus*-induced interleukin-8 synthesis by respiratory epithelial cells is controlled by the phosphatidylinositol 3-kinase, p38 MAPK, and ERK1/2 pathways and not by the toll-like receptor-MyD88 pathway. *J Biol Chem,* 283**,** 30513-21.

BAUD, V. & KARIN, M. 2009. Is NF-kappaB a good target for cancer therapy? Hopes and pitfalls. *Nat Rev Drug Discov,* 8**,** 33-40.

BEISSWENGER, C., HESS, C. & BALS, R. 2012. *Aspergillus fumigatus* conidia induce interferon-beta signalling in respiratory epithelial cells. *Eur Respir J,* 39**,** 411-8.

BELLANGER, A. P., MILLON, L., KHOUFACHE, K., RIVOLLET, D., BIECHE, I., LAURENDEAU, I., VIDAUD, M., BOTTEREL, F. & BRETAGNE, S. 2009. *Aspergillus fumigatus* germ tube growth and not conidia ingestion induces expression of inflammatory mediator genes in the human lung epithelial cell line A549. *J Med Microbiol,* 58**,** 174-9.

BERGMANN, A., HARTMANN, T., CAIRNS, T., BIGNELL, E. M. & KRAPPMANN, S. 2009. A regulator of *Aspergillus fumigatus* extracellular proteolytic activity is dispensable for virulence. *Infect Immun,* 77**,** 4041-50.

BERTUZZI, M., SCHRETTL, M., ALCAZAR-FUOLI, L., CAIRNS, T. C., MUNOZ, A., WALKER, L. A., HERBST, S., SAFARI, M., CHEVERTON, A. M., CHEN, D., LIU, H., SAIJO, S.,

FEDOROVA, N. D., ARMSTRONG-JAMES, D., MUNRO, C. A., READ, N. D., FILLER, S. G., ESPESO, E. A., NIERMAN, W. C., HAAS, H. & BIGNELL, E. M. 2014. The pH-Responsive PacC Transcription Factor of *Aspergillus fumigatus* Governs Epithelial Entry and Tissue Invasion during Pulmonary Aspergillosis. *PLoS Pathog,* 10**,** e1004413.

BERUBE, K., PRYTHERCH, Z., JOB, C. & HUGHES, T. 2010. Human primary bronchial lung cell constructs: the new respiratory models. *Toxicology,* 278**,** 311-8.

BIGNELL, E., NEGRETE-URTASUN, S., CALCAGNO, A. M., HAYNES, K., ARST, H. N., JR. & ROGERS, T. 2005. The *Aspergillus* pH-responsive transcription factor PacC regulates virulence. *Mol Microbiol,* 55**,** 1072-84.

BLASIUS, A. L., GIURISATO, E., CELLA, M., SCHREIBER, R. D., SHAW, A. S. & COLONNA, M. 2006. Bone marrow stromal cell antigen 2 is a specific marker of type I IFN-producing cells in the naive mouse, but a promiscuous cell surface antigen following IFN stimulation. *J Immunol,* 177**,** 3260-5.

BORGER, P., KOETER, G. H., TIMMERMAN, J. A., VELLENGA, E., TOMEE, J. F. & KAUFFMAN, H. F. 1999. Proteases from *Aspergillus fumigatus* induce interleukin (IL)-6 and IL-8 production in airway epithelial cell lines by transcriptional mechanisms. *J Infect Dis,* 180**,** 1267-74.

CARTERSON, A. J., HONER ZU BENTRUP, K., OTT, C. M., CLARKE, M. S., PIERSON, D. L., VANDERBURG, C. R., BUCHANAN, K. L., NICKERSON, C. A. & SCHURR, M. J. 2005. A549 lung epithelial cells grown as three-dimensional aggregates: alternative tissue culture model for *Pseudomonas aeruginosa* pathogenesis. *Infect Immun,* 73**,** 1129-40.

CHAUDHARY, N., DATTA, K., ASKIN, F. B., STAAB, J. F. & MARR, K. A. 2012. Cystic fibrosis transmembrane conductance regulator regulates epithelial cell response to *Aspergillus* and resultant pulmonary inflammation. *Am J Respir Crit Care Med,* 185**,** 301-10.

COULOT, P., BOUCHARA, J. P., RENIER, G., ANNAIX, V., PLANCHENAULT, C., TRONCHIN, G. & CHABASSE, D. 1994. Specific interaction of *Aspergillus fumigatus* with fibrinogen and its role in cell adhesion. *Infect Immun,* 62**,** 2169-77.

COUREUIL, M., JOIN-LAMBERT, O., LECUYER, H., BOURDOULOUS, S., MARULLO, S. & NASSIF, X. 2012. Mechanism of meningeal invasion by *Neisseria meningitidis*. *Virulence,* 3**,** 164-72.

DALY, P., VERHAEGEN, S., CLYNES, M. & KAVANAGH, K. 1999. Culture filtrates of *Aspergillus fumigatus* induce different modes of cell death in human cancer cell lines. *Mycopathologia,* 146**,** 67-74.

DAVIES, C. & TOURNIER, C. 2012. Exploring the function of the JNK (c-Jun N-terminal kinase) signalling pathway in physiological and pathological processes to design novel therapeutic strategies. *Biochem Soc Trans,* 40**,** 85-9.

DEHART, D. J., AGWU, D. E., JULIAN, N. C. & WASHBURN, R. G. 1997. Binding and germination of *Aspergillus fumigatus* conidia on cultured A549 pneumocytes. *J Infect Dis,* 175**,** 146-50.

DERY, O., CORVERA, C. U., STEINHOFF, M. & BUNNETT, N. W. 1998. Proteinase-activated receptors: novel mechanisms of signaling by serine proteases. *Am J Physiol,* 274**,** C1429-52.

DICKSON, R. P., ERB-DOWNWARD, J. R. & HUFFNAGLE, G. B. 2013a. The role of the bacterial microbiome in lung disease. *Expert Rev Respir Med,* 7**,** 245-57.

DICKSON, R. P., HUANG, Y. J., MARTINEZ, F. J. & HUFFNAGLE, G. B. 2013b. The lung microbiome and viral-induced exacerbations of chronic obstructive pulmonary disease: new observations, novel approaches. *Am J Respir Crit Care Med,* 188**,** 1185-6.

DICKSON, R. P. & HUFFNAGLE, G. B. 2015. The Lung Microbiome: New Principles for Respiratory Bacteriology in Health and Disease. *PLoS Pathog,* 11**,** e1004923.

DRIESBAUGH, K. H., BUZZA, M. S., MARTIN, E. W., CONWAY, G. D., KAO, J. P. & ANTALIS, T. M. 2015. Proteolytic activation of the protease-activated receptor (PAR)-2 by the glycosylphosphatidylinositol-anchored serine protease testisin. *J Biol Chem,* 290**,** 3529-41.

DULON, S., CANDE, C., BUNNETT, N. W., HOLLENBERG, M. D., CHIGNARD, M. & PIDARD, D. 2003. Proteinase-activated receptor-2 and human lung epithelial cells: disarming by neutrophil serine proteinases. *Am J Respir Cell Mol Biol,* 28**,** 339-46.

DURAND, J. K. & BALDWIN, A. S. 2017. Targeting IKK and NF-kappaB for Therapy. *Adv Protein Chem Struct Biol,* 107**,** 77-115.

ESCOBAR, N., ORDONEZ, S. R., WOSTEN, H. A., HAAS, P. J., DE COCK, H. & HAAGSMAN, H. P. 2016. Hide, Keep Quiet, and Keep Low: Properties That Make *Aspergillus fumigatus* a Successful Lung Pathogen. *Front Microbiol,* 7**,** 438.

FILLER, S. G. & SHEPPARD, D. C. 2006. Fungal invasion of normally non-phagocytic host cells. *PLoS Pathog,* 2**,** e129.

FISCHER, G., MULLER, T., SCHWALBE, R., OSTROWSKI, R. & DOTT, W. 2000. Species-specific profiles of mycotoxins produced in cultures and associated with conidia of airborne fungi derived from biowaste. *Int J Hyg Environ Health,* 203**,** 105-16.

FONTAINE, T., MAGNIN, T., MELHERT, A., LAMONT, D., LATGE, J. P. & FERGUSON, M. A. 2003. Structures of the glycosylphosphatidylinositol membrane anchors from *Aspergillus fumigatus* membrane proteins. *Glycobiology,* 13**,** 169-77.

FONTAINE, T., SIMENEL, C., DUBREUCQ, G., ADAM, O., DELEPIERRE, M., LEMOINE, J., VORGIAS, C. E., DIAQUIN, M. & LATGE, J. P. 2000. Molecular organization of the alkali-insoluble fraction of *Aspergillus fumigatus* cell wall. *J Biol Chem,* 275**,** 27594-607.

GAILLARD, P., JEANCLAUDE-ETTER, I., ARDISSONE, V., ARKINSTALL, S., CAMBET, Y., CAMPS, M., CHABERT, C., CHURCH, D., CIRILLO, R., GRETENER, D., HALAZY, S., NICHOLS, A., SZYNDRALEWIEZ, C., VITTE, P. A. & GOTTELAND, J. P. 2005. Design and synthesis of the first generation of novel potent, selective, and *in vivo* active (benzothiazol-2-yl)acetonitrile inhibitors of the c-Jun N-terminal kinase. *J Med Chem,* 48**,** 4596-607.

GALAO, R. P., LE TORTOREC, A., PICKERING, S., KUECK, T. & NEIL, S. J. 2012. Innate sensing of HIV-1 assembly by Tetherin induces NFkappaB-dependent proinflammatory responses. *Cell Host Microbe,* 12**,** 633-44.

GAUTHIER, T., WANG, X., SIFUENTES DOS SANTOS, J., FYSIKOPOULOS, A., TADRIST, S., CANLET, C., ARTIGOT, M. P., LOISEAU, N., OSWALD, I. P. & PUEL, O. 2012. Trypacidin, a spore-borne toxin from *Aspergillus fumigatus*, is cytotoxic to lung cells. *PLoS One,* 7**,** e29906.

GE, J., XU, H., LI, T., ZHOU, Y., ZHANG, Z., LI, S., LIU, L. & SHAO, F. 2009. A Legionella type IV effector activates the NF-kappaB pathway by phosphorylating the IkappaB family of inhibitors. *Proc Natl Acad Sci U S A,* 106**,** 13725-30.

GOMEZ, C. & CHANEZ, P. 2016. The lung microbiome: the perfect culprit for COPD exacerbations? *Eur Respir J,* 47**,** 1034-6.

GUPTA, S. C., SUNDARAM, C., REUTER, S. & AGGARWAL, B. B. 2010. Inhibiting NF-kappaB activation by small molecules as a therapeutic strategy. *Biochim Biophys Acta,* 1799**,** 775-87.

HIRAKATA, Y., YANO, H., ARAI, K., ENDO, S., KANAMORI, H., AOYAGI, T., HIROTANI, A., KITAGAWA, M., HATTA, M., YAMAMOTO, N., KUNISHIMA, H., KAWAKAMI, K. & KAKU, M. 2010. Monolayer culture systems with respiratory epithelial cells for evaluation of bacterial invasiveness. *Tohoku J Exp Med,* 220**,** 15-9.

HIRT, C., PAPADIMITROPOULOS, A., MELE, V., MURARO, M. G., MENGUS, C., IEZZI, G., TERRACCIANO, L., MARTIN, I. & SPAGNOLI, G. C. 2014. "*In vitro*" 3D models of tumor-immune system interaction. *Adv Drug Deliv Rev,* 79-80**,** 145-54.

HOMMA, T., KATO, A., BHUSHAN, B., NORTON, J. E., SUH, L. A., CARTER, R. G., GUPTA, D. S. & SCHLEIMER, R. P. 2016. Role of *Aspergillus fumigatus* in Triggering Protease-Activated Receptor-2 in Airway Epithelial Cells and Skewing the Cells toward a T-helper 2 Bias. *Am J Respir Cell Mol Biol,* 54**,** 60-70.

KAUFFMAN, H. F., TOMEE, J. F., VAN DE RIET, M. A., TIMMERMAN, A. J. & BORGER, P. 2000. Protease-dependent activation of epithelial cells by fungal allergens leads to morphologic changes and cytokine production. *J Allergy Clin Immunol,* 105**,** 1185-93.

KOGAN, T. V., JADOUN, J., MITTELMAN, L., HIRSCHBERG, K. & OSHEROV, N. 2004. Involvement of secreted *Aspergillus fumigatus* proteases in disruption of the actin fiber cytoskeleton and loss of focal adhesion sites in infected A549 lung pneumocytes. *J Infect Dis,* 189**,** 1965-73.

KOTHARY, M. H., CHASE, T., JR. & MACMILLAN, J. D. 1984. Correlation of elastase production by some strains of *Aspergillus fumigatus* with ability to cause pulmonary invasive aspergillosis in mice. *Infect Immun,* 43**,** 320-5.

LAFEMINA, M. J., ROKKAM, D., CHANDRASENA, A., PAN, J., BAJAJ, A., JOHNSON, M. & FRANK, J. A. 2010. Keratinocyte growth factor enhances barrier function without altering claudin expression in primary alveolar epithelial cells. *Am J Physiol Lung Cell Mol Physiol,* 299**,** L724-34.

LAFEMINA, M. J., SUTHERLAND, K. M., BENTLEY, T., GONZALES, L. W., ALLEN, L., CHAPIN, C. J., ROKKAM, D., SWEERUS, K. A., DOBBS, L. G., BALLARD, P. L. & FRANK, J. A. 2014. Claudin-18 deficiency results in alveolar barrier dysfunction and impaired alveologenesis in mice. *Am J Respir Cell Mol Biol,* 51**,** 550-8.

LAN, R. S., STEWART, G. A., GOLDIE, R. G. & HENRY, P. J. 2004. Altered expression and *in vivo* lung function of protease-activated receptors during influenza A virus infection in mice. *Am J Physiol Lung Cell Mol Physiol,* 286**,** L388-98.

LEVDANSKY, E., KASHI, O., SHARON, H., SHADKCHAN, Y. & OSHEROV, N. 2010. The *Aspergillus fumigatus* cspA gene encoding a repeat-rich cell wall protein is important for normal conidial cell wall architecture and interaction with host cells. *Eukaryot Cell,* 9**,** 1403-15.

LEVDANSKY, E., ROMANO, J., SHADKCHAN, Y., SHARON, H., VERSTREPEN, K. J., FINK, G. R. & OSHEROV, N. 2007. Coding tandem repeats generate diversity in *Aspergillus fumigatus* genes. *Eukaryot Cell,* 6**,** 1380-91.

LI, H., ZHOU, H., LUO, Y., OUYANG, H., HU, H. & JIN, C. 2007. Glycosylphosphatidylinositol (GPI) anchor is required in *Aspergillus fumigatus* for morphogenesis and virulence. *Mol Microbiol,* 64**,** 1014-27.

LIU, W., ZOU, Z., HUANG, X., SHEN, H., HE, L. J., CHEN, S. M., LI, L. P., YAN, L., ZHANG, S. Q., ZHANG, J. D., XU, Z., XU, G. T., AN, M. M. & JIANG, Y. Y. 2016. Bst1 is required for *Candida albicans* infecting host via facilitating cell wall anchorage of Glycosylphosphatidyl inositol anchored proteins. *Sci Rep,* 6**,** 34854.

LORENZINI, J., SCOTT FITES, J., NETT, J. & KLEIN, B. S. 2017. *Blastomyces dermatitidis* serine protease dipeptidyl peptidase IVA (DppIVA) cleaves ELR+ CXC chemokines altering their effects on neutrophils. *Cell Microbiol,* 19.

LU, Z., KIM, D. H., FAN, J., LU, Q., VERBANAC, K., DING, L., RENEGAR, R. & CHEN, Y. H. 2015. A non-tight junction function of claudin-7-Interaction with integrin signaling in suppressing lung cancer cell proliferation and detachment. *Mol Cancer,* 14**,** 120.

MCCANN, F., CARMONA, E., PURI, V., PAGANO, R. E. & LIMPER, A. H. 2005. Macrophage internalization of fungal beta-glucans is not necessary for initiation of related inflammatory responses. *Infect Immun,* 73**,** 6340-9.

MILLER, F., LECUYER, H., JOIN-LAMBERT, O., BOURDOULOUS, S., MARULLO, S., NASSIF, X. & COUREUIL, M. 2013. *Neisseria meningitidis* colonization of the brain endothelium and cerebrospinal fluid invasion. *Cell Microbiol,* 15**,** 512-9.

MORETTI, S., BELLOCCHIO, S., BONIFAZI, P., BOZZA, S., ZELANTE, T., BISTONI, F. & ROMANI, L. 2008. The contribution of PARs to inflammation and immunity to fungi. *Mucosal Immunol,* 1**,** 156-68.

MORIYUKI, K., NAGATAKI, M., SEKIGUCHI, F., NISHIKAWA, H. & KAWABATA, A. 2008. Signal transduction for formation/release of interleukin-8 caused by a PAR2-activating peptide in human lung epithelial cells. *Regul Pept,* 145**,** 42-8.

NOORT, A. R., VAN ZOEST, K. P., WEIJERS, E. M., KOOLWIJK, P., MARACLE, C. X., NOVACK, D. V., SIEMERINK, M. J., SCHLINGEMANN, R. O., TAK, P. P. & TAS, S. W. 2014. NF-kappaB-inducing kinase is a key regulator of inflammation-induced and tumour-associated angiogenesis. *J Pathol,* 234**,** 375-85.

PARIS, S., BOISVIEUX-ULRICH, E., CRESTANI, B., HOUCINE, O., TARAMELLI, D., LOMBARDI, L. & LATGE, J. P. 1997. Internalization of *Aspergillus fumigatus* conidia by epithelial and endothelial cells. *Infect Immun,* 65**,** 1510-4.

PENALVA, M. A., TILBURN, J., BIGNELL, E. & ARST, H. N., JR. 2008. Ambient pH gene regulation in fungi: making connections. *Trends Microbiol,* 16**,** 291-300.

PHAN, Q. T., MYERS, C. L., FU, Y., SHEPPARD, D. C., YEAMAN, M. R., WELCH, W. H., IBRAHIM, A. S., EDWARDS, J. E., JR. & FILLER, S. G. 2007. Als3 is a *Candida albicans* invasin that binds to cadherins and induces endocytosis by host cells. *PLoS Biol,* 5**,** e64.

PITTET, M. & CONZELMANN, A. 2007. Biosynthesis and function of GPI proteins in the yeast *Saccharomyces cerevisiae*. *Biochim Biophys Acta,* 1771**,** 405-20.

RACKLEY, C. R. & STRIPP, B. R. 2012. Building and maintaining the epithelium of the lung. *J Clin Invest,* 122**,** 2724-30.

RICHARD, M. L. & PLAINE, A. 2007. Comprehensive analysis of glycosylphosphatidylinositol-anchored proteins in *Candida albicans*. *Eukaryot Cell,* 6**,** 119-33.

RIZK, M. G., BASLER, C. F. & GUATELLI, J. 2017. Cooperation of the Ebola proteins VP40 and GP1,2 with BST2 to activate NF-kappabeta independently of virus-like particle trapping. *J Virol*.

SANZ, A. B., SANCHEZ-NINO, M. D., IZQUIERDO, M. C., JAKUBOWSKI, A., JUSTO, P., BLANCO-COLIO, L. M., RUIZ-ORTEGA, M., SELGAS, R., EGIDO, J. & ORTIZ, A. 2010. TWEAK activates the non-canonical NFkappaB pathway in murine renal tubular cells: modulation of CCL21. *PLoS One,* 5**,** e8955.

SCHELLER, J., CHALARIS, A., SCHMIDT-ARRAS, D. & ROSE-JOHN, S. 2011. The pro- and anti-inflammatory properties of the cytokine interleukin-6. *Biochim Biophys Acta,* 1813**,** 878-88.

SCHLINGMANN, B., MOLINA, S. A. & KOVAL, M. 2015. Claudins: Gatekeepers of lung epithelial function. *Semin Cell Dev Biol,* 42**,** 47-57.

SHARON, H., AMAR, D., LEVDANSKY, E., MIRCUS, G., SHADKCHAN, Y., SHAMIR, R. & OSHEROV, N. 2011. PrtT-regulated proteins secreted by *Aspergillus fumigatus* activate MAPK signaling in exposed A549 lung cells leading to necrotic cell death. *PLoS One,* 6**,** e17509.

SHARON, H., HAGAG, S. & OSHEROV, N. 2009. Transcription factor PrtT controls expression of multiple secreted proteases in the human pathogenic mold *Aspergillus fumigatus*. *Infect Immun,* 77**,** 4051-60.

SHIH, V. F., DAVIS-TURAK, J., MACAL, M., HUANG, J. Q., PONOMARENKO, J., KEARNS, J. D., YU, T., FAGERLUND, R., ASAGIRI, M., ZUNIGA, E. I. & HOFFMANN, A. 2012. Control of RelB during dendritic cell activation integrates canonical and noncanonical NF-kappaB pathways. *Nat Immunol,* 13**,** 1162-70.

SHUKLA, S. D., BUDDEN, K. F., NEAL, R. & HANSBRO, P. M. 2017. Microbiome effects on immunity, health and disease in the lung. *Clin Transl Immunology,* 6**,** e133.

SOH, U. J., DORES, M. R., CHEN, B. & TREJO, J. 2010. Signal transduction by protease-activated receptors. *Br J Pharmacol,* 160**,** 191-203.

SRINIVASAN, B., KOLLI, A. R., ESCH, M. B., ABACI, H. E., SHULER, M. L. & HICKMAN, J. J. 2015. TEER measurement techniques for *in vitro* barrier model systems. *J Lab Autom,* 20**,** 107-26.

STERKEL, A. K., LORENZINI, J. L., FITES, J. S., SUBRAMANIAN VIGNESH, K., SULLIVAN, T. D., WUTHRICH, M., BRANDHORST, T., HERNANDEZ-SANTOS, N., DEEPE, G. S., JR. & KLEIN, B. S. 2016. Fungal Mimicry of a Mammalian Aminopeptidase Disables Innate Immunity and Promotes Pathogenicity. *Cell Host Microbe,* 19**,** 361-74.

SUI, X., YAN, L. & JIANG, Y. Y. 2017. The vaccines and antibodies associated with Als3p for treatment of Candida albicans infections. *Vaccine,* 35**,** 5786-5793.

SUN, S. C. 2017. The non-canonical NF-kappaB pathway in immunity and inflammation. *Nat Rev Immunol,* 17**,** 545-558.

SUN, W. K., LU, X., LI, X., SUN, Q. Y., SU, X., SONG, Y., SUN, H. M. & SHI, Y. 2012. Dectin-1 is inducible and plays a crucial role in *Aspergillus*-induced innate immune responses in human bronchial epithelial cells. *Eur J Clin Microbiol Infect Dis,* 31**,** 2755-64.

SUTHERLAND, T. C., QUATTRONI, P., EXLEY, R. M. & TANG, C. M. 2010. Transcellular passage of *Neisseria meningitidis* across a polarized respiratory epithelium. *Infect Immun,* 78**,** 3832-47.

SWIDERGALL, M. & FILLER, S. G. 2017. Oropharyngeal Candidiasis: Fungal Invasion and Epithelial Cell Responses. *PLoS Pathog,* 13**,** e1006056.

TAKAHASHI, S., EBIHARA, A., KAJIHO, H., KONTANI, K., NISHINA, H. & KATADA, T. 2011. RASSF7 negatively regulates pro-apoptotic JNK signaling by inhibiting the activity of phosphorylated-MKK7. *Cell Death Differ,* 18**,** 645-55.

THAU, N., MONOD, M., CRESTANI, B., ROLLAND, C., TRONCHIN, G., LATGE, J. P. & PARIS, S. 1994. rodletless mutants of *Aspergillus fumigatus*. *Infect Immun,* 62**,** 4380-8.

TOKAREV, A., SUAREZ, M., KWAN, W., FITZPATRICK, K., SINGH, R. & GUATELLI, J. 2013. Stimulation of NF-kappaB activity by the HIV restriction factor BST2. *J Virol,* 87**,** 2046-57.

TOMEE, J. F., WIERENGA, A. T., HIEMSTRA, P. S. & KAUFFMAN, H. K. 1997. Proteases from *Aspergillus fumigatus* induce release of proinflammatory cytokines and cell detachment in airway epithelial cell lines. *J Infect Dis,* 176**,** 300-3.

TULLY, J. E., NOLIN, J. D., GUALA, A. S., HOFFMAN, S. M., ROBERSON, E. C., LAHUE, K. G., VAN DER VELDEN, J., ANATHY, V., BLACKWELL, T. S. & JANSSEN-HEININGER, Y. M. 2012. Cooperation between classical and alternative NF-kappaB pathways regulates proinflammatory responses in epithelial cells. *Am J Respir Cell Mol Biol,* 47**,** 497-508.

VAKNIN, Y., SHADKCHAN, Y., LEVDANSKY, E., MOROZOV, M., ROMANO, J. & OSHEROV, N. 2014. The three *Aspergillus fumigatus* CFEM-domain GPI-anchored proteins (CfmA-C) affect cell-wall stability but do not play a role in fungal virulence. *Fungal Genet Biol,* 63**,** 55-64.

VALIM, C. X., DA SILVA, E. Z., ASSIS, M. A., FERNANDES, F. F., COELHO, P. S., OLIVER, C. & JAMUR, M. C. 2015. rPbPga1 from *Paracoccidioides brasiliensis* Activates Mast Cells and Macrophages via NFkB. *PLoS Negl Trop Dis,* 9**,** e0004032.

VAN DE VEERDONK, F. L., KULLBERG, B. J., VAN DER MEER, J. W., GOW, N. A. & NETEA, M. G. 2008. Host-microbe interactions: innate pattern recognition of fungal pathogens. *Curr Opin Microbiol,* 11**,** 305-12.

VANCRAEYNESTE, H., CHARLET, R., GUERARDEL, Y., CHOTEAU, L., BAUTERS, A., TARDIVEL, M., FRANCOIS, N., DUBUQUOY, L., SOLOVIEV, D., POULAIN, D., SENDID, B. & JAWHARA, S. 2016. Short fungal fractions of beta-1,3 glucans affect platelet activation. *Am J Physiol Heart Circ Physiol,* 311**,** H725-34.

VENTURA, J. J., HUBNER, A., ZHANG, C., FLAVELL, R. A., SHOKAT, K. M. & DAVIS, R. J. 2006. Chemical genetic analysis of the time course of signal transduction by JNK. *Mol Cell,* 21**,** 701-10.

VILLAR, C. C., KASHLEVA, H., NOBILE, C. J., MITCHELL, A. P. & DONGARI-BAGTZOGLOU, A. 2007. Mucosal tissue invasion by *Candida albicans* is associated with E-cadherin degradation, mediated by transcription factor Rim101p and protease Sap5p. *Infect Immun,* 75**,** 2126-35.

WANG, J., YI, S., ZHOU, J., ZHANG, Y. & GUO, F. 2016. The NF-kappaB subunit RelB regulates the migration and invasion abilities and the radio-sensitivity of prostate cancer cells. *Int J Oncol,* 49**,** 381-92.

WANG, W., SHI, L., XIE, Y., MA, C., LI, W., SU, X., HUANG, S., CHEN, R., ZHU, Z., MAO, Z., HAN, Y. & LI, M. 2004. SP600125, a new JNK inhibitor, protects dopaminergic neurons in the MPTP model of Parkinson's disease. *Neurosci Res,* 48**,** 195-202.

WANG, X., BELGUISE, K., KERSUAL, N., KIRSCH, K. H., MINEVA, N. D., GALTIER, F., CHALBOS, D. & SONENSHEIN, G. E. 2007a. Oestrogen signalling inhibits invasive phenotype by repressing RelB and its target BCL2. *Nat Cell Biol,* 9**,** 470-8.

WANG, X., DESTRUMENT, A. & TOURNIER, C. 2007b. Physiological roles of MKK4 and MKK7: insights from animal models. *Biochim Biophys Acta,* 1773**,** 1349-57.

WASYLNKA, J. A., HISSEN, A. H., WAN, A. N. & MOORE, M. M. 2005. Intracellular and extracellular growth of *Aspergillus fumigatus*. *Med Mycol,* 43 Suppl 1**,** S27-30.

WASYLNKA, J. A. & MOORE, M. M. 2002. Uptake of *Aspergillus fumigatus* Conidia by phagocytic and nonphagocytic cells *in vitro*: quantitation using strains expressing green fluorescent protein. *Infect Immun,* 70**,** 3156-63.

WASYLNKA, J. A. & MOORE, M. M. 2003. *Aspergillus fumigatus* conidia survive and germinate in acidic organelles of A549 epithelial cells. *J Cell Sci,* 116**,** 1579-87.

WEIH, F., DURHAM, S. K., BARTON, D. S., SHA, W. C., BALTIMORE, D. & BRAVO, R. 1996. Both multiorgan inflammation and myeloid hyperplasia in RelB-deficient mice are T cell dependent. *J Immunol,* 157**,** 3974-9.

WHITMARSH, A. J. & DAVIS, R. J. 1996. Transcription factor AP-1 regulation by mitogen-activated protein kinase signal transduction pathways. *J Mol Med (Berl),* 74**,** 589-607.

WONG, M. H. & JOHNSON, M. D. 2013. Differential response of primary alveolar type I and type II cells to LPS stimulation. *PLoS One,* 8**,** e55545.

XU, S., XU, X. & ZHANG, L. 2013. Effect of heating on chain conformation of branched beta-glucan in water. *J Phys Chem B,* 117**,** 8370-7.

YOZA, B. K., HU, J. Y., COUSART, S. L., FORREST, L. M. & MCCALL, C. E. 2006. Induction of RelB participates in endotoxin tolerance. *J Immunol,* 177**,** 4080-5.

ZHANG, Z., LIU, R., NOORDHOEK, J. A. & KAUFFMAN, H. F. 2005. Interaction of airway epithelial cells (A549) with spores and mycelium of *Aspergillus fumigatus*. *J Infect,* 51**,** 375-82.

ZHONG, L. M., ZONG, Y., SUN, L., GUO, J. Z., ZHANG, W., HE, Y., SONG, R., WANG, W. M., XIAO, C. J. & LU, D. 2012. Resveratrol inhibits inflammatory responses via the mammalian target of rapamycin signaling pathway in cultured LPS-stimulated microglial cells. *PLoS One,* 7**,** e32195.

ZHU, H. C., QIU, T., LIU, X. H., DONG, W. C., WENG, X. D., HU, C. H., KUANG, Y. L., GAO, R. H., DAN, C. & TAO, T. 2012a. Tolerogenic dendritic cells generated by RelB silencing using shRNA prevent acute rejection. *Cell Immunol,* 274**,** 12-8.

ZHU, W., PHAN, Q. T., BOONTHEUNG, P., SOLIS, N. V., LOO, J. A. & FILLER, S. G. 2012b. EGFR and HER2 receptor kinase signaling mediate epithelial cell invasion by *Candida albicans* during oropharyngeal infection. *Proc Natl Acad Sci U S A,* 109**,** 14194-9.

APPENDICES

Appendix 1: Chemical components of *Aspergillus* complete media

A. **Trace Elements Solution (**To make 1L)

1. 40 mg $Na_2B_4O_7.10H_2O$ (di-sodium tetraborate $10H_2O$)
2. 400 mg $CuSO_4$.$5H_2O$ (cupric sulphate $5H_2O$)
3. 800 mg $FePO_4$. $2H_2O$ (ferric orthophosphate dihydrate)
4. 800 mg $MnSO_4.2H_2O$ (manganese sulphate dihydrate)
5. 800 mg $Na_2MoO_4.2H_2O$ (sodium molybdate $2H_2O$)
6. 8g $ZnSO_4$. $7H_2O$ (zinc sulphate $7H_2O$)

Autoclave

Keep in fridge

B. **Vitamin Solution** (To make 1L)

1. 400 mg PABA (4-aminobenzoic acid)
2. 50 mg aneurin (thiamine)
3. 1 mg biotin (or 10ml of biotin stock-stock 0.1 mg/ml)
4. 24 g inositol
5. 100 mg nicotinic acid
6. 200 mg Panto (DL-phantothenic acid)
7. 250 mg pyridoxine
8. 100 mg riboflavin
9. 1.4 g choline chloride

Wrap the bottle in foil paper and Autoclave
Keep in fridge.

C. **Aspergillus Salt Solution** (To make 1L)

1. Add 26 g KCl (Potassium chloride)
2. 26 g $MgSO_4$. $7H_2O$ (Magnessium dihydrogen heptahidrate)
3. 76 g KH_2PO_4 (Potassium dihydrogen orthophosphate)
4. 50 mL Trace element solution

Add 1.5 ml/l Chloroform as a preservative.
Keep in fridge
Do not autoclave.

Appendix 2: Composition of RIPA buffer

(0.05 M (50 mM) Tris-HCl pH7.5, 0.15M (150 mM) NaCl, 1% Triton X-100, 1% Sodium Deoxycholate, 0.1% SDS and 20 mM EDTA) with protease (Cat. No 78410, Thermofisher, United Kingdom) and phosphatase (Cat. No P5726-5ML, Sigma, United Kingdom) inhibitors.

Appendix 3: DAPI Counter macro to automatically process and count DAPI objects

```
// DAPI Counter macro to automatically process and count DAPI objects
// This macro is optimised for wide-field imaging with a 20x 0.75NA objective lens and a 6.45um pixel size camera, giving a digital pixel size of 0.323um. If your images are of a different resolution please contact Darren.thomson@manchester.ac.uk for assistance
// This macro was written by Darren Thomson June 2016. Any comments or quereys should be directed to Darren.thomson@manchester.ac.uk

// Instructions: Create a folder with only the fluorescent images of DAPI + create a folder to deposit the processed outlines images
// Drag and drop this macro file onto FIJI and 'Run' the script. OR create a new macro and paste this code into the window and ‘Run’ the script.
// Direct the macro to the input folder with all the DAPI images are + the output folder to deposit processed images
// Save the results data to Excel from the macro and arrange/illustrate the data accordingly in Excel.

dir1 = getDirectory("Where are the DAPI images");
format = getFormat();
dir2 = getDirectory("Where will I save the processed images?");
list = getFileList(dir1);
setBatchMode(true);
for (i=0; i<list.length; i++) {
 showProgress(i+1, list.length);
```

```
 open(dir1+list[i]);


run("Subtract Background...", "rolling=35");
 run("Gaussian Blur...", "sigma=3");
setAutoThreshold("Huang dark");
//run("Threshold...");
run("Convert to Mask");
run("Watershed");
run("Analyze Particles...", "size=400-5000 circularity=0.50-1.00 show=Outlines summarize");


 if (format=="8-bit TIFF" || format=="GIF")
 convertTo8Bit();
 saveAs(format, dir2+list[i]);
 close();
}
function getFormat() {
 formats = newArray("TIFF", "8-bit TIFF", "JPEG", "GIF", "PNG",
 "PGM", "BMP", "FITS", "Text Image", "ZIP", "Raw");
 Dialog.create("Batch Convert");
 Dialog.addChoice("Convert to: ", formats, "TIFF");
 Dialog.show();
 return Dialog.getChoice();
}
function convertTo8Bit() {
 if (bitDepth==24)
 run("8-bit Color", "number=256");
 else
 run("8-bit");
```

Appendix 4: Human HXL cytokine profiler array output

	Live fungal challenge relative to PBS expressed as fold change					CF^{48} challenge relative to PBS expressed as fold change				
Analytes	**Rep1**	**Rep2**	**Rep3**	**Rep4**	**Average**	**Rep1**	**Rep 2**	**Rep3**	**Rep4**	**Average**
PDGF-AB/BB	56.11	1.80	0.98	-9.42	**12.37**	0.07	0.02	0.22	-2.35	**-0.51**
IL-2	-2.83	1.05	5.99	34.65	**9.72**	0.35	0.34	0.79	6.17	**1.91**
MIG	37.27	1.49	0.63	-1.30	**9.52**	0.46	0.50	0.40	-1.81	**-0.11**
Cripto-1	0.25	0.65	1.44	25.16	**6.88**	0.46	0.15	0.50	6.94	**2.01**
IL-1α	21.22	0.67	2.91	1.31	**6.53**	0.51	0.28	1.43	1.04	**0.82**
MIP-3β	3.93	-0.01	10.25	11.47	**6.41**	1.93	0.16	0.11	2.00	**1.05**
IL-10	19.90	1.36	0.98	2.58	**6.20**	0.23	0.36	0.42	0.89	**0.48**
IL-18 Bpa	-21.06	8.22	0.39	36.02	**5.89**	0.45	0.15	1.78	31.99	**8.59**
IL-22	15.73	3.81	0.78	1.98	**5.58**	0.67	0.38	0.52	0.73	**0.57**
IL-1ra	3.15	0.92	1.00	16.22	**5.32**	0.52	0.61	1.06	6.14	**2.08**
IL-33	10.75	2.10	3.87	2.35	**4.77**	0.33	-0.07	1.23	1.82	**0.83**
FGF basic	8.98	5.58	1.33	2.23	**4.53**	2.84	3.05	8.22	11.10	**6.30**
IP-10	0.36	0.93	3.97	10.98	**4.06**	0.32	0.31	0.50	4.12	**1.31**
Adiponectin	4.16	1.47	1.99	8.12	**3.94**	0.31	0.26	0.37	1.57	**0.63**
MMP-9	-1.07	-0.57	11.07	5.84	**3.82**	0.41	0.21	9.93	2.58	**3.29**
Myeloperoxidase	9.02	3.33	1.63	1.13	**3.78**	0.35	0.40	0.57	0.34	**0.42**
I-TAC	2.10	-0.86	8.83	3.41	**3.37**	0.49	0.51	-0.40	0.06	**0.17**
IL-19	4.91	3.26	2.80	1.29	**3.07**	0.55	0.67	0.62	0.48	**0.58**
CD40 ligand	1.85	1.65	2.95	5.42	**2.97**	0.29	0.32	2.55	6.33	**2.37**
RAGE	4.26	3.61	0.53	2.71	**2.78**	0.31	0.19	0.26	2.00	**0.69**
SDF-1α	0.94	0.48	1.33	8.04	**2.70**	0.38	0.66	1.12	1.09	**0.81**
Kallikrein 3	2.20	0.28	4.48	3.20	**2.54**	0.33	0.35	1.99	1.59	**1.06**
MIP-1α/MIP-1β	15.61	0.30	-8.54	2.28	**2.41**	-0.99	2.52	1.77	1.35	**1.16**
IL-17A	-0.13	0.01	6.17	3.30	**2.34**	0.76	0.44	2.47	2.22	**1.47**
TfR	4.54	3.04	0.90	0.80	**2.32**	0.99	1.04	1.29	0.85	**1.04**
Growth Hormone	3.36	2.32	1.28	1.57	**2.14**	0.48	0.92	0.43	1.12	**0.74**
Pentraxin-3	5.78	0.69	1.09	0.86	**2.10**	0.52	0.38	0.52	0.52	**0.48**
RANTES	2.30	1.13	1.59	3.12	**2.04**	0.32	0.46	1.62	0.75	**0.79**
TARC	1.47	0.55	2.97	3.12	**2.03**	0.18	0.18	1.21	1.05	**0.66**
C-Reactive protein	1.28	1.02	1.05	4.72	**2.02**	0.39	0.41	0.53	2.40	**0.93**
ST2	1.03	1.23	1.73	4.04	**2.01**	0.09	0.12	0.25	0.42	**0.22**
Leptin	4.51	1.14	0.33	1.96	**1.98**	0.92	1.20	0.96	1.73	**1.20**
GM-CSF	1.18	2.50	1.13	2.79	**1.90**	0.64	0.83	0.56	0.65	**0.67**
BDNF	0.59	0.54	1.73	4.24	**1.78**	0.91	1.00	0.72	1.09	**0.93**

TFF3	-0.05	-0.04	5.78	1.29	**1.75**	0.20	0.08	6.56	0.17	**1.75**
CD30	-0.36	0.52	1.73	4.97	**1.72**	2.12	1.58	0.07	0.53	**1.07**
uPAR	1.48	1.19	2.24	1.83	**1.69**	0.47	0.77	0.44	0.08	**0.44**
SHBG	1.61	0.80	0.94	3.37	**1.68**	0.29	0.25	1.06	2.05	**0.91**
Resistin	2.90	1.47	1.25	0.68	**1.57**	0.13	0.17	0.85	0.49	**0.41**
TGF-α	2.21	0.55	1.88	1.51	**1.54**	0.25	0.66	1.56	0.41	**0.72**
EMMPRIN	1.80	1.82	1.17	1.21	**1.50**	3.90	3.74	1.19	1.58	**2.60**
MIP-3α	-0.39	2.42	1.92	2.04	**1.50**	0.35	0.85	0.08	0.23	**0.38**
IL-13	3.97	0.57	0.31	0.94	**1.45**	0.25	0.36	0.37	0.56	**0.39**
IL-27	-0.72	1.32	1.84	3.05	**1.37**	0.42	0.52	0.93	1.30	**0.79**
Thrombospondin-1	1.54	1.51	0.83	1.54	**1.36**	0.31	0.40	0.28	0.13	**0.28**
GRO-α	1.52	1.54	1.15	1.18	**1.35**	0.64	0.63	0.90	0.97	**0.78**
Endoglin	0.92	0.94	0.78	2.72	**1.34**	0.23	0.15	0.52	0.34	**0.31**
IL-4	1.73	1.56	0.39	1.68	**1.34**	0.91	0.92	0.34	0.80	**0.74**
CD14	0.91	1.13	1.28	2.03	**1.33**	0.61	0.78	0.42	0.56	**0.59**
IL-12 p70	2.37	1.11	1.03	0.74	**1.31**	0.17	0.18	0.09	0.17	**0.15**
Serpin	1.40	1.35	1.25	1.19	**1.30**	0.81	0.83	0.85	1.00	**0.87**
MIF	-0.04	2.14	1.56	1.51	**1.29**	1.11	1.25	1.09	1.16	**1.15**
IL-15	-0.23	0.60	2.40	2.34	**1.28**	0.38	0.02	0.53	1.35	**0.57**
Aggrecan	-1.14	0.65	0.65	4.88	**1.26**	0.55	0.34	0.21	0.74	**0.46**
MCP-3	0.52	1.13	1.40	1.85	**1.22**	0.19	0.17	0.06	1.82	**0.56**
Cystatin C	1.42	1.37	1.07	1.03	**1.22**	0.33	0.34	0.48	0.68	**0.46**
ENA-78	1.25	1.31	1.10	1.05	**1.18**	0.62	0.65	0.84	0.92	**0.76**
IL-8	1.30	1.29	1.04	1.03	**1.17**	0.66	0.66	0.80	0.91	**0.76**
Angiopoietin-2	0.16	0.91	2.24	1.34	**1.16**	0.55	0.48	0.82	0.18	**0.51**
FGF-19	1.44	1.44	0.92	0.82	**1.16**	0.48	0.54	0.83	0.73	**0.65**
VEGF	1.82	1.17	0.82	0.73	**1.14**	0.24	0.20	0.24	0.24	**0.23**
Dkk-1	1.36	1.33	0.89	0.90	**1.12**	0.69	0.79	0.81	0.85	**0.79**
MCP-1	1.17	1.21	1.12	0.94	**1.11**	0.65	0.71	0.79	0.69	**0.71**
Lipocalin-2	1.14	1.17	1.04	1.08	**1.11**	0.34	0.40	0.58	0.62	**0.48**
IL-24	1.09	1.45	0.69	1.17	**1.10**	0.37	0.46	0.49	0.40	**0.43**
EGF	0.18	0.74	1.35	2.06	**1.08**	0.57	0.45	0.83	0.53	**0.60**
Angiogenin	0.94	1.02	1.23	1.10	**1.07**	0.36	0.38	0.50	0.60	**0.46**
PDGF-AA	1.04	1.11	0.98	0.98	**1.03**	0.46	0.51	0.08	0.10	**0.29**
Vitamin D BP	1.04	0.73	0.99	1.35	**1.03**	0.79	0.44	0.39	0.60	**0.56**
IL-16	-0.58	-0.10	2.17	2.45	**0.98**	-1.14	-0.12	1.35	1.55	**0.41**
ICAM-1	1.25	0.84	0.61	1.18	**0.97**	0.31	0.19	0.73	0.50	**0.43**
TNF-alpha	1.27	1.02	0.49	1.06	**0.96**	0.15	0.11	0.12	0.20	**0.15**
Complement factor D	0.90	1.07	0.95	0.90	**0.95**	0.48	0.52	0.32	0.33	**0.41**
IGFBP-3	0.60	1.07	0.98	1.00	**0.91**	0.18	0.13	0.28	0.33	**0.23**
Angiopoietin-1	0.02	1.08	1.33	0.99	**0.86**	1.30	0.28	0.32	0.15	**0.51**

Fas Ligand	0.38	0.84	1.30	0.88	**0.85**	0.23	0.35	0.04	0.31	**0.23**
M-CSF	0.45	0.46	1.85	0.54	**0.82**	0.45	0.70	0.12	0.47	**0.43**
LIF	-1.64	1.79	1.66	1.44	**0.81**	0.66	0.48	0.92	0.15	**0.55**
Complement component C5/C5a	-0.09	0.50	0.49	2.33	**0.81**	0.54	0.23	0.14	0.82	**0.43**
IGFBP-2	0.03	1.33	0.85	0.95	**0.79**	0.45	0.41	0.42	0.41	**0.42**
GDF-15	0.12	0.53	0.96	1.40	**0.75**	0.57	0.66	0.51	1.13	**0.72**
RBP4	0.67	0.72	0.83	0.69	**0.73**	0.20	0.22	0.25	0.18	**0.21**
IFN-γ	-0.68	0.68	1.27	1.51	**0.70**	0.19	0.32	0.59	0.60	**0.43**
IL-11	0.13	1.04	0.75	0.78	**0.68**	0.32	0.26	0.50	0.61	**0.42**
IL-23	1.08	0.71	0.41	0.48	**0.67**	0.32	0.10	1.15	0.51	**0.52**
IL-32α/β/γ	-1.64	2.24	0.49	1.43	**0.63**	0.27	0.49	2.59	0.61	**0.99**
IL-6	0.18	0.50	1.00	0.84	**0.63**	0.40	0.46	0.75	0.45	**0.52**
Flt-3 Ligand	0.54	0.30	0.80	0.85	**0.62**	1.00	1.18	0.53	0.11	**0.71**
IL-31	0.34	0.33	-0.05	1.77	**0.60**	0.49	0.30	0.80	0.95	**0.64**
Osteopontin	0.51	0.49	0.72	0.64	**0.59**	0.70	0.70	1.04	1.13	**0.89**
BAFF	-0.77	0.37	0.66	1.23	**0.37**	0.85	0.45	2.41	0.58	**1.07**
Chitinase 3-like 1	-1.17	0.51	0.61	0.88	**0.21**	0.43	0.07	0.33	0.34	**0.29**
IL-3	0.80	1.07	1.93	-3.17	**0.16**	0.06	-3.57	0.52	-0.58	**-0.89**
HGF	-0.47	0.45	-0.09	0.66	**0.14**	0.14	0.38	0.33	0.44	**0.32**
FGF-7	-0.16	-1.44	0.52	0.09	**-0.25**	0.45	0.40	0.29	1.44	**0.64**
PF4	-2.07	0.82	0.57	-1.86	**-0.63**	0.22	0.25	2.39	0.14	**0.75**
IL-1β	-2.39	-0.18	3.89	-5.73	**-1.10**	0.42	0.42	3.83	-3.65	**0.26**
Relaxin-2	0.47	0.39	2.77	-8.44	**-1.20**	0.85	1.15	0.16	-3.05	**-0.22**
IL-5	0.53	1.44	1.72	-8.51	**-1.21**	0.96	0.57	0.40	-3.92	**-0.50**
G-CSF	-1.21	0.98	-17.40	5.61	**-3.00**	0.95	0.11	-18.56	1.97	**-3.88**
DPPIV	-13.98	0.23	4.60	-3.49	**-3.16**	0.21	0.90	3.36	-1.02	**0.86**
IL-34	1.11	0.44	0.00	-74.88	**-18.33**	-1.13	-0.87	-0.97	7.54	**1.14**

Footnote: The cytokines/proteins highlighted were selected for further qualitative and quantitative analysis